THE EFFECT OF SEASONAL VARIATIONS IN THE RED RIVER AND UPPER CARBONATE AQUIFER ON RIVERBANK STABILITY IN WINNIPEG

by

JEFFREY M. TUTKALUK

A Thesis
Submitted to the Faculty of Graduate Studies
in Partial Fulfilment of the Requirements for the Degree of

MASTER OF SCIENCE

Department of Civil and Geological Engineering
University of Manitoba
Winnipeg, Manitoba

June, 2000

THE UNIVERSITY OF MANITOBA

FACULTY OF GRADUATE STUDIES

*****

COPYRIGHT PERMISSION PAGE

The Effect of Seasonal Variations in the Red River and Upper Carbonate Aquifer on Riverbank Stability in Winnipeg

BY

Jeffrey M. Tutkaluk

A Thesis/Practicum submitted to the Faculty of Graduate Studies of The University of Manitoba in partial fulfillment of the requirements of the degree of Master of Science

ABSTRACT

A transient Finite Element seepage model has been developed which incorporates a confined aquifer, river, and groundwater within a lacustrine riverbank. The transient seepage modeling is performed over a period when the piezometric elevations of the unconfined aquifer are increasing and river levels are decreasing. The transient groundwater regime computed, within an idealized riverbank section, are similar to those observed through piezometer monitoring of a site on which the model is based. The seepage results are then incorporated into slope stability analysis and the influence of seasonal fluctuations in piezometric elevation of the aquifer and river are examined. Parallel slope stability analysis is also performed using assumed static groundwater elevations. The results of the slope stability modeling of the two different methods of determining piezometric elevations within a riverbank are compared and contrasted using a range of effective shear strength parameters from $c' = 3$ kPa, $\phi' = 8°$ to $c' = 5$ kPa, $\phi' = 17°$.

Safety factors computed using FEM generated porewater pressures are typically higher than those using assumed static groundwater levels for a given set of effective shear strength parameters. However, the reduction in safety factor over the modeling duration is greater when using FEM porewater pressures compared to assumed groundwater levels. The difference in computed safety factors is attributed to the transient model incorporating the combined destabilizing influence of the recharging unconfined aquifer and decreasing river levels (FE computed piezometric elevations) compared with only the destabilizing influence of decreased river level (assumed groundwater elevations) in the static analysis.

ACKNOWLEDGEMENTS

I would like to acknowledge the support of my advisor, Dr. James Graham who provided insight, advice, and encouragement. It was a lengthy process but he never gave up on me and for that I will be eternally grateful. He has helped in the way I write and think and aided me in developing a more critical way of thinking.

I would like to thank the other graduate students in the Civil and Geological Engineering Department. In particular, I wish to acknowledge James Blatz and David Farell for their modeling help earlier in my program. I would also like to thank Dr. S. Lee Barbour of the University of Saskatchewan for his help early on in my program, Dr. Rob Kenyon, and Charles Wright for their assistance.

Financial support was provided by an Industrial Orientated Research (IOR) grant from the Natural Sciences and Engineering Research Council of Canada and KGS Group Inc.

This study was made possible by the City of Winnipeg's Department of Waterways who partially funded earlier field experiments that measured groundwater potentials in two Winnipeg riverbanks.

Finally, I would like to express my sincere thanks and love to family for their encouragement, support, and interest. In particular, my wife Rachelle, parents Taras and Sandra, Rachelle's parents Ed and Mona, and brother Toby and his family.

TABLE OF CONTENTS

LIST OF FIGURES

Figure 4.2 River level boundary condition (function) assigned to riverbank between regulated summer river level and unregulated winter river level in the SEEP/W FE model

Figure 4.3 Bedrock aquifer boundary condition (function) assigned to base of glacial till in the SEEP/W FE model

Figure 4.4 Comparison of observed bedrock aquifer piezometric elevations with SEEP/W modelled bedrock piezometric elevations

Figure 4.5 Porewater dissipation function assigned to riverbank between regulated summer river level and unregulated winter river level

LIST OF TABLES

CHAPTER 1. INTRODUCTION

Slope instability along existing waterways within the City of Winnipeg has probably been occurring for approximately ten thousand years. Initially, the waterways (rivers, streams, and creeks) cut their paths through recently deposited Lake Agassiz sediments, creating channels, which are broadly similar to what exists today. Concerns over slope stability have arisen periodically in the last 100 years as increased development occurred adjacent to the waterways. When property loss occurs or bank remediation is necessary, the financial burden on private landowners can be significant. However it is minor compared to the financial impact faced by administrations owning public land. Given sufficient financial resources, current engineering practices have generally been able to stabilize critical failures along the banks of waterways. However, there is some indication that the designs may at times be either too conservative and costly, or else unconservative leading to failure. This suggests that the stability of Winnipeg riverbanks is still not fully understood.

In 1964 Mishtak undertook a survey of riverbanks within the City of Winnipeg as part of an extensive study for the Red River Floodway construction (Mishtak 1964). The survey was conducted to determine the slopes of natural stable riverbanks. This information was later used as part of the input for designing appropriate slopes for the Winnipeg Floodway system. Mishtak's survey found that of the 141 riverbanks surveyed, 135 were unstable or showed signs of movement. Figure 1.1 (Baracos and Graham 1981) shows the locations of active and inactive slide areas with the City of Winnipeg at that time. It is immediately clear that the locations of slides are concentrated along the outside bends of the waterways. Observations by the author indicate that the typical morphology of

slope instability along these bends consists of upstream sections failing first, followed by a progression of failures to the downstream limit of the bend. Currently, it appears that waterways are experiencing the later stages of this failure progression, with most of the active slopes being located at the downstream end of the outside bends.

Research into slope instability along the waterways within the limits of Winnipeg has largely been conducted by local geotechnical engineering companies in conjunction with the City of Winnipeg's Waterway Department and the University of Manitoba. Research at the university was formerly led by Professor A. Baracos (Baracos 1960, Baracos 1978, Baracos and Graham 1981) and is continued through Professor J. Graham (Graham 1979, Graham 1984, Graham 1986, Graham *et al.* 1987, Lew and Graham 1988). Research undertaken by their undergraduate and postgraduate students examined the strength characteristics of Lake Agassiz clays, possible reasons for slope instability, remediation techniques, and the influence of groundwater pressures on slope stability. One research topic that was not considered in detail was the influence of groundwater movements on slope stability. Modeling groundwater movements using finite element methods and then using the generated data in slope stability analysis will in principle allow calculation of the factor of safety. This was the approach adopted in the research described in this thesis document. It provides important insights into understanding the seasonal effects of groundwater fluctuation on the stability of slopes.

This chapter begins with a brief examination of the economic impacts of slope instability in Winnipeg. Next, a discussion of previous research into slope instability is presented along with a brief review of current slope engineering practices. This leads to an explanation of aspects of slope instability which require further study. The chapter ends with details of the objectives and organization of the thesis.

1.1 ECONOMIC AND INFRASTRUCTURE IMPACTS OF SLOPE INSTABILITY WITHIN THE CITY OF WINNIPEG

Of the approximately 230 km of waterway frontage in Winnipeg, approximately 105 km is owned by the City. Winnipeg's Waterways Department has estimated that the construction cost to repair existing unstable riverbank slopes would be approximately $83.5 million (1997) dollars. In addition the cost of lost property has been estimated at approximately $1 million dollars per annum (D. Kingerski, personal communication).

The first and most obvious result of a slope failure is loss of property. The loss of usable property (back from the crest of the slope) per site is typically small, usually only a few feet during a single instability event. However, if this trend is repeated over many years, then the accumulated loss of property can be significant. For example, geotechnical reports on file at the Department of Waterways indicate clearly that a section of riverbank upstream of St. Johns Ravenscourt School has lost approximately 9 m of bank in the last 30 years while a section of riverbank along Kildonan Park has lost an average of 5 m to 8 m in the last fifteen to twenty years. Further costs which are not factored into either construction or property loss are costs related to infrastructure. Infrastructure costs can be subdivided into immediate and delayed or deferred costs. Immediate costs are those associated with the replacement of items such as underground services. Delayed or deferred costs involve the realignment of roadways or underground services that are too close to an active failure zone along a waterway. The actual physical reconstruction of infrastructure may not occur until several years after the initial problem is recognized. This frequently leads to remediation being delayed until major movements make it absolutely necessary.

The City of Winnipeg does not currently have money specifically allocated for remediation of riverbank instability. However, individual departments like Waterworks and Waste, collectively have small annual budgets of $300,000 to $400,000 (R.M. Kenyon, personal communication) for improvement initiatives at such sites as sewer outfalls to ensure that excessive erosion will not lead to slope failure or damage to the outfall.

In recognition of the unstable nature of riverbank slopes in Winnipeg, the city created the City of Winnipeg Rivers and Streams Authority (currently known as Waterways Department) in 1951. The mandate of this department, under by-law 5888/92 proclaimed by the Province of Manitoba December 15, 1995, is to review and approve any and all construction, within specified setbacks from normal summer river level of watercourses within city limits, to ensure that any proposed construction will not adversely impact existing stability conditions. The specified setback from regulated (summer) river level for the major rivers, such as the Red and Assiniboine, is 350 feet while the setback is 250 feet for smaller waterways such as Bunns Creek and Sturgeon Creek.

In 1996, the total value of construction for which permits were requested was approximately $45 million. This dollar figure shows the importance and value of riverbank construction. It also indicates the need to identify stable slopes with confidence and to provide reliable, cost effective remediation for failing slopes.

1.2 SLOPE STABILITY RESEARCH

Research into slope stability along Winnipeg riverbanks began at the University of Manitoba in the early 1960's. The research concentrated on characterizing the strength properties of the Lake Agassiz clays (Van Cauwenberghe 1972, Freeman and Sutherland 1974, Baracos 1978, Baracos *et al.* 1980, Baracos and Graham 1981, Baracos *et al.* 1983, Graham *et al.* 1983, Graham 1986, Graham *et al.* 1987) and understanding the reasons for slope instability. Recent research has focused on the impact of groundwater on slope stability (Wright 1993, Hamilton 1995). The current research program has been aided by long term piezometric data recorded by KGS Group Inc. (KGS Group 1994) on behalf on the Winnipeg Waterways Department.

Research at the University of Manitoba also included triaxial shear strength testing, direct shear strength testing, and remediation techniques to improve slope stability. This research led to a good understanding of the upper and lower bounds of shear strength parameters as well as understanding the processes that create slope instability, (Crawford 1964, Graham et al. 1983, Graham and Shields 1985).

In addition to these studies of strength, the effects of piezometric elevations in the lacustrine clays, tills, and upper carbonate aquifer have also been studied at the University of Manitoba (Baracos 1978, Baracos and Graham 1981), by local water resources experts (Render 1970), and by the local consulting industry (KGS Group Inc. 1994). Simultaneous analysis of seepage and slope stability has not yet been studied.

In Winnipeg, the analysis of stable and unstable slopes for design purposes has become relatively routine. For stable slopes shear strength parameters are selected based on

research, commercial testing, and local experience. Groundwater levels are generally selected on a 'worst' case basis. Using these assumptions, commercially available software is used to determine the critical slip surfaces along which failure is likely to occur. Similar techniques are employed when performing back analysis of failing or failed slopes. Typically a worst case groundwater level is assumed. This is commonly taken to be a saturated slope with the groundwater level at or close to the slope surface. Combinations of shear strength parameters, c' and ϕ', are then selected to achieve a computed safety factor (FS) equal to unity. In all these analyses the groundwater is assumed to be controlled only by conditions in the clay and the river. The underlying limestone bedrock is assumed, in the analysis, to play no role in establishing porewater pressures in riverbanks. It is known however, that the limestone bedrock is an aquifer in which piezometric elevations (hydraulic potentials) vary seasonally. Considerable experience supported by field instrumentation indicate non-static groundwater conditions (KGS Group Inc. 1994).

The influence of these non-static conditions on riverbank stability is the principle focus of research described in this thesis document. The following hypothesis formed the principles on which the research program was designed.

HYPOTHESIS: Seasonal changes in groundwater potentials have significant impact on riverbank behaviour in Winnipeg and should be incorporated into slope stability analyses.

1.3 OBJECTIVES OF RESEARCH

Objectives of the research program include the following:

1. to use finite element seepage analysis to determine relationships between piezometric elevations in the Agassiz clays, piezometric elevations in the carbonate aquifer below the clay, river levels, and slope stability
2. to test the validity of the current practice of assuming static piezometric conditions when performing slope stability calculations
3. to investigate alternative slope remediation techniques.

The objectives require a thorough understanding of local hydrogeology, shear strength parameters, and current slope engineering practices in order that the effect of each variable can be considered separately. Once this has been presented in initial sections of the following document, new studies are reported of integrated calculations of seepage and stability in generalized, though typical, cross sections of Winnipeg riverbanks. The research has used these new insights in further studies of several sites whose hydrogeology had been investigated in detail through instrumented field research supported by the City of Winnipeg through a contract to KGS Group in 1992.

1.4 ORGANIZATION OF THESIS

Following this introduction, Chapter 2 presents a review of published literature on soil properties and behaviour, local hydrogeology, slope instability of Lake Agassiz clays in

the Winnipeg area, riverbank monitoring data, and current methods of slope stability analysis. This background permits the introduction of seepage analysis and its integration with slope stability analysis to form the basis of the research program outlined previously. Chapter 3 outlines the procedures and software used for the research program. Chapter 4 provides detailed information about the modeling procedures used with respect to shear strength parameters, slope stability analysis methods, seepage analysis, and confirmation of previous results. Chapter 5 presents detailed analysis procedures of the coupled seepage/slope stability model and presentation of the results. Chapter 6 presents a discussion of the analysis results in Chapter 5 and relates them to the hypothesis stated at the end of Section 1.2. Finally, Chapter 7 details the conclusions that can be drawn from the research and makes recommendations for further research.

CHAPTER 2. LITERATURE REVIEW

2.1 INTRODUCTION

The research program presented in this thesis will examine how seasonal variations in the piezometric elevation of a confined bedrock aquifer, the Upper Carbonate aquifer, affect riverbank stability in Winnipeg. In order to gain an insight into how riverbank stability is affected by the Upper Carbonate aquifer and to justify the work that has been undertaken it is necessary to present a review of literature already compiled on the subject.

This chapter begins by reviewing the properties of the stratigraphic units that overlie bedrock. A series of papers has been published discussing the composition and behaviour of these surficial deposits. These include Mishtak (1964), Teller (1976), Baracos (1977), Loh and Holt (1974), Baracos *et al.* (1983a,b), and Graham and Shields (1985). The discussion of soil properties is followed by a discussion of local hydrogeology. The hydrogeology of the Winnipeg area is complex and was discussed in detail by Render (1970).

The discussion of soil properties and local hydrogeology leads to a discussion of slope instability problems in Lake Agassiz clays, particularly within the City of Winnipeg. Riverbanks within Winnipeg have a long history of instability, with literature dating back to at least the 1950 flood. Slope stability of Winnipeg riverbanks has been examined by several authors including Baracos (1960), Freeman and Sutherland (1974), and Baracos and Graham (1981). Initial efforts to examine slope instability in Winnipeg used total

stress analysis that provided unrealistically high estimates of safety factor. The use of effective stress analysis and residual strength concept provided more satisfactory results.

Next, the results of two long-term riverbank monitoring programs are discussed. Both monitoring programs utilized piezometers and slope movement indicators to record groundwater levels and riverbank movements. Slope stability analysis methods are then briefly discussed. Fredlund and Krahn (1977) and Graham (1984) reviewed the most common methods of slope stability analysis in detail and therefore only a brief overview will be given later in the chapter. These topics lead to a justification and scope of the program that has been undertaken.

2.2 PROPERTIES OF WINNIPEG SOILS

The soils which constitute overburden (soils overlying bedrock) were deposited under varying conditions including recent depositional environments, late post-glacial, post-glacial, and interglacial. Three distinct layers or units are identifiable based on their geotechnical properties and depositional environments. From the ground surface downward, these layers are an upper complex zone, glaciolacustrine clays, and glacial tills consisting of basal till and some water-laid till. The geotechnical properties of each layer will be summarized in the following sections.

2.2.1 Upper Complex Zone

The upper layer of the soil profile in Winnipeg is characterized by clays, silts, and varying amounts of organic soils, man-made fills, sands, and alluvial silts. The upper complex zone is typically 3 m thick but can vary from less than 1 m to a maximum of 4.5 m (Baracos *et al.* 1983a). The laminated brown silty clays are intermediate to highly plastic, are smectitic, are highly fissured, and have a nuggety structure of less than 25 mm in size (Baracos *et al.* 1983b). The upper complex zone represents the late post-glacial and recent depositional environments (Baracos *et al.* 1983b). The silts occur in the form of interlayers that can vary from a few centimeters to one metre in thickness with a maximum thickness of about 3 m (Baracos *et al.* 1983a). They are believed to be in part aeolian deposits brought by wind from the Assiniboine delta deposits to the west. The silt interlayers can sometimes form perched water tables and are usually soft. The bottom of the silt usually indicates the lower boundary of the upper complex zone.

2.2.2 Glaciolacustrine Clays

The clays found in Winnipeg and the surrounding area were deposited during the most recent glacial impoundment of the Red River Valley, referred to as Lake Agassiz, between 11,700 and 7,500 years ago (Fenton *et al.* 1983). At its maximum size, Lake Agassiz was the largest lake in North America with its waters covering, at various times, a total area of about 950,000 km^2 although its maximum size at any one time was approximately 350,000 km^2 (Teller and Clatyon 1983). Deposition of the clays in the Red River valley lasted approximately 2,000 years (Teller, personal communication). The source materials for the lacustrine deposits are thought to be mainly Cretaceous age

shales to the south and west, with minor contributions from local carbonates, and Precambrian rock to the east (Quigley 1980, Baracos *et al.* 1983b). The average thickness of the plastic clay is 9 to 13 m with a range of thickness from 0 to 20 m.

The upper clays, 1.5 to 6 m thick, have been weathered and oxidized resulting in a brown to mottled brown color. The clay below this weathered, oxidized zone is classified as grey clay (also locally known as blue clay). It is believed that the brown and grey clays are part of a single depositional sequence, differing only in color due to the degree of oxidation downward from the ground surface (Baracos 1977, Graham *et al.* 1983). The upper brown clay is fissured or jointed, with some of the fissures extending to the underlying till surface. The structure of the brown clay has resulted from the combination of several processes. Successive drying-rewetting and freeze-thaw cycles (Graham and Au 1985, Graham and Shields 1985) have left the upper brown clay with a structure referred to locally as "nuggety". The deposit typically consists of alternating clay-rich and silt-rich layers which are frequently 2 mm thick (Freeman and Sutherland 1974, Baracos 1977). The lower levels of the deposit, the grey clay, are coarser and more massively bedded than the upper layers (Baracos *et al.* 1983b). The grey clay occasionally contains ice-rafted rock fragments that may approach boulder size, along with frequent uncemented silt inclusions/clasts (Teller 1976, Baracos 1977, Baracos *et al.* 1983b). The clay size fraction is often 70 to 80 % resulting in a USCS classification as highly plastic. However, some zones in the grey clay can approach intermediate plasticity due to an increase in occurrence of silt inclusions/clasts.

The mineralogy of Winnipeg soils has been studied by several authors including Quigley (1968), Loh and Holt (1974), Teller (1976), and Baracos (1977). Table 2.1 (Baracos 1977) shows the results of the most recent study. The table lists the occurrence of both

clay and non-clay minerals in order of decreasing amount found in each of the examined samples. Baracos cited differences in his results compared with previous work and attributes the differences to technique, interpretation, and nomenclature. The main clay minerals present are smectite, illite, and kaolinite while the main non-clay minerals are dolomite, calcite, and feldspar. Non-clay minerals show up very strongly in inclusions/clasts, light colored varves, and in the light colored swirls or veins that create a mottled or marbled appearance.

The strength properties of the clay deposits have been investigated by several authors including Mishtak (1964), Crawford (1964), Freeman and Sutherland (1974), Baracos (1978), and Baracos *et al.* (1983a,b). Mishtak (1964) was one of the first authors to report the results of detailed triaxial testing on lacustrine clays in Winnipeg. This work formed part of an extensive field investigation concerned with the construction of the Red River Floodway. During one phase of the field investigation that involved excavation of a full-scale test trench, block samples were obtained at 1.5 m intervals, beginning at a depth of 1.5 m and continuing to a depth of 13.7 m. Specimens were obtained from the block samples and tested by the Prairie Farm Rehabilitation Administration (PFRA). Mishtak reported primarily the results of tests performed on specimens from the 9.1 m depth. He determined that the effective shear strength parameters for clay were in the order of $c' = 45$ kPa, $\phi' = 12°$ for consolidated undrained tests and $c' = 31$ kPa, $\phi' = 16.5°$ for intact specimens in drained tests. Mishtak also noted curvature of the shear strength envelope at low confining pressures.

Crawford (1964) performed similar triaxial tests using a block sample from the same location and depth as reported by Mishtak (1964). Crawford's consolidated undrained tests gave effective stress values of $c' = 59$ kPa, $\phi' = 9°$. These results were confirmed to

a reasonable degree by the results of consolidated drained tests with the lateral stress decreasing to failure. Crawford also performed tests to examine the effect of softening on shear strength. Specimens were immersed in de-aired water prior to testing. As suggested by Crawford, the test results indicated a considerable reduction in shear strength at low confining stresses. Only two specimens were tested in this manner as the supply of clay from the block sample had been exhausted. As will be discussed later, this apparent reduction in strength due to softening at low confining stresses may be more a function of the clay structure.

Freeman and Sutherland (1974) reported on the results of a detailed triaxial testing program to investigate shear strength anisotropy of Winnipeg clays. The testing program consisted of performing drained triaxial tests and undrained triaxial tests with pore-water pressure (pwp) measurement on specimens orientated at various angles with respect to the in situ vertical axis of the samples. The results indicated that the shear strength across the layers was greater than the shear strength along the layers, although scatter made interpretation of results from the upper brown clay more difficult (Figure 2.1). The specimens were tested with confining pressures in the working stress range between 0 to 200 kPa. The range of strengths across the layers for the grey clay was c' = 6 to 11 kPa, ϕ' = 18 to 26° while the brown clay had values of c' = 42 kPa, ϕ' = 19°. The range of strengths along the layers for the grey clay was c' = 2 to 5 kPa, ϕ' = 14 to 26° while the shear strength of the brown clay had reduced significantly to c' = 3 kPa, ϕ' = 14°. Meanwhile Rivard and Lu (1978) noted that fissures have a major influence on the strengths of clays.

Loh and Holt (1974) performed a series of undrained triaxial tests on block samples of Winnipeg clay obtained from a depth of about 4.9 m. Specimen preparation was similar to that performed by Freeman and Sutherland (1974) with samples being trimmed to produce specimens with laminations at various orientations to the horizontal between 0 and 90° (typically every 15°). The block sample was classified as laminated brown clay and contained silt inclusions, occasional gypsum intrusions, and small pebbles. Specimens were tested in both 'undisturbed' and remoulded states. The remoulded specimens were trimmed at the same angles as the 'undisturbed' samples but since the remoulded block lacked an intact structure the reference for trimming specimens was the base of the remoulded block. The test results, shown in Figure 2.2 (Loh and Holt 1974), indicated that the 'undisturbed' specimens displayed anisotropic strength behaviour while the remoulded specimens had isotropic strength properties. The lowest shear strengths occurred from specimens trimmed with bedding planes at approximately 45° to the horizontal, with the highest strengths occurring for specimens with bedding planes at 82° to the horizontal. Specimens with bedding planes between 0 and approximately 45° had intermediate undrained shear strengths. The results of the testing program performed by Loh and Holt (1974) indicate anisotropic strength behaviour more clearly than that reported by Freeman and Sutherland (1974).

One of the most recent detailed testing programs investigating the shear strength of Winnipeg clays was undertaken by Baracos *et al.* (1980). A series of consolidated undrained triaxial tests with pore-water pressure measurement was performed on Winnipeg grey clay samples at various stress levels to investigate stress characteristics for different field applications. The results, as shown in Figure 2.3 (Baracos *et al.* 1980), indicate that the effective shear strength parameters depend on stress level and can be

divided into three linear groupings as indicated in Table 2.2 (after Baracos *et al.* 1980). Further evidence for at least the first two linear groupings can be seen in the results presented by Mishtak (1964), Crawford (1964), and Freeman and Sutherland (1974). In all three instances, the failure envelopes show this behaviour of low c′ and high ϕ' at low effective stresses and higher c′, lower ϕ' values at intermediate effective stress levels. The explanation for this shear strength behaviour can be summarized as follows:

- at low effective stresses the clay shear strength properties are dominated by fissuring of the clay, in particular by low (or zero) tensile stresses.
- at intermediate stresses, the shear strength properties are dominated by overconsolidated behaviour and,
- at high effective stresses, the shear strength properties are dominated by normally consolidated behaviour.

Although peak shear strength parameters are significant in understanding the behaviour of Winnipeg clays, residual shear strength parameters are equally important. Residual shear strength parameters are necessary for establishing effective slope remediation works once an unstable slope has been identified or analysis of a pre-existing failure. The range of residual shear strength parameters for Winnipeg clays is significant. Based on direct shear test results, Freeman and Sutherland (1974), Baracos (1978), and Baracos *et al.* (1980) reported ranges of residual shear strengths contained in Table 2.3.

The most common range of residual shear strength parameters for Winnipeg clays appear to be $c_r' = 3\text{-}5$ kPa and $\phi_r' = 8\text{-}13°$ (Graham 1986). Typically, the direct shear test involves obtaining residual (large strain) strength of a specimen under a normal load. Once a residual strength in achieved the normal load is increased and the specimen is

again sheared until a new residual strength is achieved. This process continues until the residual strength envelope of the soil has been defined within the desired stress range. Baracos *et al.* (1980) also performed direct shear tests by beginning the tests at high normal stresses and then decreasing the normal stress after each corresponding residual strength was obtained. The results indicated that although ϕ_r' was similar to the increasing normal load testing method, the c_r' values were much lower and tended to approach $c_r' = 0$ kPa. Also, the residual strengths were reached after only small displacements. Baracos *et al.* (1980) concluded that standard direct shear test results may overestimate the stability of previously failed slopes.

The behaviour and structure of Winnipeg clays has been significantly altered due to geologic processes. These processes and their effects have been discussed by Baracos *et al.* (1980) and Graham and Shields (1985). Two factors have significantly influenced the properties of Winnipeg clays. The first is the climate in which the annual temperature may range from -35 to +35 °C. Drying-rewetting and freeze-thaw cycles have led to a heavily fissured, brown clay to depths of 5-9 m (Graham and Au 1985). The effects of the physical weathering are evident only in the upper brown clays. The second factor is the influence of the groundwater. Existing piezometric levels in the Upper Carbonate aquifer are significantly lower than they were near the end of glaciation (Teller 1976, Graham and Shields 1985) and considerably lower than they were 100 years ago (Render 1970). Upward percolation resulting from high piezometric levels in the Upper Carbonate aquifer in the past has resulted in the introduction and deposition of sulphates and carbonates into the clays (Teller 1976, Baracos *et al.* 1980, and Graham and Shields 1985). These salts would not have been present at the time of deposition since post-glacial Lake Agassiz was a fresh water (or at worst brackish) lake (Teller 1976,

Quigley 1980). Evidence of the deposition of the salts is present both directly and indirectly. Direct evidence is in the form of fibrous white inclusions or streaks that occur particularly in the near surface deposits of brown clay. These deposits were typically formed in the fissured structure of the brown clays. The salts were brought near the surface by upward flow from the Upper Carbonate aquifer as well as gradients created at the freezing front in the brown clays (Graham and Shields 1985). Deposition was probably due to high summer evaporation rates that lowered the groundwater in the clays (Graham and Shields 1985). The indirect evidence of the deposition of these salts has been presented by Graham *et al.* (1983). The strength behaviour and pore-water pressure response of Winnipeg clays suggest that it is cemented. Electron microscopy, however, is not able to view the interparticle contacts where these bonds would form. Therefore, although evidence suggests cementation, some uncertainty still remains.

The geotechnical properties of Winnipeg clays are summarized in Table 2.4 (Baracos *et al.* 1983a).

2.2.3 Glacial Tills

It is believed that the till units which overlie the bedrock in the Winnipeg area were deposited between 11,000 and 24,000 years ago during a complex series of retreats and readvancements of the continental ice sheet during Late Wisconsinan glaciation (Teller and Fenton 1980). The till thicknesses in the Winnipeg area range from 0 to 10 m, with an average of 3-6 m (Baracos *et al.* 1983b). The till units have a significant range of compositions and stiffnesses varying from soft clayey tills to very dense cemented tills. Five separate till units have been identified coinciding with glacial retreat and

readvancement (Teller and Fenton 1980). Typically, the lower units are dense to very dense, cemented, well graded basal tills with ranges in particle size from clay to boulder size. Underlying the glaciolacustrine clays in some areas, are soft clayey water-laid tills commonly having a similar particle size range as the lower tills. The most dominant particle sizes in the tills are silt sizes followed by sand and finally clay sizes. The dense basal tills have high unconfined compressive strengths ranging from 3,350 to 3,590 kPa (Baracos *et al.* 1983a) and high residual angle of shearing resistance of about 31° (Baracos 1978). The soft clayey tills often have unconfined compressive strengths under 50 kPa (Baracos 1960). A summary of the geotechnical properties of Winnipeg tills is presented in Table 2.5 (Baracos *et al.* 1983b).

A separate geologic unit was also deposited during the same geologic period as the tills. This unit is comprised of glaciofluvial sands and gravels which can occur below, within, or above the till units, and may in some cases exist without the presence of till. These variably distributed sand and gravel deposits are of limited extent and typically do not exceed 1 m in thickness. Their perched water tables have had a major impact on construction projects in Winnipeg, including braced and tieback excavation systems and soft-ground tunnelling. Figure 2.4 shows a photograph of a glaciofluvial deposit overlying bedrock.

2.3 WINNIPEG HYDROGEOLOGY

The City of Winnipeg is underlain by an extensive confined aquifer, known as the Upper Carbonate aquifer, which occurs in the top 15 to 30 m of the Paleozoic carbonate rocks

(Render 1970). The Upper Carbonate aquifer is partially confined above by glacial tills and Lake Agassiz clays and below by slightly pervious underlying carbonate rock.

Winnipeg hydrogeology, as it relates to slope stability, can be divided into two distinct units. The first unit is the surficial deposits (glacial tills, clays) and the second is the Upper Carbonate aquifer. The hydrogeology of these units will now be discussed.

2.3.1 Surficial deposits

As discussed in Section 2.2, the surficial deposits consist of glacial tills, glaciofluvial sands and gravels, and Lake Agassiz clay deposits. Within this unit, two minor water-bearing zones can be identified. The first is located in the upper 4.5 m of the Lake Agassiz deposits in the form of irregular sandy and silty deposits. The second occurs adjacent to the bedrock in the form of glaciofluvial sands and gravels. In a few locations large diameter wells have been installed to provide domestic water supply from these two minor water-bearing zones (Render 1970).

It will be remembered that overlying the bedrock are glacial tills and glaciofluvial sands and gravels. The tills may consist of dense to very dense cemented basal tills, overlain by soft or loose, wet uncemented water-laid tills. At a given location some, none, or all of these deposits may overlie the bedrock. Render (Goff, see Baracos *et al.* 1983a) reports that the average hydraulic conductivity of the tills east of Winnipeg is $3x10^{-8}$m/s and $1.5x10^{-7}$m/s slightly north of Winnipeg (Day, see Baracos *et al.* 1983a). Render (1970)

also observed hairline joints in the cemented tills and these probably account for most of its permeability.

The Lake Agassiz deposits, which usually overlie the till, consist of an upper complex zone which overlies highly plastic clays. The lower highly plastic clay zone has an intergranular hydraulic conductivity of 10^{-11} to 10^{-13} m/s and horizontal permeabilities that are about twice the vertical values (Baracos and Mishtak after Render 1970). More recent laboratory testing has measured values of hydraulic conductivity for the glaciolacustrine clays at around 10^{-10} m/s (Yuen 1995). Hairline fractures were observed in the lower clay unit during the Floodway excavation and may form a secondary permeability system (Render 1970). The Upper complex zone has variable permeabilities due to the discontinuous nature of its soils. Typically though, the permeability will be greater than that found in the lower high plastic clay zones. The most important hydrogeologic aspects of the lower Agassiz unit are its restriction of recharge to the Upper Carbonate aquifer (Render 1970).

2.3.2 Upper Carbonate Aquifer

The bedrock surface is quite irregular as a result of pre-glacial weathering, glacial, and interglacial modification (Teller 1976, Baracos *et al.* 1983b). The top 0.5 to 1.0 m of the bedrock is generally highly disturbed (Baracos *et al.* 1983b) with depressions and variable size fractures and openings. These disturbed zones may be infilled with sands, gravels, rock fragments, and even clayey or silty material. Horizontal and vertical openings may be present several meters below the bedrock surface as shown in Figures 2.5 and 2.6, which were photographed by the author at a major construction site in

downtown Winnipeg. In some instances the limestone bedrock has been dissolved leaving behind a channel through which groundwater can flow (Figure 2.7).

The upper 7.5 m of the bedrock is the major zone of permeability and is therefore the zone of most active flow (Render 1970). Since the permeability is the highest in the upper zone of the bedrock, the slope of the bedrock surface has a controlling influence on local and regional groundwater movement. The transmissivity of the Upper Carbonate aquifer ranges from under 24.8 to 2480 m^3/m/day (Render 1970).

The Upper Carbonate aquifer is the most important part of the extensive zone of groundwater movement within the upper bedrock in the Red River basin. Groundwater movement is predominantly lateral in the upper portion of the bedrock. In the Winnipeg region it consists of three major recharge directions:

- from the east
- from the northwest
- from the southwest

These zones of recharge are shown on Figure 2.8 (Render 1970). Recharge for the eastern zone occurs in the glacial sand and gravel uplands east of Winnipeg and from the Bird's Hill aquifer; recharge for the northwestern zone occurs by infiltration through areas of thin glacial till northwest of Winnipeg; and recharge for the southwestern zone occurs by infiltration through a thin veneer of glacial till and fluvial deposits on the western side of the basin (Render 1970). In addition to the overall lateral flow systems described, there are local vertical flow regimes that move water stored in the surficial deposits down into the Upper Carbonate aquifer. However due to the low permeability of

the Lake Agassiz clays, this contribution is negligible, probably less than one percent of the annual pumpage from the aquifer during the 1960's and 1970's (Render 1970).

An analogue model study reported by Render (Hobson *et al.*, see Render 1970) indicated that the river is at least partially connected to the Upper Carbonate aquifer. In central Winnipeg, the potential difference between the river and Upper Carbonate aquifer is greatest during the annual spring flood events and during the mid to late summer months when commercial and industrial pumping demand is the greatest. The quantitative contribution of this flow system appears to be significant.

2.3.4 Groundwater Usage

The Upper Carbonate aquifer has been an important source of water for Winnipeg since the late 1800's. The Upper Carbonate aquifer supplied all of Winnipeg's demand for water until the Winnipeg aqueduct was completed in 1919. In 1918, groundwater withdrawal reached a maximum value of 1.6×10^{10} l/yr and then sharply decreased with the completion of the Winnipeg aqueduct as shown in Figure 2.9 (Render 1970). Pumping rates continued to rise after completion of the aqueduct as commercial and industrial development increased. In the 1960's and early 1970's the Upper Carbonate aquifer supplied approximately 17% of the annual demand for water (Render 1970).

The most recent trend in groundwater usage has been that of non-consumptive nature (KGS Group 1994, Render, 1997, personal communication). Groundwater that is pumped from the Upper Carbonate aquifer for such things as heating or air conditioning is returned after it has been used. Also, some major industrial users have closed down,

further decreasing the annual demand for groundwater, but the total annual pumping is still significant.

The annual demand for groundwater coupled with recharge of the aquifer creates cycles of drawdown and regain in the piezometric elevation of the bedrock aquifer. This is illustrated in a series of representative hydrographs (Figures 2.10a to 2.10e, Manitoba Natural Resources, Water Resources Branch 1998). The peak piezometric elevations represent the effects of recharge of the aquifer during the annual spring thaw. Shortly after completion of the spring thaw, commercial and industrial usage increases resulting in drawdown of the aquifer. Drawdown of the aquifer continues until approximately late August or early September when groundwater demand decreases and the aquifer begins to recharge into November and December. At this point the aquifer remains relatively constant until the next annual spring thaw. The location of bedrock aquifer monitoring wells in Winnipeg is shown in Figure 2.11 (Manitoba Natural Resources, Water Resources Branch 1998)

2.3.5 Construction Problems

The most common groundwater related construction problem in Winnipeg is excessive discharge into deep excavations. Several construction projects adversely affected by groundwater discharges are discussed in detail by Render (1970). Excessive groundwater discharges may result in minor design revisions such as driven piles replacing cast-in-place piles or major revisions such as the use of a grout curtain or pumping wells. A less common occurrence, but one which has had negative impact on several projects, is hydraulic fracturing and failure of the base of the excavation due to

high pore-water pressures in the underlying till or bedrock. This process is significantly more dangerous and can cause serious damage to earth retaining structures. This event, on a much smaller scale, is shown in Figures 2.12(a) through 2.12(d). The photographs were taken by the author during a riverbank remediation project. The hydraulic fracturing of the grey clay is evidence of the high piezometric pressures in the Upper Carbonate aquifer and their potential to influence the stability of riverbanks in Winnipeg.

2.4 SLOPE STABILITY PROBLEMS IN LAKE AGASSIZ CLAYS

Difficulties in assessing riverbank stability in Winnipeg date back to the early 1950's. Baracos (1960) investigated a series of riverbank failures after the 1950 flood and found that there was a poor correlation between theoretical and actual safety factor values. Safety factors greater than unity were indicated for riverbanks that showed signs of failure. Total stress analysis of riverbank failures suggested that the average undrained shear strength mobilized was between 19 and 29 kPa, much lower than values measured in laboratory tests on intact specimens. These reduced values of undrained shear strength were used successfully in the design of secondary dikes, along restricted zones of the riverbank, using safety factor values as low as 1.2.

By considering the effects of tension cracks, lower observed strengths along the clay-till contact, lower observed strengths at the toe, and lower strengths along old failure surfaces, Baracos (1960) determined that the mobilized shear strengths were approximately 30 to 50% of the undrained shear strengths measured in the laboratory. It was also noted that many slides included a large component of horizontal displacement

and that following initial movement, some riverbanks continued to fail in a retrogressive manner behind the original failure surface. Baracos concluded that stability analysis in terms of effective stress would prove more satisfactory for predicting when failures occur and the failure geometry.

Peterson *et al.* (1960) examined failures that occurred in the dikes of the Seven Sisters Falls Hydroelectric project, located east of Winnipeg. The dikes were constructed of medium to highly plastic clay and founded on highly plastic lacustrine clay of the same origin as the clays found in Winnipeg. In a seven year period, after construction of the dikes was completed in 1949, 13 failures had occurred in a 5.6 km length even though the dikes have an estimated safety factor of at least 1.5. The failures were all similar in nature and first showed up as cracks between the dike centerline and the edge of the crest on the reservoir side. Shear strength tests were performed on the dike fill material and the high plastic foundation clay. The undrained shear strength of the foundation clay ranged from c_u = 19 to 53 kPa while representative effective shear strength parameters were determined to be c' = 10.3 kPa and ϕ' = 19°, again from intact specimens (Rivard and Lu 1978).

Total and effective stress stability analysis were performed on the cross section shown in Figure 2.13 (Peterson *et al.* 1960). The calculated safety factor value for total stress analysis was 1.31 and 1.40 for effective stress analysis. The remaining 12 failure areas that were analyzed used total stress and were found to have FS values ranging from 0.9 to 2.1. This clearly represents an inadequacy in modeling since at failure, all these sites had FS = 1.0 by definition.

In an effort to re-evaluate the shear strength parameters and stability of the Seven Sisters dikes, a series of large diameter thin-walled tubes samples were obtained from boreholes near the slide area shown in Figure 2.13. Intact specimens from the sample tubes were tested at Harvard University under the direction of Professor Casagrande. The effective shear strength parameters determined from these studies were c' = 13.8 kPa and ϕ' = 14.5°. These newly determined shear strength parameters were used in additional analyses of the slide area in Figure 2.13. However, the results were less than satisfactory, with a safety factor of 1.33 being obtained.

Peterson *et al.* (1960) concluded that the stability of clay dikes on lightly overconsolidated highly plastic foundation was overestimated by both total and effective stress method of analysis. They also commented that shear strengths obtained in the laboratory must be modified so that calculated safety factor values would be reduced.

Prior to construction of the Red River Floodway, extensive geotechnical and hydrogeologic investigations were conducted. As part of the geotechnical investigation a full-scale test trench was excavated, along the floodway route, to examine the stability of clay slopes after rapid excavation and drawdown (Mishtak 1964). Excavation of the test trench began in mid August 1961, and was completed to a depth of 13.7 m during the last week of October. The north slope was designed at a slope of 1H:1V and the south slope was designed at a slope of 4H:1V. Previous borehole drilling had allowed samples to be retrieved and tested in the laboratory in undrained shear. The average undrained shear strength was determined to be c_u = 52 kPa which, based on total stress analysis, suggested that the test trench would have to be approximately 14 m deep to induce failure along the 1H:1V slope. Both slopes had been extensively instrumented to record

groundwater levels and slope movements as the excavation proceeded towards inducing a slope failure. During excavation of the test trench, large block samples were retrieved at intervals of 1.5 m. Laboratory triaxial testing was performed by PFRA and consisted of undrained, consolidated undrained (with pore pressure measurement), and drained triaxial tests as discussed in Section 2.2.2. Additional testing, on soil retrieved from the test trench, was performed by Crawford (1964), Freeman and Sutherland (1974), and Baracos (1977).

Initial movement of the 1H:1V slope was first observed from slope inclinometer and alignment hub monitoring data at the west end of the trench when the average depth of the test trench was 7.6 m. However, at this stage there were still no visible signs of movement such as tension cracking. The first definite visible movements occurred when the average depth of the test trench was 10.4 m and were recorded by slope inclinometer movement at a depth of 14.6 m (the approximate depth of the clay-till interface). Upon completion of the test trench excavation, it was allowed to fill with water. Complete failure of the 1H:1V slope occurred during the fall of 1962 when water was pumped out of the trench simulating a rapid drawdown scenario.

Total and effective stress analyses were performed on two sections of the 1H:1V slope. Total stress analysis indicated that the undrained shear strength required for stability was 30 kPa, significantly lower than the undrained shear indicated by triaxial testing on intact specimens. Effective stress analysis indicated safety factor values of 1.28 to 2.08, depending on the assumed failure surface and shear strength assumptions.

At the invitation of the City of Winnipeg's Rivers and Streams Authority No. 1, Professor H.B. Sutherland (1966) examined the problem of riverbank instability in Winnipeg.

Sutherland's assessment included inspection of riverbanks, review of consultant's reports applying for construction permission along riverbanks, and review of the results of the Red River Floodway test trench excavation. Based on this review, Sutherland concluded that conventional methods of slope stability using laboratory determined shear strengths should not be used to analyze riverbanks in Winnipeg. He recommended that total stress analysis be adopted provided that c_u = 24 kPa is used and a safety factor of 1.5 is obtained in the analysis. He further recommended that the toe of riverbanks should be protected against erosion, adequate drainage of slopes must be provided, and no fill should be placed on slopes unless justified by analysis.

The first long-term study of the influence of a transient or dynamic groundwater regime on slope stability of riverbanks was reported by Baracos (1978) as discussed in Section 2.5. Groundwater movement within the studied riverbank sites tended to be in a downward direction with evidence suggesting that this pattern was caused by local pumping wells installed in the bedrock aquifer. Slope movement data collected during the study indicated that riverbank movement was related to seasonal events and aided in identifying or 'fitting' slip surfaces for stability analysis.

As part of this long-term study, slope stability analyses were performed based on groundwater observations, observed movement data, and residual shear strength parameters. The residual shear strength parameters were obtained from a series of direct shear tests as detailed by Baracos (1978). The residual shear strength parameters used varied from c_r' = 0 to 1.4 kPa and ϕ_r' = 8 to 12.7°. The results of the stability analyses indicated that the selected residual strength parameters were found to satisfy the seasonal changes in stability. Also, 'fitted' slip surfaces were used in the analyses that approximately matched the slide surfaces interpreted from slope indicator

movements. The 'fitted' slip surfaces were found not to coincide with critical slip surfaces (lowest safety factors) obtained in the stability analyses. If these critical slip surfaces had been used to back calculate required shear strength parameters, higher values than those used in the analyses, would have resulted.

Rivard and Lu (1978) and Lefebvre (1981) reported on the use of 'fully softened' or normally consolidated shear strengths, for first time slides in fissured plastic clays, by reviewing a series of case studies from western Canada and eastern Canada, respectively. In particular, Rivard and Lu re-examined the Seven Sisters dike failures discussed at the beginning of this section. Using normally consolidated shear strengths of c'= 0 kPa and ϕ' = 16° (Peterson *et al.* after Rivard and Lu 1978 and Peterson *et al.* 1960), Rivard and Lu were able to obtain safety factors approximately equal to unity for the failure condition. In comparison, safety factors generated using representative effective shear strength parameters determined at Harvard University (Peterson *et al.* 1960) gave safety factors equal to approximately 1.7.

More recent information (Graham 1986) has determined ranges of shear strengths applicable for slope stability analysis of Winnipeg riverbanks. Successful analyses have been performed in failed slopes with c_r' = 3-5 kPa and ϕ_r' = 8-12° and for first time slides using fully softened strengths of c' = 5 kPa and ϕ' = 15-17°. Currently, these ranges of strengths are used by the local consulting industry in Winnipeg. The approach is based on the understanding that straining at propagating fissures can modify an originally overconsolidated or cemented clay and produce an effective microstructure similar to that of normally consolidated clay (Rivard and Lu 1978).

2.5 WINNIPEG RIVERBANK MONITORING

Long term monitoring of riverbanks or slopes for both groundwater behaviour and slope movement is beyond the scope of most geotechnical investigations. While topographic, stratigraphic, and soil property data are collected in most routine geotechnical investigations, only very large geotechnical projects or research programs have the resources needed for a detailed slope monitoring program.

Within metropolitan Winnipeg, only two long-term riverbank monitoring projects have been undertaken in the last thirty years. The first (Baracos 1978) involved detailed monitoring of piezometric elevations and slope movement at two sites. The second (KGS Group 1994) also consisted of detailed monitoring of piezometric elevations and slope movement at two riverbank sites. The approximate locations of these projects are shown in Figure 2.14.

The first research program (Baracos 1978) commenced in early 1969 and continued for approximately 3.5 years. Two locations along the Red River were monitored. The first site was in St. Vital near the junction of St. Mary's Road and St. Anne's Road. The second site consisted of two monitoring locations approximately 190 m apart in St. Boniface south of the Provencher Bridge along Tache Avenue. Both sites were located on the east side of the Red River on outside bends of broad meanders and had shown signs of instability dating back to at least the 1950 flood (Baracos 1978).

The second research program (KGS Group 1994) began in March 1992 and terminated at the end of August 1993. Two sites were again selected. One site was the same site in

St. Vital used by Baracos, while the other was at the south end of St. Mary's Road, near the Perimeter Highway, on a section of the Red River which was actively failing.

2.5.1 Piezometric Data

Piezometric data obtained from the sites monitored by Baracos (1978) and KGS Group (1994) indicate that there is an overall downward flow of groundwater from the upper clays toward the underlying glacial till and bedrock aquifer as shown in Figure 2.15 (KGS Group 1994). These observations by themselves indicate that current hydrostatic groundwater assumptions for the purposes of slope stability calculations are unrealistic and result in safety factors that are too low. (Downward flow into the slope increases stability).

The downward flow of groundwater from the upper clays into the bedrock aquifer was investigated by Baracos (1978). Records of bedrock pumping wells adjacent to the monitoring sites were examined. In one instance, a bedrock pumping well record was compared with a piezometric record for the silt till zone. The piezometric record paralleled the pumping well record indicating the influence of industrial and commercial use of groundwater. Based on this examination and comparison of records Baracos concluded that groundwater usage from the bedrock aquifer was responsible for the direction of flow of the local groundwater regime. As indicated in Section 2.2.2 groundwater flow in the past had a strong upward component resulting in deposition of sulphates in the upper brown clays. The result of groundwater withdrawal, at least in part, is responsible for a reversal in the direction of groundwater flow.

The South Perimeter site monitored by KGS Group had results that differed from the other sites. Based upon the field data obtained, Figure 2.16 shows that upward flow from the bedrock aquifer appears to be a much more significant component of the local flow regime (KGS Group 1994). The groundwater flow at the crest and along the slope of the riverbank is still in a downward direction. However, upward flow from the bedrock aquifer is significant in the region of the riverbank toe. Unfortunately, only one monitoring well was installed to record piezometric elevations in the bedrock aquifer. As a minimum two monitoring wells (ideally three monitoring wells) would have provided valuable data regarding the gradient and flow direction in the aquifer.

The distribution of equipotentials in the glacial tills and bedrock aquifer (Figures 2.15 and 2.16) requires further comment. Based upon the tangent law of refraction (Fetter 1994), flow lines will refract when entering a porous medium of different hydraulic conductivity than the porous medium they are exiting. The magnitude of this refraction is given by:

$$\frac{K_1}{K_2} = \frac{\tan\theta_1}{\tan\theta_2} \qquad (2.1)$$

where K_1, K_2 and θ_1, θ_2 are the hydraulic conductivities and flow line angles (with respect to the vertical) of the respective porous media. Figure 2.17 (Fetter 1994) shows the path of a flow line crossing a conductivity boundary from a region of low hydraulic conductivity to a region of high hydraulic conductivity. Based upon the tangent law of refraction and given the published ranges of hydraulic conductivities from both soil types, the flow lines entering the glacial till from the overlying clay would refract considerably and become close to horizontal.

2.5.2 Riverbank Movement Data

Slope movement data were gathered by both Baracos (1978) and KGS Group (1994) at their respective sites for the duration of each of the long term monitoring projects. The slope movement indicators were monitored at regular intervals that depended on the time of year. For instance, KGS Group generally monitored slope indicators at their sites four to five times a year coinciding with river flows. Slope indicators were monitored prior to annual spring high river levels, after river levels had decreased to summer elevations, before annual lowering of Red River in mid fall, after river levels had decreased to their winter levels, and monitored during mid winter. The monitoring schedule allowed rates of slope movement to be correlated primarily with changes in levels of the Red River.

Cumulative movement versus time plots are presented in Figures 2.18 (Baracos 1978) and Figure 2.19 (KGS Group 1994). The patterns of movements are similar in both plots, particularly for riverbanks experiencing minor movements. They can be correlated to annual seasonal events that occur in Winnipeg as follows:

- Virtually no movements occur during spring high water and summer regulated river levels. Piezometric elevations in the bedrock aquifer are at their highest level during the annual spring thaw in response to melt-water and high river levels. The high river levels create a stabilizing effect against the piezometric elevations in the bedrock aquifer. At about the same time as the river levels begin to decrease, industrial and commercial groundwater demand increase and the piezometric elevations in the bedrock aquifer decrease in response to this demand.

- Rates of movement increase dramatically with the lowering of river levels during mid fall. The lowering of the Red River to an unregulated level is a destablizing event that lowers the safety factor of riverbanks. However, a further destabilizing influence is the increase in piezometric elevation of the bedrock aquifer due to reduced industrial and commercial demand. The increase in piezometric elevation of the bedrock aquifer increases the pore-water pressures at the clay-till interface decreasing the effective stresses and reducing the maximum available shear strength in this region.

- Rates of movement decrease during winter until spring high river levels occur. Several processes may occur to reduce the rates of movement during the winter months. Of these, a reduction in groundwater levels in the clays and increased resistance to movement due to frost penetration, are the most obvious. Piezometric data collected by KGS Group (1994) have shown that the water table surface elevation in the clay decreases slightly during the fall-winter period due to decreased infiltration on a regional basis. This small decrease in water table elevation increases the effective stresses in the upper clays and therefore increases the available shear strength in this region.

The depth of frozen soil in Winnipeg can reach 2 to 3 meters below the ground surface depending on snow cover and winter temperatures. Frozen soil in the upper regions of a riverbank increase the stiffness of the soil and increase its strength. Although quantitative data is unavailable, a small increase in strength is likely sufficient to contribute to the decreased rates of movement observed in Winnipeg during the winter months.

Baracos (1978) pointed out an additional scenario of riverbank movement associated with snowmelt run-off and low winter river levels. This is indicated on Figure 2.18, line m-n. Riverbank movements may occur as the slope thaws and softens due to spring run-off while the river remains at a low winter level. This observation may be extended to include early spring rainfall events coupled with low winter river levels. The effective stresses in the slope will decrease with increasing groundwater levels while the stabilizing benefit of higher river levels is not yet present.

Two critical time periods of riverbank movement are therefore defined by the observed movement of riverbanks obtained from instrumentation, one in the fall and the second in the spring. The major critical time period for riverbank movements generally occurs during the mid fall period when the Red River is lowered to a regulated winter river level. The reduction in river levels has a destabilizing effect but may be further enhanced by increased piezometric elevations in the bedrock aquifer.

2.6 METHODS OF SLOPE STABILITY ANALYSIS

Geotechnical engineers commonly use limit equilibrium methods of analyses when examining slope stability problems (Graham 1984). The method of slices is the most common limit equilibrium slope stability analysis technique because of its ability to handle complex geometries and variable soil and groundwater conditions. The most common methods of slices are the following:

- Ordinary or Fellenius
- Simplified Bishop's

- Janbu's simplified
- Janbu's rigorous
- Spencer's
- Morgenstern-Price

The first four methods outlined above can be considered simplified methods since they only satisfy moment or force equilibrium while the last two are rigorous methods, satisfying both moment and force equilibrium (Fredlund *et al.* 1992). A brief discussion will be presented here on the methods of slices. Fredlund and Krahn (1977) and Graham (1984) have presented detailed discussions on the methods of slices and comparisons of the slope stability methods. They show that all commonly used methods are statically indeterminate and that assumptions must be made to permit solutions to be obtained.

The above methods differ to some extent in the statics used to derive the safety factor equation, but more significantly in assumptions used to make the problem determinate. Figure 2.20 (Graham 1984) shows the forces acting upon a typical slice. The first simplifying assumption is to make the slices narrow enough so that the normal force, P, acts at the center of the base of each slice eliminating one unknown. The second simplifying assumption is to assume a value or function for the interslice force inclinations. This set of assumptions overspecify the problem allowing two safety factors to be generated, one safety factor based on moment equilibrium and the other based on force equilibrium. Typically, a solution is taken to have been obtained when the safety factors of force and moment equilibrium are equal.

2.6.1 Common Methods of Slope Stability Analysis

Two equations form the basis of the modern methods of slices, one for moment equilibrium and one for force equilibrium as follows:

$$F_f = \frac{\sum \left(c'l\cos\alpha + (P - ul)\tan\phi'\cos\alpha\right)}{\sum P\sin\alpha + \sum kW \pm A - L\cos\omega} \tag{2.2}$$

$$F_m = \frac{\sum \left(c'lR + (P - ul)R\tan\phi'\right)}{\sum Wx - \sum Pf + \sum kWe \pm Aa + Ld} \tag{2.3}$$

The difference in the methods of slices listed previously lies in the how the forces between neighbouring slices are defined. With the exception of the Ordinary or Fellenius method of slices, the normal force P across the base of a slice can be defined as follows:

$$P = \left[W - (X_R - X_L) - \frac{c'\sin\alpha}{F} + \frac{ul\tan\phi'\sin\alpha}{F}\right] / m_\alpha \tag{2.4}$$

where:

$$m_\alpha = \cos\alpha + \left(\sin\alpha\tan\phi'\right) / F \tag{2.5}$$

The Ordinary method of slices assumes that the interslice forces can be neglected in the analysis because they are parallel to the base of each slice in turn (Fredlund and Krahn 1977). This assumption can lead to significant errors since interslice forces of adjacent slices are not equivalent due to change in direction. The safety factor is computed using

Equation 2.3 with the normal force equal to the component of slice weight that is perpendicular to the slice base (excluding horizontal seismic loading).

The Simplified Bishop's method neglects interslice shear forces, X_R and X_L, and assumes that the interslice forces can be adequately defined by normal or horizontal forces acting along the vertical sides of each slice. The factor of safety is obtained by summing moments about a common point, usually the center of rotation. The factor of safety equation is the same as that obtained for the Ordinary method, Equation 2.3, but the equation of the normal force P is different.

Janbu developed two methods of slices both based on force equilibrium. The first method, simplified, ignores the interslice shear forces and applies a correction factor, f_0, to the safety factor obtained from Equation 2.2. The correction factor is based on the cohesion of the soil, angle of internal shearing resistance of the soil, and geometry of the failure surface. The correction factor lies between 1.0 to 1.15. The corrected safety factor is taken to be the calculated safety factor multiplied by the appropriate correction factor. Janbu's rigorous method assumes that the point at which interslice forces act can be defined by a 'line of thrust'. The safety factor and normal force and are given by Equations 2.2 and 2.4, respectively, while the interslice forces are defined as follows:

$$X_L = E_L \tan\alpha_t - (E_L - E_R) f_L / b + KW / bh / 2 \qquad (2.6)$$

$$(E_L - E_R) = [W - (X_L - X_R)] \tan\alpha - S_m / \cos\alpha + KW \qquad (2.7)$$

where $f_L, f_R,$ and α_t define the location, measured vertically from the base of each slice, and inclination, measured from the horizontal, of the line of thrust. The rigorous method differs from the simplified method since the interslice shear and normal forces are used to determine a safety factor. To solve for a safety factor requires an iterative process and

evaluation of the interslice shear forces. On the first iteration the interslice shear forces are set to zero. Thereafter, the interslice shear forces are solved by summing moments about the midpoint of the base of each slice. The safety factor has been determined when a consistent line of thrust and safety factor value have been obtained.

Spencer's method assumes that there is a constant relationship between the magnitude of the interslice shear and normal forces as follows:

$$\tan\theta = \frac{X_L}{E_L} = \frac{X_R}{E_R} \qquad (2.8)$$

where θ is the angle of the resultant interslice force with respect to the horizontal.

Spencer's method produces two safety factors, one based on force equilibrium and one based on moment equilibrium, for each resultant force angle. Iterations continue until a θ angle produces the condition $F_m = F_f$ at which point the analysis is complete. Both moment and force equilibrium have been satisfied by a series of assumptions resulting in the same safety factor.

The Morgenstern-Price method assumes that the inclinations of the interslice forces vary across the slide mass according to:

$$\tan\theta = X / E = \lambda f(x) \qquad (2.9)$$

where λ is a scaling factor to be evaluated in solving for the safety factor and f(x) is an assumed functional relationship with respect to x as shown in Figure 2.21 (Graham 1984). Two special cases of the Morgenstern-Price method occur when f(x) = 0 and f(x) = constant. When f(x) = 0 the solution is the same as Bishop's simplified and when f(x) = constant the solution is the same as Spencer's. Equations 2.2 and 2.3 are used to determine safety factor values for moment and force equilibrium while the interslice

forces are determined using equations 2.6 and 2.7. Like Janbu's rigorous method, evaluation of the interslice forces involves initially setting the interslice shear forces equal to zero. During subsequent iterations the horizontal interslice forces are computed using Equation 2.7 and the vertical interslice forces are determined by assuming a λ value and side force function f(x) as follows:

$$X_L = E_L \lambda f(x) \qquad (2.10)$$

Experience and judgement are required in selecting the appropriate f(x) function to best estimate the manner in which the interslice forces vary across the slide mass. The interslice forces are recomputed for every iteration until acceptable arithmetic precision has been achieved for F_m and F_f. The analysis is repeated for the same side force function but a different scaling factor value is used. The final safety factor value is obtained for a given f(x) function and λ value when $F_m = F_f$. Since f(x) is assumed, other side force functions should also be examined. The analyst must be careful when selecting f(x) distributions since some f(x) functions may produce a line of thrust outside the slide mass or imply interslice shear forces which exceed available shear strengths (Graham 1984).

2.6.2 Comparison of Methods

Fredlund and Krahn (1977) presented slope stability analysis of circular and non-circular (or composite) slip surfaces using the methods of slices described in the preceding section. Figure 2.22 (Fredlund and Krahn 1977) shows the slope geometry, piezometric conditions, and strength assumptions used in the analysis. Six different combinations of shear strength, slip surface type, and piezometric conditions were used to define the slope properties. For each combination, a safety factor was computed using the six

methods outline earlier. The results of the comparative analysis are contained in Table 2.6 as cases 1 to 6. Figure 2.23 (Fredlund and Krahn 1977) illustrates a plot of safety factor versus λ for case 1. The results from moment-equilibrium analysis (F_m) indicate that Simplified Bishop's, Spencer's, and Morgenstern-Price produce safety factors that are very similar. The Ordinary method consistently produces safety factors which are lower than three methods listed above while the Janbu methods produce results which can be higher, lower, or similar compared with the three methods listed above. Examination of Figure 2.23 illustrates the effect of interslice force assumptions on computed safety factors for the six methods used in the comparative study. The force equilibrium methods of slices are quite sensitive to λ values, while moment equilibrium methods of slices are relatively insensitive to λ values (Graham 1984). In all cases, Bishop's, Spencer's, and Morgenstern-Price methods yielded results that were very similar, though the results varied significantly depending on whether the failure surface was circular or composite.

When analyzing a slope stability problem, it can be expected that rigorous methods will produce similar safety factors while simplified methods, especially force equilibrium methods, may produce significantly different results (Fredlund *et al.* 1992) as illustrated by Figure 2.23.

It has become accepted practice to use the center of rotation as the axes of moment equilibrium when employing moment equilibrium methods of slices. Fredlund *et al.* (1992) examined the effect of the position of the axes of moment equilibrium on three methods of slices. The methods of slices chosen for the study were Ordinary, Simplified Bishop's, and General Limit Equilibrium (GLE). Figure 2.24 (Fredlund *et al.* 1992) shows

the basic slope used to study the effect of the position of the axes of moment equilibrium. Several parameters were varied to determine the effect of the position of the axes of moment equilibrium including shear strength (c', ϕ'), slip surface radius, depth to hard stratum, and slope angle. The GLE method was used to generate a reference safety factor for each combination of parameters to be compared with safety factors generated by Ordinary and Simplified Bishop's for the same parameters. Any differences that were found were presented in terms of percentage difference as compared with the GLE safety factors. In comparing safety factors computed for circular slip surfaces, it was found that the Simplified Bishop's method produced very similar results compared to the GLE method when the axes of moment equilibrium was the same as the centre of rotation. However, when the axes of moment equilibrium was moved vertically, the maximum difference was 8 %. The safety factors computed using the Ordinary method were strongly influenced by position of the axes of moment equilibrium as it was moved in a horizontal direction. When the centre of rotation was selected as the axes of moment equilibrium, significant differences occurred between Ordinary method safety factors and the reference safety factors. To generate similar safety factors, the axes of moment equilibrium had to be positioned to the right of the centre of rotation in Figure 2.24.

When computing safety factors for composite slip surfaces, the Simplified Bishop's method produced safety factors that were, generally, different from the reference safety factors when the centre of rotation was used as the axes of moment equilibrium. The maximum difference observed in the study was 12 % when the center of rotation was used as the axes of moment equilibrium. The location of the axes of moment equilibrium which generated similar safety factors compared to the reference safety factors was consistently found to lie above the center of rotation. The position of the axes of moment

equilibrium above the center of rotation was designated *dy* (Fredlund *et al.* 1992). The *dy* values varied from negligible to values of several meters (depending on parameter combinations) and were strongly influenced by the radius of the circular portion of the slip surface and the perpendicular distance from the hard stratum to the projected circular surface. The greater the magnitude of the above two parameters the greater was the *dy* value. As in the circular case, the Ordinary method produced very different safety factors compared to reference values when the center of rotation was used as the axes of moment equilibrium. The position of the axes of moment equilibrium required to compute similar safety factors as the reference values was located to the right of the center of rotation.

The Ordinary method of slices is subject to significant errors, compared to rigorous methods, whether it is used to analyze circular or composite slip surfaces. The Simplified Bishop's method, however, computes safety factors that are very similar to safety factor values computed by rigorous methods such as Spencer's, Morgenstern-Price, and GLE (Fredlund and Krahn 1977, Fredlund *et al.* 1992). Differences between Simplified Bishop's and rigorous methods can occur when the center of rotation is used as the axes of moment equilibrium to analyze composite slip surfaces. The Simplified Bishop's method can produce comparable results with rigorous methods provided an appropriate axis of moment equilibrium is chosen.

2.7 JUSTIFICATION AND DETAILS OF MODELING PROGRAM

Slope stability analysis of Winnipeg riverbanks has become a well defined process aided by research at the University of Manitoba and within the local consulting community. The

geotechnical properties of Winnipeg soils have been extensively investigated and slope instability problems examined in detail.

As discussed in Chapter 1, one unknown that has not been fully explored is the influence of the confined bedrock aquifer, the Upper Carbonate aquifer, on the stability of Winnipeg riverbanks. Available data show that the piezometric levels in the Upper Carbonate aquifer are variable and are a function of annual precipitation events and time of year. The influence of the bedrock aquifer on slope stability in Winnipeg has been qualitatively assessed as having both stabilizing and destabilizing effects. However, quantitative analysis to verify these effects had not been performed before this research project.

The influence of the bedrock aquifer is an integral component of riverbank stability and should be included when performing slope stability calculations. Incorporation of the influence of the Upper Carbonate aquifer raises the following questions. For a given riverbank, what is the stabilizing/destabilizing effect of the Upper Carbonate aquifer compared to local conventional slope stability analysis techniques? Do effective shear strength parameters need to be redefined if the Upper Carbonate aquifer is accounted for? The following section describes the methodology that was employed in order to answer these questions and fulfil the objectives stated in Chapter 1.

2.7.1 Modeling Program

In order to achieve the objectives of the research program, an integrated groundwater flow-slope stability model should use realistic parameters to simulate the strength,

hydraulic, and geometric properties of a natural riverbank. This will ensure confidence in the results generated in the model. More importantly, the results generated in the research program should be, at least in part, transferable to the local consulting community.

The overall modeling program was comprised of two parts or steps. The first step was the development of a finite element model that would simulate seasonal groundwater flow patterns observed in Winnipeg riverbanks. To ensure accurate analyses results two conditions had to be met. Firstly, the hydraulic properties of the materials being modelled had to be realistic. The properties were taken from published literature and then arithmetically averaged for use in the groundwater flow model. Secondly, the seasonal variations of river levels and piezometric elevations of the bedrock aquifer also had to be realistic. Seasonal variation of piezometric data for the Red River and bedrock aquifer was obtained from instrumentation monitoring records of full-scale projects.

Typical geological sequences in Winnipeg consist of the three major stratigraphic units mentioned earlier. In order of occurrence from the ground surface these units are the clays (brown and grey), glacial tills, and carbonate bedrock. The thickness of the clays and glacial tills can vary considerably within Winnipeg. Thickness data were obtained primarily from boreholes drilled along the Red River. The clay and glacial till thickness used in the research program reflected conditions at a research site where piezometric data was used to develop the finite element groundwater model.

The groundwater model was set up primarily to examine the late-summer to late-fall time period during which the bedrock aquifer begins to recharge and the Red River is allowed to drop to an unregulated level. Just prior to this annual cycle beginning, the piezometric

elevations in the Red River and bedrock aquifer are relatively constant. This provided a good starting point for the groundwater flow model. Analysis of the groundwater flow consisted of two components. The first was to perform Steady-State analysis. This analysis provided the initial conditions or starting point for the second component of the groundwater flow model. A Steady-State analysis was used to approximate the groundwater flow since hydraulic conditions are relatively constant at this time.

The second component of the groundwater flow model was a study of the seasonal variation of piezometric elevations in the river and bedrock aquifer. These seasonal variations were modelled as time dependent boundary functions in a transient analysis. Time steps used in the transient analysis were made sufficiently small to ensure that convergence difficulties did not occur. The results generated in the transient analysis were then compared to results obtained from field instrumentation to determine the accuracy of the groundwater flow model.

The results generated in the groundwater flow model were then used in the second step of the overall modeling program. The safety factor of the modelled riverbank was examined based upon the seasonal variation of the groundwater flow regime. Safety factors were calculated at discrete time increments generated in the groundwater flow model. This allowed the safety factor to be mapped as a function of time and variations in the piezometric elevations of the river and bedrock aquifer. Also, the effect of increasing or decreasing the thickness of the clay and glacial till was examined.

Chapters 3, 4, and 5 provide detailed descriptions of the software used to perform the modeling and analysis, procedures and assumptions, and results of the analyses

described in the preceding section. The results are discussed in Chapter 6 and Chapter 7 contains conclusions and suggestions for further work.

CHAPTER 3. COMPUTER SOFTWARE AND PROCEDURES

3.1 INTRODUCTION

The computer software used for the research was developed by GEO-SLOPE International Limited based in Calgary, Alberta, Canada. GEO-SLOPE offers several Windows based software packages including SLOPE/W, SEEP/W, and SIGMA/W. The software was selected for several reasons including:

1. ease of use
2. the ability to integrate individual software packages so that data files from one program can be used in others
3. good graphical displays and output

GEO-SLOPE software operates in a Windows environment, making it easy to learn and use. Secondly, porewater pressures or effective stresses generated by finite elements in SEEP/W or SIGMA/W can be incorporated into SLOPE/W instead of using the simpler built-in pore pressure options of SLOPE/W. Finally, the most appealing aspect of GEO-SLOPE software is its excellent graphical capabilities. The graphical features allow for easy visual verification of input and output data.

The focus of the research program is seasonal groundwater changes and their effect on riverbank stability. The seasonal variation of groundwater in riverbanks is a time dependent condition requiring transient analysis. The SEEP/W finite element software allowed the research program to examine the transient behaviour of groundwater in

riverbanks and then incorporate the resulting porewater pressure predictions into SLOPE/W. In this way, it provided more realistic modeling of slope stability.

3.2 USING GEO-SLOPE SOFTWARE

Within each software package of the Geo-Slope family, three functions are common to all, namely:

1. DEFINE
2. SOLVE
3. CONTOUR

The DEFINE function allows the user to input all parameters required to fully specify the problem. This includes the problem geometry, soil properties, and desired method of analysis. Having completed the DEFINE step the user can then solve the problem that has been defined. The SOLVE function is the mathematical engine which performs the calculations required for the analysis the user has chosen and the problem that has been defined. When the SOLVE function is complete, the results of the analysis can be viewed in CONTOUR. This function presents the results of calculations performed by SOLVE in a graphical format. A more detailed summary of the use of the SLOPE/W and SEEP/W used in the research program is presented below.

3.2.1 Using SLOPE/W

SLOPE/W is a computer program which allows the user to input the data required to specify a slope, calculate a factor of safety for that slope, and finally view the results in a

graphical format. To specify all the parameters of the slope the user must select the DEFINE function. Figure 3.1 (SLOPE/W user's guide) illustrates the DEFINE function screen with its menu and tool bars. The most important menu or tool bar feature is the KEYIN menu that allows the slope geometry and its corresponding parameters to be specified.

The information required to properly define a slope cross section is a topographic survey and subsurface investigation to determine the stratigraphic profile. The user can proceed in several different ways to begin setting up a problem. Typically, the soil properties are input first. They can be obtained either through a geotechnical investigation and laboratory testing or from a database compiled from local experience. The soil types and their properties are input in order of occurrence from the surface to the stratigraphic basement.

The user can choose to draw the cross-section using the DRAW function or can manually input coordinates defining the cross section in the KEYIN menu. A combination of these two functions is generally the easiest approach. Based on the survey and stratigraphic data, the user manually inputs points or coordinates defining the surface and stratigraphic geometry. Lines are then drawn between corresponding points, using the DRAW menu, to define the surface and boundaries of stratigraphic units. The graphical capabilities of the SLOPE/W allow the user to view the cross section as it is being defined. This makes verification of the input data easy and intuitive.

The remainder of the data to be input relates to the analysis that will be performed. SLOPE/W allows the user to select nine different limit equilibrium methods of slope stability analysis such as Bishop's, Janbu, and Morgenstern-Price, as well as a finite

element slope stability option that requires the use of SIGMA/W. Having chosen a limit equilibrium method the user must input analysis-specific data such as details of the slip surface type, piezometric conditions and convergence limits.

Three types of slip surfaces are available for selection:

- Circular
- Block
- Fully specified

Circular slip surfaces are generated by defining a grid of rotation centers and a series of radius or tangent lines. The grid of rotation centers is located above the slope being solved, while the radius or tangent lines are defined within the slope. The computer analyzes a slip surface centered at each grid point in turn and intersecting the slope in a way defined by the radius or tangent line specification. Initially, it is best to begin with a fairly large, widely spaced grid of rotation centers and widely spaced radius lines, and then gradually refine both the grids and radius lines. Results are viewed using the CONTOUR function.

The program also permits sliding to be specified by sliding blocks that are defined by three linear segments. Two blocks of points, a left and a right block, are defined within the slope and an axis point is specified above the slope that is used in the analysis for moment equilibrium. Slip surfaces are generated by connecting each point in the left block with each point in the right block, creating one of the linear segments. The two remaining linear segments are generated from the right and left blocks back to the surface, at the toe and crest of the slope. These segments are projected to the surface at angles that have been specified to ensure numerical stability of the solution. As with circular slip surfaces, described in an earlier paragraph, it is advantageous to begin with

large blocks of widely spaced points and then refine the search parameters after viewing the results. While SLOPE/W generates slip surfaces for circular and block-specified analyses, a third form of slip surface is also available, one defined by the user through a series of pre-selected points.

Input of porewater pressure data is done by selecting one of nine possible options that include coefficients $r_u = u/\gamma z$, piezometric lines, and data generated in the related program SEEP/W. The final input to define the analysis properties is convergence. This option allows the user to specify the number of slices used in each failure surface analysis as well as the tolerance for acceptance of the solution. When the difference in safety factor values between two iterations is less than the tolerance, for example 0.001, the problem has converged and the iteration process will stop. The SLOPE/W default values are adequate for most problems.

Once the problem has been defined, the user can proceed with the SOLVE function. This is the numerical engine that calculates the factors of safety based on user specified input data. For each slip surface within the specified search limits, the SOLVE function iterates the chosen safety factor equation until the convergence criteria have been satisfied. Once the SOLVE function has completed its computations, the SOLVE window displays the most critical factor of safety for the chosen methods of analyses.

The final step for the user is to view the results generated in the SOLVE function using the CONTOUR function. This function offers the choice of a significant amount of information including:

- free body diagram and force polygon for each slice of a particular slip surface

- shear resistance (shear strength and shear mobilized) along the slip surface from crest to toe
- strength (cohesive, frictional, and suction) along the slip surface from crest to toe
- selected slip surfaces for each analysis performed

Typically, the most commonly viewed results are the critical slip surface and corresponding safety factor (FS) for the chosen input data. When the CONTOUR function is selected, the lowest FS value and corresponding slip surface are shown by default. By drawing contours of FS values in the rotation center grid, it can be determined if the lowest FS value that has been calculated is also the critical (or lowest possible) FS value. If the critical slip surface has been found, the contours nearest the critical FS value will be closed and confine the minimum FS value. If the minimum FS value has not been found then the contours will not be closed but will be open in the direction where the critical FS value will be found. The critical FS value is then found by moving the grid of rotation centers in the direction where the current lowest FS value is located. The grid of rotation centers is then moved by the user until the critical FS value and slip surface have been found. Similarly, in block-specified analysis, the CONTOUR function shows the lowest FS value and slip surface for the data input. However, the lowest FS value may not be the critical value. The user must verify that the critical slip surface has been found. Once this has been done, the user can choose to alter the soil properties or piezometric conditions and perform further stability analysis based on different conditions.

3.2.2 Using SEEP/W

SEEP/W is a finite element (FE) software product that can be used to model and analyze porewater pressure distribution and movement within porous materials such as soil or rock. SEEP/W allows the user to model and analyze various types of problems including saturated/unsaturated flows, steady state or transient conditions, and confined and unconfined flow boundaries.

The process of developing, solving, and viewing results in SEEP/W is very similar to that previously described for SLOPE/W. Once again the user begins by selecting the DEFINE function. There are two important menu options in the DEFINE function namely KEYIN and DRAW. The KEYIN menu option allows the user to input all data necessary to fully specify the problem. However, the DRAW option plays a much more significant role in the development of the problem than in SLOPE/W. There are now several important options the user must specify.

The user begins to define the problem by selecting options from the KEYIN menu that will form the analysis that will be performed. The KEYIN menu can be subdivided into 3 categories of input.

1. Analysis
2. Material properties and functions
3. Finite element mesh characteristics

The user can choose to select either steady-state or transient analysis and view the problem in two dimensions, axisymetrically, or plan view. These choices relate to the problem being analyzed. For example a pumping well in a homogenous, isotropic

unconfined aquifer may use transient analysis and an axisymetric view to define the problem. If the transient analysis option is selected then the user must define the time increments to be used. Time increment data may consist of constant time increments or increments which are each successfully larger than the previous increment by a factor such as 2 or 3. The total time increment (duration) from beginning to the end of analysis is defined by the user. As in SLOPE/W the user must also specify convergence criteria which control the iteration process. The user can specify the maximum number of iterations the SOLVE function will execute as well as the tolerance (as a percentage), successive iterations. A maximum number of iterations defined by the user provides a finite limit to the solution process.

The second category of input in the KEYIN menu is material properties and functions. The user must input the hydraulic characteristic of each material within the domain of the problem. The hydraulic characteristics of the soil include hydraulic conductivity, volumetric water content, and 'K-ratio' that defines anisotropy. If the hydraulic conductivity functions of the various soils are known, the user can input them. Alternatively, the user can select hydraulic conductivity functions from a SEEP/W database that ranges in material types from uniform sand to clayey silt. A third option is also available which is particularly useful for modeling unsaturated conditions. This option allows the hydraulic conductivity of a soil to be estimated from the volumetric water content function of that soil. Hydraulic conductivity of a given soil is relatively constant when the soil is saturated and porewater pressures are positive. However it can decrease rapidly if the soil becomes unsaturated and porewater pressures become negative. The volumetric water content function is also relatively constant at positive porewater pressures but may decrease rapidly once porewater pressures become negative. The volumetric water content can either be estimated by the user or obtained

from a soil water characteristic curve (SWCC) data for each soil in turn. The final important hydraulic characteristic is the 'K-ratio', $K_{vertical}/K_{horizontal}$. This must be specified if the soil is known to have anisotropic hydraulic conductivity.

Finite element mesh characteristics, such as nodes, elements, and boundary conditions can all be manually input from the KEYIN menu. This is generally very time consuming. It is more efficient to manually input the set of principal coordinates that define the ground surface and various stratigraphic boundaries. Once these have been input, a FE mesh is created using the DRAW menu. When the DRAW menu is selected, the user can select material type and element shape, either quadrilateral or triangular.

To ensure SEEP/W analysis is accurate the following guidelines are recommended (SEEP/W User's Guide):

- quadrilateral and triangular elements should have aspect ratios near 1.0.
- quadrilateral elements should have interior angles equal to 90°.
- triangular elements should have an interior angle equal to 90°.

Finite elements can either be selected individually or multiple elements can be selected in uniform regions of the cross section. Individual elements are drawn by selecting the corresponding nodes that define the corners of the element. An element is then generated within those limits. Large groups of elements can be drawn in the same manner. The corner nodes of the region being defined are selected. The user then defines the number of elements to be selected in the vertical and horizontal directions. For example, a region which is 10 m by 10 m can be defined as having 10 vertical divisions and 10 horizontal divisions resulting in 100 elements, each 1m x 1 m,

generated by SEEP/W. This process continues until the domain of the problem has been fully defined by a FE mesh. The remaining user inputs, boundary conditions, boundary functions, and flux sections are defined using the DRAW menu.

Within the DRAW menu the user can choose to draw single or multiple elements, boundary conditions, boundary functions, or flux sections. Boundary data can be assigned to individual nodes or to groups of nodes depending on the user. Typically a boundary is a vertical or horizontal feature and selection of multiple nodes for input of boundary data is routine.

After the data, material properties, and FE mesh data have been input for the analysis, the last operation before the problem is solved is to sort and verify the input data. The utility menu is chosen and the user selects the verify option. This checks the correctness of the data and also performs such operations as ensuring that every node is attached to an element and identifying selected elements which have non-existent node numbers. If verification produces no errors, node data and element data may be sorted either vertically or horizontally. This sorting should be in the direction of the minimum dimension (SEEP/W Users Guide). Sorting in this manner decreases the nodal point differences and results in more efficient computing. These last two steps are among the most important processes in producing a well defined FE domain.

After the user is satisfied that the problem has been properly defined and the input data have been verified and sorted, the SOLVE function is selected to compute the finite element solution to the problem. SEEP/W is based on Darcy's Law for both saturated and unsaturated flow. The governing equation used in the formulation of SEEP/W is:

$$\frac{\partial}{\partial x}\left(k_x \frac{\partial H}{\partial x}\right) + \frac{\partial}{\partial y}\left(k_y \frac{\partial H}{\partial y}\right) + Q = \frac{\partial \Theta}{\partial t} \qquad (3.1)$$

where k_x and k_y are the horizontal and vertical hydraulic conductivities, respectively; H is head; Q is flux; and Θ is volumetric water content. This equation is based on the application of Darcy's Law and the conservation of mass. Under steady-state conditions with homogeneous and isotropic hydraulic conductivities. Equation 3.1 reduces to the Laplace equation. In words, Equation 3.1 states that the difference in flow entering or leaving a unit element at a point in time is equal to the change in the volumetric water content. The Galerkin method is applied to the governing differential equation resulting in finite element equations which are solved using Gauss elimination techniques (more detail is presented in the Theory section of the SEEP/W User's Guide, GEO-SLOPE International Ltd., © 1991-1994). There are six different files created when the SOLVE function is activated. Of these the 'head' file and 'velocity' file are the most important. The 'head' file contains the computed total heads at each node while the 'velocity' file contains the Darcian velocity (specific discharge) and hydraulic gradients for each Gauss integration point in each element.

Once the SOLVE function has been completed the user may view the results in graphical format using the CONTOUR function. By default CONTOUR shows the velocity vectors based on the computations performed in SOLVE. The velocity vectors indicate direction and magnitude of flow within the problem boundaries. They also provide a qualitative measure of the model performance, allowing users to judge the correctness or accuracy of the model they developed. The most useful menu bar option is the DRAW option. Using this option contours can be drawn for all the data computed in SOLVE. These include total head, pressure head, x or y velocity, x or y gradient, and

volumetric water content. The DRAW option allows the user to view data in a graphical format. This makes understanding of the results much easier.

3.2.3 Integrating SEEP/W results with SLOPE/W analysis

Most slope stability software requires the input of static groundwater conditions to simulate the piezometric properties of a slope. This limits modeling of the interaction between groundwater, confined aquifers, rivers or reservoirs, and how it can affect slope stability. The advantage of using SEEP/W and SLOPE/W in this research program is that an integrated slope stability/seepage analysis could be performed.

Flow conditions in the slope under examination are first defined and solved using SEEP/W. Then (Figure 3.2) in the SLOPE/W program, the user can import the FE mesh generated in SEEP/W. The user defines the soil properties and analysis method in the usual way as if the FE mesh had not been imported. Once this has been done the SOLVE function is selected in SLOPE/W. A dialogue box appears and prompts the user to select the appropriate file containing SEEP/W results for porewater pressure distributions. SOLVE then completes the analysis based on the SLOPE/W input data and the SEEP/W pressures. Results for slope stability calculations can be viewed in the usual way using the CONTOUR function. The process is continued until the user is confident that the most critical (lowest) FS value has been found.

The user may now proceed in one of two ways depending on the analysis to be performed. One, the user can select to hold constant the boundary conditions of the seepage analysis and perform a sensitivity analysis based on varying soil strengths.

Conversely, the soil strength data can be kept constant, and the boundary conditions of the seepage analysis altered to reflect changing groundwater conditions.

CHAPTER 4. DETERMINATION OF MODEL INPUT DATA

4.1 INTRODUCTION

Selection of input data required to perform the analyses and modeling, as outlined in Section 2.7, was obtained from the published literature and observations of existing riverbanks in Winnipeg. Most of the data, such as shear strength parameters and hydraulic conductivities, obtained from previous literature was of a quantitative nature. The observational data were primarily related to the geometry of riverbanks above and below water levels in rivers within Winnipeg.

4.2 SHEAR STRENGTH PARAMETERS

The shear strength parameters chosen for slope stability analyses reflect methods currently used by local consulting industry as indicated, for example, by Graham (1986). The parameters discussed in the following paragraphs have been successfully used in local consulting practice to perform analyses on Winnipeg riverbanks. Use of these parameters will enable comparisons to be made between this research program and current practice.

4.2.1 Post-Peak Shear Strengths

Post-peak strengths were used to specify the shear strength of the clays in the riverbank cross section selected for seepage and slope stability analysis. Post-peak strengths have been used with success in first-time slides in Winnipeg (Graham 1986). The post-peak strength values are generally about $c' = 5$ kPa and $\phi' = 17°$. These parameters were used in this project for most of the clay soil above the clay-till contact. Previous research analyses (Rivard and Lu 1978; Lefebvre 1981) has shown that intact (peak) strengths do not produce satisfactory results when used in slope stability. The reason involves plastic straining around crack tips in fissured plastic clay. Safety factors computed using peak strengths are generally in excess of unity for slopes that show signs of instability or have failed. Lower shear strengths are required to produce results that agree with observed slope behaviour and which are consistent with the occurrences of slickensided surfaces.

4.2.2 Residual Shear Strengths

A zone of softer, lower strength clay has been identified along the clay-till contact in Winnipeg clays (Freeman and Sutherland, 1974). Within this zone a strength lower than post-peak strength was assigned to the clays. This lower strength zone at the clay-till contact also permitted modeling of non-circular or composite slip surfaces commonly observed along Winnipeg riverbanks.

One set of shear strength parameters assigned to this zone was of $c' = 3$ kPa and $\phi' = 12°$ which falls within the upper bounds of residual strengths commonly used in

Winnipeg clays. It is about 30% lower than the post-peak strengths described in Section 4.2.1. Some calculations were done using a slightly higher set of shear strength parameters, c ′ = 4 kPa and ϕ' = 15°. These shear strength parameters are just slightly lower than the post-peak shear strengths described in Section 4.2.1. The shear strength parameters assigned to this weaker zone were not intended to represent residual strengths but rather to be just slightly lower than observed post-peak shear strengths.

The location and extent of the soil layers within the cross section used for the seepage and slope stability modeling are shown in Figure 4.1. The carbonate bedrock that underlies the till was not required for the majority of modeling performed and has been omitted from Figure 4.1. The stratigraphy for the cross section was selected based on the conditions observed at KGS Group's South Perimeter research site (KGS Group 1994).

4.3 SLOPE GEOMETRY AND MORPHOLOGY

The slope geometry and morphology used in the analysis was idealized but representative of the characteristics of Winnipeg riverbanks. They were selected by considering data from the published literature, preliminary analysis, and field observations.

Mishtak (1964) surveyed riverbanks along the Assiniboine and Red Rivers within Winnipeg, focusing on whether the riverbanks had failed, showed signs of previous failure, or were stable. Each riverbank was characterized by its geometric features including height of bank and slope. Of the 141 riverbanks that were surveyed, only 6

were determined to be stable while the remainder had either failed or showed signs of distress. The majority of the riverbanks which had failed rotationally became stable at slopes of 4.5H to 6.75H:1V. Mishtak's observations were used in the design of the Winnipeg Floodway which has a slope of 6H:1V for nearly its entire length (personal communication, Steve Wicek, Water Resources Department, Manitoba Department of Natural Resources, 1999). This design slope was deemed to be acceptable based on Mishtak's observations of natural riverbanks in Winnipeg.

Preliminary analysis was performed to determine an adequate riverbank slope for use in the model. Three geometric sections of riverbank had to be considered, the upper bank, mid bank, and toe. Each section of riverbank has its own characteristics related to initial formation in the soft lacustrine sediments, influence from regulating river levels, and effects of erosion and slope instabilities. It is probable that slope instabilities and failures were common when the initial channel was formed in the soft lacustrine sediments. Over the last several thousand years the river channels in Winnipeg has meandered and reshaped the riverbank geometries. The geometry of the upper bank section is most likely related to the steepest slope at which the riverbank is currently stable based on annual precipitation, groundwater fluctuations, and river level fluctuations. The mid-bank section is less steep and is influenced by the current regulation of river levels. The toe section of the riverbank is usually much steeper than the mid bank section. It results from year-round submergence and continued erosion. An alternative explanation suggests that the morphology of riverbanks is related to migration and erosion of meander features.

Characteristics of the slopes used in the analyses were chosen to be consistent with riverbanks on the outside bends of rivers within the City of Winnipeg. These areas are

typically the most active with respect to downslope movement and failure. Riverbanks on inside bends of rivers typically have much different geometry and often different stratigraphy. The idealized riverbank cross section used in the research project is shown in Figure 4.1. The cross section consists of a regular shape that omits some of the irregularities that may occur in real riverbanks. The author has had considerable experience plotting riverbank survey data for the purposes of performing slope stability calculations. In most instances, intermediate survey points between changes in riverbank geometry can be eliminated because they fall on a relatively straight line. This is particularly true between the riverbank crest to regulated river elevation (upper bank) and from regulated river level elevation to the unregulated river level elevation (mid bank). The second reason for the regular shape of the riverbank used in the model is related to creation of the finite element mesh for seepage modeling. A straight or linear portion of riverbank cross section is easy to discretize. The slope of a straight section of riverbank can be determined and then used to identify locations of nodes making up elements defining the FE mesh along a linear portion of riverbank.

4.3.1 Slope Height

Slope height is the vertical distance from the (mostly) horizontal ground at the top of the riverbank to the toe of the riverbank where it again becomes relatively horizontal. This is illustrated in Figures 2.22 and 2.24. The height of slopes for the research modeling reported here was selected on the basis of existing (surveyed) riverbanks in Winnipeg. Top of bank (crest) elevations range from about 230 to 232m (geodetic elevation). Toe elevations range from about 218 to 220m. The slope height chosen for the modeling

program was 12m which represents a common vertical distance for a natural riverbank in Winnipeg.

4.3.2 Upper Slope

As described in Section 4.3, the upper slope is the section of slope from the crest of the riverbank to an elevation where the regulated summer river level intersects the bank. This section is often thought of as a major contributing factor to riverbank instability and the corresponding computed safety factor values. As shown on Figure 2.24, the upper slope is on the disturbing side of the center rotation in circular failures and is primarily responsible for the disturbing moments in Limit Equilibrium computations.

Based on preliminary analyses and examination of field data, the upper slope was selected to have a gradient of 6H:1V. The primary criterion for selection of appropriate upper bank slope was safety factor. The safety factor, under the extreme conditions of a fully saturated riverbank and unregulated winter river level, was targeted to be in the range of 1.2 to 1.3. This range of safety factor was chosen since it was hypothesised by the author that introduction of influence of the Upper Carbonate aquifer would tend to reduce computed safety factors. The selected safety factor range (1.2 to 1.3) allowed improved analysis to produce lower safety factors that did move below unity.

4.3.3 Mid Bank

The mid-slope section of Winnipeg riverbank is located between the regulated level in the summer and unregulated winter level. This section is generally characterized by lack

of mature vegetation and is relatively flat. However its slope is highly variable from location to location.

For the purposes of this research, the mid-slope section of riverbank was selected to be at 10H:1V (Figure 4.1). This slope falls within the range of mid-bank slopes that are commonly found along Winnipeg riverbanks.

4.3.4 Riverbank Toe

The toe section of the riverbank is often the steepest part of a riverbank due to erosion by the river. This section is always submerged and therefore experiences erosion, to different degrees, all year long. This part of the riverbank extends from the winter level of the unregulated river to the river bottom. This section is typically examined primarily through river bottom soundings (some done by the author in his professional practice) but data were also obtained from flood risk maps for the City of Winnipeg. The toe section of riverbank was selected to have a slope of 4H:1V.

4.4 RIVER LEVEL

River levels play an important role in stability of riverbanks. Higher or lower than normal river levels will increase or decrease, respectively, the safety factor. Evidence of this can be seen by examining Figure 2.18 (Baracos 1978) and Figure 2.19 (KGS Group 1994). In both figures there is a strong correlation between river level and riverbank movement.

Although river level alone is not solely responsible for observed riverbank movements in Winnipeg it does contribute to time-dependent riverbank movements.

Commonly, in a climate such as Winnipeg's, river levels can be categorized by season as follows:

- In spring, flows and levels are generally at a yearly high as a result of spring run-off.
- During summer, flows decrease to yearly average levels. Water levels are controlled by adjustable weirs at Lockport, Manitoba located approximately 20 km downstream of Winnipeg. These are influenced to a small extent by precipitation in Winnipeg and to a much larger extent by rainfall in the watershed, including tributary rivers such as the Pembina, Morris, Souris, and LaSalle.
- Flows and levels decrease during the fall and winter as precipitation in the form of rain diminishes and temperatures drop below the freezing point. Also the adjustable weirs in Lockport are lowered allowing river levels to decrease to unregulated flows.

The river levels within Winnipeg are somewhat unique in that they are artificially controlled during the summer months and allowed to decrease to unregulated levels in the fall. Further discussion is given in the following paragraphs. This transition from regulated to unregulated level is of major interest since it relates to observed riverbank movements.

4.4.1 Regulated River Level

The river level within Winnipeg is artificially maintained approximately 2m above the normal unregulated level during the summer months. The Red River is maintained at this level to allow navigation downstream of Winnipeg which would otherwise be impossible because of bedrock outcropping (Lister Rapids) in the river bed near St. Andrews, Manitoba (personal communication, Brian Bodnaruk, KGS Group, 1998).

The artificially maintained river level has a stabilizing effect on deep-seated movements on riverbanks within Winnipeg though some concerns have been raised that it may adversely affect surficial erosion. The river level used for modeling and analyses purposes in this project was 223.9m (geodetic elevation). The level chosen represents a level seen primarily along the southern (upstream) section of the Red River in Winnipeg. This also corresponds to the controlled river level at one of the locations (South Perimeter site) where a research program was undertaken by KGS Group to monitor piezometric elevations in a riverbank as water levels and piezometric elevations changed.

4.4.2 Unregulated River Level

During a three-week period beginning in mid-October the river level is allowed to drop to its natural unregulated level (Figure 4.2). The lowering of river level is performed in anticipation of the coming spring run-off and associated higher river levels. The objective is to provide additional flow capacity and reduced volume of ice during spring break-up. Lowering of the Red River in this way has a destabilizing effect on riverbanks in the area

affected by this annual event. This includes a portion of the banks of the Assiniboine River within Winnipeg.

A value of 222.1m (geodetic elevation) was selected for modeling the unregulated river level. This value, like the regulated river level, was selected to correspond to levels experienced along the upstream section of the Red River within Winnipeg, that is, in the southern part of Winnipeg.

4.5 FAILURE SURFACE CLASSIFICATION

Selection of the appropriate failure surface geometry was one of the fundamental components of the research program. The failure surfaces used in the research program were based on observed movements and from data collected from instrumented research sites (Baracos 1978, KGS Group 1994).

Although failure conditions may be modelled fairly successfully with computed safety factors often close to unity, failure surfaces generated from computer analyses seldom match exactly the position and size of actual or observed failure surfaces. However, an attempt should be made to select failure surfaces for analysis that are representative of the failure surface that is likely to occur. In practice this is difficult or impossible to accomplish unless instrumentation is in place to measure displacements. Failure surface geometry can also be determined from observations and investigation. Test holes and survey data can be used to identify backscarps and exit locations as well as slickensided shear zones. Information of this type allows a reasonable approximation of the likely failure surface to be investigated. The process does not require the failure surface to be

identified exactly. What is needed is selection of the correct general shape of the surface. Systematic analysis then finds the most critical surface of this generic shape.

4.5.1 Model Failure Surface

The program of modeling and analyses undertaken in this project utilized a non-circular or composite failure surface as the primary mode of failure. Baracos (1978), Baracos and Graham (1981), and Graham (1986) have shown or discussed the nature of failure surfaces along riverbanks in Winnipeg and have indicated that a large number of slides tend to have a considerable component of horizontal displacement. To ensure composite slip surfaces would develop in the computer models, a 0.6m thick zone of lower shear strength was assigned to the clay overlying the till. The shear strengths were just slightly lower than the remainder of the clay within the idealized cross section. The use of lower shear strengths produced slip surfaces that were circular at the crest and toe but were linear along the clay-till interface. These slip surfaces simulated the shapes that are commonly observed in instrumented riverbanks.

4.6 SEEPAGE

Seepage or groundwater modeling comprised the bulk of the computational time for the research program undertaken in this thesis. The seepage model developed was calibrated with field data from the research site at South Perimeter investigated by KGS Group (1994). Although the riverbank at the research site and the model riverbank were quite similar in geometry, the goal of the seepage model was not necessarily to duplicate

observed site-specific responses but rather to produce groundwater behaviour that exhibited similar generic trends to those observed at the research site.

The time period chosen for modeling coincided with the monitoring data collected at the South Perimeter research site. The beginning of the modelled period was selected to be in late August 1992, and the end of the period selected to be November 30,1992. This period encompassed the recharge of the bedrock aquifer and lowering of the river from regulated to unregulated levels. The seepage modeling utilized transient FE analyses in order to follow the time dependent behaviour of both the river and bedrock aquifer.

Following sections describe seepage parameters used in the FE seepage modeling.

4.6.1 Hydraulic Conductivity

Initially, values of saturated hydraulic conductivities, K, for soils in the model riverbank were selected on the basis of previous research and published data. Intact lacustrine clays in the region have saturated hydraulic conductivity from 10^{-9}m/s to 10^{-13}m/s (Baracos 1960, Yuen *et al.* 1997). The tills are often fractured and have an approximate range of 10^{-7}m/s to 10^{-8}m/s (Render 1970). However, test data are limited. These values represented a starting point for the seepage analyses. During calibration of the FE seepage model, the saturated hydraulic conductivities of the clays were adjusted in order to produce behaviour similar to that observed from piezometric instrumentation at the South Perimeter site (KGS Group, 1994).

4.6.2 Initial Conditions

Transient FE modeling was performed in order to assess the influence of fluctuations in the river level and bedrock aquifer on riverbank stability. Prior to beginning the transient analysis, a set of initial conditions was required to provide a starting point for the transient analysis.

The initial conditions were selected at a point in time when the bedrock aquifer was at its most constant piezometric elevation. This occurs near the end of summer (late August or early September) when demand for groundwater begins to decrease and just before the bedrock aquifer begins to recharge. A Steady-State analysis was used to compute the initial conditions for input into the transient model. The piezometric elevation was obtained from the bedrock hydrograph (Figure 2.10 b) while the piezometric surface was determined from monitoring data recorded at the South Perimeter research site (KGS Group 1994).

4.6.3 Boundary Conditions

Three boundary conditions or functions were used in the transient FE model. These functions were assigned to simulate the river level, piezometric elevation of the bedrock aquifer, and porewater pressure reductions in the toe of the riverbank. The river level was modelled by assigning piezometric elevations to the nodes along the applicable section of riverbank, from the regulated summer river level elevation to the end of the cross section along river bottom. The piezometric elevation assigned to each node matched the elevations experienced with respect to time at the South Perimeter

research site over the modeling duration. The boundary function simulated the lowering of the river level from a regulated to unregulated level (Figure 4.2).

Nodes along the base of the finite element (FE) model of the slope, representing the surface of the bedrock aquifer, were also assigned a boundary function. This function represented the piezometric elevation of the aquifer as it varied with time during the period of interest (Figure 4.3). The piezometric data obtained from the bedrock monitoring well consisted of daily measurements. Data were plotted and a best-fit line was manually plotted through the data in order to reduce the number of data points required to be input into the boundary function as shown in Figure 4.4.

The final boundary function required in the seepage model was not readily apparent at the beginning of the modeling process. During the initial stages of seepage modeling, the model consistently produced results that were significantly higher than those observed along the toe of the riverbank between the regulated and unregulated river levels. The higher piezometric elevations resulted because a boundary condition was not specified for the toe of the riverbank after the river level had dropped. In the case of an actual riverbank, the toe section, between regulated and unregulated river level, remains saturated even though it is no longer submerged. The excess porewater pressures are dissipated by seepage from the toe and by evaporation. In the case of the seepage model, no condition was initially specified to account for porewater pressure dissipation once the toe of the riverbank was no longer submerged. After some initial trial and error a boundary function simulating porewater pressure dissipation from the riverbank toe was found to produce conditions similar to those observed. The boundary function is shown in Figure 4.5. This process is known as 'history matching'.

4.7 FINITE ELEMENT MODELING PROCEDURES

The idealized 6H:1V slope chosen for the research project was initially discretized assuming that a uniform hydraulic conductivity function would be used for the lacustrine clay. With the exception of remedial modeling discussed in Section 5.5, two stratigraphic units were used in the FE seepage model, namely lacustrine clay and till. For most of the modeling, the bedrock aquifer did not have to be included except as a potential boundary. The bedrock aquifer was modelled by assigning a boundary function to the bottom of the glacial till simulating the piezometric surface of the aquifer. Transition zones with smaller elements were used between the clay and the glacial till but otherwise the mesh was relatively uniform in the area of interest. Hydraulic conductivity functions were then assigned to the lacustrine clay and glacial till based on the results of previous research discussed in Section 4.6.1. The final and most important input parameter to be defined was the boundary conditions. As mentioned previously, only two boundary conditions were identified initially, the bedrock aquifer and river level. In both instances the piezometric elevations vary with time as a result of seasonal changes in of bedrock aquifer recharge and lowering of the river level from a regulated to unregulated level. A third boundary condition, simulating porewater pressure dissipation at the riverbank toe, was identified later on in the modeling program as described in Section 4.6.3.

4.7.1 Modeling Interval

The period of interest for the FE modeling was from the last week in August 1992 to the end of November 1992. This period was of interest for three reasons. One, KGS Group

collected extensive piezometric data at the South Perimeter research site during this time period. Two, the time interval encompasses both the recharge of the bedrock aquifer and the lowering of the river level. Third, at the start of the modeling interval the bedrock aquifer has been at a relatively constant elevation for a period of approximately two weeks while the river level has been relatively constant for several months. Under these conditions a steady state approximation was generated for use as the initial conditions in the transient seepage model as discussed in Section 4.6.2.

The time period used was 97 days that were subdivided into half-day time steps for the purposes of the transient FE modeling. Data generated at selected time steps were then used in the model calibration and subsequent stability analysis.

4.7.2 Model Calibration

Calibration was the final step in the FE model development process. The model was calibrated by comparing data observed at the South Perimeter research site with data generated by the model. Nodes were created within the FE mesh that had the same relative location within the idealized section as the pneumatic piezometers at the research site as shown on Table 4.1. Figure 2.16 shows the location of the actual pneumatic piezometers installed and monitored at KGS Group's South Perimeter research site. Computed heads (potentials) from the FE model were compared with the observed data. Depending on the agreement between computed and observed porewater pressures, changes were made to the hydraulic conductivity functions, boundary functions, and FE mesh and the model reanalyzed. The final transient FE mesh is shown Figure 4.6. The hydraulic conductivity boundaries are shown on Figure

4.7 and summarized in Table 4.2. Yuen *et al.* (1998) discuss hydraulic conductivities in clays that are similar to Winnipeg clay. The hydraulic boundaries shown in Figure 4.7 were required to achieve agreement between the observed piezometric data and the computed piezometric data. In the case of the third boundary condition/function, it was the calibration process that led to the need for this boundary function being required. Iteration and adjustment of input parameters continued until the computed results agreed well with the observed data. Results will be discussed in detail in the next chapter.

CHAPTER 5. RESULTS OF SEEPAGE AND SLOPE STABILITY ANALYSIS

5.1 INTRODUCTION

This chapter describes the Finite Element (FE) seepage modeling results and the slope stability analyses that were performed. The first part of the research project was the development of a transient seepage model and integrated seepage-slope stability analyses. The seepage model produced predictions for porewater pressure distributions within an idealized riverbank cross section over a 97-day modeling interval. The porewater predictions were then integrated into slope stability analyses of a generic riverbank. The analyses examined how the safety factor changed as a confined bedrock aquifer (modeling the Upper Carbonate aquifer) recharged and river level decreased from a regulated summer level to an unregulated level.

The second part of the research program examined slope stability using assumed groundwater conditions. The same shear strength parameters were used as in the slope stability analysis that used FE derived porewater pressures but the porewater pressures were now assumed to be represented by a piezometric line (representing the phreatic surface). As is common practice, the porewater pressures were calculated from vertical distances below the piezometric line. These simplified groundwater assumptions were used to determine the validity of such assumptions when detailed piezometric data or groundwater conditions are not available. Comparisons can then be drawn between the two different methods of treating groundwater conditions in slope stability calculations.

5.2 FINITE ELEMENT SEEPAGE ANALYSIS

The FE seepage model was based on an understanding developed from the Winnipeg South Perimeter research site during the late summer and fall of 1992 (KGS Group, 1994). The riverbank at this location was extensively instrumented with a total of sixteen pneumatic piezometers and one bedrock monitoring well (Natural Resources monitoring well OC022). Data collected from the piezometers were used to check that the seepage model was relatively consistent with observed groundwater behaviour. As discussed in Section 4.6.3, the data collected from the bedrock monitoring well at the South Perimeter site was used as one of the boundary conditions in the FE model.

Initially the formulation of the FE seepage model was very simple. However, as the process of verification and calibration continued, the model became increasingly complex. Several model configurations and boundary conditions were examined until the seepage model generated acceptable data. The following section discusses results of the FE seepage modeling.

5.2.1 Finite Element Seepage Analysis Results

As described in Section 4.7 calibration of the seepage model was performed until acceptable results were achieved. This usually means that differences between measured and computed porewater potentials are rather better than ±1m. The results of the FE seepage analysis are presented in Figures 5.1 to 5.16. The FE modeling results are plotted alongside the corresponding pneumatic piezometer results from the South

Perimeter research site. As previously mentioned in Section 4.7.2, the pneumatic piezometer locations are shown in Figure 2.16. Generally, the FE modeling results agree well with the observed piezometric data. Specifically, results are very similar for piezometer locations P3, P8, P11, and P14 (Figures 5.3, 5.8, 5.11, and 5.14, respectively). The similarity is due to the fact that the piezometric elevations in the bedrock aquifer have a controlling influence along this section of the riverbank. The boundary condition (function) assigned to the base of the till layer was based on observed monitoring data from a bedrock well located at the site and therefore it is not surprising that the model data matches closely with observed data. The remainder of the piezometer locations have good agreement with respect to magnitude and trends between the FE generated data and the observed data.

As would be expected, the observed and computed piezometric conditions and responses both reflect the influence of the piezometric boundaries. Near the toe of the slope (Figures 5.1, 5.2, 5.4, and 5.5) piezometric conditions within the clay are influenced by changes in river level. Along the clay-till interface (Figures 5.3, 5.8, 5.11, and 5.14) piezometric conditions are influenced by the bedrock aquifer. However, as observation locations become further removed from the influences of piezometric boundaries, piezometric elevations become more constant. The relatively constant piezometric elevations are illustrated in Figure 5.15 and 5.16 (P15 and 16 locations, respectively). These observation locations are located near the crest of the riverbank and show little piezometric variation during the modeling period.

5.3 SLOPE STABILITY ANALYSIS

Slope stability analysis was performed using two different porewater pressure distributions. First, porewater pressure data generated from the Finite Element Model (FEM) analysis described in Section 4.7.2 and 5.2 were incorporated into the slope stability analysis in the way outlined in Chapter 3. Analysis was then performed at discrete time intervals over the 97-day modeling period. In particular, slope stability analysis was performed to coincide with specific river levels that were selected for ease of modeling in the seepage analysis.

Slope stability analysis was then performed utilizing "hydrostatic" porewater pressure distributions. In the context of the research project, "hydrostatic" refers to groundwater potentials being constant vertically but varying horizontally within the domain of the idealized cross section. A piezometric line was assumed for three different groundwater levels within the idealized slope. This second set of slope stability analysis were performed at the same river levels (time intervals) described in the preceding paragraph.

Results of the stability analysis will be described and compared in the following sections.

5.3.1 Slope stability analysis using FEM generated porewater pressures

Slope stability analysis was performed at discrete time intervals to coincide with particular river levels for the duration of the modeling period as outlined in Section 4.7.1

(Figure 4.2). The time intervals coincide with uniform 0.2m decreases in river level beginning at a river level of 223.9m. The initial slope stability analysis was performed with three combinations of effective shear strength parameters using the concept of a weaker clay layer along the clay-till interface as outlined in Section 4.2.2 and Table 4.3. The results of the initial slope stability analysis are shown on Figures 5.17 to 5.19. The time t = 0 safety factors vary from approximately 1.6 (Figure 5.17) to 1.9 (Figure 5.19). The relatively high safety factor values correspond to the maximum drawdown of the bedrock aquifer and the river level is at its highest level within the modeling duration considered. Under normal conditions this time period is when riverbanks are the most stable. As the bedrock aquifer recharges prior to the river level beginning to drop, FS values slowly decrease with respect to time as porewater pressures at the clay-till interface begin to increase. The final safety factors vary from approximately 1.3 (Figure 5.17) to 1.7 (Figure 5.19). In each figure, 5.17 to 5.19, there is a change in slope at 39 days. This discontinuity represents the first FS values computed after the river level has begun to decrease in elevation. At this time in the modeling duration two factors are now contributing to the decreases in FS values; increasing piezometric elevations in the bedrock and decreasing river level elevations. As shown in Figure 5.40 the recharge of the bedrock aquifer and decrease in river level elevation are relatively linear with respect to time. Therefore the corresponding FS versus time plots also show this relatively linear pattern. The FS values continue to decrease until approximately two-thirds of the way into the modeling duration when they become relatively constant. At this time the river level has stopped decreasing and the piezometric elevation of the bedrock aquifer is relatively constant.

The overall reduction in safety factor during the modeling duration is summarized in Figures 5.20 to 5.22. The decrease in safety factor varied from approximately 13% in

Figure 5.22 to 17% in Figure 5.20. This reduction comprises the effect of the bedrock aquifer recharge and reduction in river level from a regulated to an unregulated level.

Additional slope stability analysis was performed which focused on varying the effective angle of internal shearing resistance (ϕ') while holding the effective cohesion intercept (c') constant. The cohesion intercept was set at $c' = 3$ kPa and ϕ' was selected as 8, 10, and 14°. The additional analysis was required to examine the lower bound of effective shear strength parameters used in the analysis and examine the sensitivity of ϕ' on safety factors. The results of the additional analysis are summarized on Figures 5.23 (FS versus time plot) and 5.24 (% change in FS versus time). The safety factors vary from approximately 1.3 to 1.7 at the beginning of the modeling duration to approximately 1.1 to 1.4 at the end of the modeling duration. The decrease in safety factor varied from approximately 16 to 17%.

5.3.2 Slope stability analysis using assumed groundwater levels

The second part of the research program, outlined in Section 5.1, was performing the stability analyses using assumed groundwater levels. Three groundwater assumptions were chosen to investigate the validity of using such assumptions, in the absence of any piezometric information, when performing in slope stability analysis of riverbanks. The groundwater assumptions used are summarized below:

- Groundwater level along ground surface of riverbank (saturated slope)
- Groundwater level 2m below crest of slope
- Groundwater level 4m below crest of slope

For the 2 and 4m below crest groundwater assumptions, the assumed phreatic surface consisted of a straight line from vertically below the crest of the slope to the point of intersection of the riverbank toe and river level. This is shown more clearly later in Figure 6.6. This range of assumed groundwater levels encompasses typical values assumed for Winnipeg riverbanks when groundwater data is unavailable.

The slope stability analyses used the same shear strength parameters as the initial slope stability analysis described in Section 5.3.1 and also the same river levels. The only difference in the numerical procedure was that the FEM generated porewater pressures were replaced with porewater pressures based on assumed groundwater levels.

Results of these analyses are presented in Figures 5.25 to 5.27 for the same set of shear strength parameters shown in Figures 5.17 to 5.19. Unlike the results presented in Figures 5.17 to 5.19, each figure has three lines of FS versus time values representing the three groundwater assumptions used. In each instance, the plots of FS versus time are constant at the beginning up to day 33 when the river level is constant. However, when the river level begins to decrease, a corresponding reduction in safety factor results since the river level is the only component in this analysis that influences safety factor.

The range in safety factors at the beginning of the analysis period were as follows:

- 1.05 to 1.28 for the groundwater assumed at the slope surface
- 1.26 to 1.55 for an assumed groundwater level 2m below the crest
- 1.35 to 1.65 for an assumed groundwater level 4m below the slope crest

The range in safety factors at the end of the analysis period were as follows:

- 1.0 to 1.26 for a saturated slope groundwater assumption
- 1.17 to 1.53 for an assumed groundwater level 2m below the crest
- 1.25 to 1.61 65 for an assumed groundwater level 4m below the slope crest

The reduction in safety factor for each set of effective shear strength parameters are shown in Figures 5.28 to 5.30. The minimum decrease in safety factor over the modeling duration was approximately 1% for the uniform shear strength case with groundwater at the surface. The maximum decrease in safety factor over the modeling duration was approximately 7% for the weak clay layer shear strength case of $c' = 3$ kPa, $\phi' = 12°$ and groundwater assumed to be 4m below the crest of the slope.

Additional slope stability analyses examined the upper end of the cohesion intercept. Two additional sets of effective shear strength parameters were assigned to the weak clay layer namely:

- $c' = 5$ kPa, $\phi' = 12°$
- $c' = 7$ kPa, $\phi' = 12°$

The additional slope stability analysis was performed since initial combinations of effective shear strength parameters produced relatively low safety factors. A summary of the additional slope stability analyses is summarized on Figures 5.31 and 5.32. The reduction in safety factors for the two additional effective shear strength parameters are shown on Figures 5.33 and 5.34. The reductions are generally small.

5.4 COMPARISON OF SLOPE STABILITY ANALYSIS RESULTS

One of the goals of the research was to examine the influence of piezometric conditions on slope stability analysis. Two different methods of determining porewater pressures were used, namely assuming a groundwater level and simulating observed piezometric conditions by performing FE seepage analysis. For each of these two piezometric conditions, the same set of effective shear strength parameters were input into the slope stability model and FS values computed. The computations have been summarized in Section 5.3. Figures 5.35 to 5.37 compare the results of the slope stability analysis performed. Each figure consists of an FS versus time plot for a particular set of effective shear strength parameters. The comparisons drawn are with respect to time during the modeling duration and are summarized below:

- Early time – bedrock aquifer beginning to recharge, river level constant
- Intermediate time – bedrock aquifer continuing to recharge, river level decreasing
- Late time – bedrock aquifer near completion of recharge, river level constant

5.4.1 Early Time Comparison

During the initial period of the analyses, approximately 33 days, safety factors generated using the assumed groundwater levels are significantly lower than those generated using the FEM porewater pressures. This is primarily because the porewater pressures along the slip surface are much lower using the FEM porewater pressures compared to assumed groundwater levels. This is illustrated in Figures 5.38 and 5.39 which are for a riverbank modelled with a weak layer at $c' = 3$ kPa, $\phi' = 12°$ and without a weak clay

layer, respectively. Figures 5.38 and 5.39 show the distribution of porewater pressures along the base of the slip surface for three of the groundwater assumptions used in the stability analysis at the start of the analysis duration (0 days). Given the same effective shear strength parameters, the FEM porewater pressures will produce higher safety factor results because porewater pressures are lower along the base of the slip surface at this time. The lower porewater pressures are due to the porewater pressure assumptions used in the analysis. At the beginning of the modeling duration the bedrock aquifer is at its lowest point and has a controlling influence on the porewater pressures at the base of the slip surface. Even based purely on observation of bedrock monitoring wells, this time period is when the bedrock aquifer has been drawn down to its minimum annual piezometric elevation.

5.4.2 Intermediate Time Comparison

During the intermediate time duration (days 33 to 76) two critical piezometric events occur. The river level decreases from its maximum regulated value to its minimum unregulated value and the piezometric elevation of the bedrock aquifer increases to a maximum value within the modeling duration. These events result in the greatest reduction in safety factor per time increment of the entire modeling duration. The rate of FS decrease is highest in the FEM based stability analysis because both the recharge of the aquifer and lowering of the river level (Figure 5.40) combine to lower FS values as shown in Figures 5.35 to 5.37. The FS values generated using FEM porewater pressures are initially much higher than the FS values generated using hydrostatic porewater pressures. However, by the end of the modeling increment the FS values are beginning to converge. Specifically, the assumed groundwater level at 4m below the

crest of the riverbank is comparable to the FEM based slope stability analysis. The porewater pressure distributions taken at the middle of the modeling duration are shown in Figures 5.41 and 5.42. The difference in porewater pressure distributions of Figures 5.41 and 5.42 is related to slip surface shape. The weak clay layer produces a composite slip surface tangent to the clay-till interface while the "no weak layer" analysis produces a circular slip surface (discussed in Section 6.3.1). The different slip surface geometries produce different porewater pressure distributions along each slip surface. The porewater pressures along the base of the slip surface have not changed in magnitude for the assumed groundwater levels but have initially increased and then decreased slightly for the FEM computed porewater pressures.

5.4.3 Late Time Comparisons

During this final modeling increment (days 76 to 97), the river level is constant while the bedrock aquifer fluctuates slightly. Values of FS calculated using the FEM groundwater assumptions are still higher than the two assumed groundwater levels used but are relatively similar if the groundwater is assumed 4m below the crest (Figures 5.35 to 5.37). Corresponding porewater pressure distributions along the base of the slip surfaces are shown in Figures 5.43 and 5.44.

5.5 RIVERBANK REMEDIATION ALTERNATIVES

One of the objectives of the research program stated in Section 1.3 was to investigate alternative remediation techniques. The most common technique used to remediate

failed or failing riverbanks is replacing clay with crushed or uncrushed "shot rock" limestone from quarries north of Winnipeg. Typically, soil is excavated at the toe of the slope and replaced with limestone. The excavation may consist of either a backhoe-excavated slot or large diameter drilled boreholes that key into the underlying till. Secondary methods of slope remediation include large diameter limestone rip rap erosion protection at the riverbank toe and slope regrading which typically supplement soil replacement. These methods are usually extremely invasive and are often accompanied by riverbank movement. These techniques of riverbank remediation have been used successfully at several locations along the banks of the Red and Assiniboine Rivers within Winnipeg.

The increase in safety factor achieved by soil replacement and rip rap is typically around 30%. Economics and practicality often limit this increase in safety factor. Larger increases could be ultimately achieved but the costs and physical space required to construct such options would not be practical.

The current techniques of riverbank remediation have been examined and analyzed in great detail by the local consulting community and will not be revisited here. From an analytical perspective a new technique will be considered.

5.5.1 Riverbank remediation by groundwater withdrawal from the bedrock aquifer

Results presented in the preceding sections indicate that piezometric elevations in the bedrock aquifer have a controlling influence on the stability of riverbanks in Winnipeg. In this regard groundwater withdrawal from the bedrock aquifer was considered as

riverbank remediation alternative. From an analytical perspective, decreasing piezometric elevations within the bedrock aquifer would have a positive influence on the safety factor of a riverbank.

The FE seepage model developed and used to perform the seepage analysis was altered to accommodate groundwater withdrawal from the bedrock aquifer. Eight meters of bedrock was added to the bottom of the cross section shown in Figure 4.6 representing the layer of most active groundwater flow within the bedrock aquifer (Render 1970). The boundary condition (function) representing piezometric elevations with the bedrock aquifer was moved from the base of the till layer to the base of the bedrock layer. To ensure compatibility of results using the altered FE model with the original seepage analysis, two checks were performed. First, seepage analysis calculations performed with the altered FE mesh (additional 8m of bedrock at bottom) were compared with the results from the original FE mesh (without bedrock). Second, the slope stability analysis described in Section 5.3.1 was also repeated. In both instances the results generated using the altered FE model were virtually identical to those generated in the original FE model. Therefore, subsequent analysis calculations (seepage and stability) would only be influenced by groundwater withdrawal from the bedrock aquifer and could be compared to the original seepage and stability calculations.

The pumping location(s) within the bedrock aquifer layer were then selected. Several combinations of single and double pumping locations as well as pumping rates were examined until a suitable combination of pumping rate and location was achieved. The results of the groundwater withdrawal from the bedrock aquifer are presented below.

5.5.2 Results of alternative remediation techniques

A system of two pumping wells spaced at 25m (Figure 5.45) was determined to be the best combination and location based on limited optimization. The wells were pumped at a rate of $2.5x10^{-3}$ m^2/sec/m that is approximately a half order magnitude higher than the hydraulic conductivity assumed for the bedrock aquifer (Render 1970) used in the FE model. The wells were pumped continuously from the beginning of the modeling duration to the end of the modeling duration. Figures 5.46 and 5.47 illustrate the change in porewater pressures along the base of slip surfaces at the end of the modeling duration using two different effective shear strength combinations.

The new FE porewater pressures were incorporated into the slope stability analysis as in Section 5.3.1. The results of the slope stability analysis are shown on Figures 5.48 and 5.49, plotted with the safety factors computed from the original FE porewater pressure distributions. There is a significant increase in safety factor resulting from groundwater withdrawal from the bedrock aquifer. The increase in safety factor is shown on Figures 5.50 and 5.51 and is approximately 25%.

The implications of pumping from the bedrock aquifer are briefly discussed in Section 6.5.

CHAPTER 6. DISCUSSION OF SEEPAGE AND SLOPE STABILITY RESULTS

6.1 INTRODUCTION

Chapter 1 listed the following objectives of this study:

1. To determine relationships between piezometric elevations in the Agassiz clay, piezometric elevations in the bedrock aquifer, river level, and slope stability using a finite element (FE) seepage model.
2. To determine the validity of current piezometric assumptions when performing slope stability computations.
3. To investigate alternative slope remediation techniques.

These objectives require study because the current piezometric trends indicate that the bedrock aquifer is in a period of recharge, due to less consumption of groundwater by local commercial/industrial users. If this trend continues, piezometric elevations in the bedrock aquifer may reach the highest levels experienced in the last 80 years. Such an increase in piezometric elevations could result in increased incidents of riverbank movements and failures.

The variation of piezometric elevations in the bedrock aquifer is well defined. The Water Resources Department of the Manitoba Department of Natural Resources has been monitoring piezometric elevations in the bedrock aquifer for many decades through a series of monitoring wells. However, data have never previously been incorporated into slope stability analyses. The data used in the slope stability analyses have been

described in Chapter 4 and the subsequent FE seepage modeling and slope stability analyses described in Chapter 5.

This chapter will examine the significance of the results presented in Chapter 5. Specifically, groundwater assumptions will be examined with respect to observed riverbank movements.

6.2 DISCUSSION OF FEM SEEPAGE ANALYSIS RESULTS

The FE seepage model was based on a range of known hydraulic properties of Winnipeg lacustrine clays and tills coupled with observed piezometric results from a research site (KGS Group 1994). The FE seepage model was calibrated to produce piezometric conditions that were similar in magnitude and behaviour to piezometric conditions observed.

The results, shown in Figures 5.1 to 5.16, indicate that the FE seepage model was able to produce similar piezometric conditions to those observed based on the modeling techniques employed. It must be stated that no new hydraulic conductivity testing (laboratory or in situ) was performed on the soils at the South Perimeter research site. It is difficult, therefore, to comment on how accurately the hydraulic properties used in the seepage model reflect the actual properties at the research site. The hydraulic properties used in the seepage model fall within the range of observed hydraulic conductivities described in previous research but information on specific hydraulic properties at the research site was not available.

An additional fact to be considered is that the piezometric observation locations (nodes) within the FE seepage model were not in the identical location of the piezometers installed in the riverbank at the research site. As discussed in Section 4.7.2 and shown in Table 4.1, the observation locations used were chosen to be as close to the actual piezometer locations as was permitted by FE mesh construction. These differences in location will contribute to some uncertainty of the results of the FE seepage calculations.

Overall, the FE seepage model produced piezometric results that were comparable (±1m) to observed piezometric conditions at the South Perimeter research site. It is therefore logical to assume that use of these FE seepage results into slope stability analysis should produce reasonable results with regards to piezometric conditions.

6.2.1 Impact of Porewater Pressure Assumptions on Laboratory Testing

Selecting correct porewater pressure assumptions is probably the single most important criterion in establishing the stress state of a laboratory specimen that has been sampled at depths below the phreatic surface. Once a specimen has been removed from its sampling device it is no longer at the total stress state where it originated. To determine the behaviour and shear strength properties of the specimen at the depth it was obtained from, it must be returned to its original stress state. In order to do this however, the stresses at depth must first be calculated. Typically, a groundwater elevation is assumed and the overburden stresses are calculated based on the unit weight of the soil. In Winnipeg, previous researchers have often assumed a hydrostatic groundwater elevation three meters below ground surface in order to determine the effective stresses below the water table. Figure 6.1 shows the porewater pressure distribution versus

depth, in terms of total head, of such a hydrostatic groundwater assumption compared with the porewater pressure distribution computed from the FE seepage model in this research project. The total head distribution of the hydrostatic assumption is constant with depth. This contrasts with the decreasing total head distribution of the FE model. The decreasing total head with depth relationship is a result of a downward groundwater flow direction from the clays towards the glacial tills and bedrock. Figure 6.2 shows porewater pressure distribution versus depth, in terms of pressure head, for the same conditions as in Figure 6.1. At a depth of approximately fifteen meters below ground surface (elevation 217.0m) the difference in porewater pressure is approximately 50 kPa. Depending on location within the City of Winnipeg and on the time of year, this difference in porewater pressure could be more or it could be less. An example of this type of piezometric distribution is shown in Figure 6.3 at the Brady Road landfill during June to August, 1986 (City of Winnipeg Hydrogeologic Study, Brady Road Landfill, UMA Engineering Ltd., 1987). Given the porewater pressures for an assumed hydrostatic distribution, specimens would have been routinely isotropically consolidated at stresses that were less than actual values.

6.3 DISCUSSION OF RESULTS OF SLOPE STABILITY ANALYSIS

The slope stability analysis performed during the research utilized two different groundwater or piezometric conditions. The first was based on porewater pressures obtained from FE seepage analysis. The second assumed a groundwater or phreatic surface within the idealized riverbank. The use of porewater pressures determined from FE analysis in riverbank stability analysis has not been done in Winnipeg due to economic factors and time constraints. The latter assumption (of a phreatic surface)

represent the groundwater assumptions typically used when determining safety factors (FS) of riverbanks in Winnipeg.

The slope stability analysis focused on using the same effective shear strength parameters and comparing results obtained for the two different groundwater conditions during the period that was being modelled. Each set of shear strength parameters produced results that were always higher for FE groundwater conditions than for assumed (hydrostatic) groundwater conditions. The largest difference in safety factor values occurred at the beginning of the modeling duration when the bedrock aquifer is at its lowest annual piezometric elevation (for example Figure 4.2). As the modeling period advances, safety factors calculated from FE groundwater conditions decrease at a greater rate than those calculated using assumed groundwater conditions. By the end of the modeling duration, the FS results for the two groundwater conditions are much closer together. This was shown in Figures 5.35, 5.36, and 5.37. The FS results converge because of the differing influences of the groundwater conditions used. In the case of the FE groundwater condition, the decrease in FS is due to a decrease in river level as well as an increase in piezometric elevation in the bedrock aquifer (Figure 5.40). The decreases in FS using assumed groundwater condition are slower and are only related to the lowering of the river level from a regulated to an unregulated level. If the porewater pressures along slip surfaces are examined for each of the two groundwater conditions (Figures 5.38 and 5.39 and Figures 5.41 to 5.44), the FE groundwater conditions are initially much lower than the assumed groundwater conditions but increase during the modeling duration as the bedrock aquifer recharges.

As a separate exercise, an examination was made of the effects of individually changing the river level with constant aquifer potentials, and changing the aquifer potentials with

constant river levels using a steady state approximation for each set of conditions. Conditions that were examined include:

a) Aquifer potential constant at 222.8m, river level at 223.9, 223.1, and 222.1m
b) Aquifer potential constant at 224.2m, river level at 223.9, 223.1, and 222.1m
c) River level constant at 223.9m, aquifer potential at 222.8 and 224.2m
d) River level constant at 223.1m, aquifer potential at 222.8 and 224.2m
e) River level constant at 222.1m, aquifer potential at 222.8 and 224.2m

In each of these cases, the reduction in safety factor varied between 10 and 12%. Based on this analysis as well as the transient analysis shown earlier, it appears that river level decreases and bedrock aquifer recharge produce approximately the same reduction in safety factor at this site and are relatively independent of each other over the modeling duration.

Given the two different groundwater conditions used for the slope stability analysis, the porewater pressures are lower along more of the slip surface for the FE groundwater conditions compared with the assumed groundwater conditions. The lower porewater pressures (from the FE seepage analysis) produce lower FS values throughout the modeling duration.

6.3.1 Slip Surface Geometry

Slip surface geometry can have a significant impact on computed safety factors particularly if a section of the slip surface is subject to changes in porewater pressures or

loading conditions. Slip surface geometry is a function of several factors, including porewater pressure conditions and shear strength. These points are illustrated in Figures 6.4 to 6.11. Figures 6.4 and 6.5 show the failure surface geometry for an assumed saturated slope with no weak clay layer. The figures show "worst case" circular surfaces at the beginning and at the end of the modeling duration, respectively. For this case the slip surface geometry does not change significantly and as a result is not greatly impacted by the decreasing river levels as shown on Figures 5.27 and 5.30. The safety factor does not change significantly even though the river level has dropped from regulated to unregulated levels. Figures 6.6 and 6.7 show the slip surface geometry for the same conditions as Figures 6.4 and 6.5 but the groundwater is now assumed to be four meters below the crest of the slope. In Figure 6.6, the slip surface is circular but by the end of the modeling duration (Figure 6.7) the slip surface has become composite. That is, it consists of circular sections at the crest and toe that are joined by a linear portion along the clay-till interface. As indicated in Figures 5.27 and 5.30 the change in safety factor is greater than when the assumed groundwater level is coincident with the ground surface.

Figures 6.8 and 6.9 show the slip surface for the saturated slope case but with a weaker clay layer at the clay-till interface. The slip surface geometry starts off being composite because of the weaker clay layer. As the river level drops, the linear portion of the slip surface along the clay-till interface increases in length. This results in the slip surface exiting well into the river. As a result, the safety factor is influenced by the river level to a greater extent compared to a cross section without a weak layer. Finally, Figures 6.10 and 6.11 show the slip surface geometry, at the beginning and end of the modeling duration, respectively, for FEM computed porewater pressures and no weak clay layer.

The resulting slip surfaces are similar to those produced in Figures 6.6 and 6.7. In both instances the slip surface geometry is initially circular but gradually becomes composite.

Based on these observations, an assumed saturated slope with uniform shear strengths produces slip surfaces that are unrealistic. However, if the groundwater is assumed to be four meters below the crest of the riverbank, the slip surface tends to become composite and is more adversely impacted by reduced river levels producing more realistic safety factors. Similarly, slip surfaces calculated using the FE porewater pressures are initially circular but become composite. This may be a result of the lower groundwater levels in riverbanks or slopes tending to force slip surfaces deeper due to increased unit weights of the soils above the water table. It may support the observation that a "saturated slope" assumption is unrealistic because it does not produce a typical composite slip surface under unregulated river levels. It also supports the observation that groundwater levels in riverbanks are 3 to 4m below the crest of the slope since a groundwater assumption of 4m below the crest produces similar slip surfaces compared with FE assumed groundwater elevations.

6.4 OTHER FACTORS AFFECTING RIVERBANK STABILITY

The research examined the influence of only one variable on the stability of riverbanks, namely groundwater conditions. However, many other factors can also influence the stability of a riverbank. Most of these factors are difficult to quantify but their potential influence on riverbank stability is understood. The most obvious of these factors are discussed below.

6.4.1 Location

Location is one of the most important factors not considered in this project. The research used piezometric data observed at the South Perimeter research site for developing the FE seepage model. The South Perimeter site is located approximately ten kilometers from the center of Winnipeg which is also approximately the center of the bedrock aquifer drawdown cone. Piezometric conditions in the bedrock aquifer used in the project will be different from conditions closer to the center of the drawdown cone. This can be seen by examining bedrock aquifer hydrographs for monitoring wells located at the periphery of Winnipeg (Figure 2.10b) and near the center of Winnipeg (Figure 2.10c). The trends are similar with respect to recharge and drawdown cycles but the magnitudes of the maximum and minimum piezometric elevations are quite different. With respect to absolute FS values, riverbanks located closer to the center of Winnipeg will be more stable than those considered in this project, but reductions in FS produced by river lowering and aquifer recharge will be greater. Therefore while the fluctuation in river level is relatively constant from location to location along Winnipeg rivers, the piezometric elevations in the bedrock aquifer will not be the same and may have to be evaluated on a site by site basis. Further sensitivity analysis may produce useful results.

6.4.2 Riverbank Geometry

As outlined in Section 4.3, the idealized cross section used in this research was chosen on the basis of initial slope stability analysis and the morphology of natural riverbanks. Obviously, different riverbank geometries will influence results of slope stability analysis. Specifically, the geometry of the upper portion of a riverbank, from the crest to the

regulated summer river level, has the most significant influence on riverbank stability. All things being equal, the flatter this upper slope the greater the safety factor. Steeper slopes produce lower safety factors.

6.4.3 Erosion

Erosion is a significant contributor to riverbank instability by reducing mass at the toe and decreasing forces resisting riverbank movement. Erosion was not considered in the research project due to the complexity required to model both seepage and erosion together. For each change in geometry associated with erosion at the toe, a new FE mesh would be required for seepage analysis. This was not included in the program.

The effects of erosion are not typically the result of a single year but are the cumulative effect of several years of erosion. The erosion is most evident on the outside bends of riverbanks where velocities are greatest. The erosion is the result of a rivers' tendency to meander when velocities are relatively low (no downcutting) and the gradient of the river is relatively low. Such is the case of the Assiniboine and Red Rivers in Winnipeg, particularly under winter ice cover. Both rivers contain meanders that result in higher velocities on the outside bends. These higher velocities result in erosion of the toe. Typically the maximum erosion will occur between the unregulated river level and the river bottom. This section of the riverbank is continuously exposed to current and is unvegetated. The decrease in safety factor is difficult to quantify without accurate yearly soundings of the river bottom to identify loss in soil. However, experience from this research suggests it would be realistic to estimate that reductions in safety factor could be in the order of five to ten percent. Although this does not seem like a dramatic

decrease in safety factor, it does become critical when other influences such as annual bedrock aquifer recharge and allowing river levels to decrease to unregulated levels are considered.

6.4.4 Vegetation

Vegetation has a significant role in riverbank stability with regards to both strength (reinforcement) and porewater pressure influences. Increases in effective shear strength parameters of soil have been measured and attributed to soil-root interaction. For example the contribution of strength from tree roots was estimated to be 5.9 kPa (Wu *et al.* 1978) for shallow slip surfaces in cohesionless soils. Tree root tensile strength has also been measured and found to be as high as 25% of the tensile strength of mild steel (Greenway 1987). For trees such as Poplar the range in tensile root strength is in the order of 30 to 50 MPa. Recent research (Wu and Watson 1998) has shown that for a thick shear zone the shear strength contribution of root mass is much less than previously reported. However, the estimated contribution of a root mass was still approximately 30% of the estimated soil resistance. Therefore, a riverbank within mature trees (especially at the crest) would be much more stable than a riverbank without such vegetation. A network of mature tree roots would act similar to reinforced earth by provided tensile reinforcement against movement. However, when trees age and topple, the root mat can cause severe damage to slopes and accelerated scour patterns under flood conditions.

Vegetation is also an important factor when considering influences of porewater pressures on riverbank stability. Vegetation can reduce piezometric elevations in the soil

in two ways. Vegetation increases evapotranspiration and also limits the amount of water entering the soil by interception. The pore system of vegetation generates capillary suctions that virtually "suck up" water from the region of the roots. This dramatically reduces the amount of water accessible to the soil. Depending on the depth, the root systems can increase soil strength while decreasing hydraulic conductivity by increasing suctions or making the soil more unsaturated. Vegetation can also increase infiltration into soils. Below the ground surface, roots can cause shrinkage and desiccation in soils creating cracks that will increase infiltration. At the ground surface vegetation, particularly grasses, can slow runoff allowing increased time for infiltration.

The second way vegetation can reduce infiltration is by interception. This method is limited primarily to trees and is also a function of rainfall intensity. Trees can intercept a significant amount of rainfall depending on the type and density of trees and also on rainfall intensity. Generally, the denser the concentration of trees the smaller the percentage of rainfall that will reach the ground surface.

6.5 BEDROCK AQUIFER PUMPING AS A REMEDIAL OPTION

Although this technique of remediation is analytically viable, several issues need further clarification, including the following. First, the pumping rate selected for the analysis was significantly lower than an actual pumping rate would be if such a system were to be employed. The limitation is due to the fact that SEEP/W cannot model fractured flow and therefore the subsequent drawdown area achieved in the model was much smaller than would occur in practice as shown in Figure 6.12. This resulted in the need for two pumping wells in the model but in reality only one well would probably be required since

a much larger pumping rate could be selected creating a much larger area of influence. The pumping rate to be selected in practice would depend on the condition of the bedrock, that is how intact or fractured the bedrock is. Second, where would the pumped water be disposed of and what, if any, would be the possible environmental impacts? Recharge into the aquifer is a possibility in an area away from the riverbank.

Obviously, the environmental impacts would have to be assessed if groundwater from the bedrock aquifer was discharged into a river. However, groundwater discharge from the bedrock aquifer does naturally occur along the Red River downstream of Winnipeg in the St. Andrews, Manitoba area and between Lockport and Selkirk, Manitoba. A major environmental concern would be the salinity of the water being pumped from the bedrock aquifer and the possibility of salt-water intrusion if the pumping rate were too great. To avoid this situation a series of smaller wells could be used in order to provide the desired drawdown over a section of riverbank. Smaller pumping rates, enough to keep the bedrock aquifer at a level to improve overall bank stability, could be used without the potential for environmental problems. The amount of aquifer drawdown is small, in the order of 2m, to effectively reduce its destabilizing effect on riverbank stability.

CHAPTER 7. CONCLUSIONS

7.1 CONCLUSIONS

This program of research was designed to provide an improved understanding of riverbank stability in Winnipeg. Specifically, it investigated the influence of transient groundwater conditions on riverbank stability. Modeling utilized observed groundwater data superimposed on an idealized riverbank cross section that was similar to the riverbank cross section where the piezometric data was collected. Groundwater conditions developed in the seepage analyses were then incorporated into slope stability analyses. Results were then compared to parallel computations using assumed groundwater conditions that were typical of current local practice.

The objectives of the research program were listed in Chapter 1 and reviewed in Chapter 6. They will not be described here. Results presented in Chapters 4 and 5 indicate that the objectives have been generally met.

As stated in Section 1.2 the hypothesis of the research program was: "Seasonal changes in groundwater potentials have significant impact on riverbank behaviour in Winnipeg and should be incorporated into slope stability analyses". The following conclusions can be made.

7.1.1 Major Conclusions

1. A finite element seepage model was developed which reasonably predicted porewater pressure conditions when compared to observed piezometric behaviour within a natural riverbank.
2. The seepage and slope stability modeling performed were based on site-specific data. The results, therefore, are only valid for the site selected in the research program. However, it is likely that generally similar observations and results would be expected at other locations along the Red River.
3. Lowering of the Red River from a regulated to an unregulated level during the fall and accompanying, though independent, recharge of the bedrock aquifer have approximately the same net destabilizing influence on riverbank stability for the site selected in the research program.
4. The commonly used assumption of a "saturated slope" significantly overestimates the porewater pressures within these riverbanks. A less conservative assumption using a groundwater level four meters below the crest is a much better approximation under conditions of substantial bedrock aquifer recharge and unregulated river level.
4. The trend of increased non-consumptive usage of groundwater for industrial and commercial purposes may lead to increasing incidences of riverbank failure in Winnipeg. Although no clear record of riverbank failure occurrences is available the data suggest that there may be an increasing trend toward more riverbank failures or at the very least riverbank movements.

7.1.2 Minor Conclusions

1. Previous laboratory testing of Winnipeg clays should be re-examined in light of the porewater pressure distributions obtained from the finite element seepage model. Specifically, strength test results of samples obtained from within a few meters of the clay-till interface should be re-examined to investigate the influence of utilizing assumed porewater pressures that may be higher than the real ones.
2. The integrated seepage-slope stability model is only valid for the location where the original piezometric observations were made.
3. Groundwater withdrawal from the bedrock aquifer has been shown to be a technically possible method of improving the stability of a riverbank. Economic and environmental impacts remain to be investigated.

7.2 RECOMMENDATIONS FOR FUTURE RESEARCH

The research program undertaken had a narrow focus, only considering the influence and interaction of groundwater systems on riverbank stability. The research has advanced the understanding of riverbank stability but is only one piece of a larger puzzle. Additional research and study is required to incorporate aspects of riverbank stability not considered in this research program. Some of these aspects are summarized below.

1. Establish two or three riverbank monitoring sites along the Red River instrumented with piezometers and slope inclinometers. Ideally the sites would

be along riverbanks that experience different seasonal piezometric conditions in the bedrock aquifer. The data gathered could then be used to develop a better understanding of the influence of the bedrock aquifer and its impact on riverbank stability. It may be possible that a simpler groundwater-slope stability model could be developed that doesn't require FE seepage analysis but rather piezometric data, based on observation, input directly into slope stability software.

2. Investigate the influence of porewater pressures on laboratory test results of Winnipeg clays especially within the zone influenced by the bedrock aquifer.
3. Examine the influence of suctions due to unsaturated soils on shear strength and permeability in the upper few meters of the soil profile.
4. Determine if a correlation exists between riverbank movements or failures and piezometric conditions. It may be possible to identify areas more susceptible to riverbank movements based on their location.
5. Quantify the annual loss in riverbank toe due to erosion of unprotected slopes and translate this into an annual decrease in safety factor.

REFERENCES

Baracos, A. 1960. "The Stability of River Banks in the Metropolitan Winnipeg Area." Proc. 14th Canadian Soil Mechanics Conference, NRCC Technical Memo. No. 69, 185-198.

Baracos., A. 1977. "Compositional and structural anisotropy of Winnipeg soils - a study based on scanning electron microscopy and X-ray diffraction analysis." Canadian Geotechnical Journal, 14, 125-137.

Baracos, A. 1978. "The Effects of River Levels, Groundwater and Other Seasonal Changes on River Banks in Winnipeg." 31st Canadian Geotechnical Conference, Winnipeg, Manitoba.

Baracos, A. and Graham, J. 1981. "Landslide Problems in Winnipeg." Canadian Geotechnical Journal, 18, 390-401.

Baracos, A., Graham, J. and Domaschuk, L., 1980. "Yielding and rupture in a lacustrine clay." Canadian Geotechnical Journal, 17, 559-573.

Baracos, A., Shields, D.H, and Kjartanson, B.H. 1983a. Geological Engineering Maps and Report for Urban Development of Winnipeg. February 1983, Cantext Publications, Winnipeg, Manitoba.

Baracos, A., Graham, J., Kjartanson, B.H., and Shields, D.H. 1983b. "Geology and soil properties of Winnipeg." Geological Environment and Soil Properties. ASCE Convention, Houston, TX, October 1983, 39-56..

Crawford, C. B., 1964. "Some Characteristics of Winnipeg Clay." Canadian Geotechnical Journal, 1(4), 227 -235.

Fenton, M., Moran, S., Teller, J., and Clayton, L., 1983. "Glacial Lake Agassiz" Special Paper 26, Geological Association of Canada, 49-74.

Fredlund, D.G. 1978. "Usage, Requirements and Features of Slope Stability Computer Software (Canada, 1977)." Canadian Geotechnical Journal, 15, 83-95.

Fredlund, D.G. and Krahn, J. 1977. "Comparison of Slope Stability Methods of Analysis." Canadian Geotechnical Journal, 14, 429-439.

Fredlund, D.G., Zhang, Z.M., and Lam, L. 1992. "Effect of the axis of moment equilibrium in slope stability analysis." Canadian Geotechnical Journal, 29, 456-465.

Freeman, W.S. and Sutherland, H.B., 1974. "Slope Stability Analysis in Anisotropic Winnipeg Clays." Canadian Geotechnical Journal, 11(1), 59-71.

Graham, J. 1979. "Embankment stability on anisotropic soft clays." Canadian Geotechnical Journal, 16, 295-308.

Graham, J. 1984. "Methods of Slope Stability Analysis" in D. Brundsen and D.B. Prior, "Slope Instability", John Wiley & Sons Ltd., New York.

Graham, J., 1986. "Slope Stability Analysis: Applications in Plastic Clays." 34th Annual Soil Mechanics and Foundation Engineering Conference, Minneapolis, MN.

Graham, J. and Au, V.C.S. 1985. "Effects of Freeze-Thaw and Softening on a Natural Clay at Low Stresses." Canadian Geotechnical Journal, 22, 69-78.

Graham, J., Noonan, M.L., and Lew, K.V. 1983. "Yield states and stress-strain relationships in a natural plastic clay." Canadian Geotechnical Journal, 20, 502-516.

Graham, J. and Shields, D.H., 1985. "Influence of Geology and Geologic Processes on the Geotechnical Properties of a Plastic Clay." Engineering Geology, 22, 109-126.

Graham, J., Lew, K.V., de Tremaudan, F., and McRae, K.J. 1987. "Circular and Non-Circular Analysis of Slopes by Microcomputer." First Canadian Symposium on Microcomputer Applications to Geotechnique, Regina, Saskatchewan.

Gray, D.H. and Sotir, R.B., 1992 "Biotechnical Stabilization of Highway Cut Slope" ASCE Journal of Geotechnical Engineering, 118 (9), 1395-1409.

Greenway, D. R. 1987. "Vegetation and Slope Stability" in M. G. Anderson and D.S. Richards, "Slope Stability", John Wiley & Sons Ltd., New York.

Hamilton, A. 1995. "The Influence of Porewater Pressures on Slope Stability in Winnipeg: A Back Analysis of Riverbank Instability on the Red River at St. Mary's Road and the Perimeter Highway." B.Sc. Thesis, University of Manitoba.

Lafleur, J. and Lefebvre, G. 1980. "Groundwater Regime Associated with Slope Stability in Champlain Clay Deposits." Canadian Geotechnical Journal, 17, 44-53.

Lefebvre, G. 1981. "Strength and slope stability in Canadian soft clay deposits." Canadian Geotechnical Journal, 18, 420-442.

Lefebvre, G. 1986. "Slope Instability and Valley Formation in Canadian Soft Clay Deposits." Canadian Geotechnical Journal, 23, 261-270.

Lew, K.V. and Graham, J., 1988. "Riverbank Stabilization by Drains in Plastic Clay." Proc. of the Fifth International Symposium on Landslides, Lausanne, Switzerland.

Loh, A.K. and Holt, R.T. 1974. "Directional Variation in Undrained Shear Strength and Fabric of Winnipeg Upper Brown Clay." Canadian Geotechnical Journal, 11, 430-437.

Misfeldt, G.A., Sauer, E.K., and Christiansen, E.A. 1991. "The Hepburn Landslide: An Interactive Slope-Stability and Seepage Analysis." Canadian Geotechnical Journal, 28, 556-573.

Mishtak, J., 1964. "Soil mechanics aspects of the Red River Floodway." Canadian Geotechnical Journal, 1(3), 133-146.

Morris, P.H., Graham, J., and Williams, D.J. 1992. "Cracking in Drying Soils." Canadian Geotechnical Journal, 29, 263-277.

Peterson, R., Jaspar, J.L., Rivard, P.J., and Iverson, N.L. 1960. "Limitations of laboratory shear strength in evaluating stability of highly plastic clays." ASCE, Research conference on shear strength of cohesive soils, 765-.

Quigley, R.M., 1968. "Soil Mineralogy, Winnipeg Swelling Clays." Canadian Geotechnical Journal, 5, 120-122.

Quigley, R.M., 1980. "Geology, mineralogy, and geochemistry of Canadian soft soils: a geotechnical perspective." Canadian Geotechnical Journal, 17, 261-285.

Render, F.W., 1970. "Geohydrology of the Metropolitan Winnipeg Area as related to ground water supply and construction." Canadian Geotechnical Journal, 7(3), 243-274.

Rivard, P.J. and Lu, Y. 1978. "Shear Strength of Soft Fissured Clays." Canadian Geotechnical Journal, 15, 382-390.

Sutherland, H.B., 1966. "The stability of the river banks in the Winnipeg area." Unpublished report to the Rivers and Streams Authority, No. 1, Winnipeg, Mb.

Teller, J.T. and Clayton, L., 1983. "Glacial Lake Agassiz" Special Paper 26, Geological Association of Canada, 3-5.

Teller, J.T. and Fenton, M. M., 1980. "Late Wisconsinan glacial stratigraphy and history of southeastern Manitoba." Canadian Journal of Earth Sciences, 17, 19-35.

Teller, J.T., 1976. "Lake Agassiz deposits in the main offshore basin of southern Manitoba." Canadian Journal of Earth Sciences, 13, 27-43.

Wright, C. 1993. "The Role of Groundwater in the Understanding of Slope Stability." B.Sc. Thesis, University of Manitoba.

Wu, T.H., Beal, P.E., and Lan, C. 1988. "In-situ Shear Test of Soil-Root Systems" ASCE Journal of Geotechnical Engineering, 114 (12), 1376-1394.

Wu, T.H., McOmber, R.M., Erb, R.T., and Beal, P.E. 1987 "Study of Soil-Root Interaction" ASCE Journal of Geotechnical Engineering, 114 (12), 1351-1375.

Wu, T.H., McKinnell III, W.P., and Swanston, D.N. 1979 "Strength of Tree Roots and Landslides on Prince of Wales Island, Alaska." Canadian Geotechnical Journal, 16, 19-33.

Wu, T.H. and Watson, A. 1998 "In Situ Shear Tests of Soil Blocks With Roots" Canadian Geotechnical Journal, 35, 579-590.

Yuen, K., Graham, J., and Janzen, P. 1998. "Weathering-induced fissuring and hydraulic conductivity in a natural plastic clay" Canadian Geotechnical Journal, 35, 1101-1108.

FIGURES

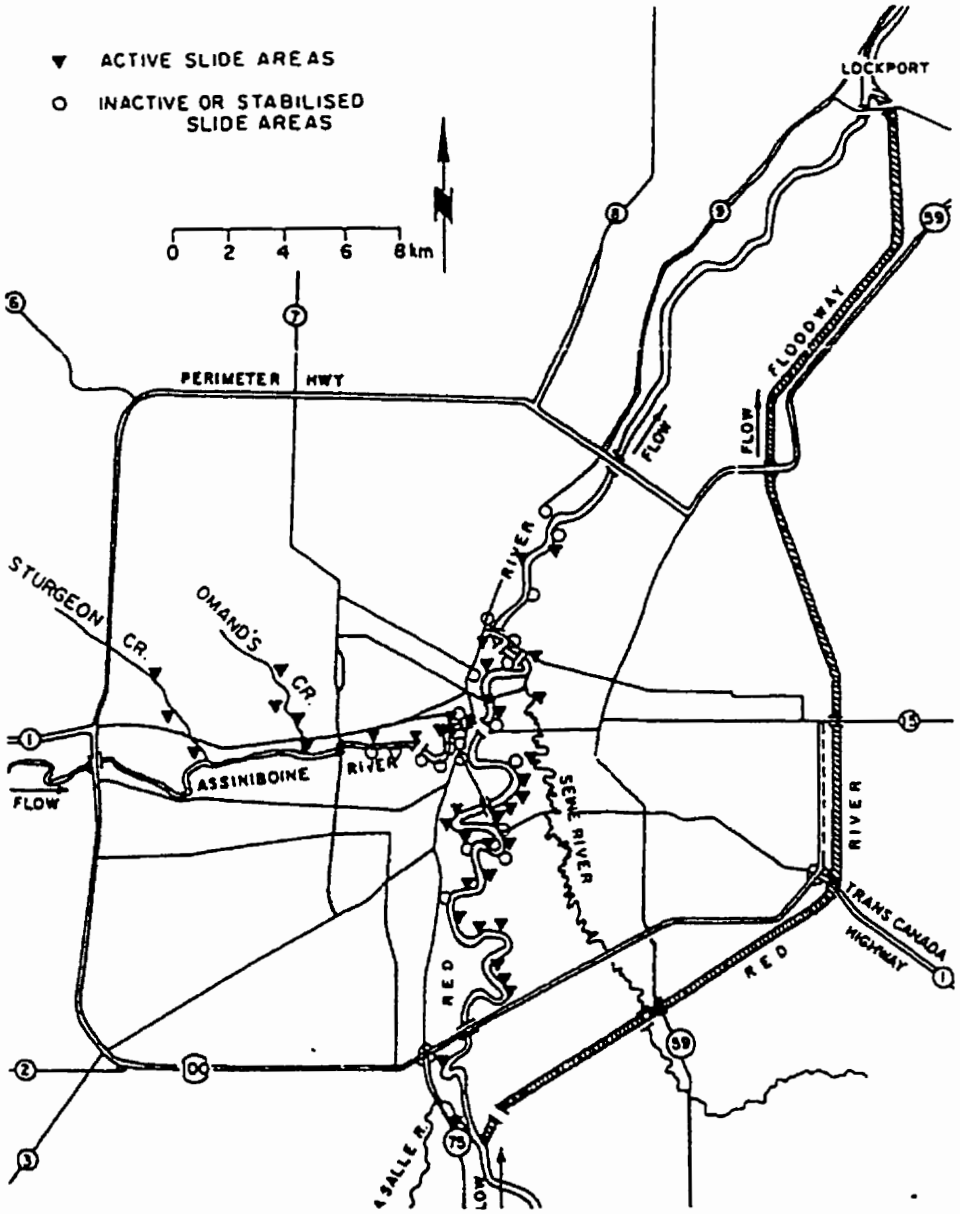

Figure 1.1 Identified active and inactive slide locations along Winnipeg riverbanks (Baracos and Graham, 1981)

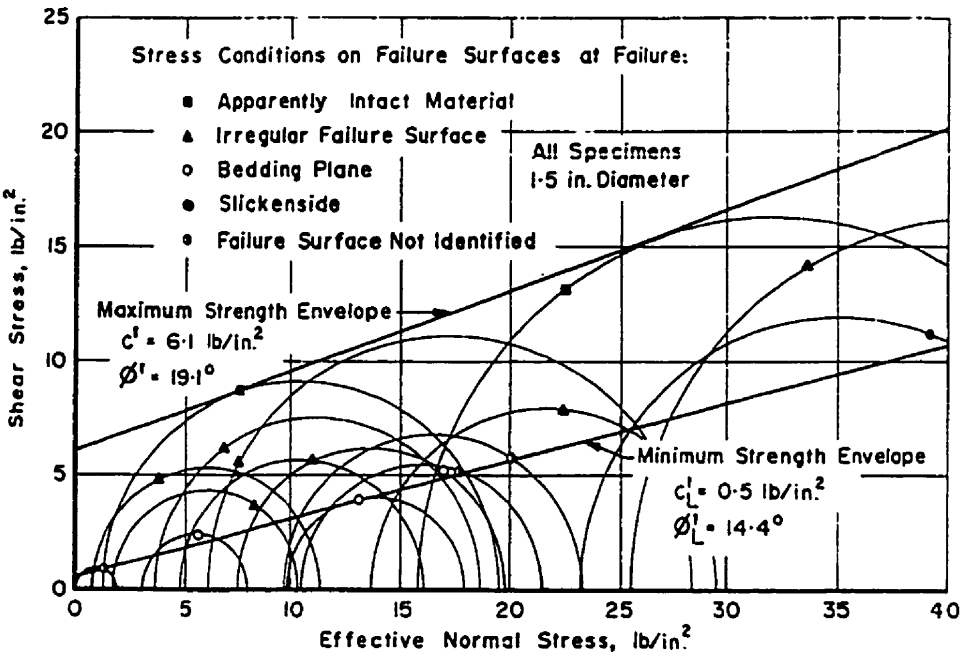

Figure 2.1 Triaxial test results for Winnipeg brown clay (Freeman and Sutherland 1974)

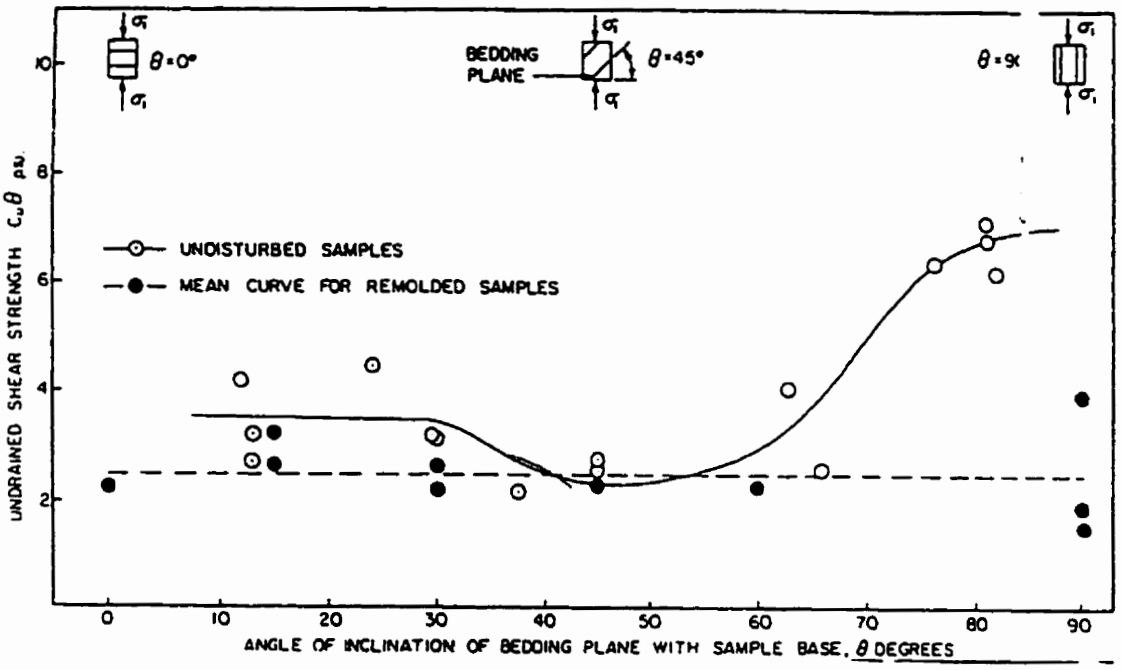

Figure 2.2 Unconfined compression test results of Winnipeg brown clay (Loh and Holt 1974)

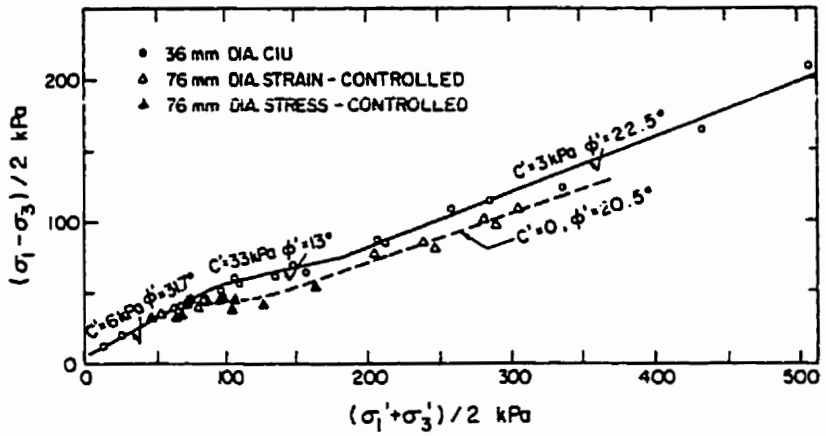

Figure 2.3 Triaxial test results for Winnipeg grey clay (Baracos *et al.* 1980)

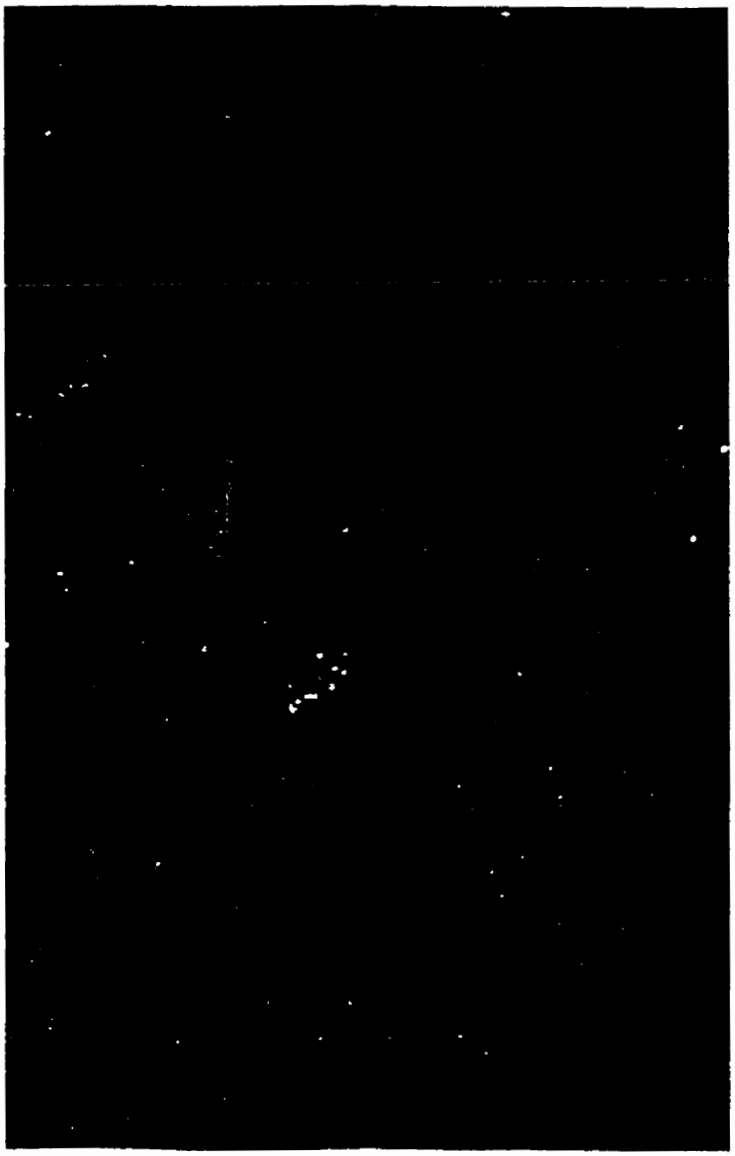

Figure 2.4 Glaciofluvial gravel deposit overlying bedrock along the Assiniboine River in Winnipeg (1995)

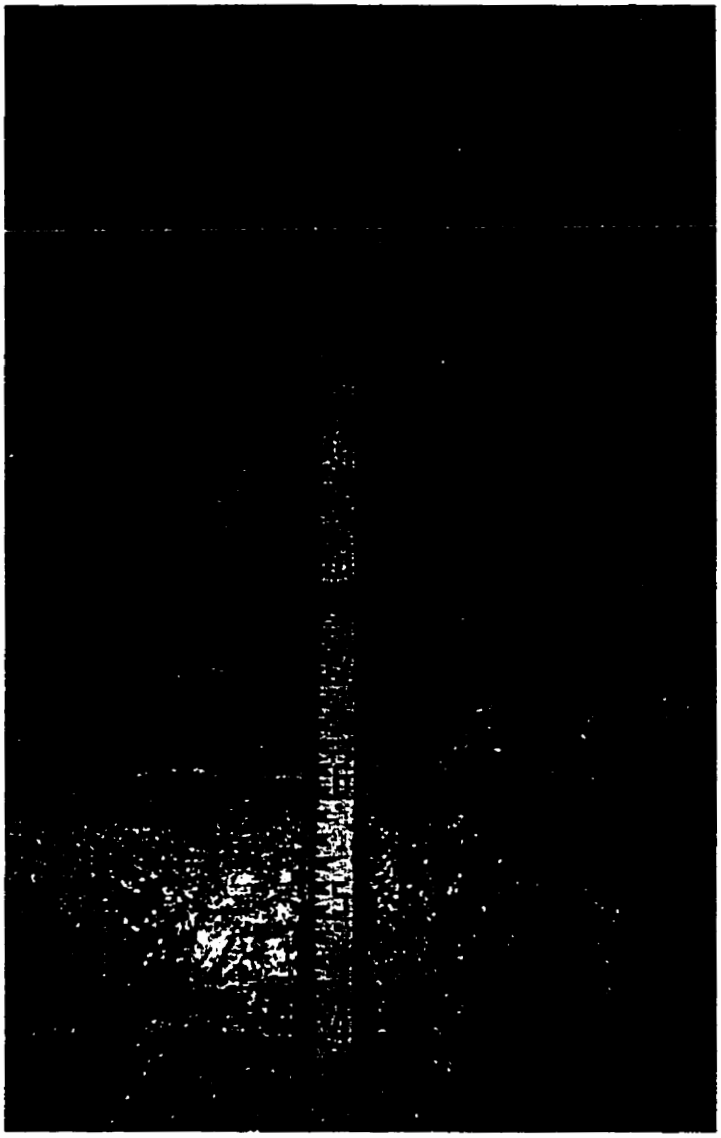

Figure 2.5 Photograph of horizontal and vertical fractures in the bedrock along the Assiniboine River in Winnipeg (1995)

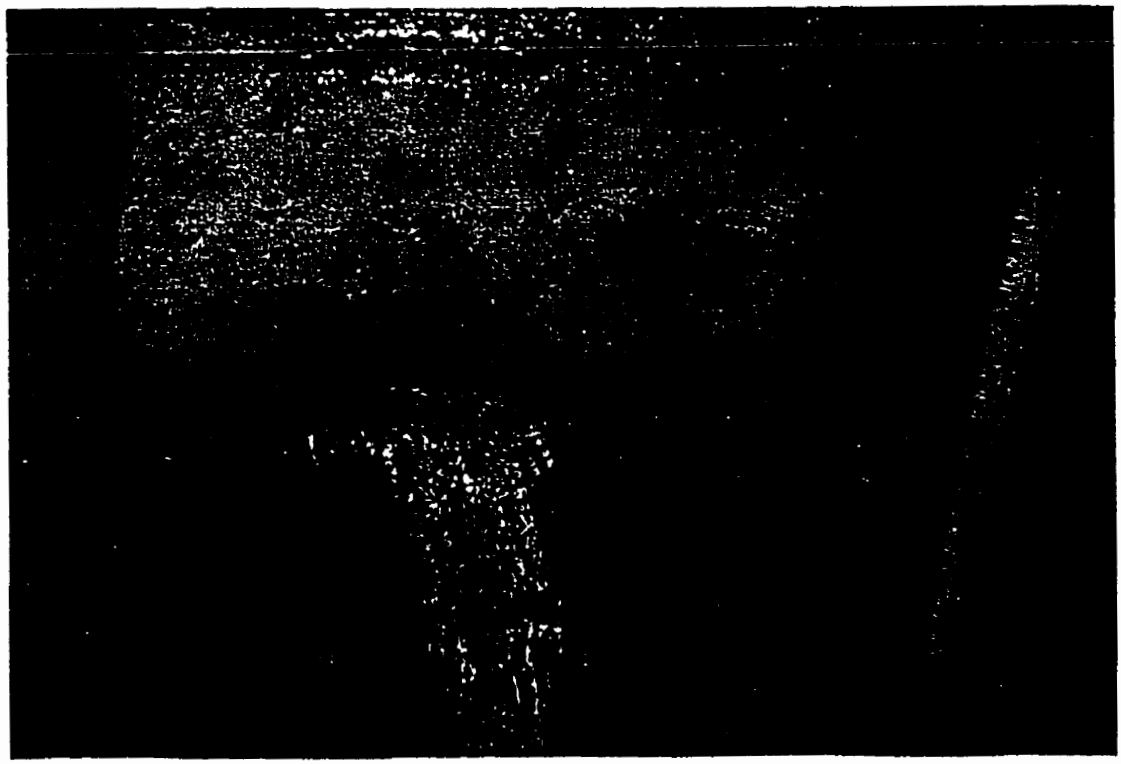

Figure 2.6 Photograph of seepage from open fracture in bedrock along the Assiniboine River in Winnipeg (1995)

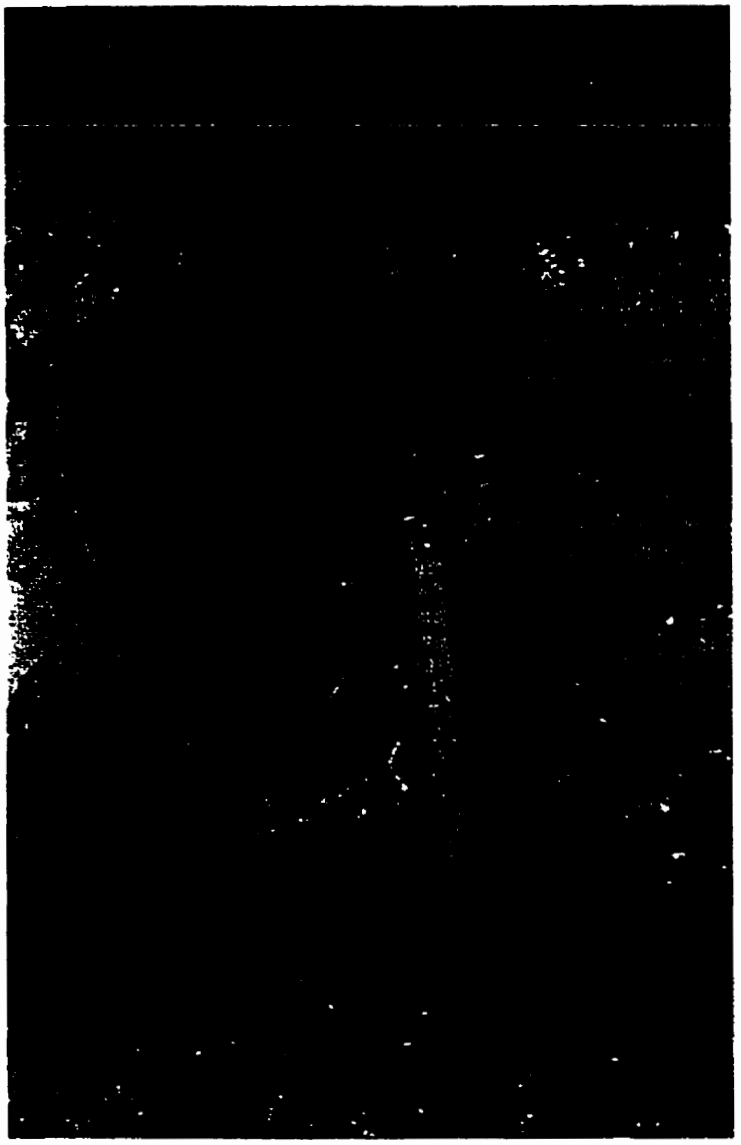

Figure 2.7 Photograph of solution channel in bedrock along Assiniboine River in Winnipeg (1995)

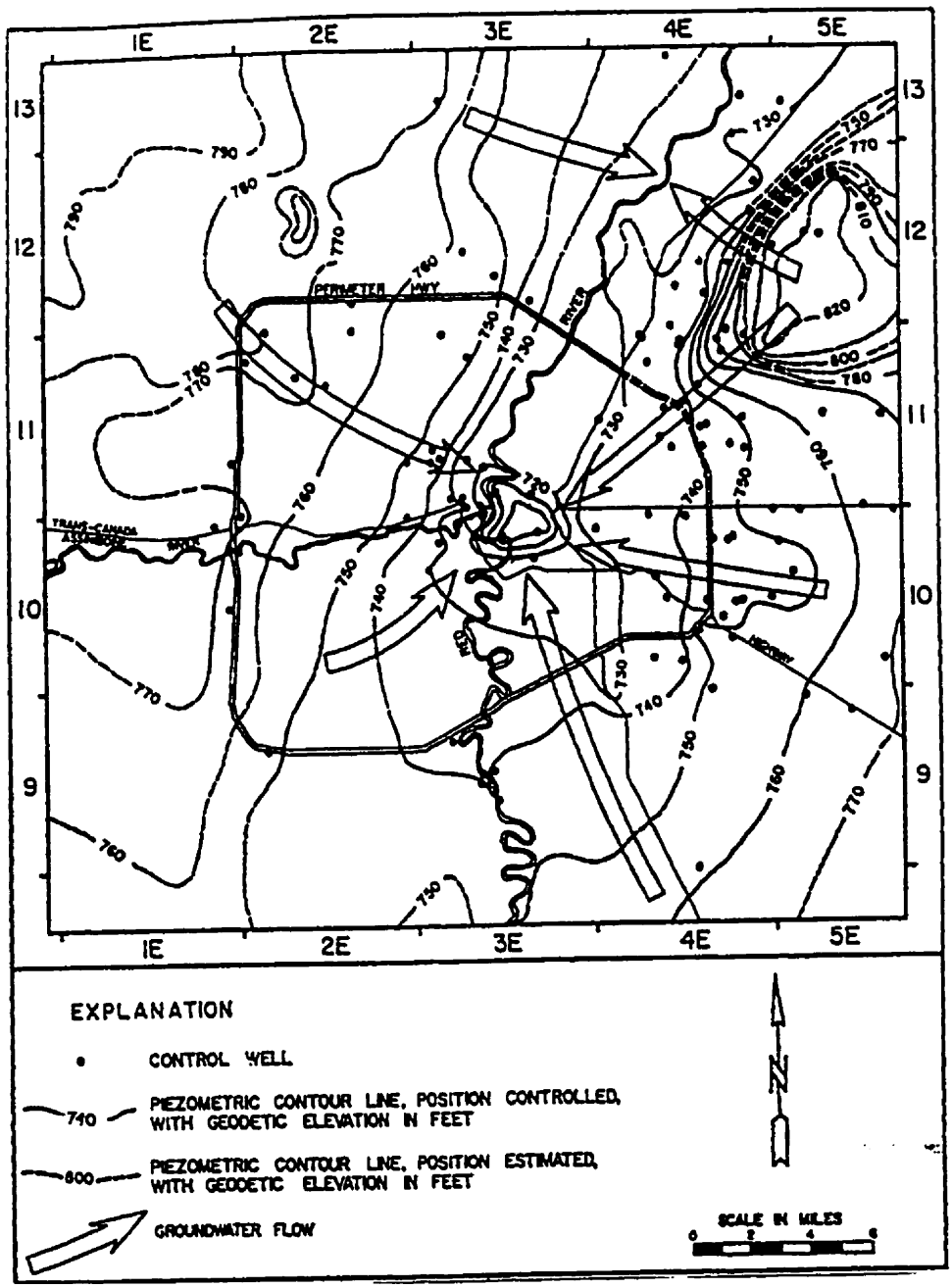

Figure 2.8 Regional groundwater flow in the Winnipeg area (Render 1970)

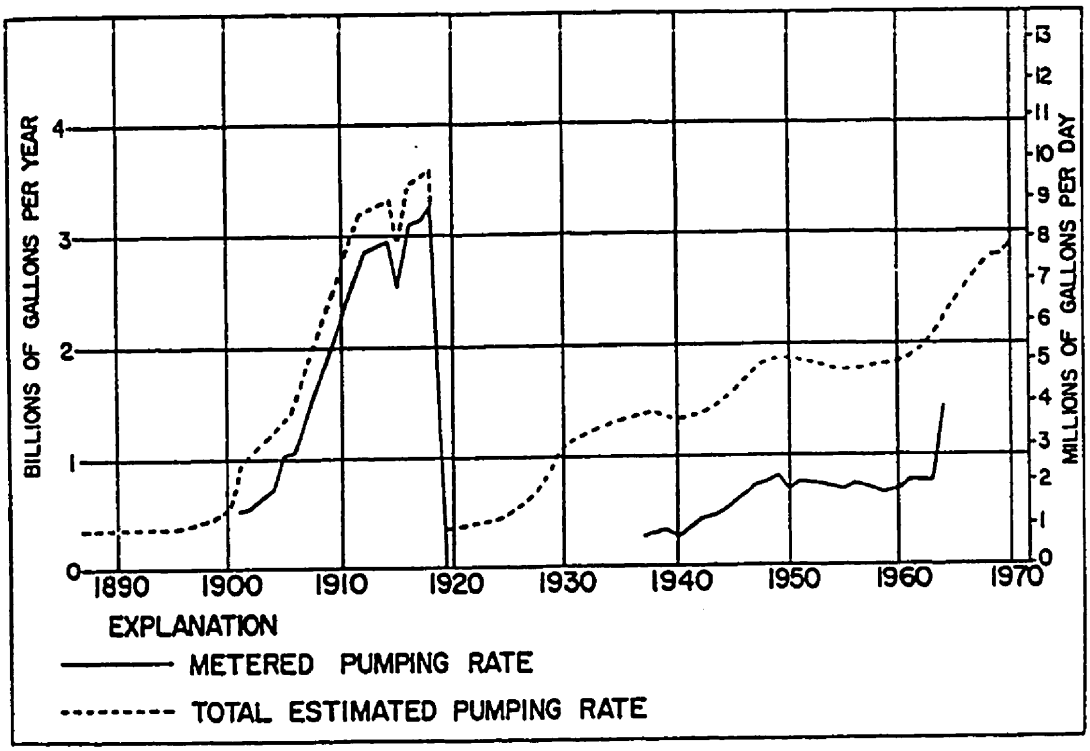

Figure 2.9 Historical groundwater withdrawal from the Upper Carbonate Aquifer (Render 1970)

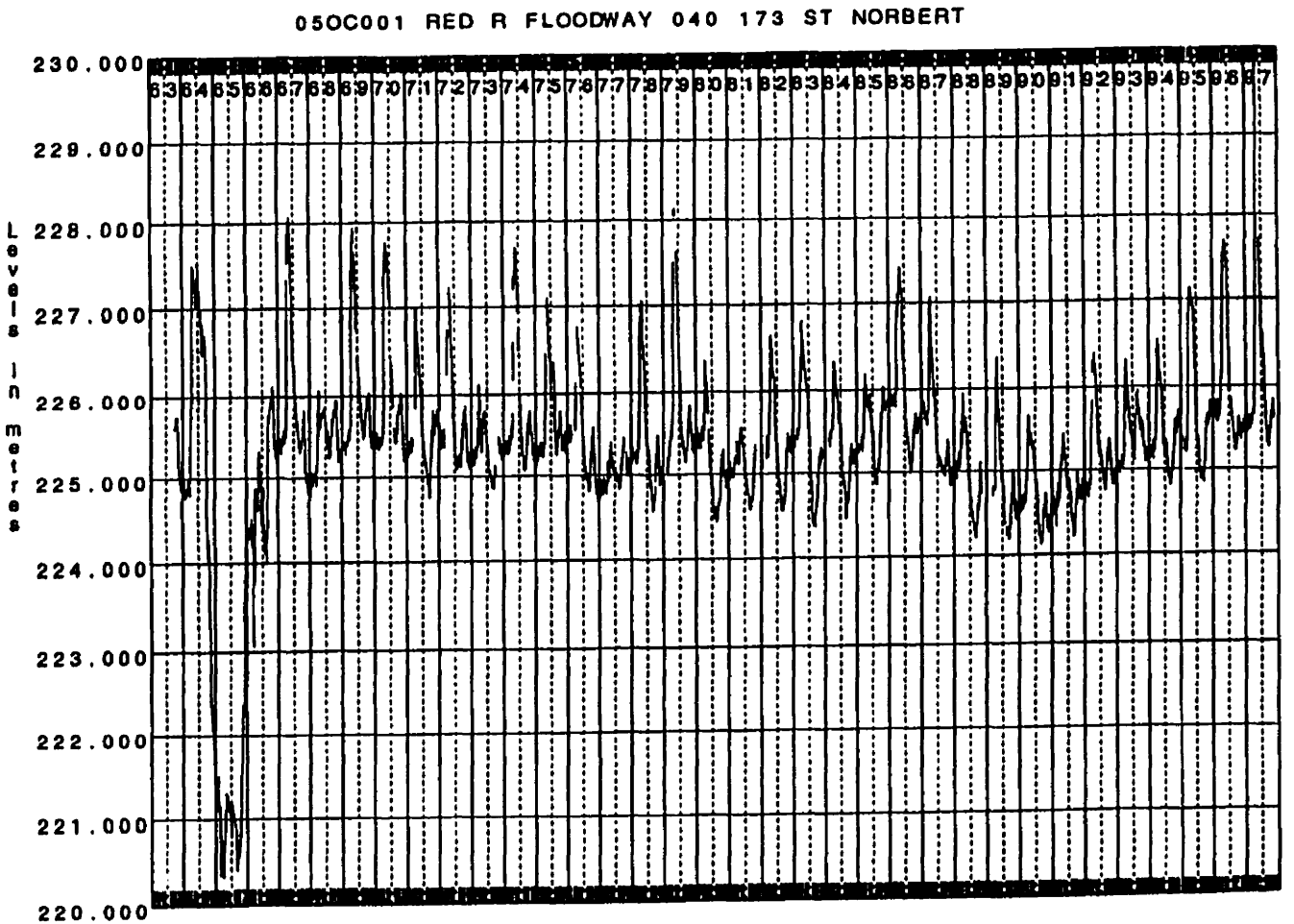

Figure 2.10a Upper Carbonate Aquifer hydrograph for monitoring well OC001 (Manitoba Water Resources 1997)

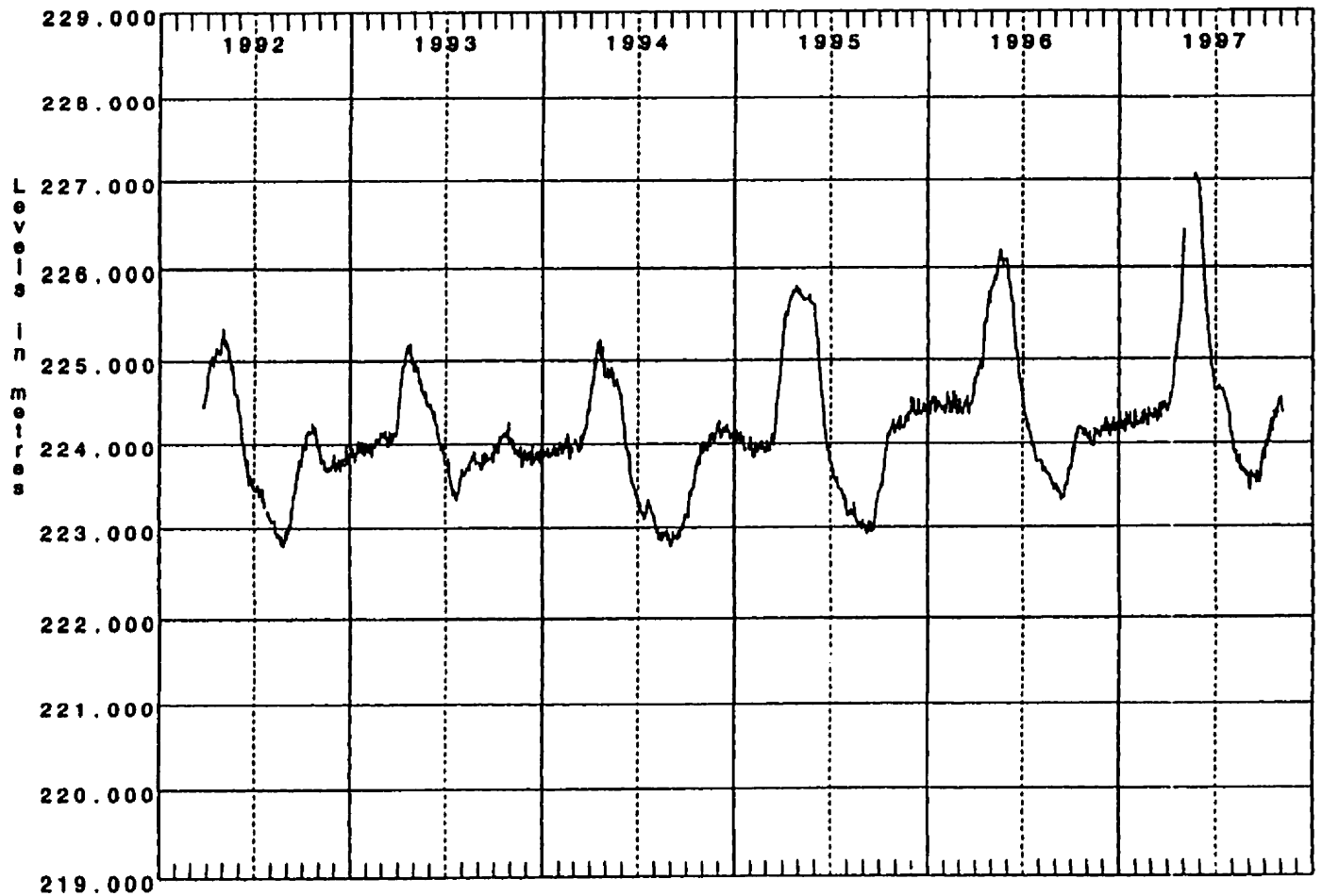

Figure 2.10b Upper Carbonate Aquifer hydrograph for monitoring well OC022 (Manitoba Water Resources 1997)

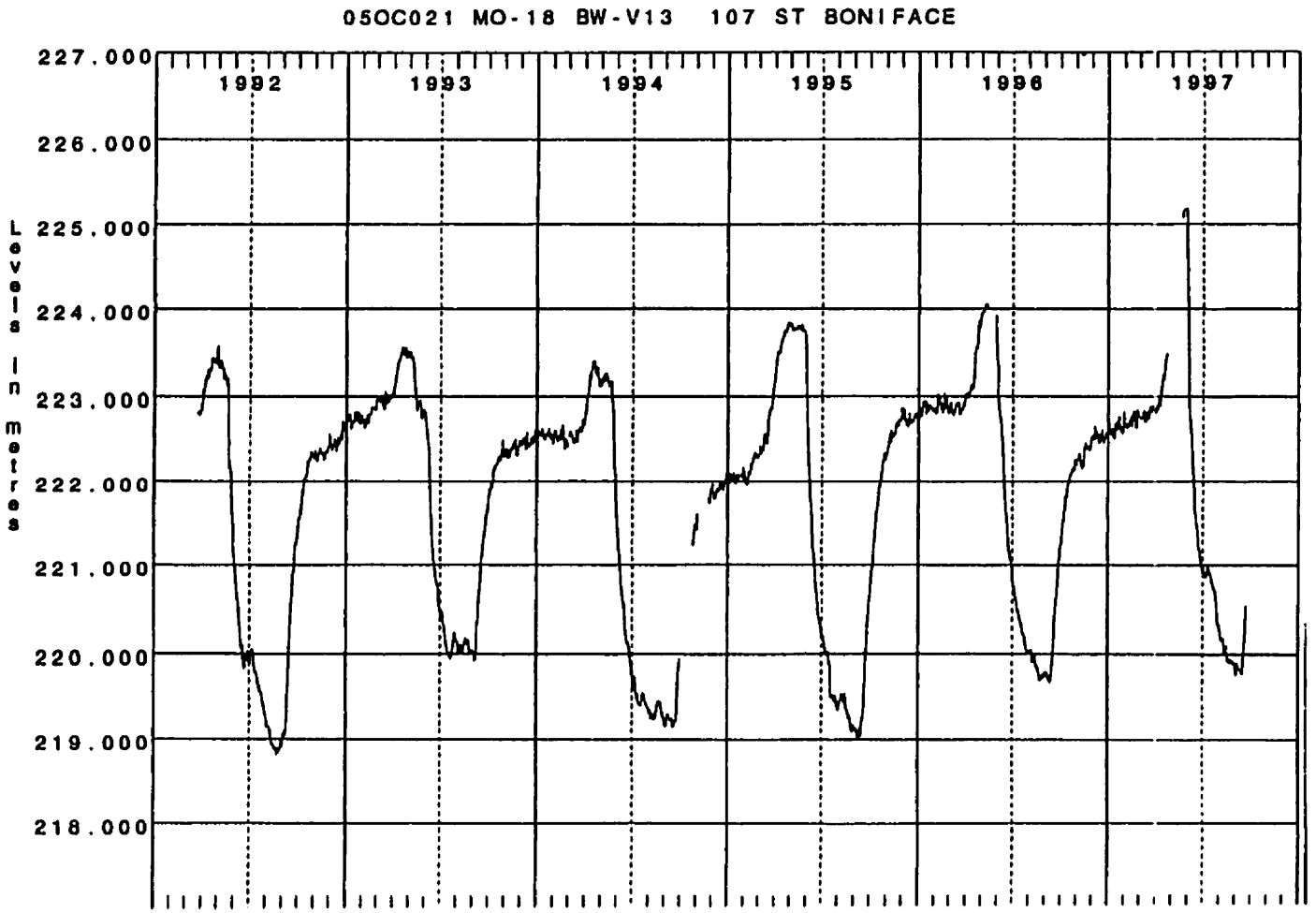

Figure 2.10c Upper Carbonate Aquifer hydrograph for monitoring well OC021 (Manitoba Water Resources 1997)

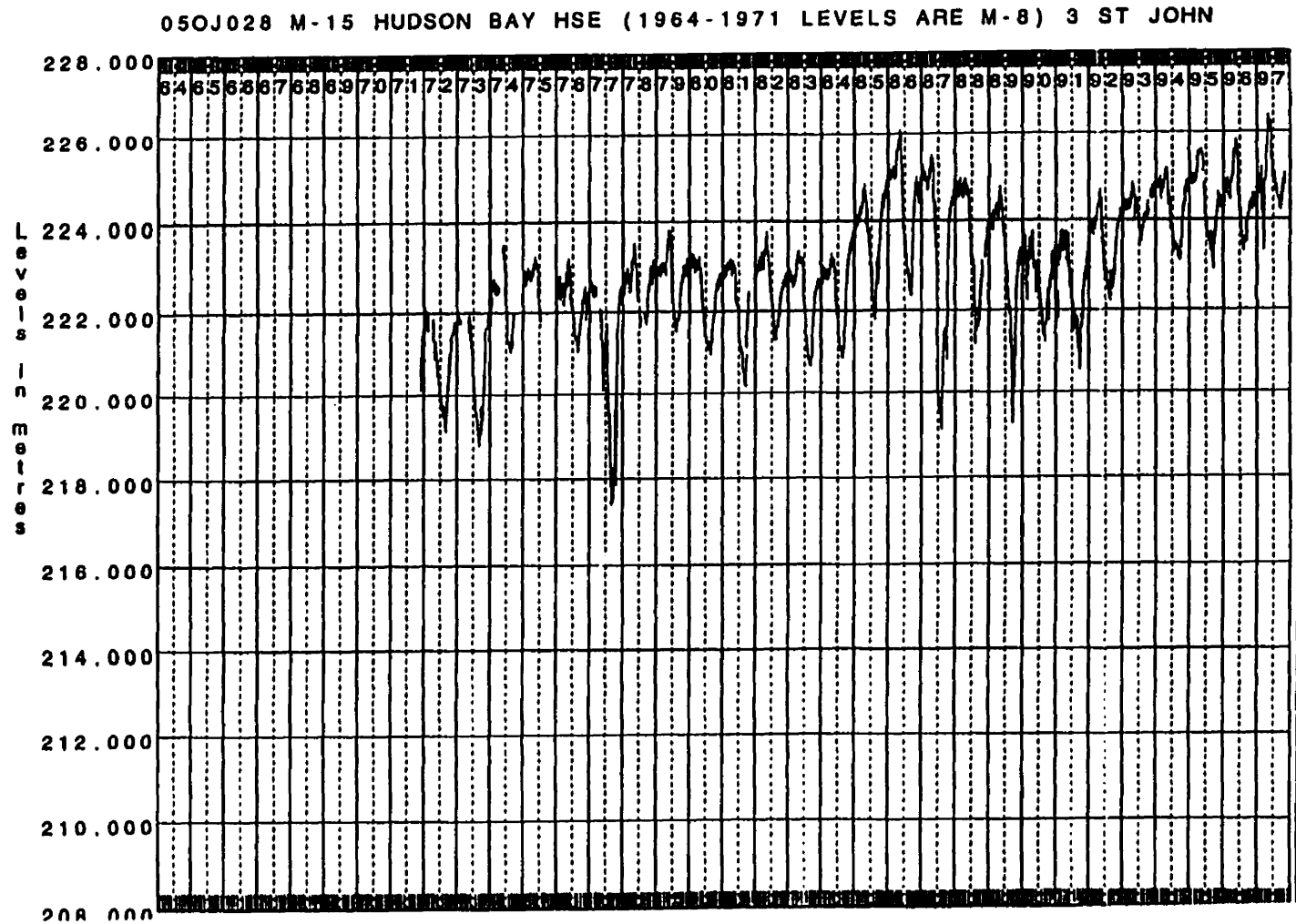

Figure 2.10d Upper Carbonate Aquifer hydrograph for monitoring well OJ028 (Manitoba Water Resources 1997)

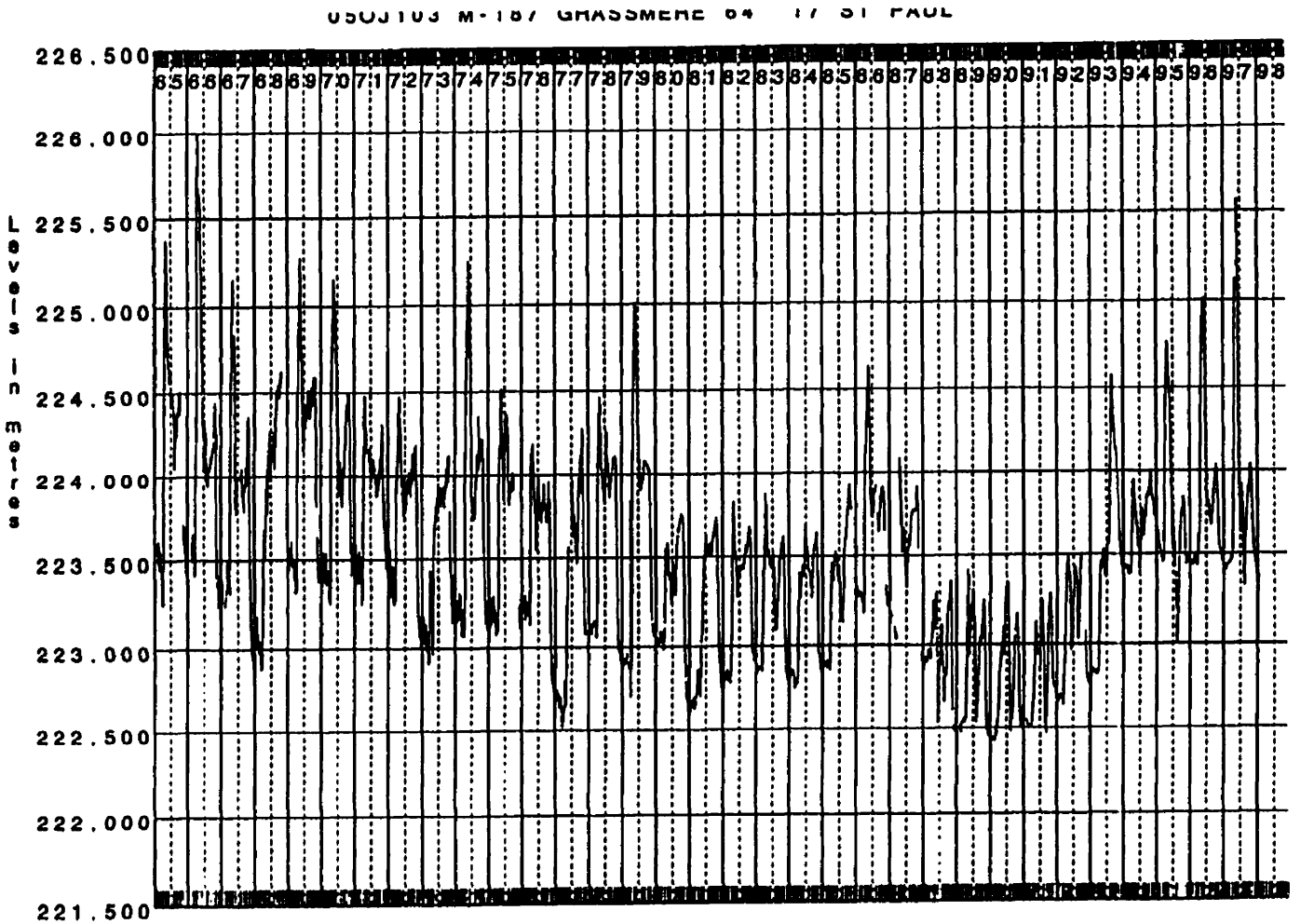

Figure 2.10e Upper Carbonate Aquifer hydrograph for monitoring well OJ103 (Manitoba Water Resources 1997)

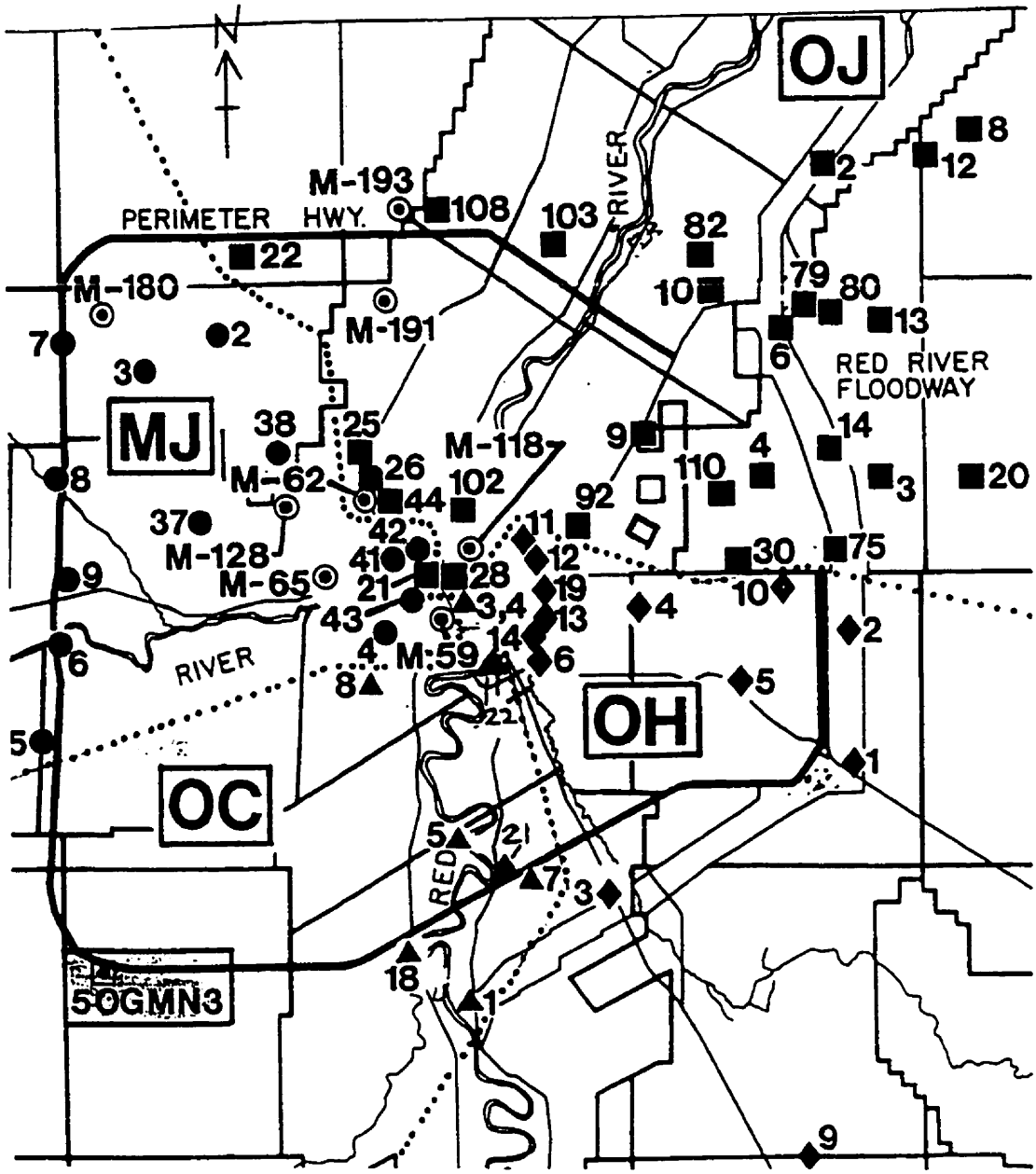

Figure 2.11 Location of Upper Carbonate Aquifer monitoring wells in Winnipeg (Manitoba Natural Resources, Water Resources Branch 1998)

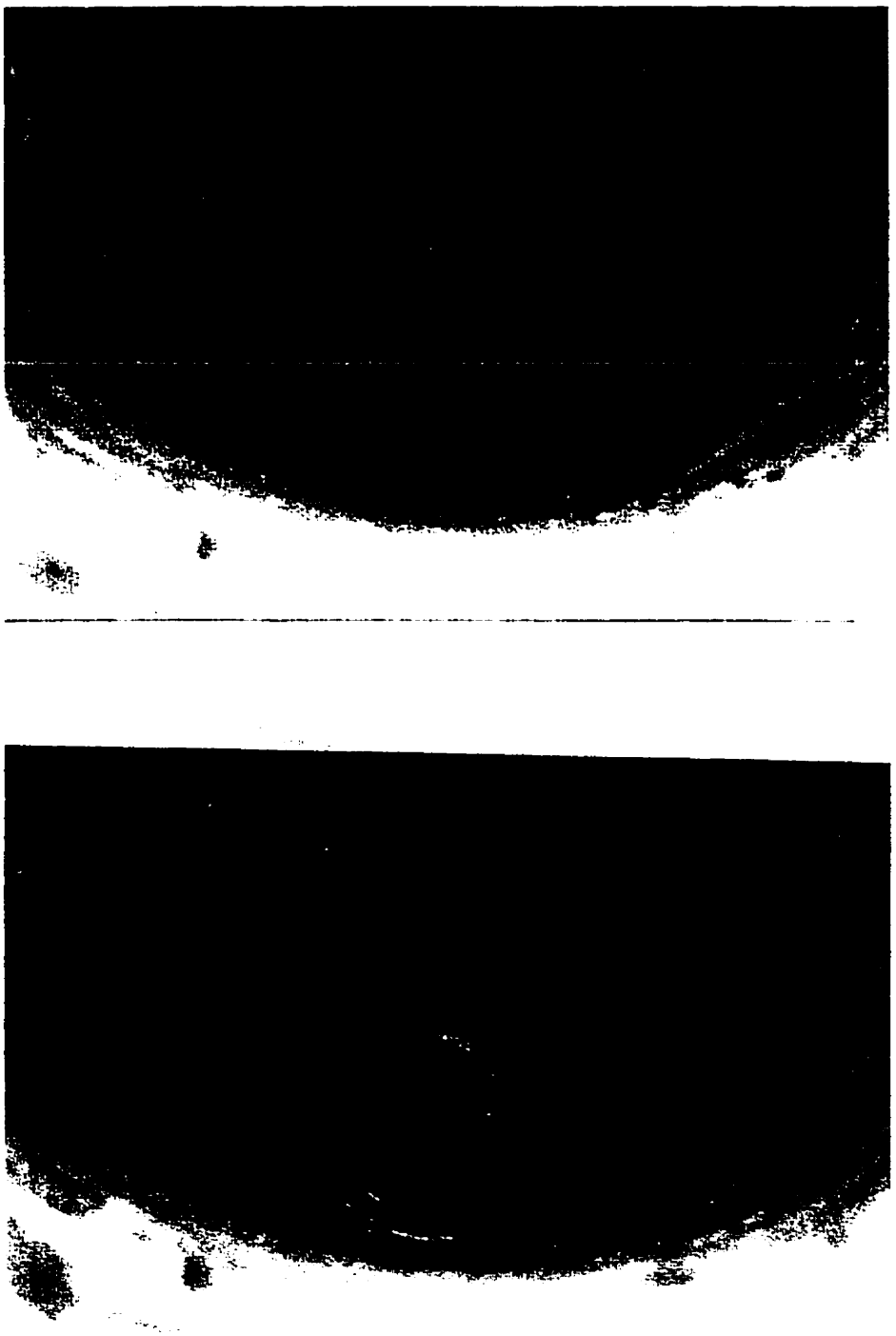

Figure 2.12 Initiation of hydraulic fracturing of Winnipeg grey clay resulting from high piezometric elevation in Upper Carbonate aquifer (upper photo). Groundwater from Upper Carbonate aquifer entering 2.1m diameter borehole (lower)

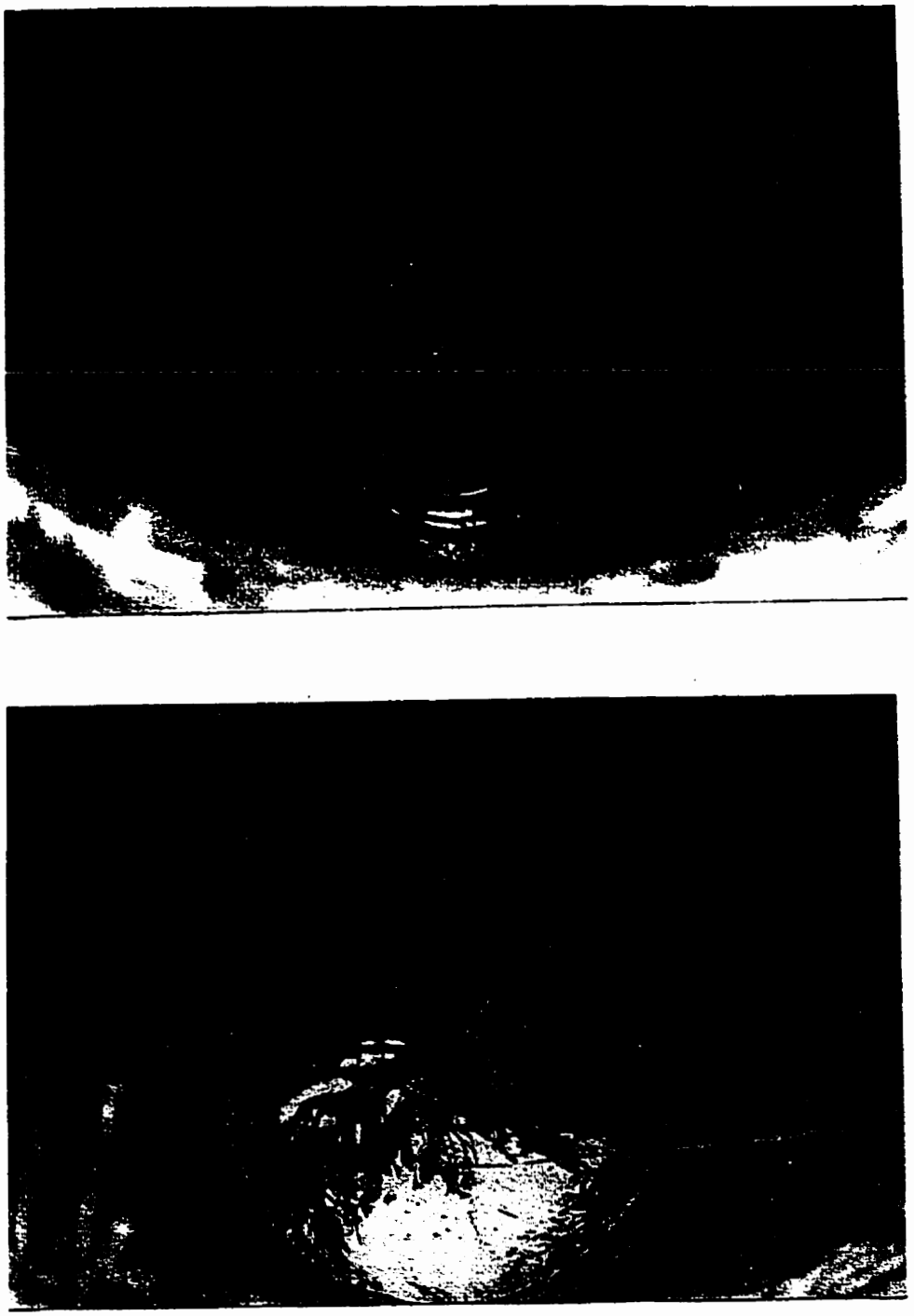

Figure 2.12 (cont.) Increased hydraulic fracturing of grey clay resulting increasing seepage volumes (upper photo). Water level in borehole near static level (lower photo).

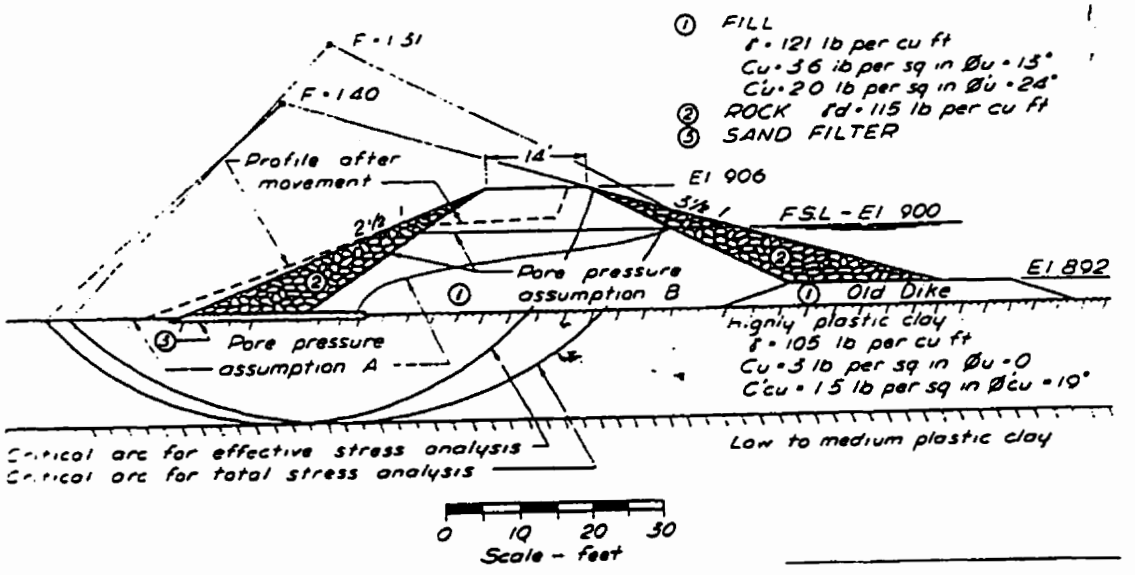

Figure 2.13 Typical cross section and failure arcs, Seven Sisters dykes (Peterson *et al.* 1960)

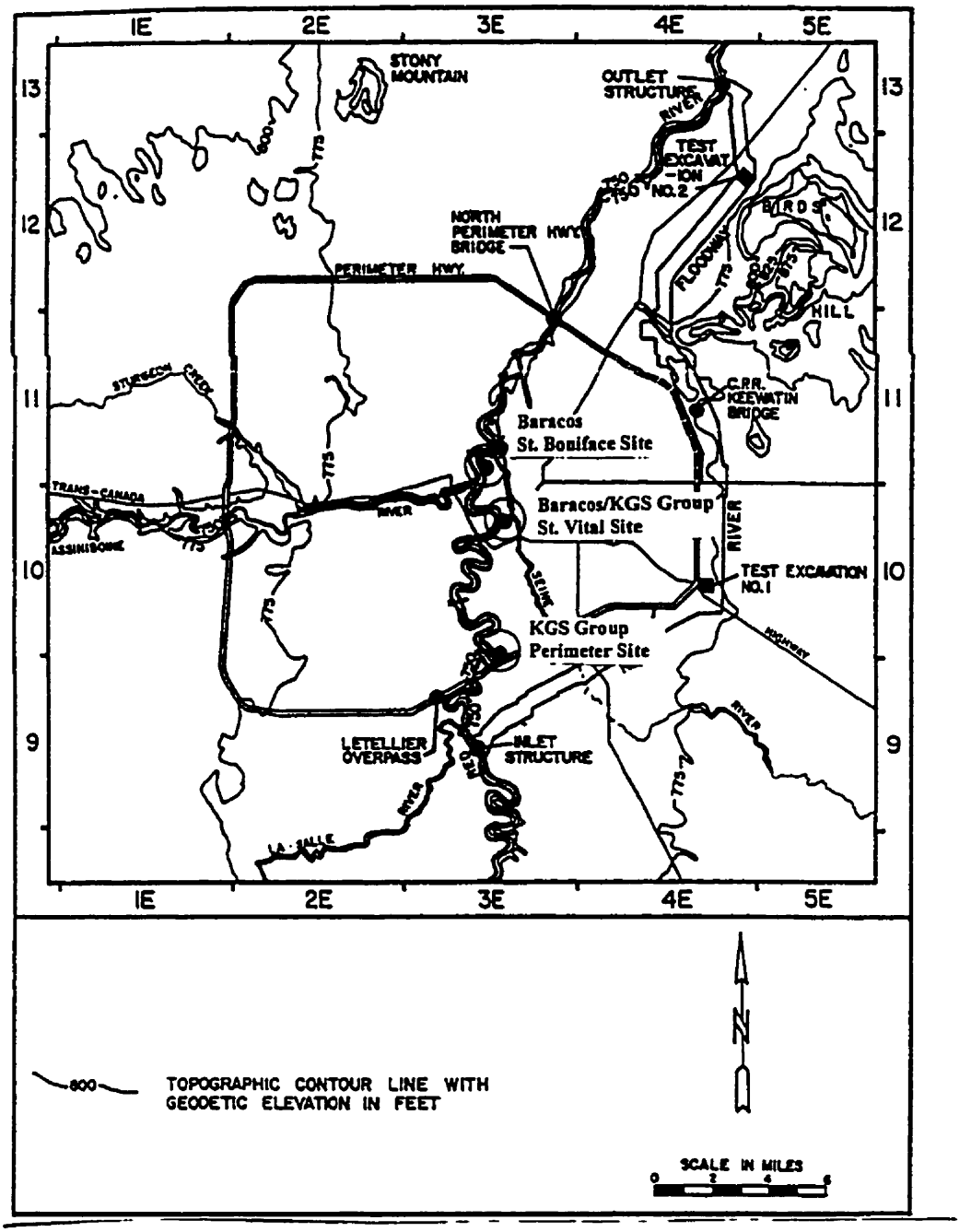

Figure 2.14 Location of riverbanks monitored by Baracos (1978) and KGS Group (1994)

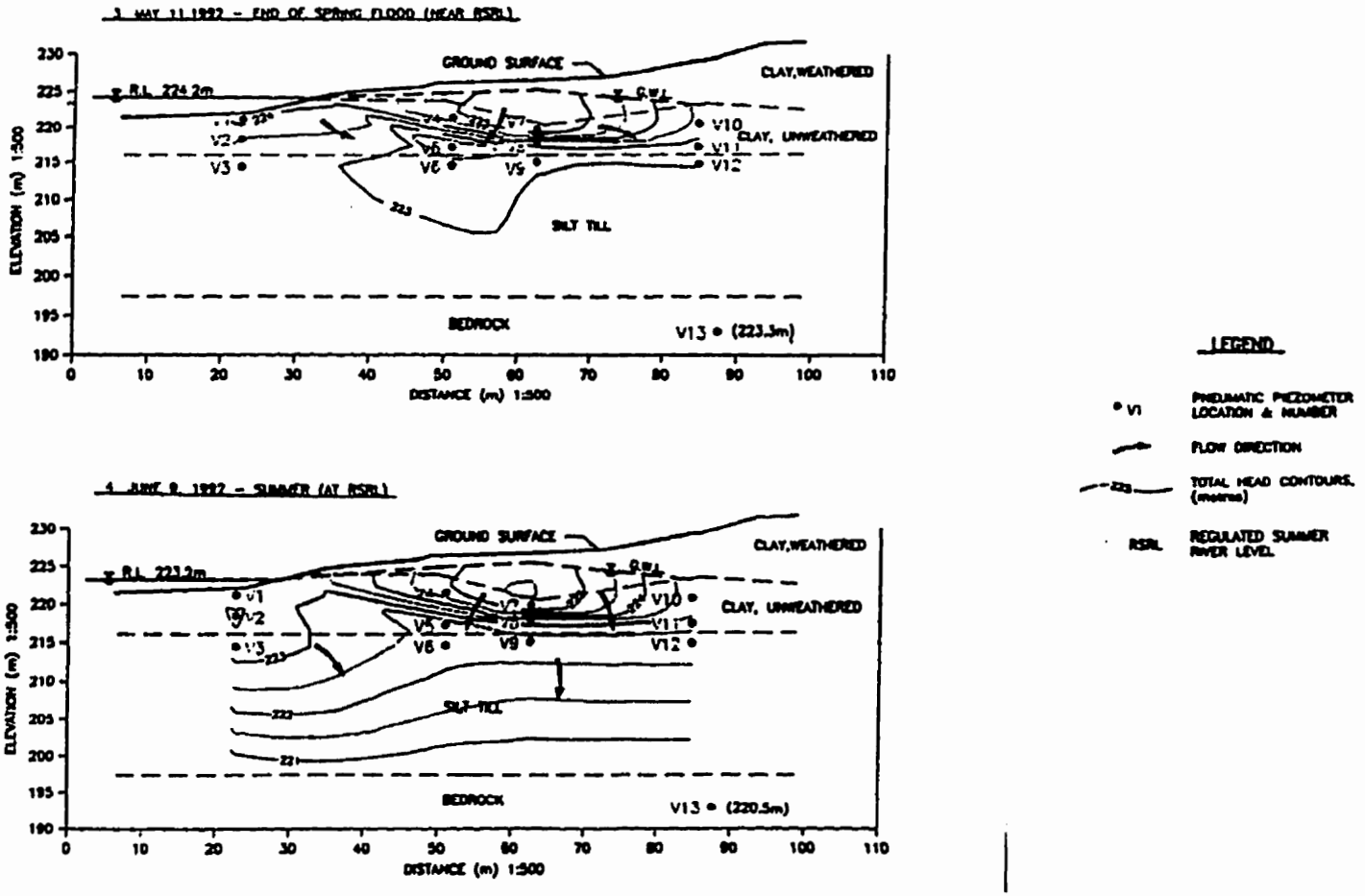

Figure 2.15 Piezometric elevations observed within the riverbank at KGS Group's St. Vital (KGS Group 1994)

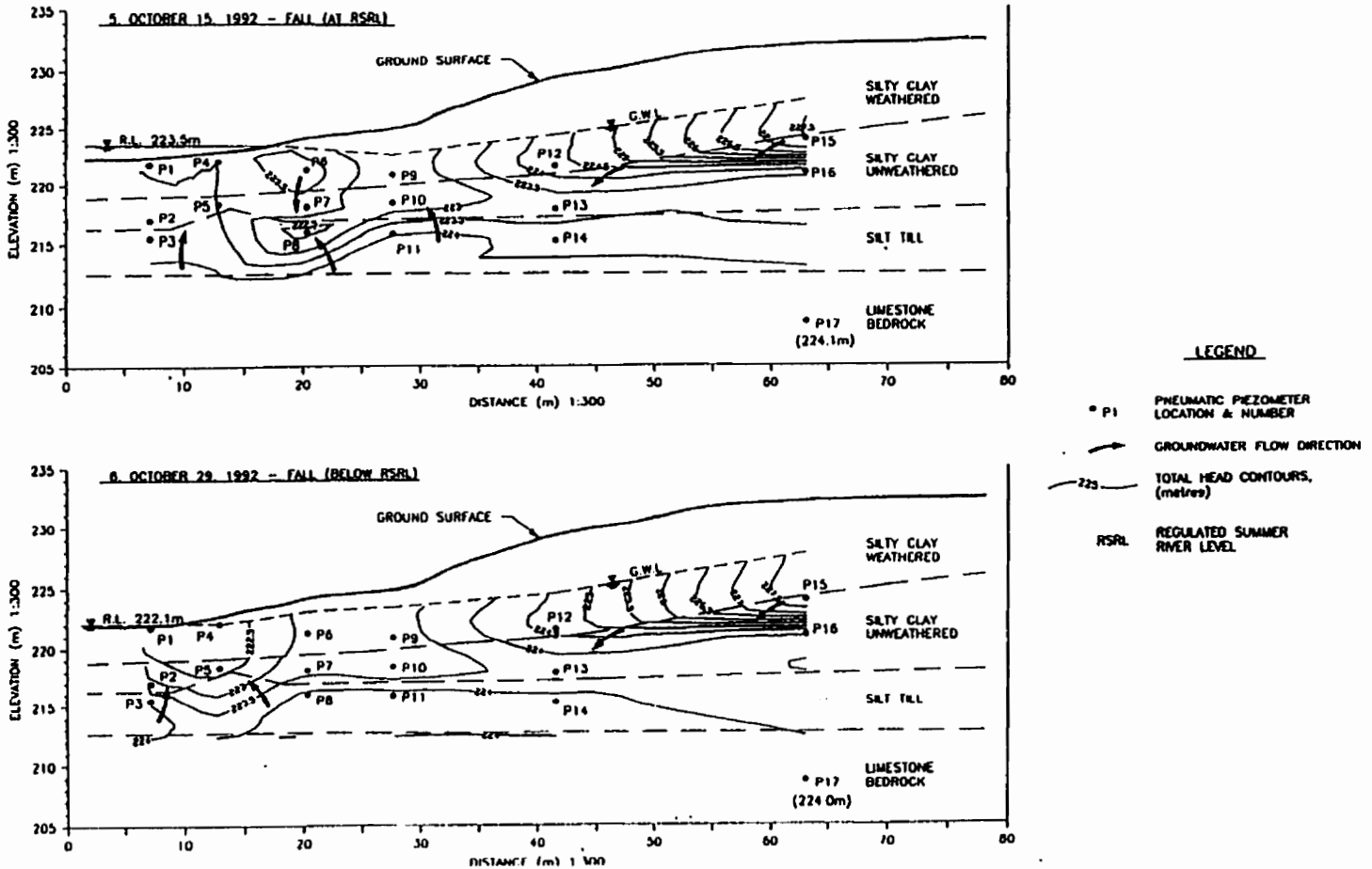

Figure 2.16 Piezometric elevations observed within the riverbank at KGS Group's South Perimeter site

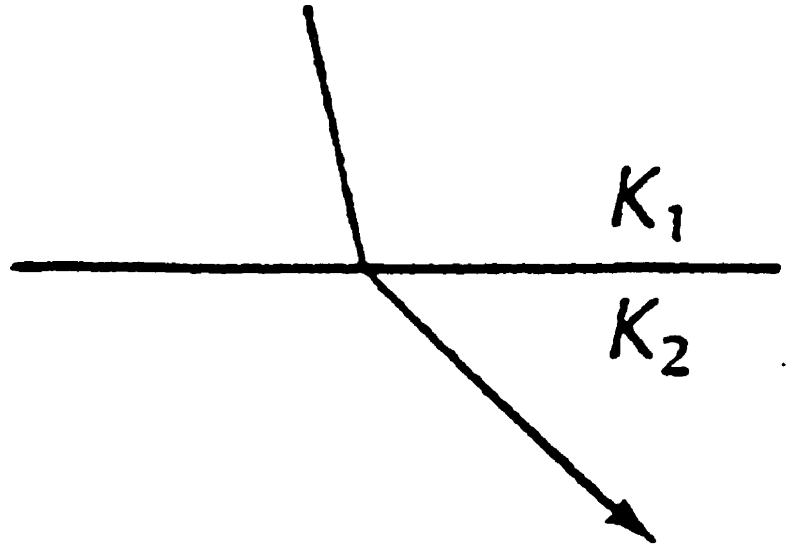

Figure 2.17 Refracted flow line travelling from low hydraulic conductivity material to high hydraulic conductivity material (Fetter 1994)

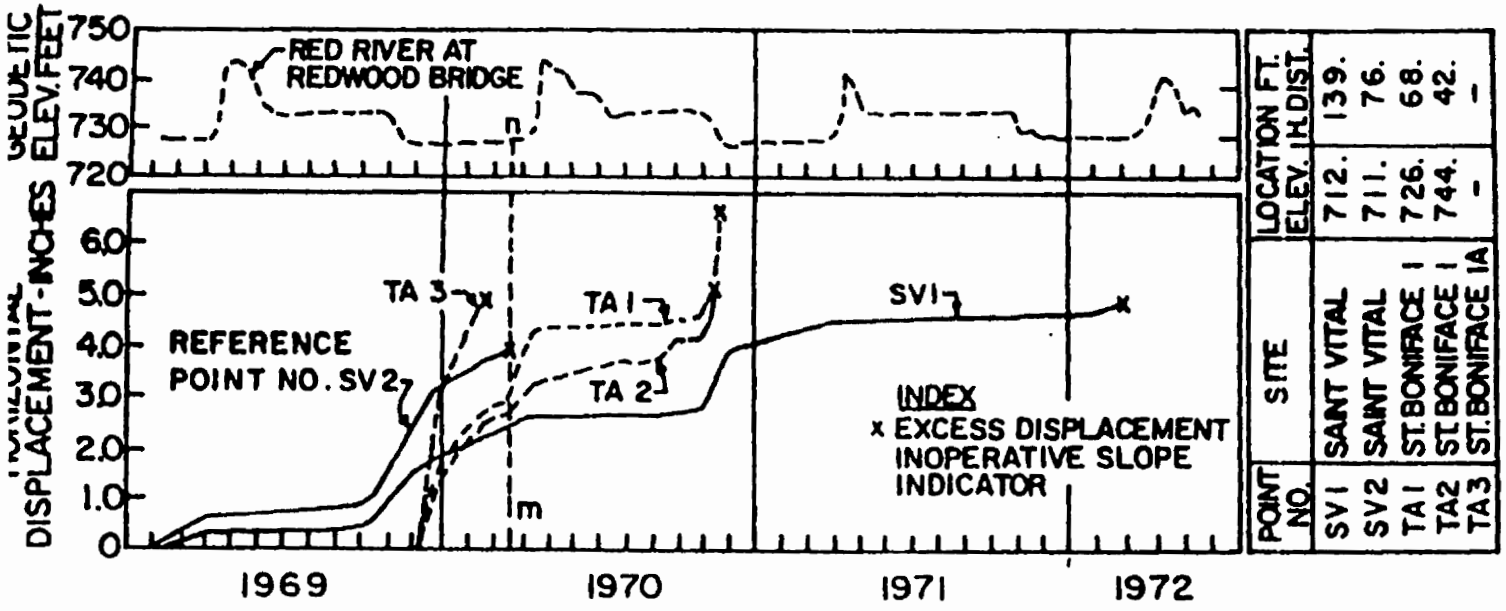

Figure 2.18 Cumulative riverbank movement recorded by slope movement indicators (Baracos 1978)

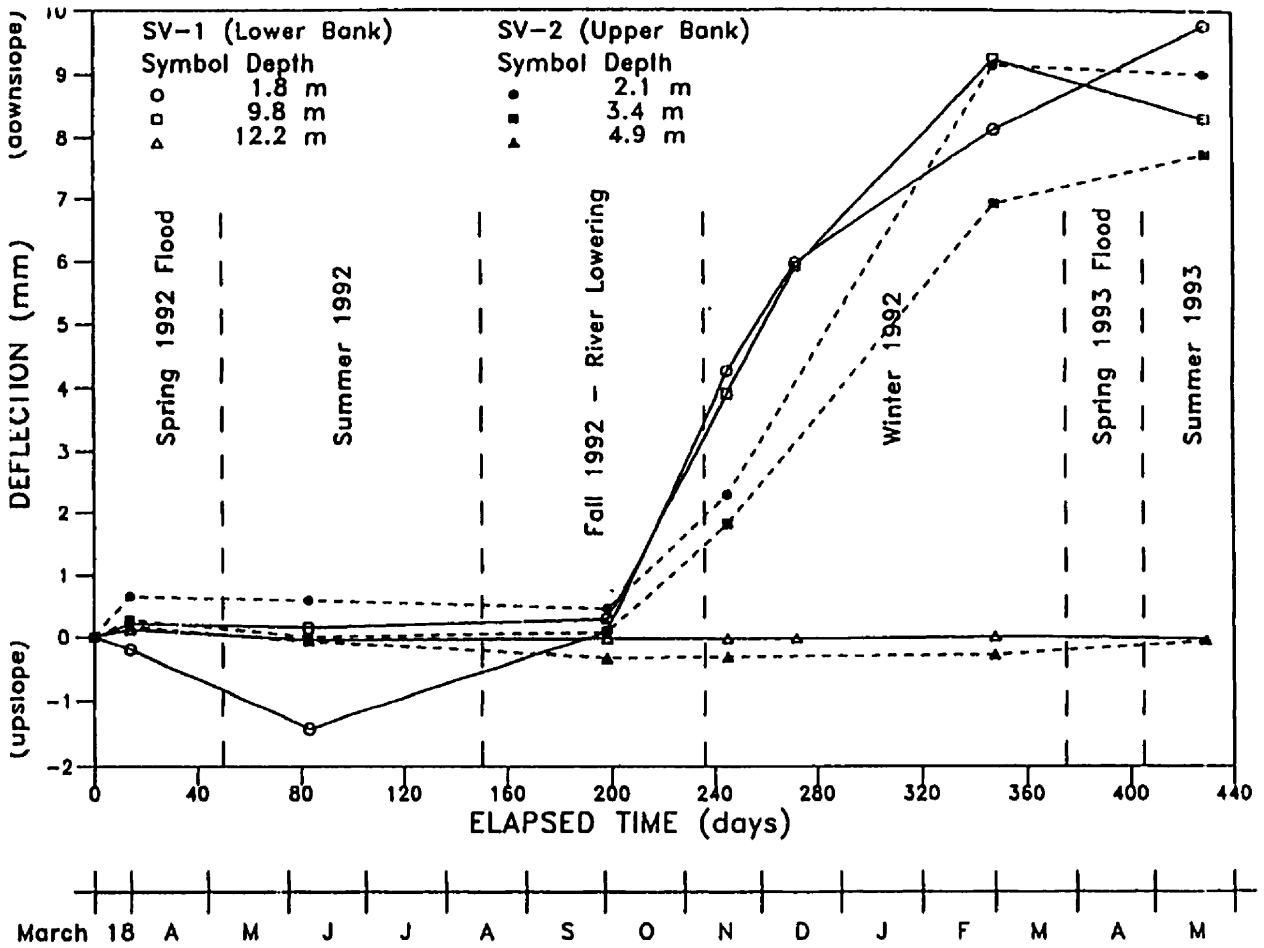

Figure 2.19 Cumulative riverbank movement recorded by slope movement indicators (KGS Group 1994)

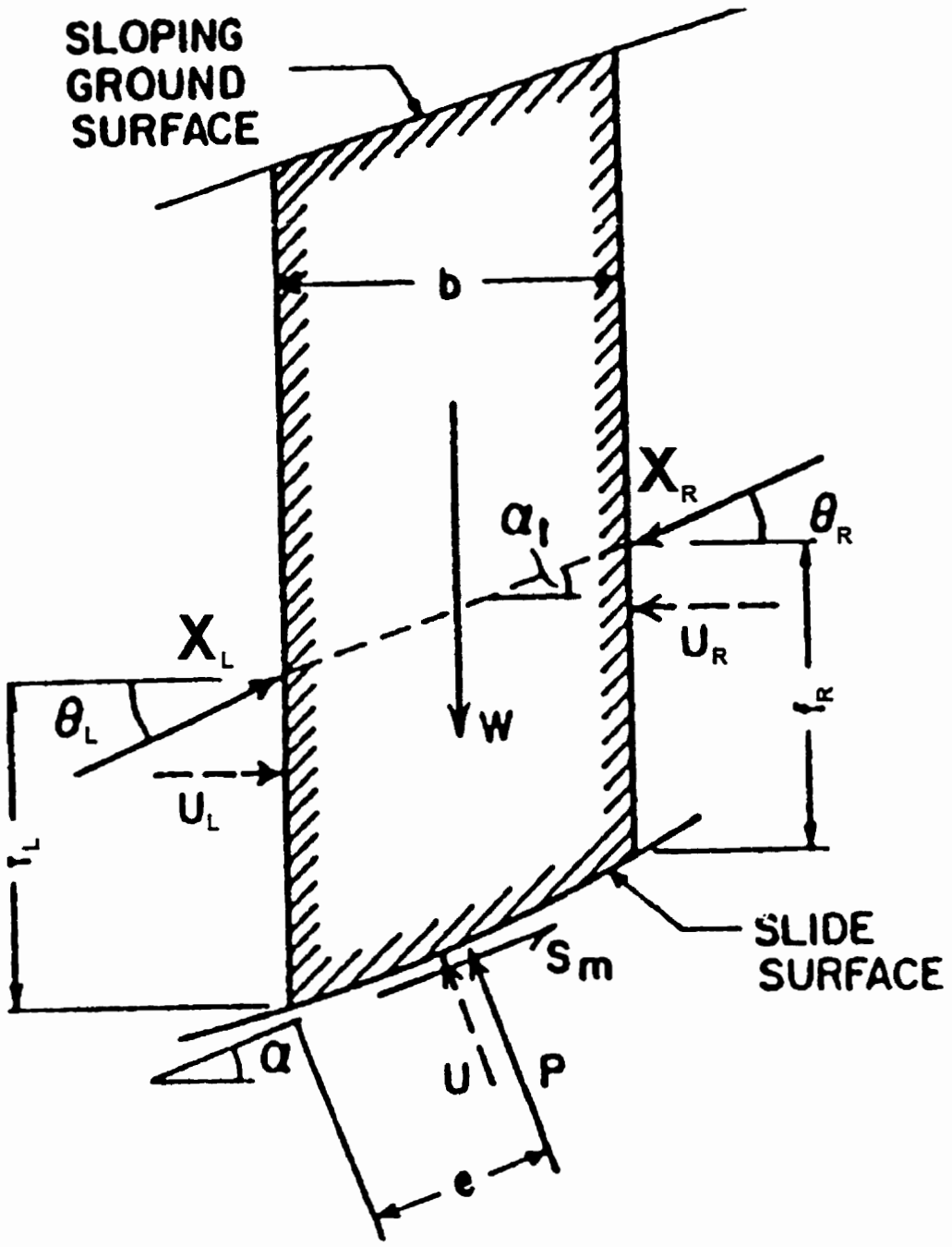

Figure 2.20 Forces acting on a typical slice within a slip surface (Graham 1984)

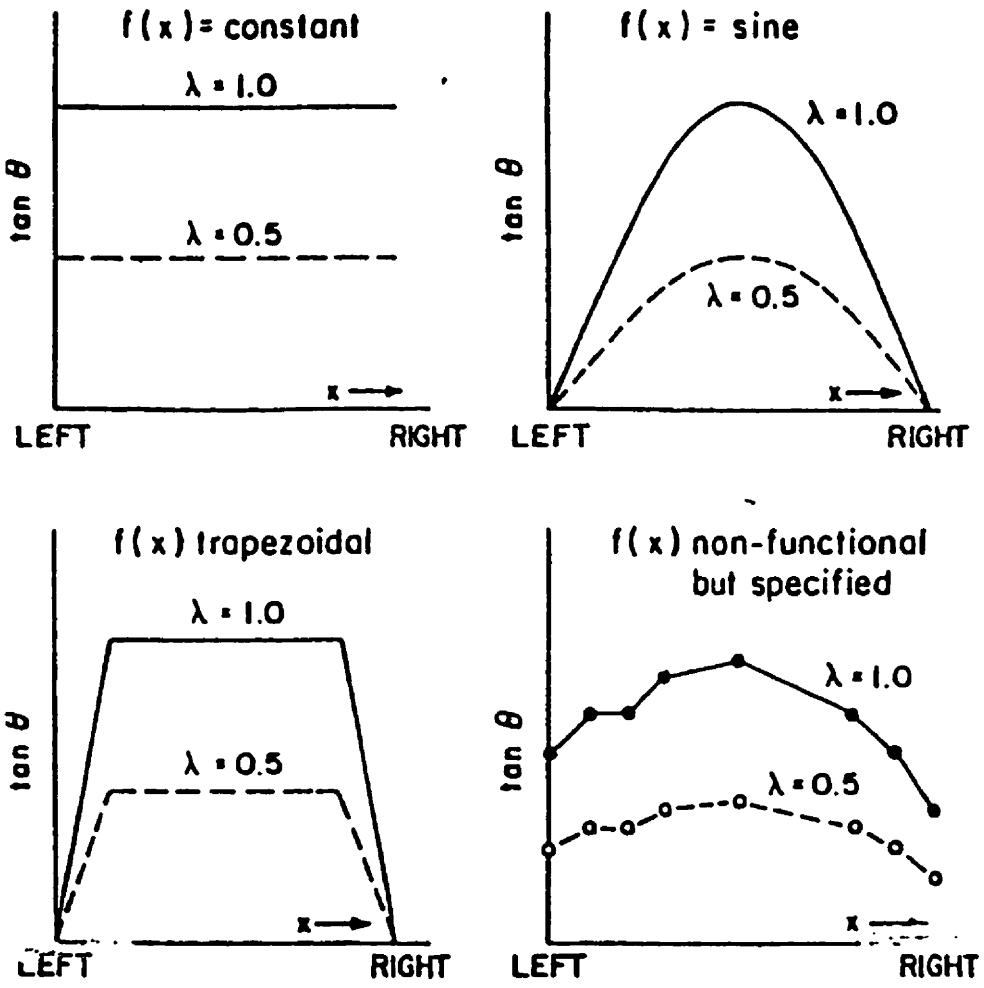

Figure 2.21 Interslice force functions used in the Morgenstern-Price method of slices (Graham 1984)

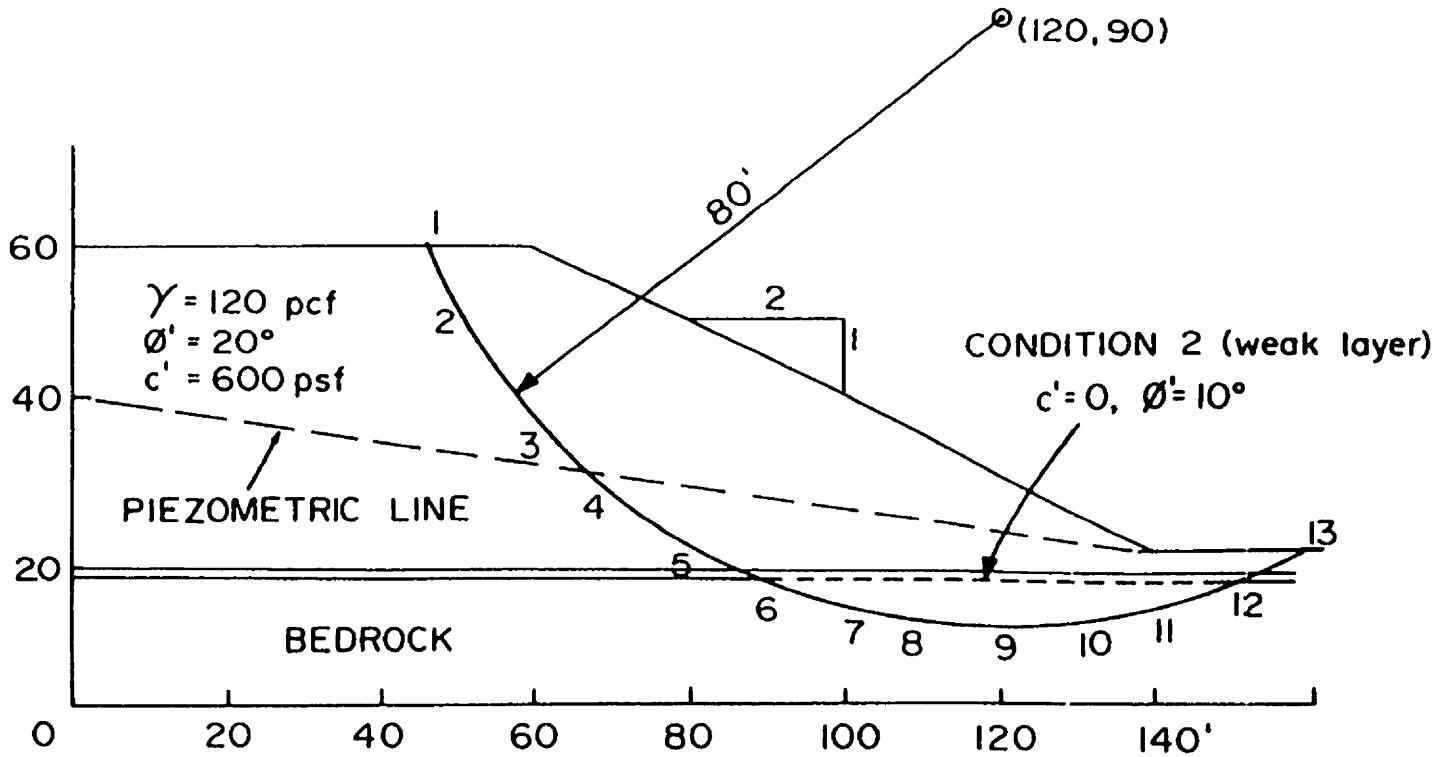

Figure 2.22 Slope geometry and properties used in the comparative study (Fredlund and Krahn 1977)

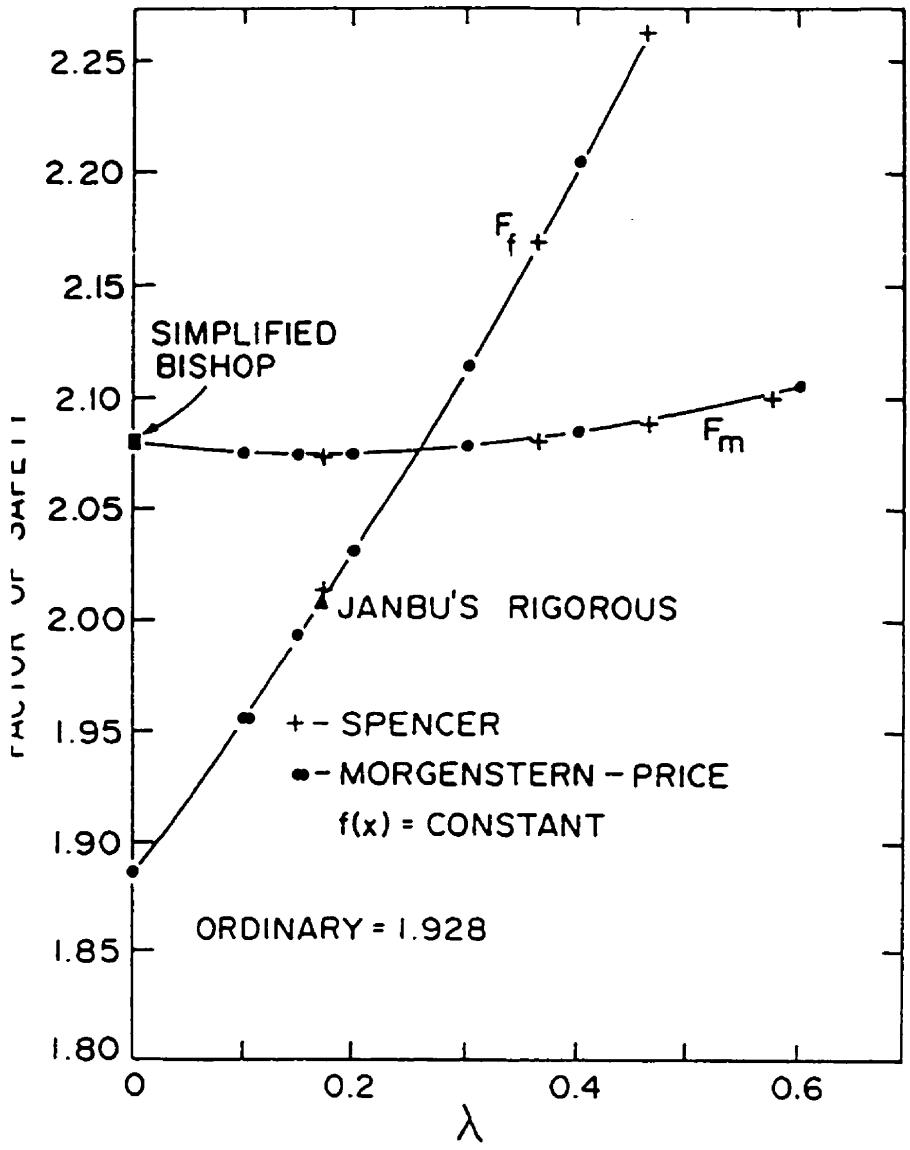

Figure 2.23 Comparison of safety factors determined for Case 1 (Fredlund and Krahn 1977)

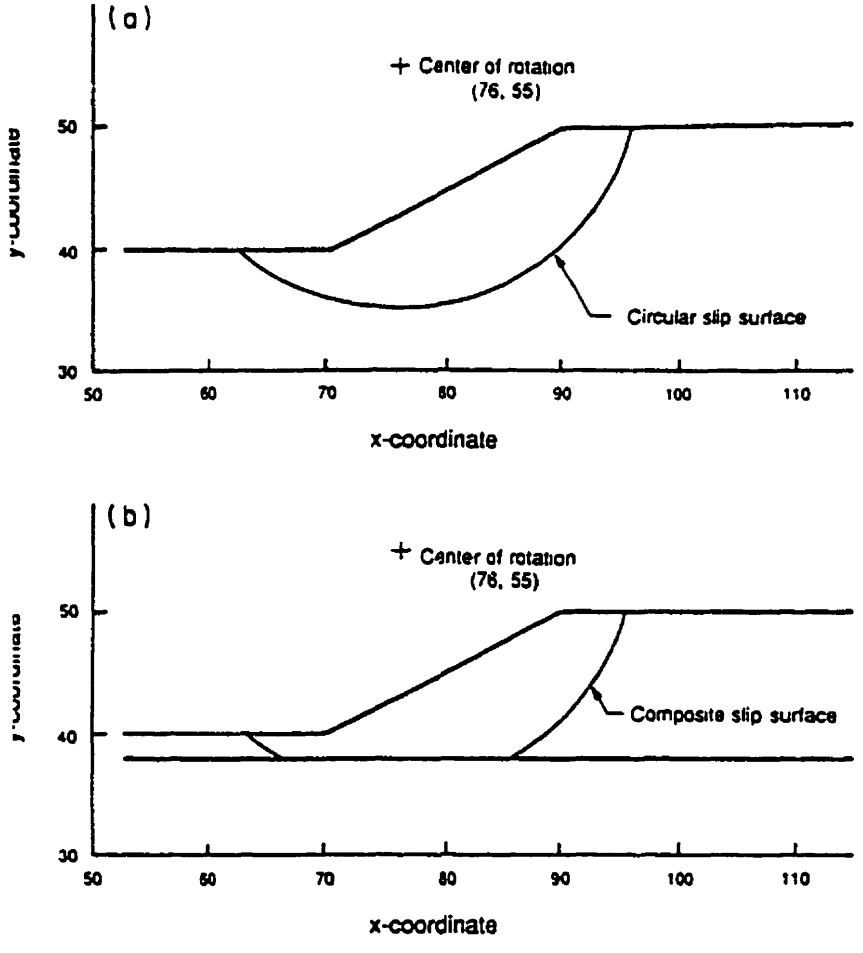

Figure 2.24 Cross sections used to examine the effect of the axis of moment equilibrium (Fredlund *et al.* 1992)

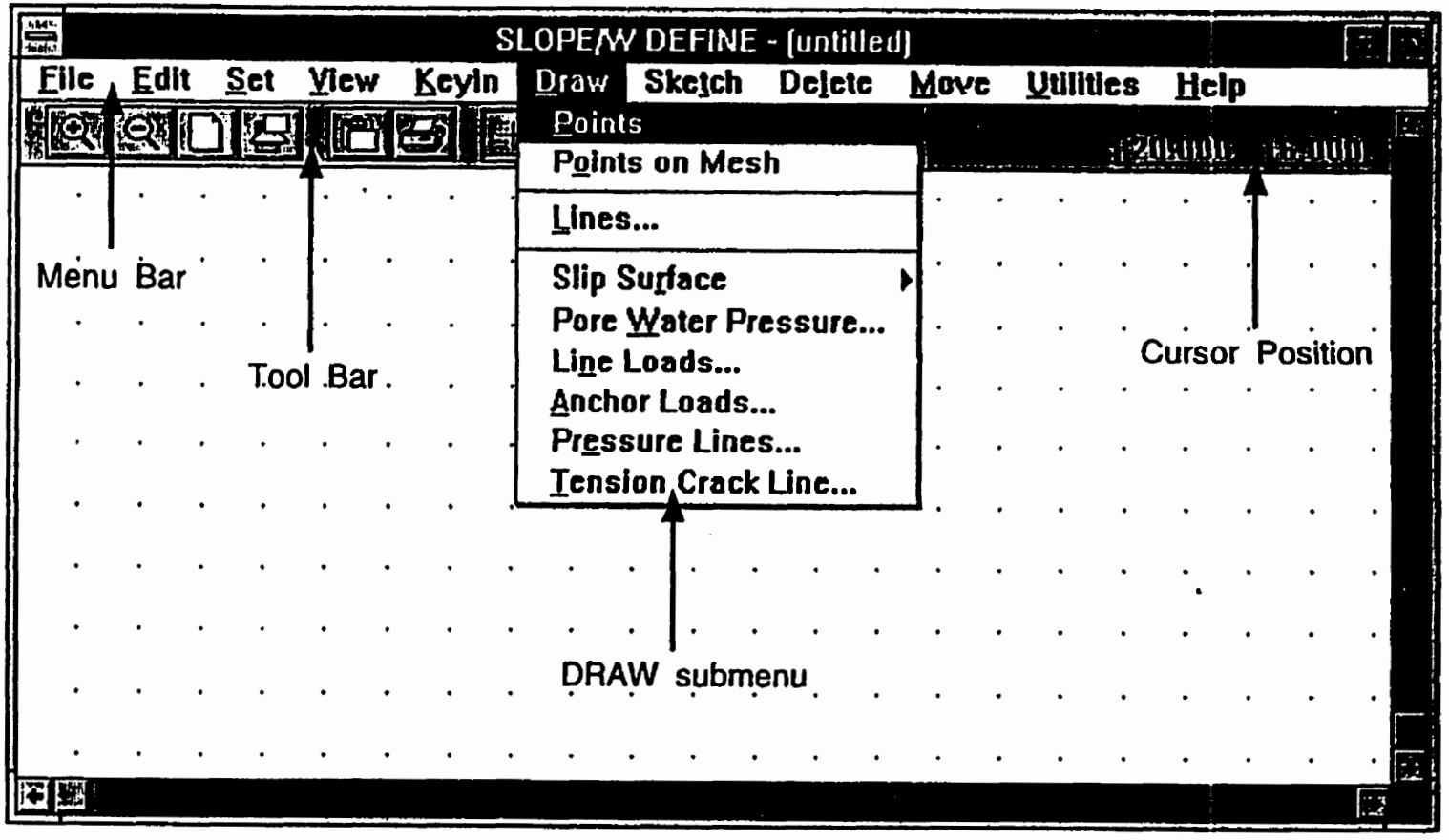

Figure 3.1 SLOPE/W DEFINE window (SLOPE/W User's guide, Geo-slope International)

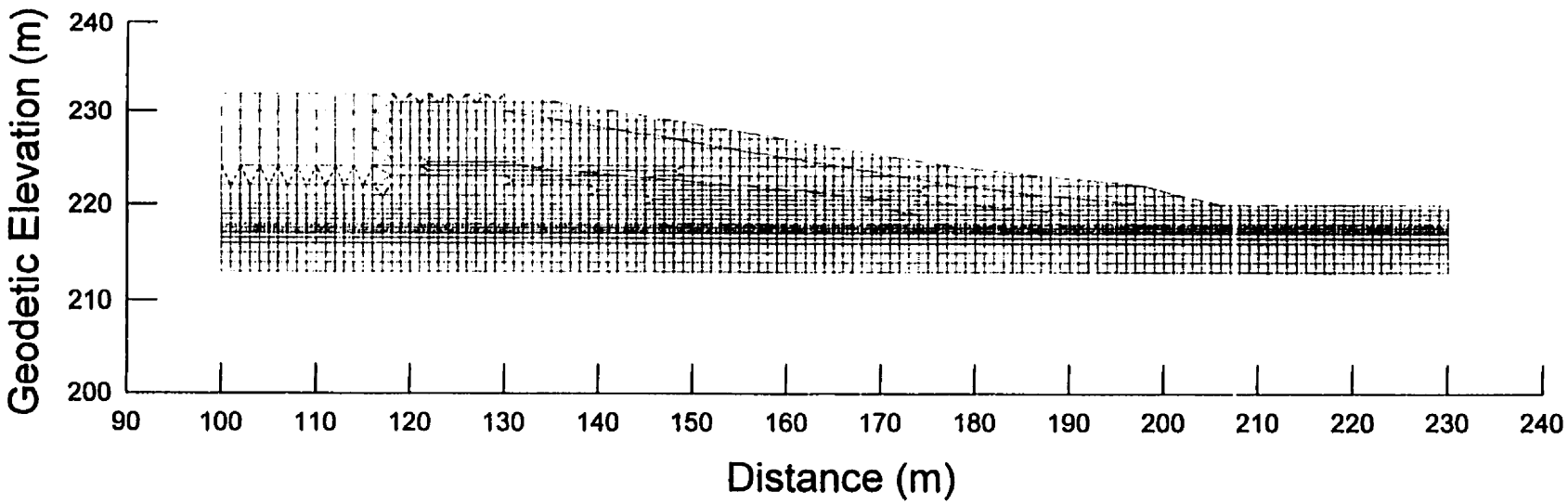

Figure 3.2 SEEP/W finite element mesh as it appears after import into SLOPE/W

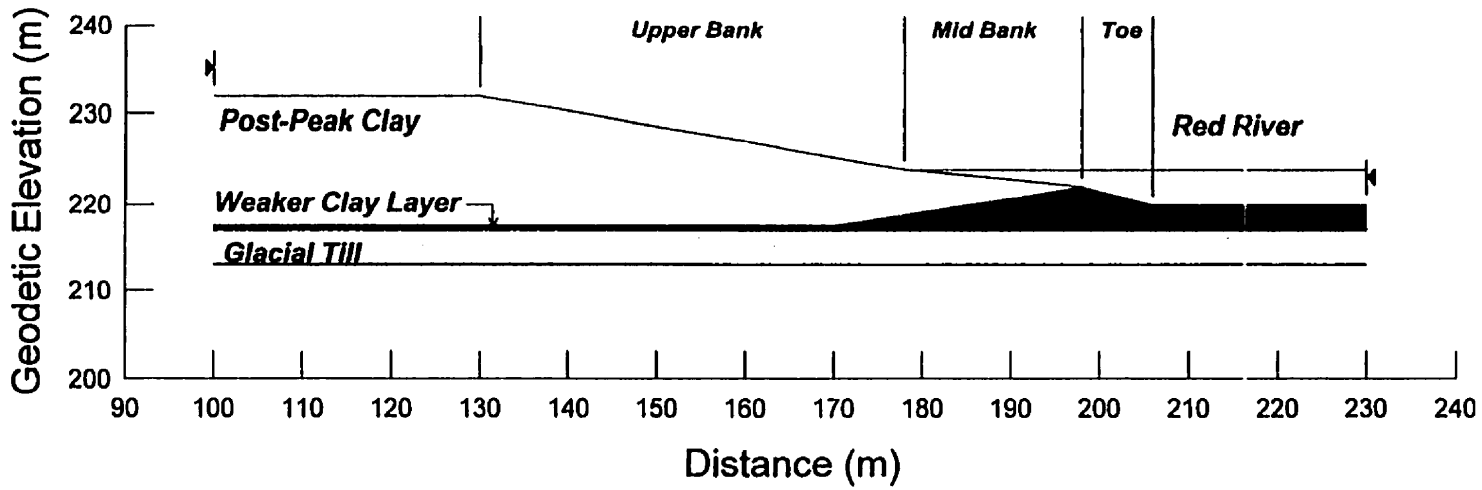

Figure 4.1 Stratigraphic units of the idealized riverbank used for stability analysis

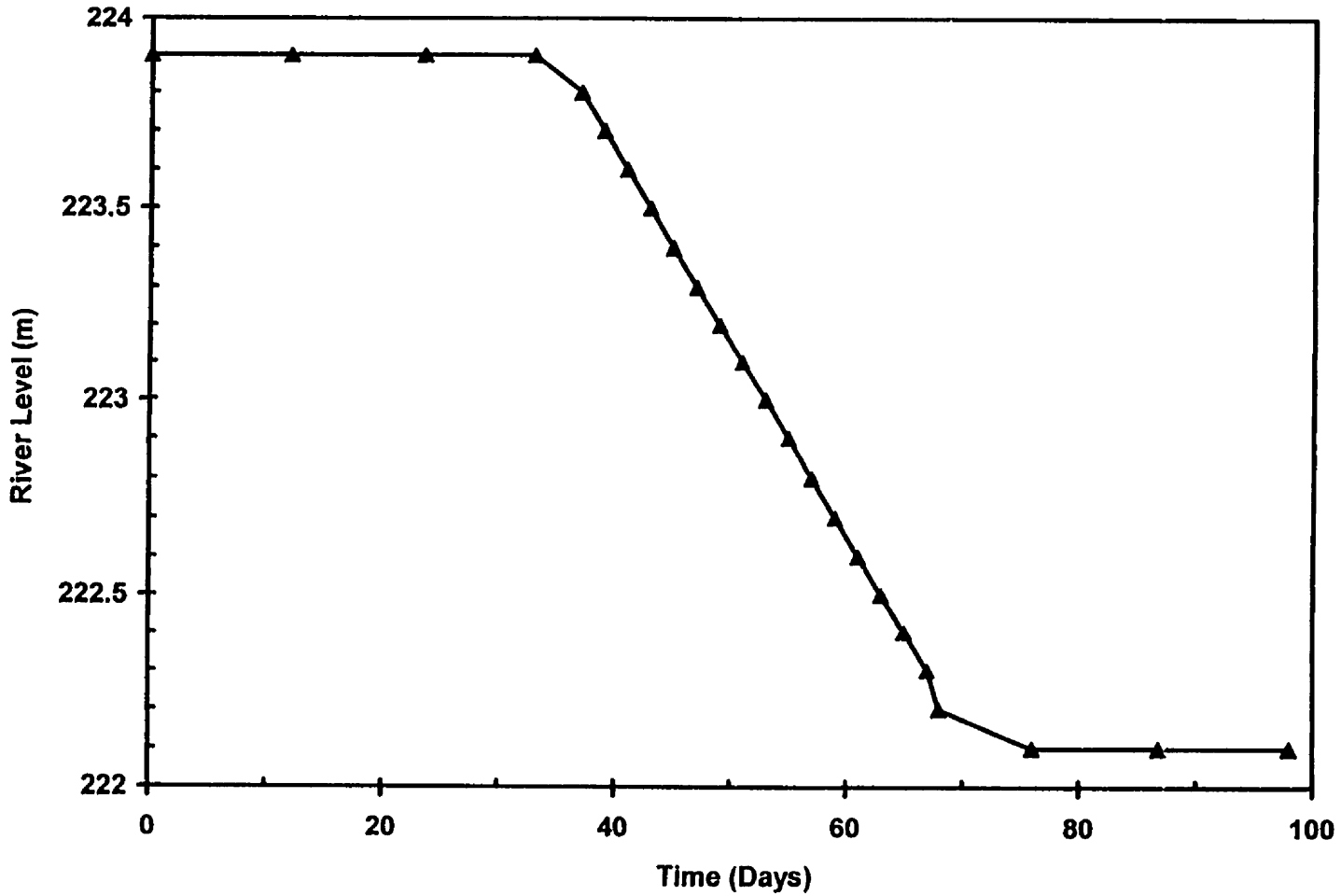

Figure 4.2 River level boundary condition (function) assigned to riverbank between regulated summer river level and unregulated winter river level in the SEEP/W FE model

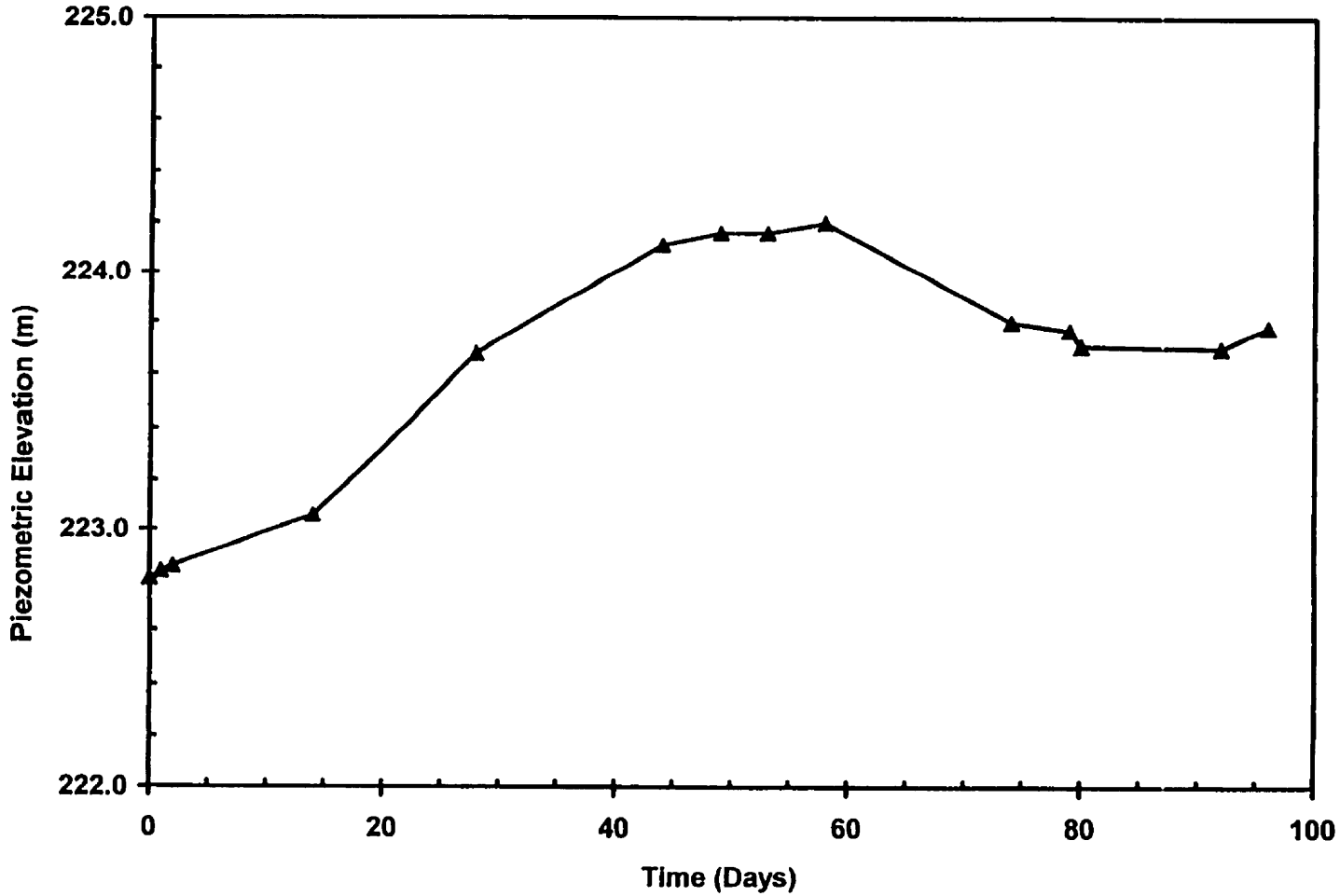

Figure 4.3 Bedrock aquifer boundary condition (function) assigned to base of glacial till in the SEEP/W FE model

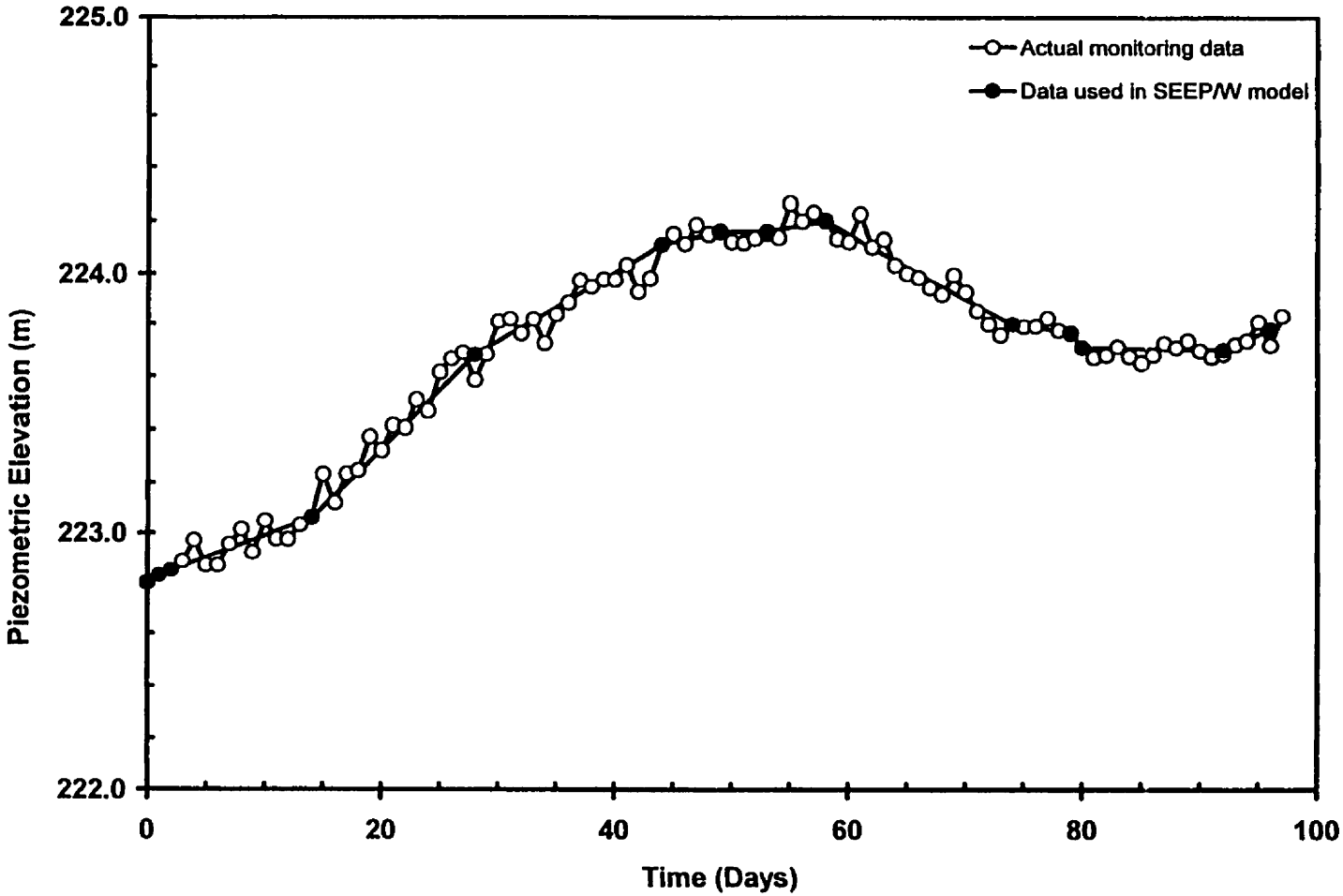

Figure 4.4 Comparison of observed bedrock aquifer piezometric elevations with SEEP/W modeled bedrock piezometric elevations

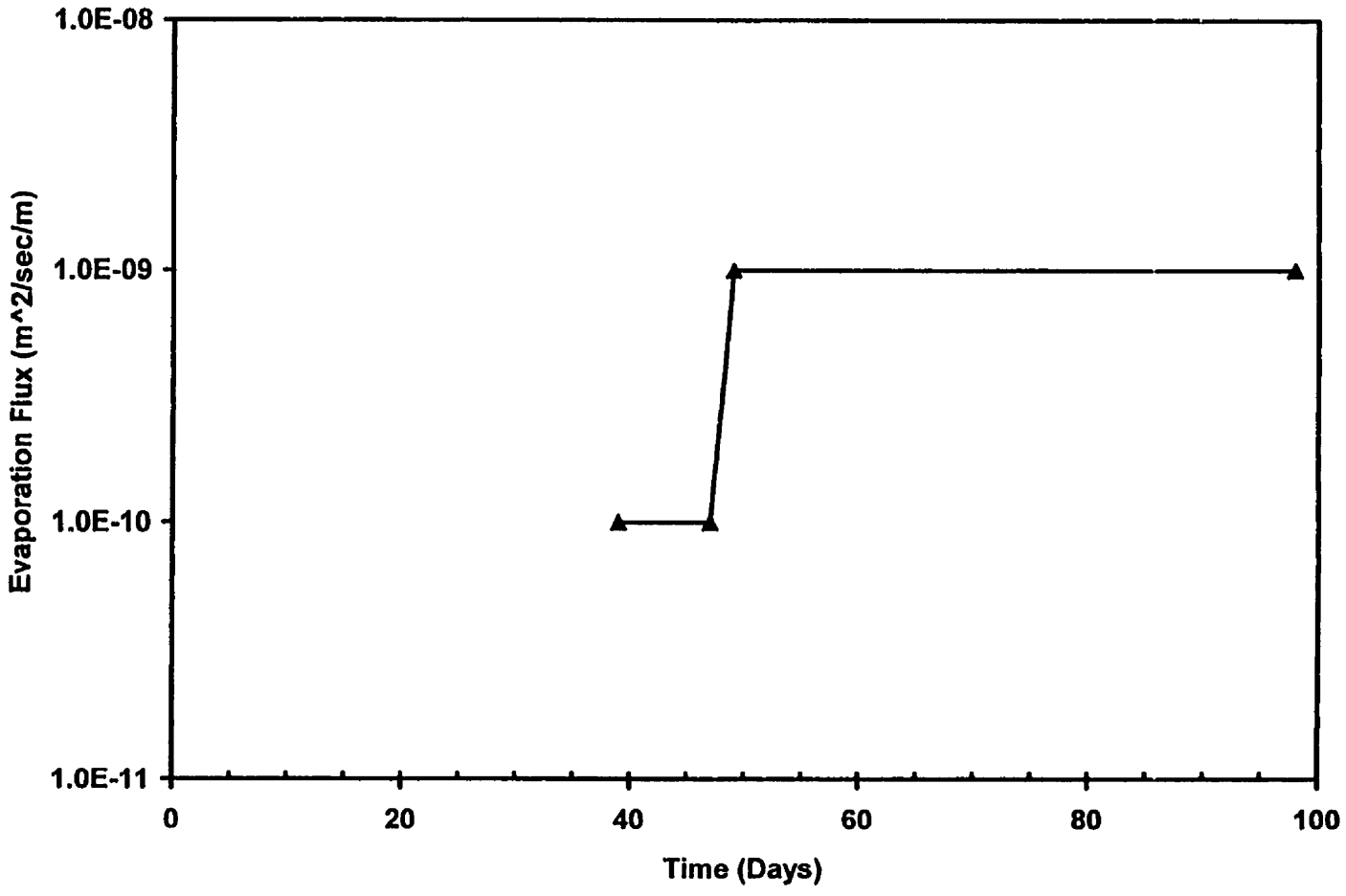

Figure 4.5 Porewater dissipation function assigned to riverbank between regulated summer river level and unregulated winter river level

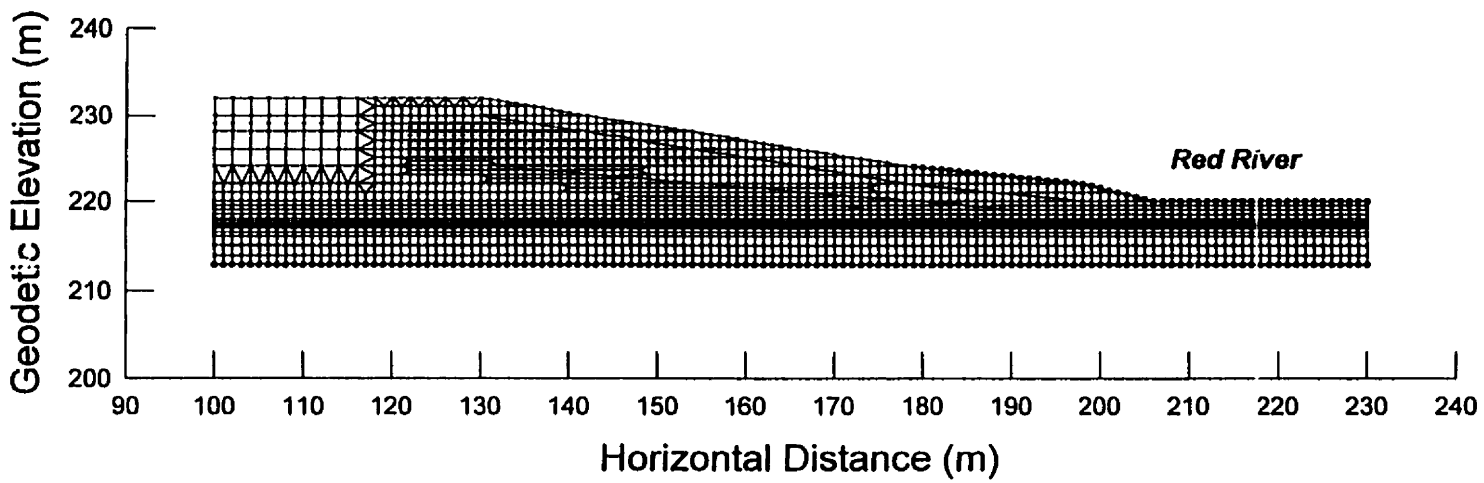

Figure 4.6 SEEP/W finite element mesh developed for seepage modeling

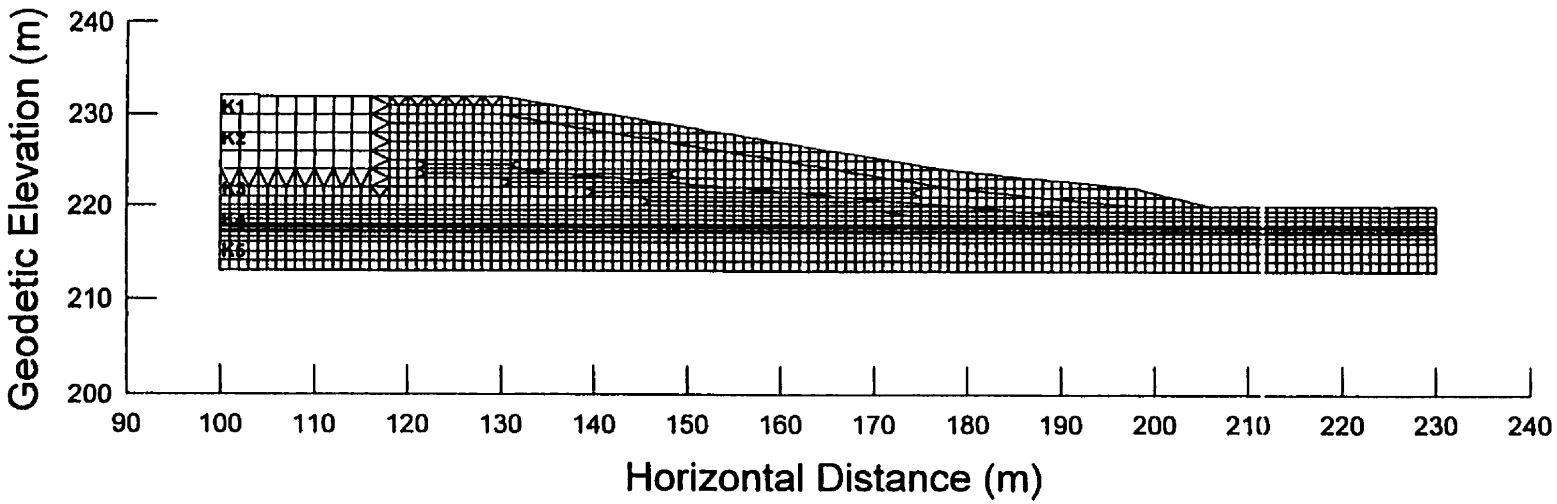

Figure 4.7 Differing hydraulic conductivity zones for the idealized riverbank

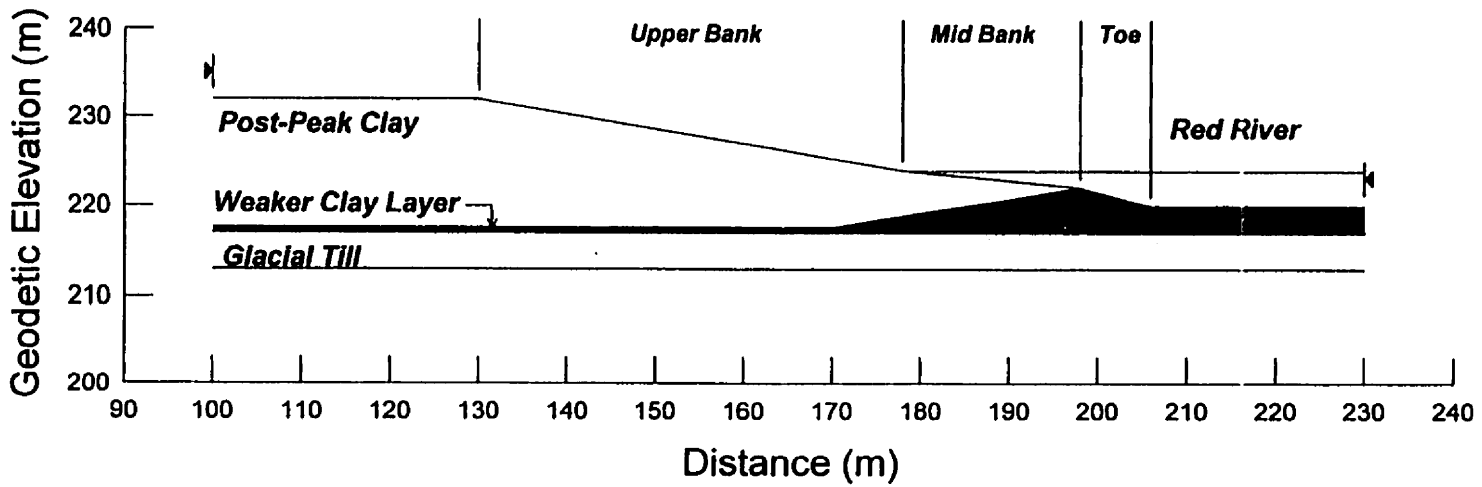

Figure 4.1 Stratigraphic units of the idealized riverbank used for stability analysis

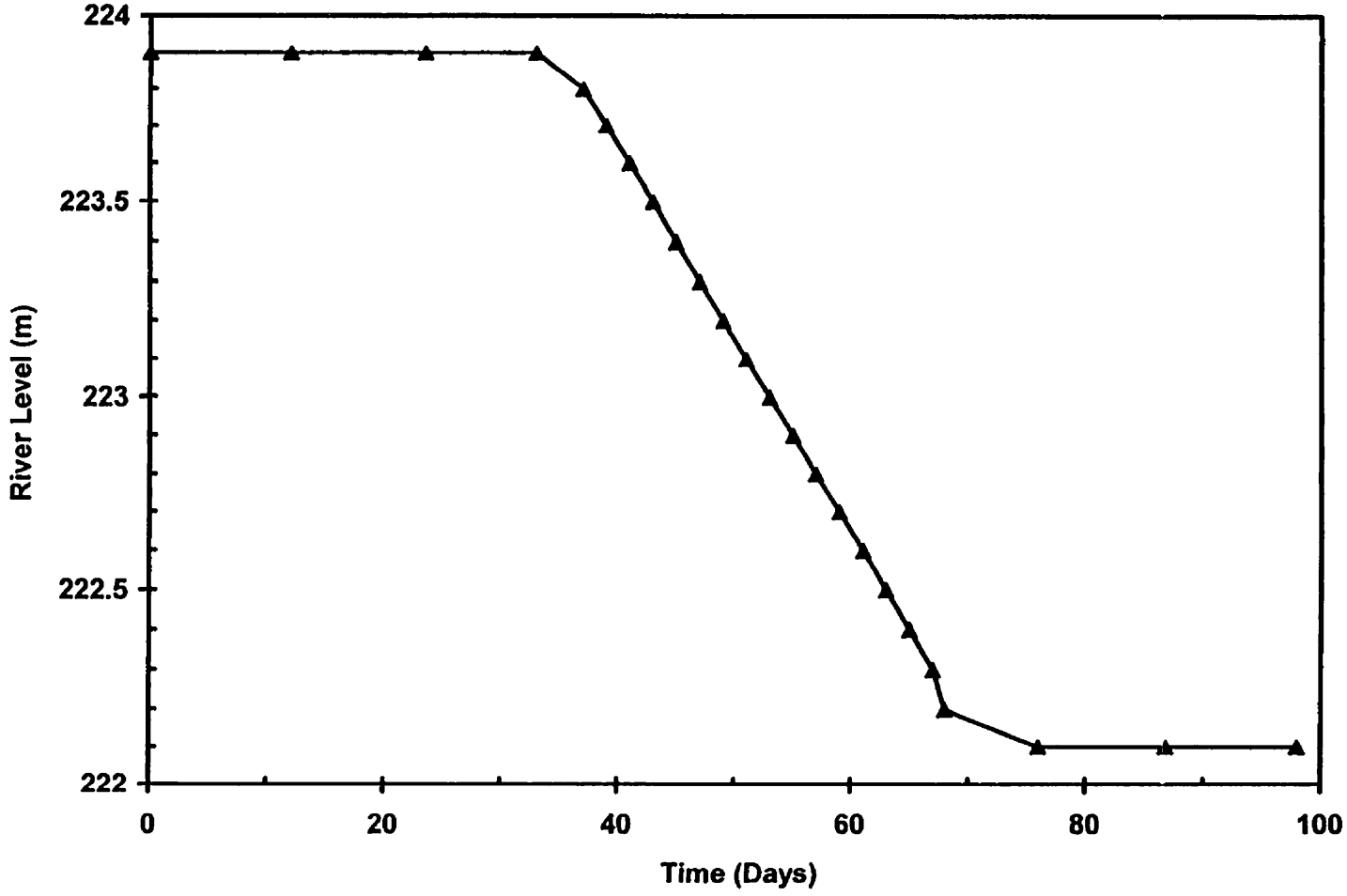

Figure 4.2 River level boundary condition (function) assigned to riverbank between regulated summer river level and unregulated winter river level in the SEEP/W FE model

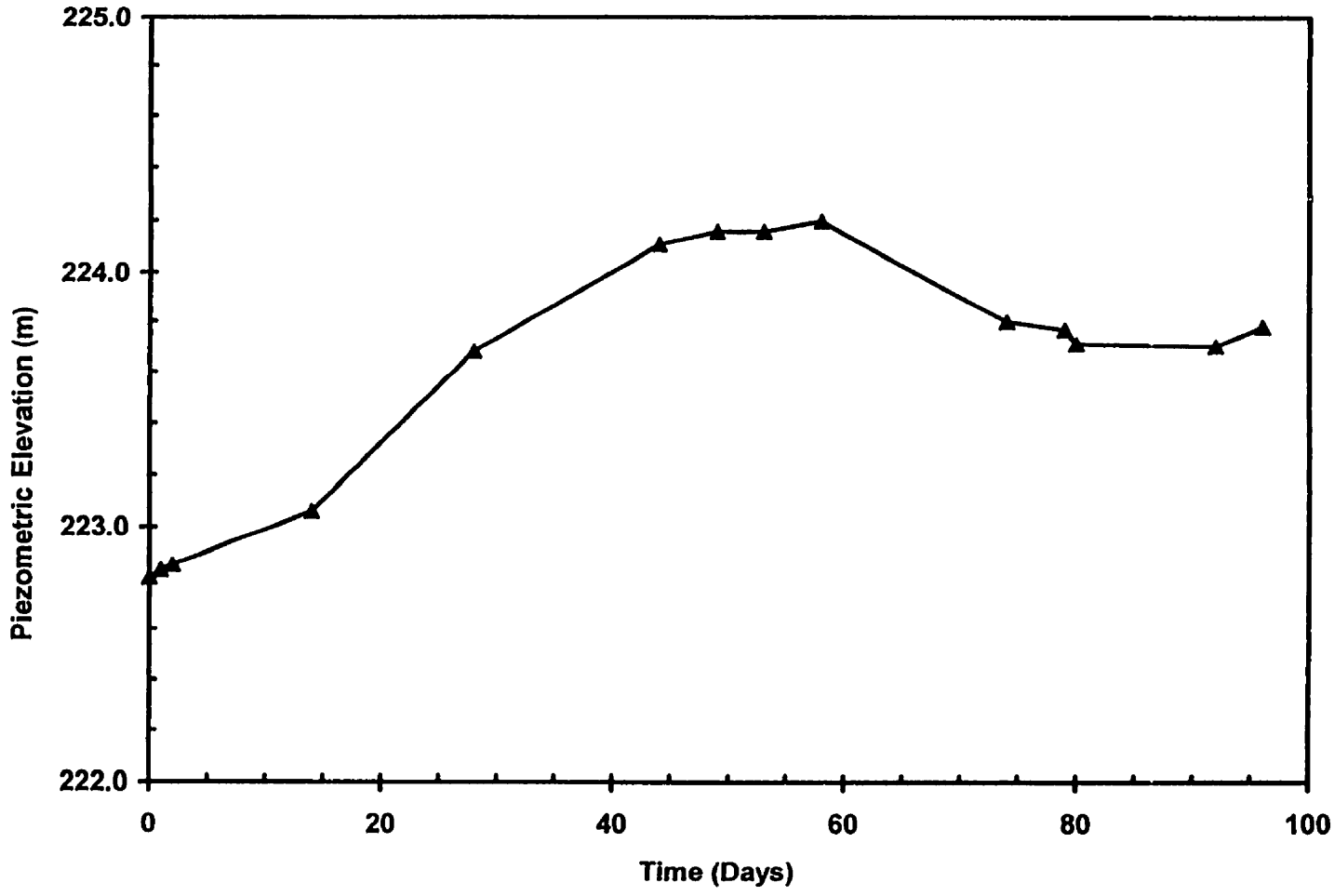

Figure 4.3 Bedrock aquifer boundary condition (function) assigned to base of glacial till in the SEEP/W FE model

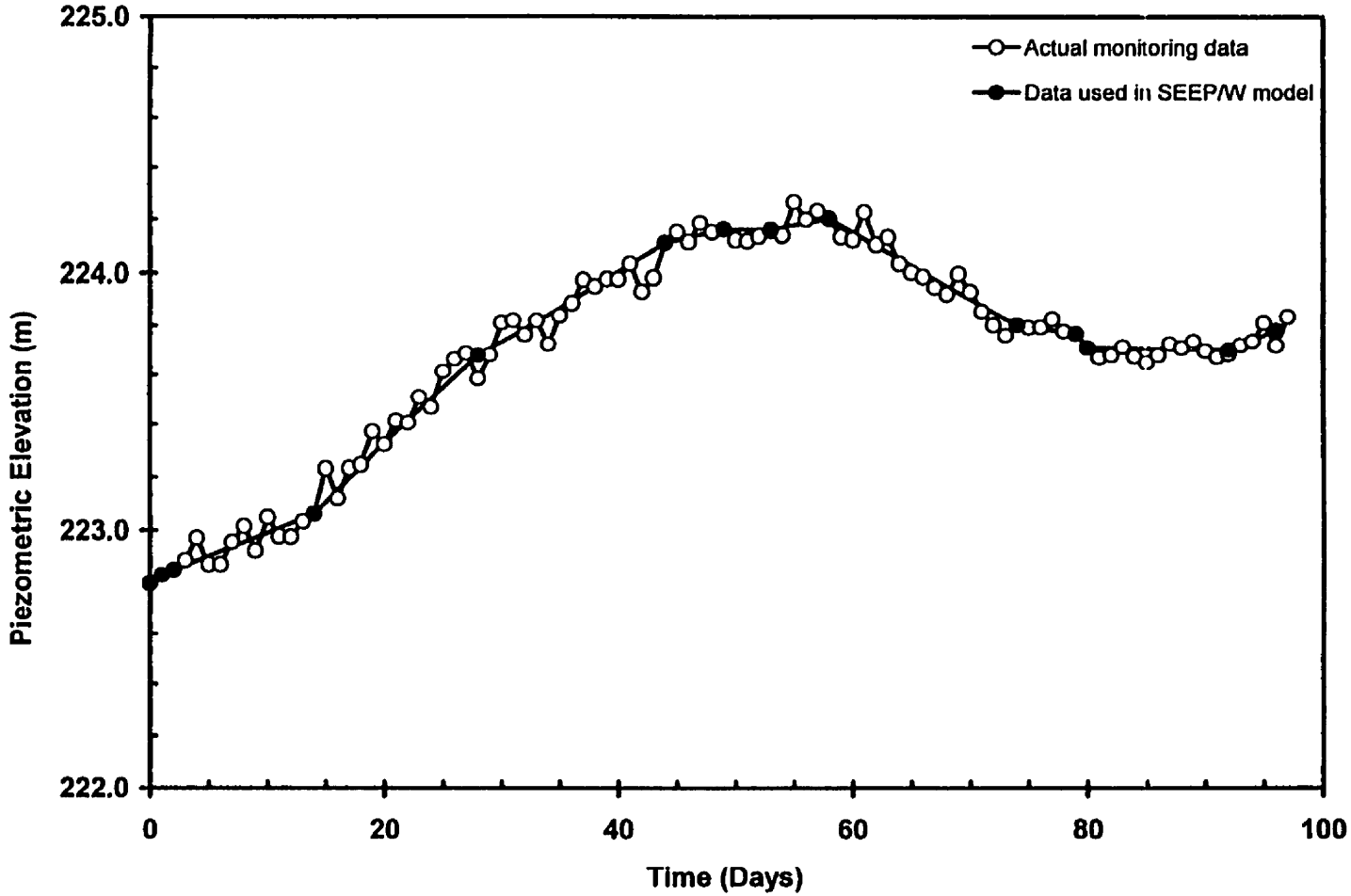

Figure 4.4 Comparison of observed bedrock aquifer piezometric elevations with SEEP/W modeled bedrock piezometric elevations

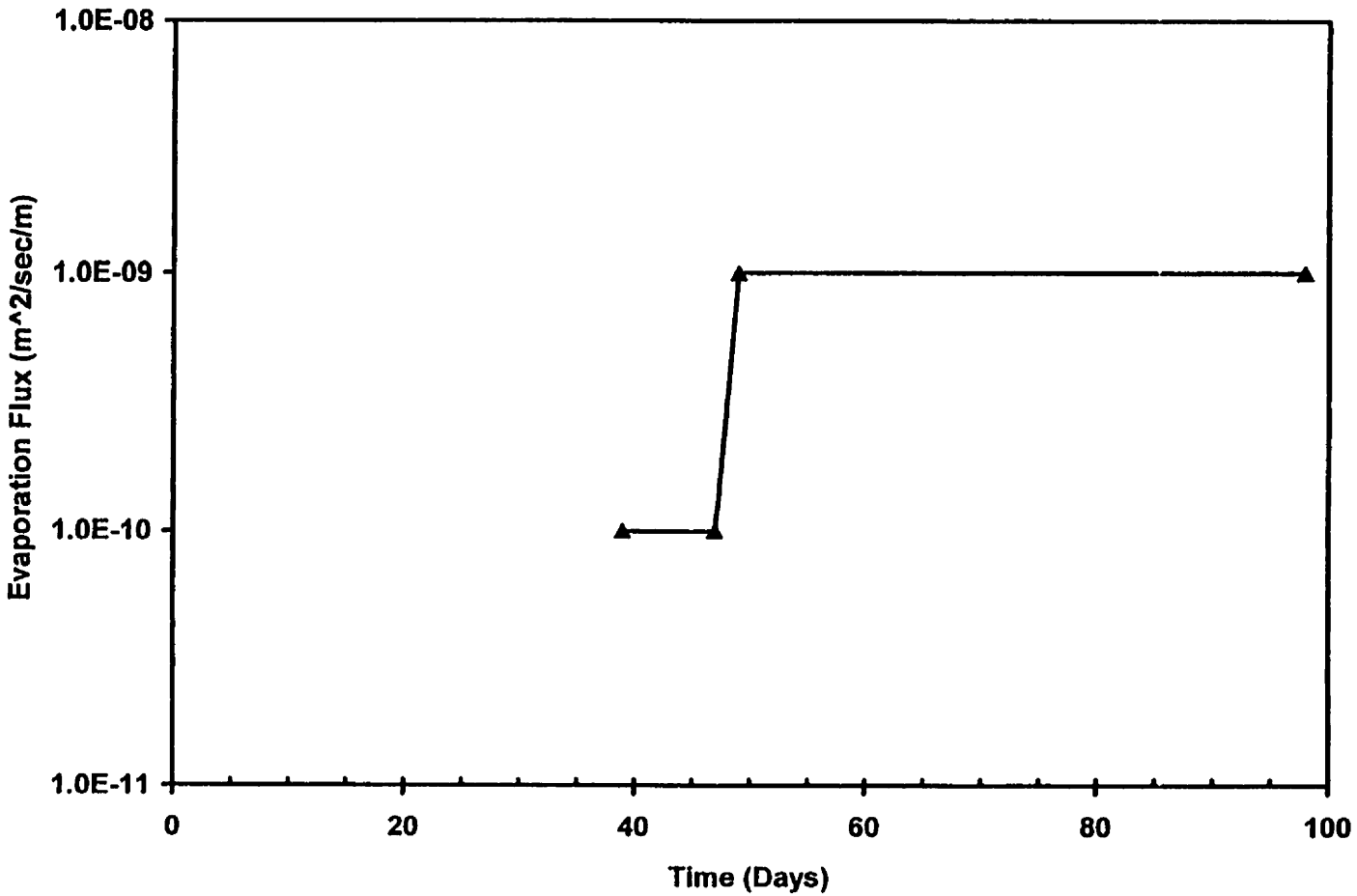

Figure 4.5 Porewater dissipation function assigned to riverbank between regulated summer river level and unregulated winter river level

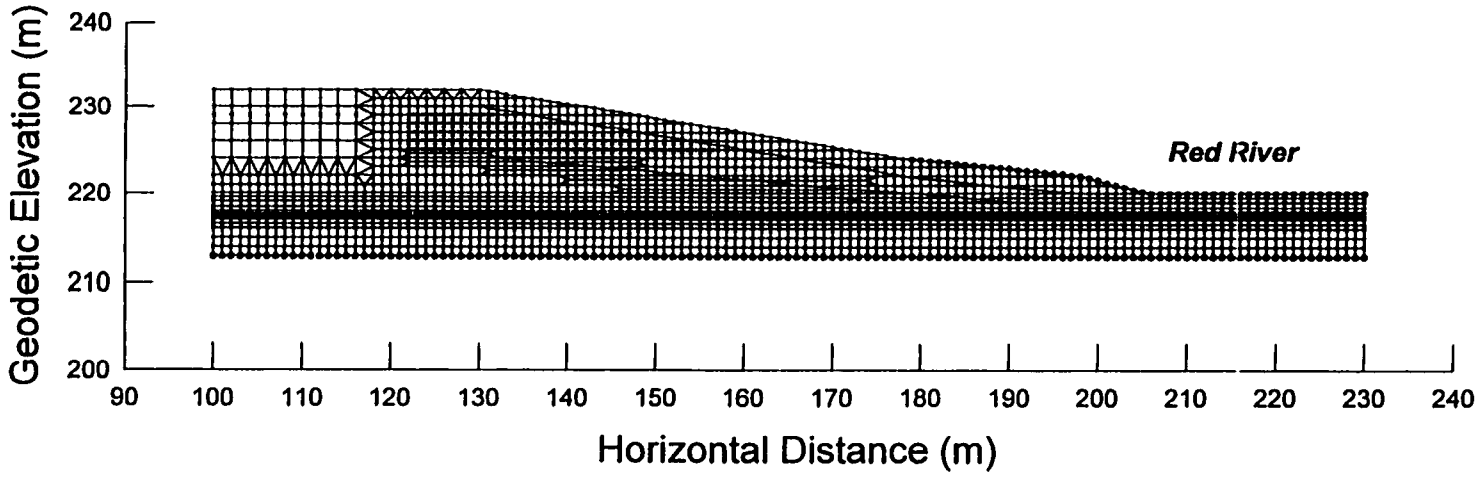

Figure 4.6 SEEP/W finite element mesh developed for seepage modeling

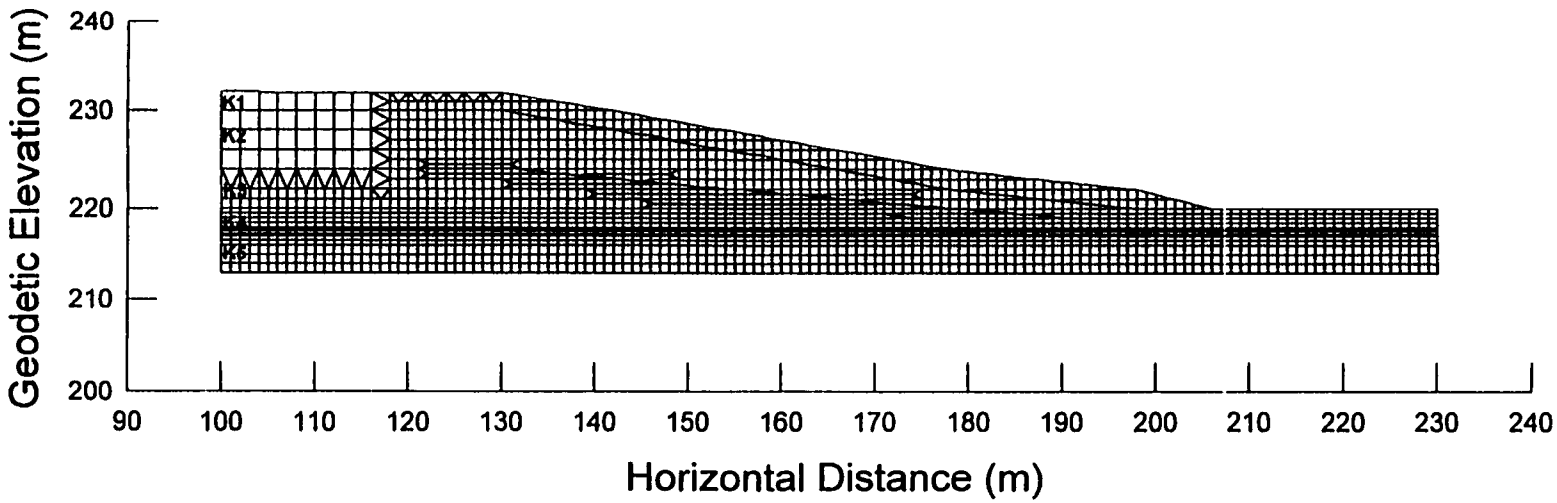

Figure 4.7 Differing hydraulic conductivity zones for the idealized riverbank

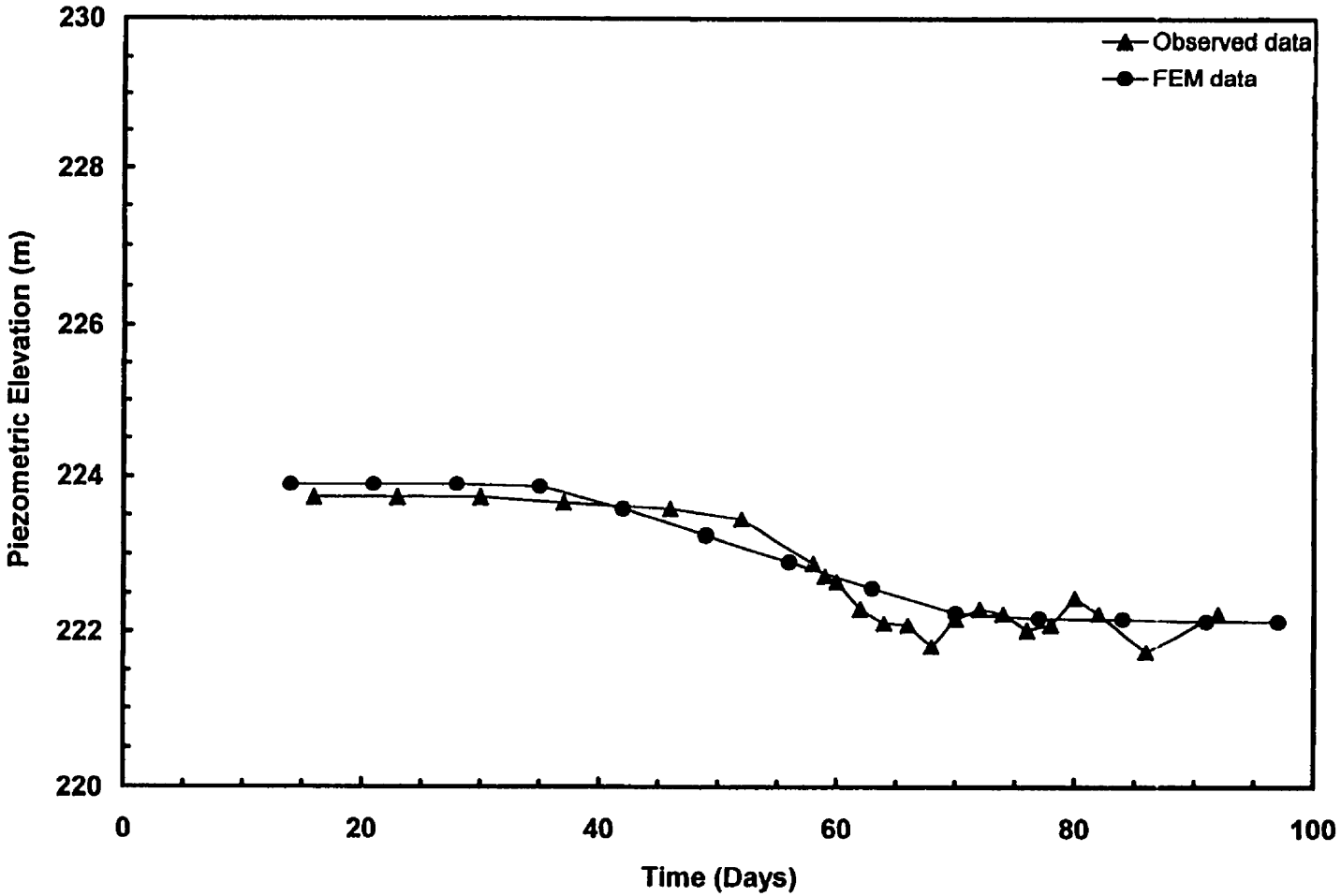

Figure 5.1 Comparison of observed piezometric elevation versus FE model data for P1 location

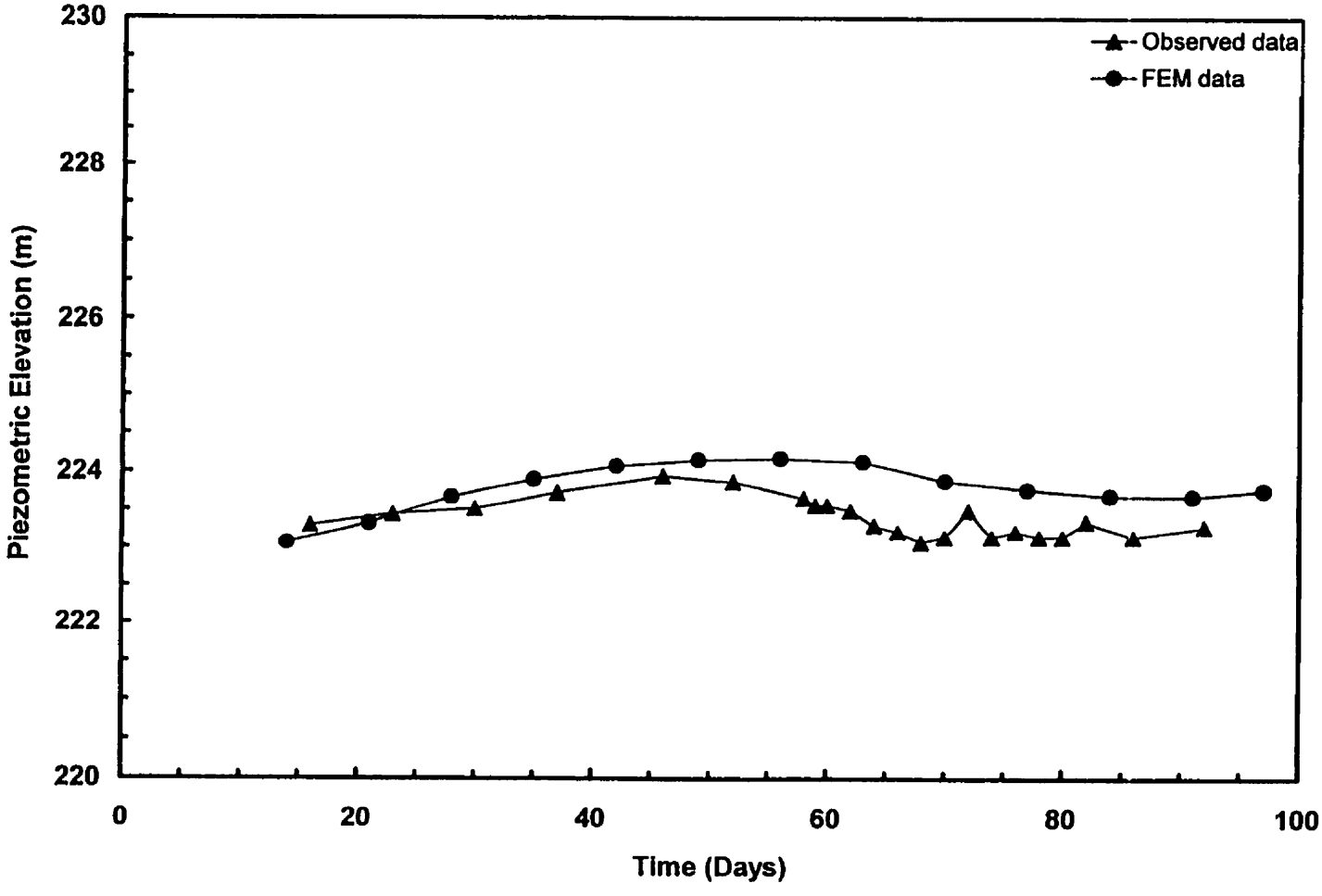

Figure 5.2 Comparison of observed piezometric elevation versus FE model data for P2 location

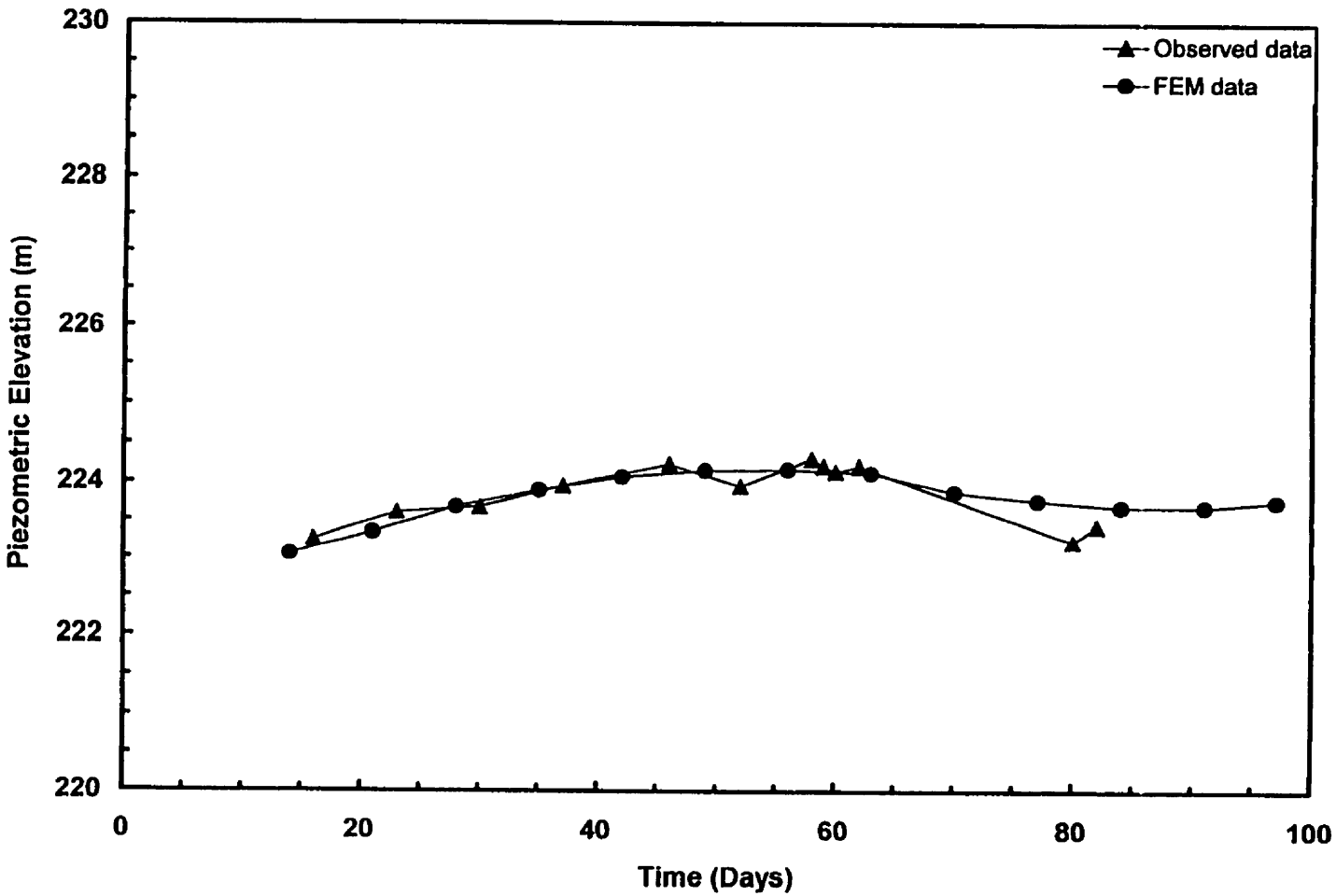

Figure 5.3 Comparison of observed piezometric elevation versus FE model data for P3 location

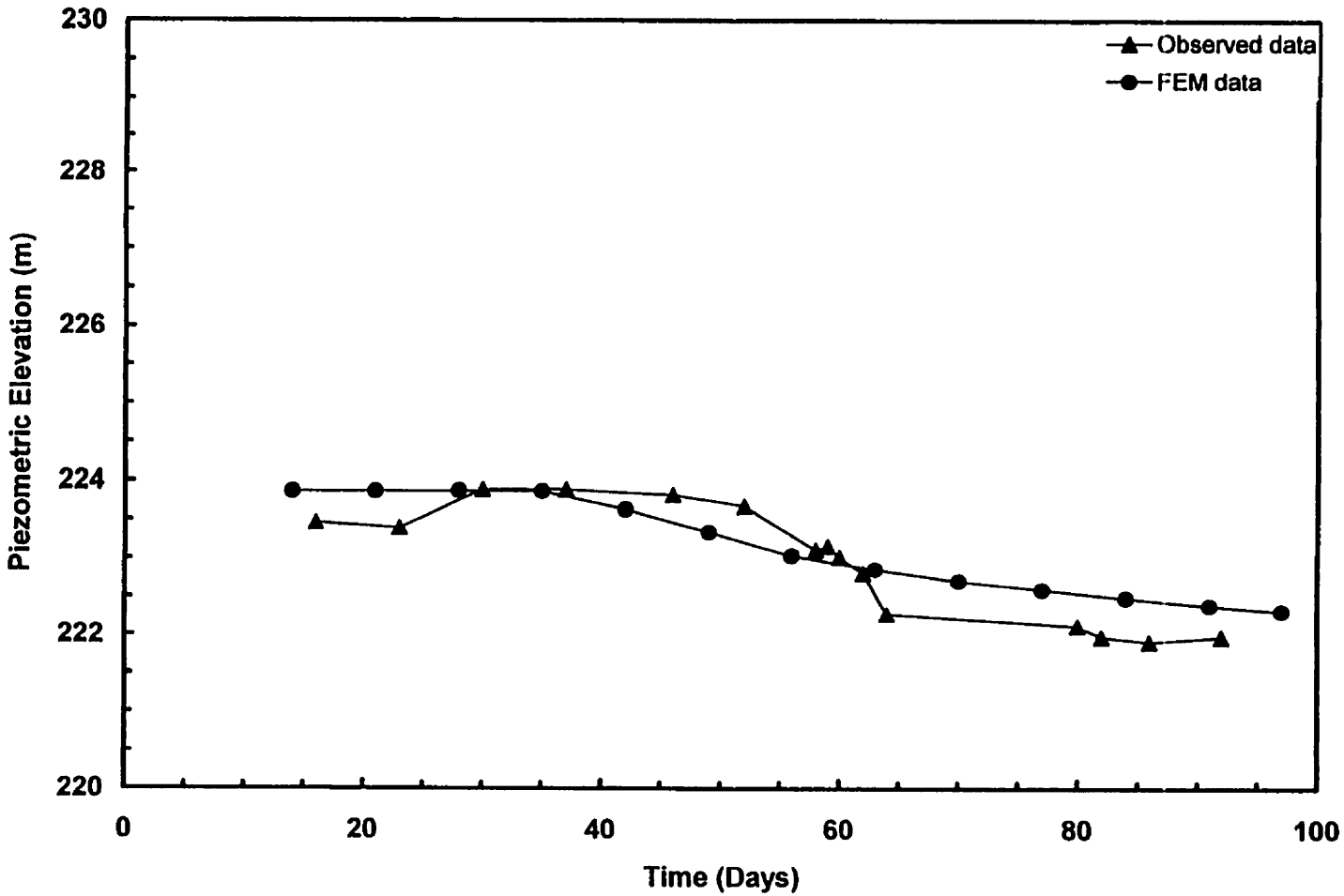

Figure 5.4 Comparison of observed piezometric elevation versus FE model data for P4 location

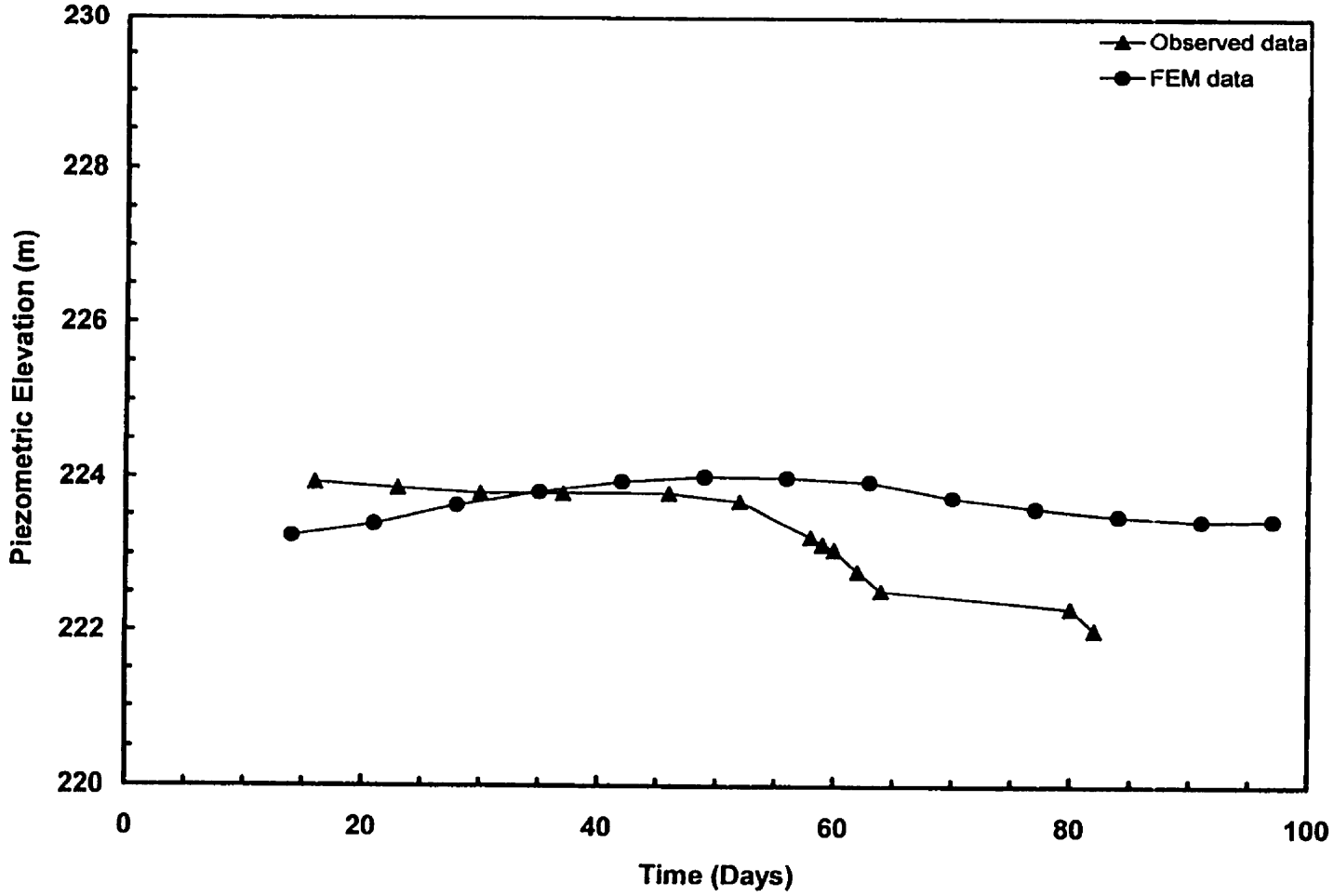

Figure 5.5 Comparison of observed piezometric elevation versus FE model data for P5 location

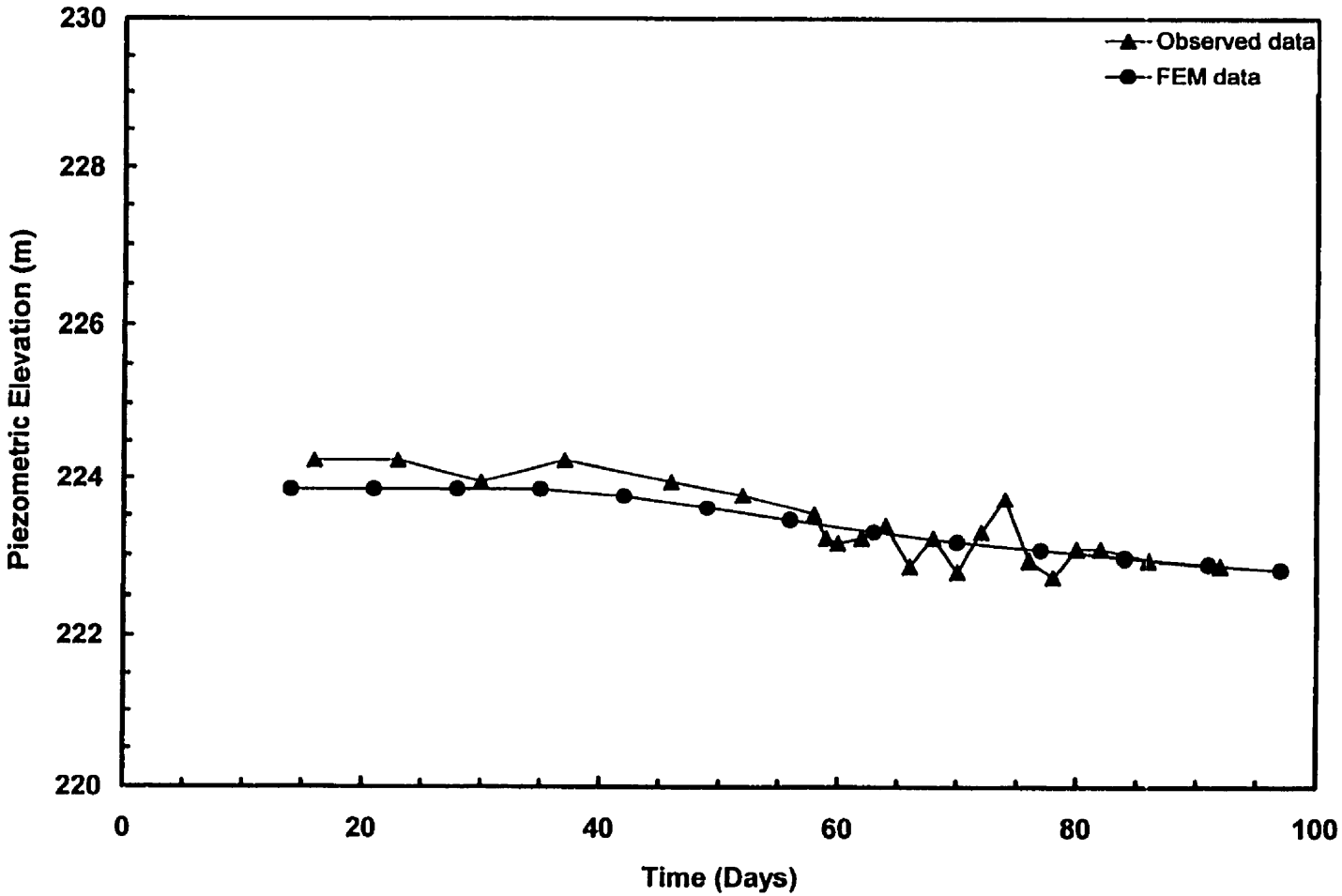

Figure 5.6 Comparison of observed piezometric elevation versus FE model data for P6 location

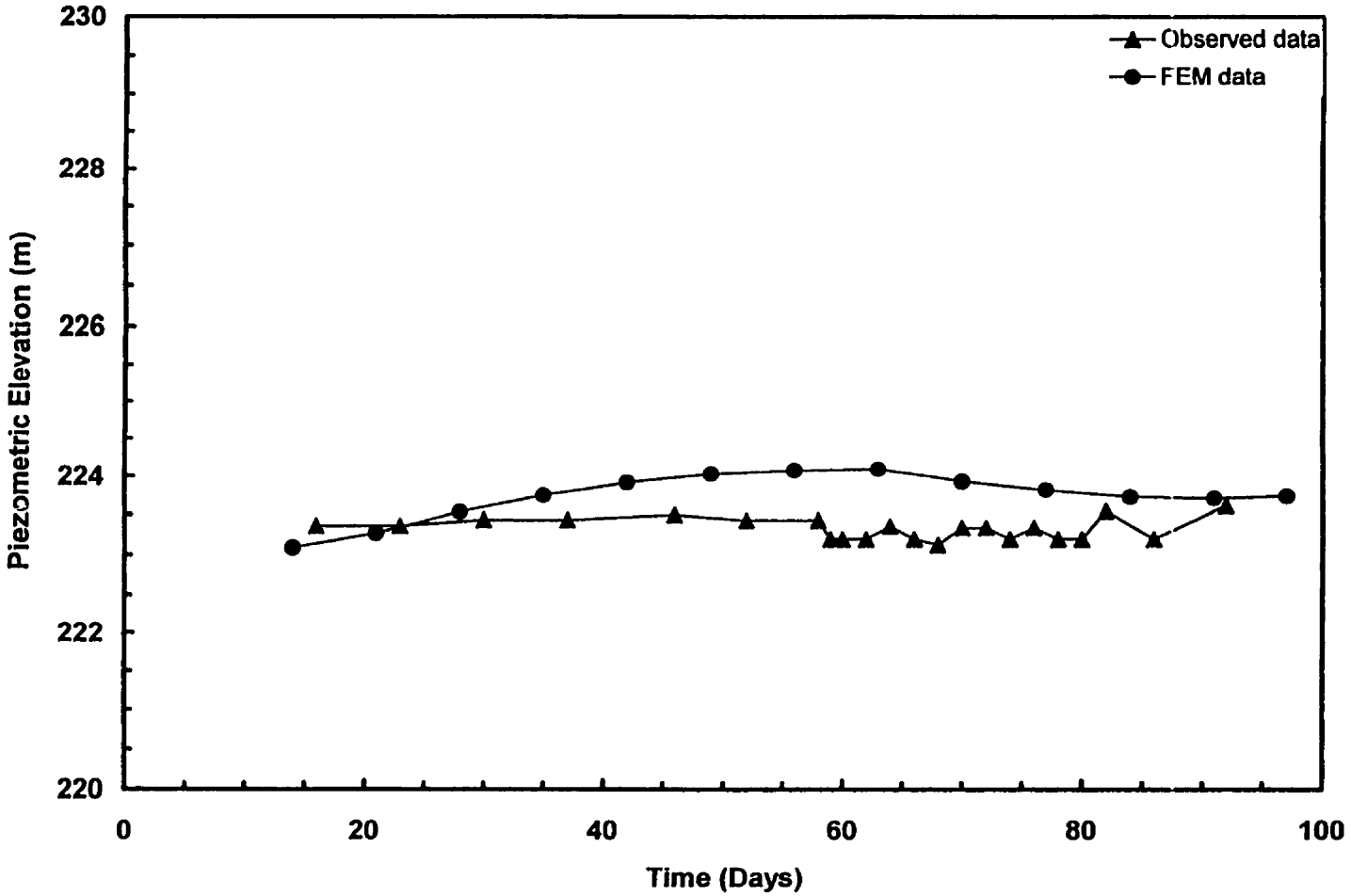

Figure 5.7 Comparison of observed piezometric elevation versus FE model data for P7 location

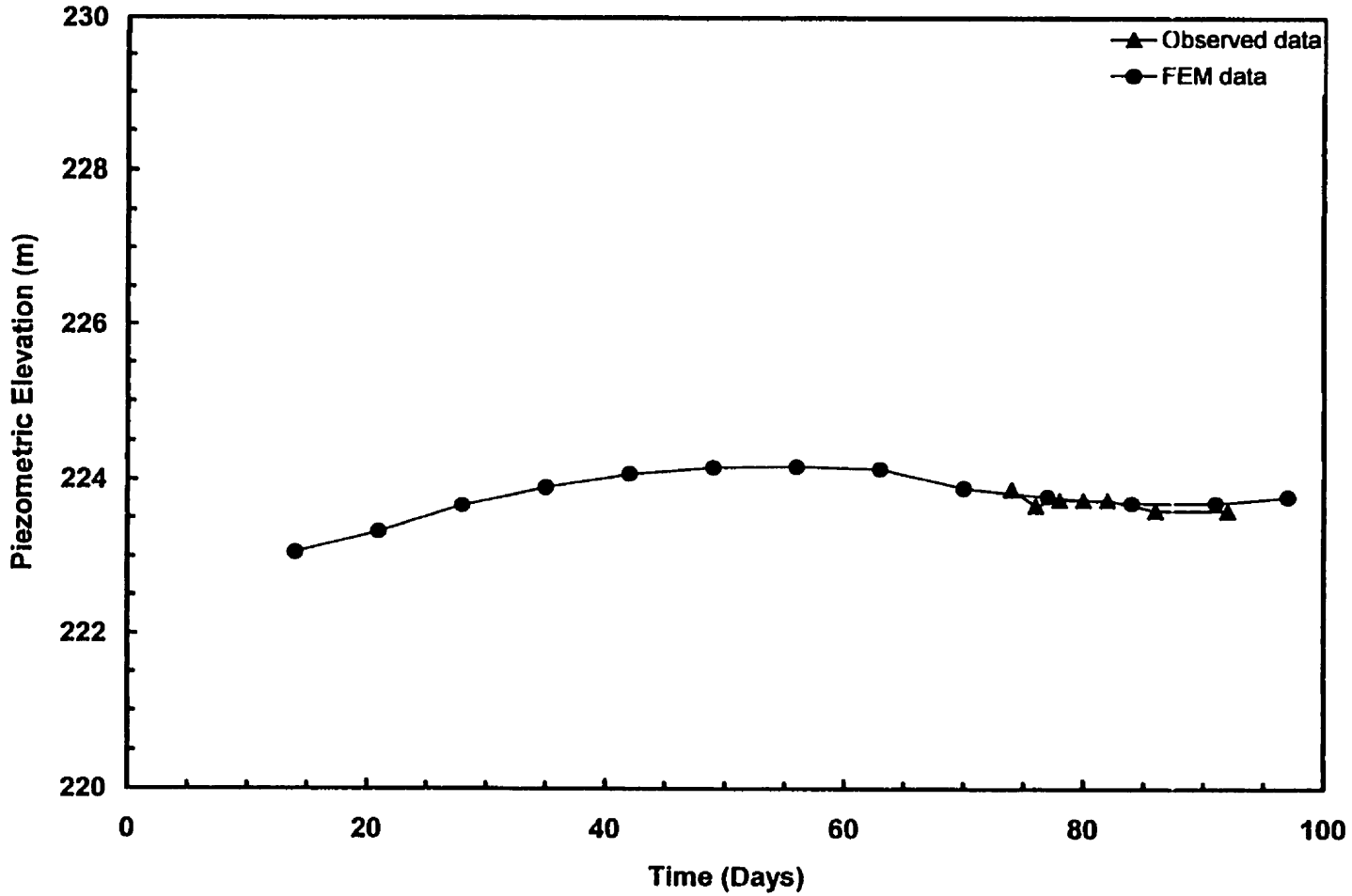

Figure 5.8 Comparison of observed piezometric elevation versus FE model data for P8 location

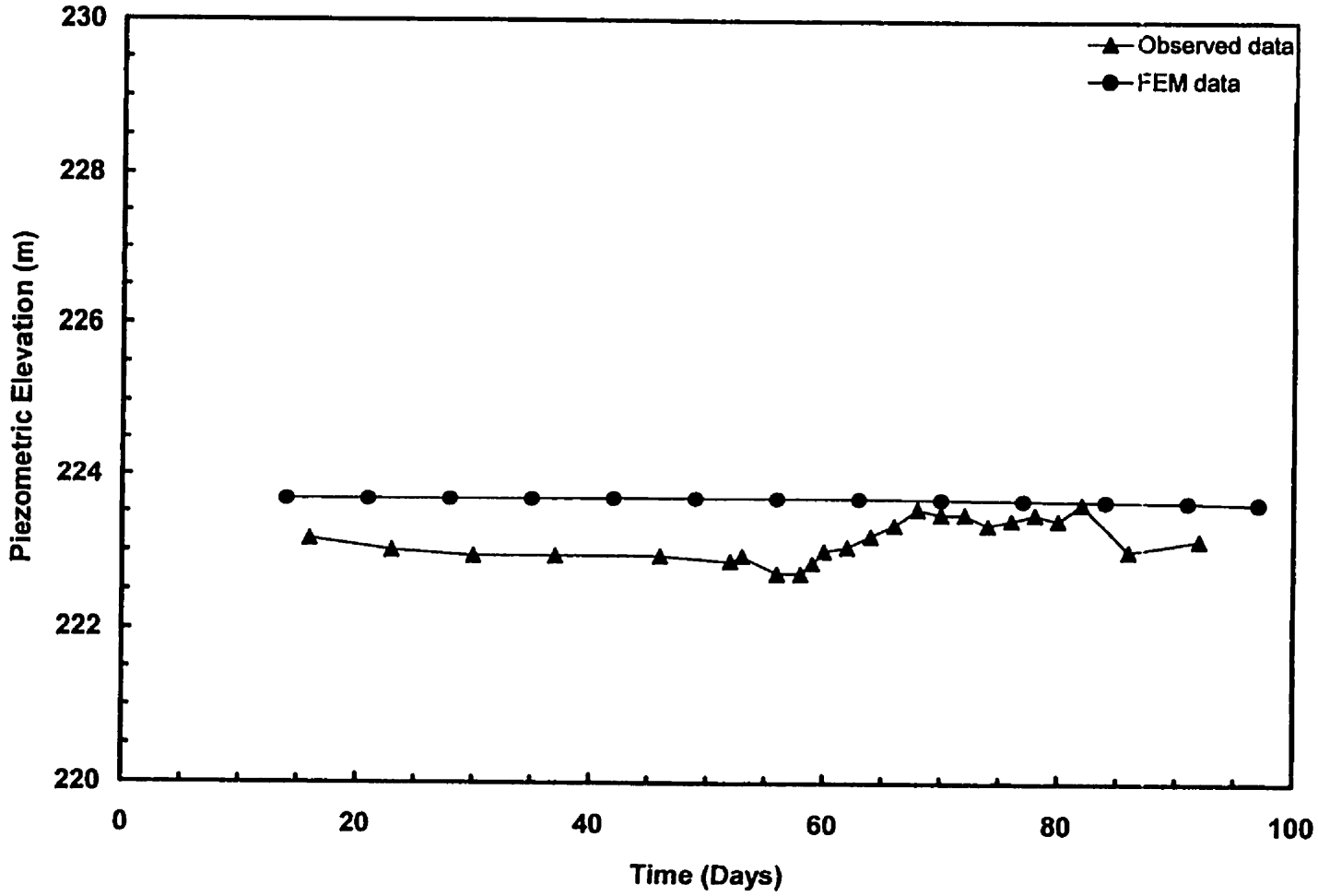

Figure 5.9 Comparison of observed piezometric elevation versus FE model data for P9 location

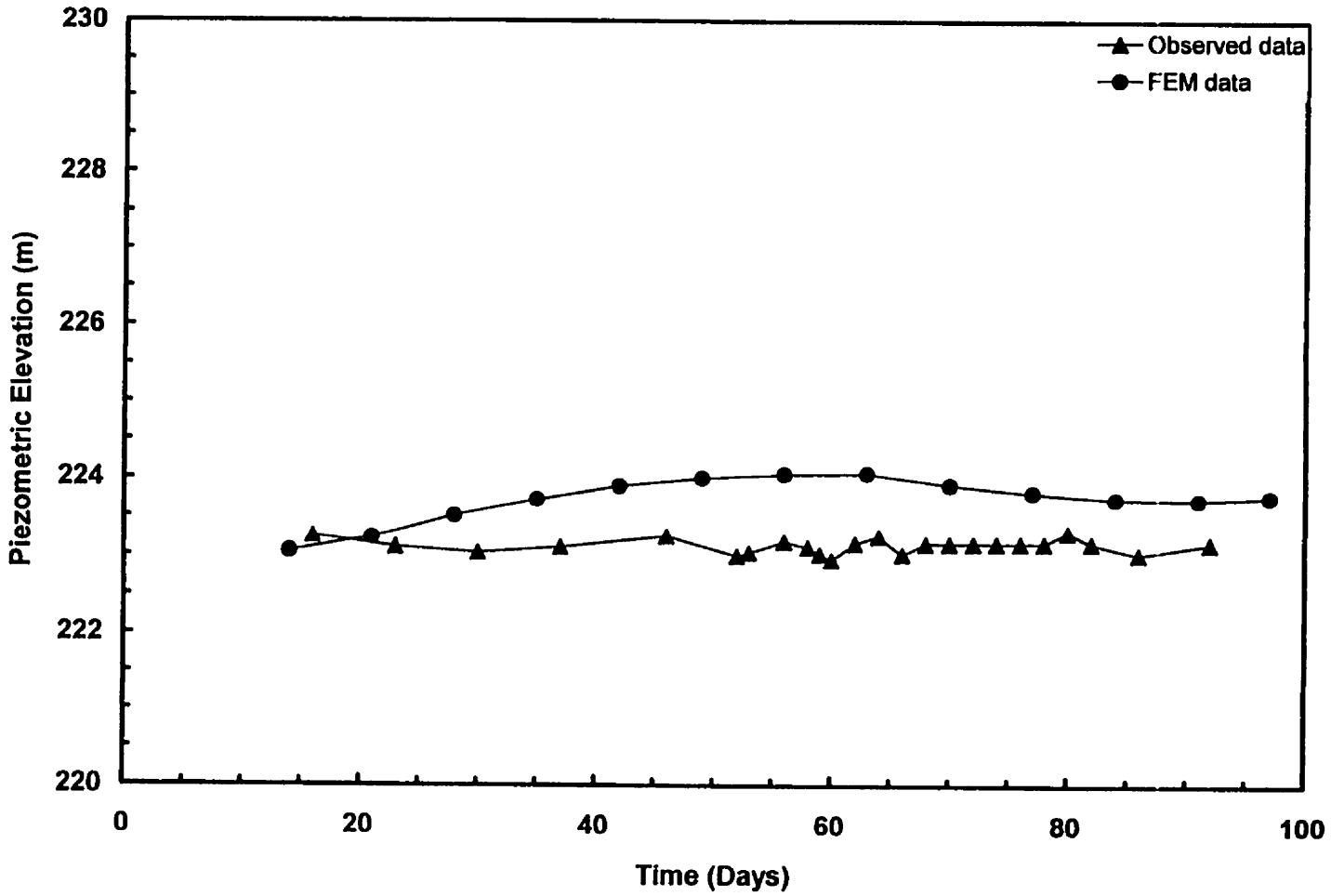

Figure 5.10 Comparison of observed piezometric elevation versus FE model data for P10 location

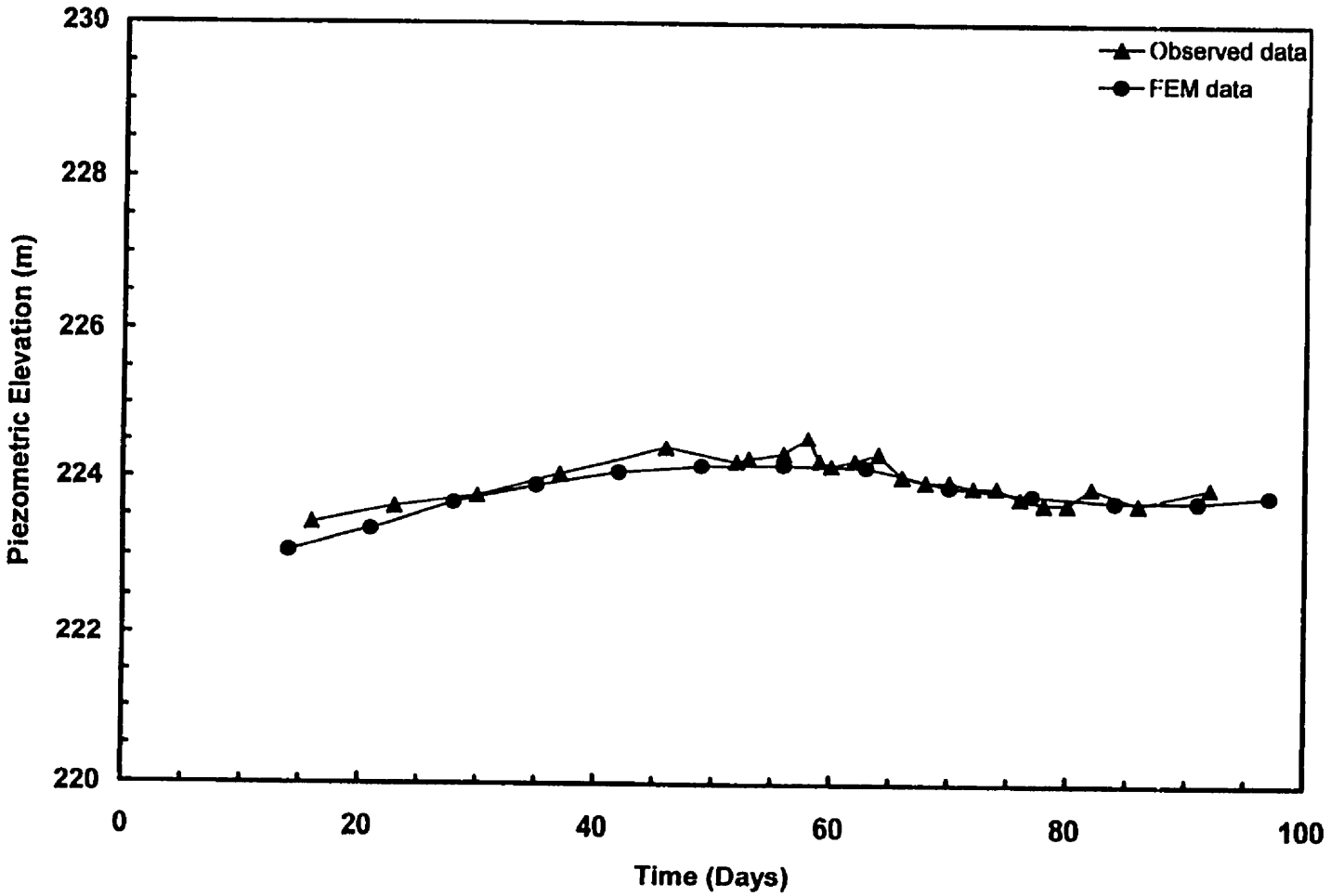

Figure 5.11 Comparison of observed piezometric elevation versus FE model data for P11 location

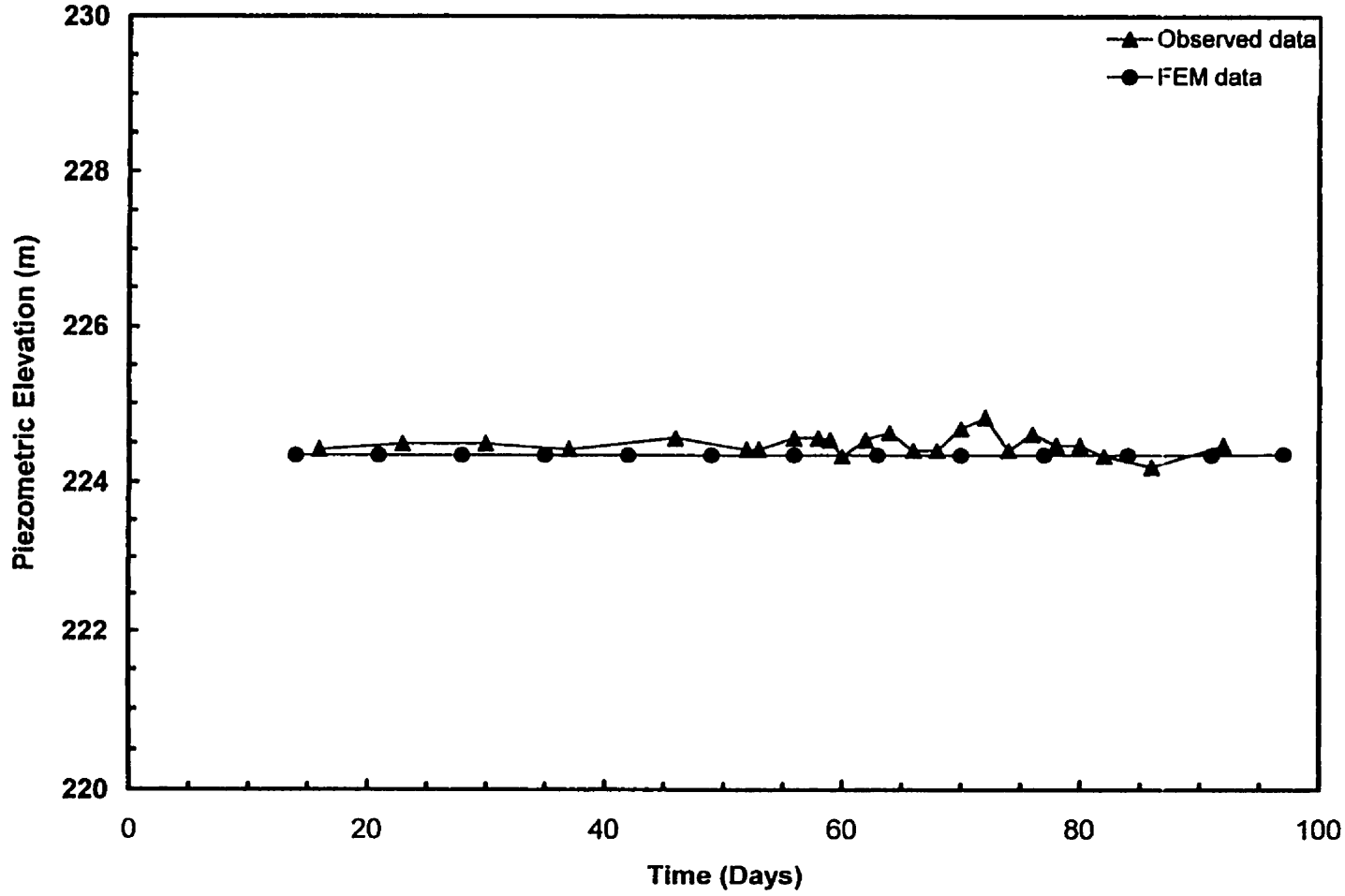

Figure 5.12 Comparison of observed piezometric elevation versus FE model data for P12 location

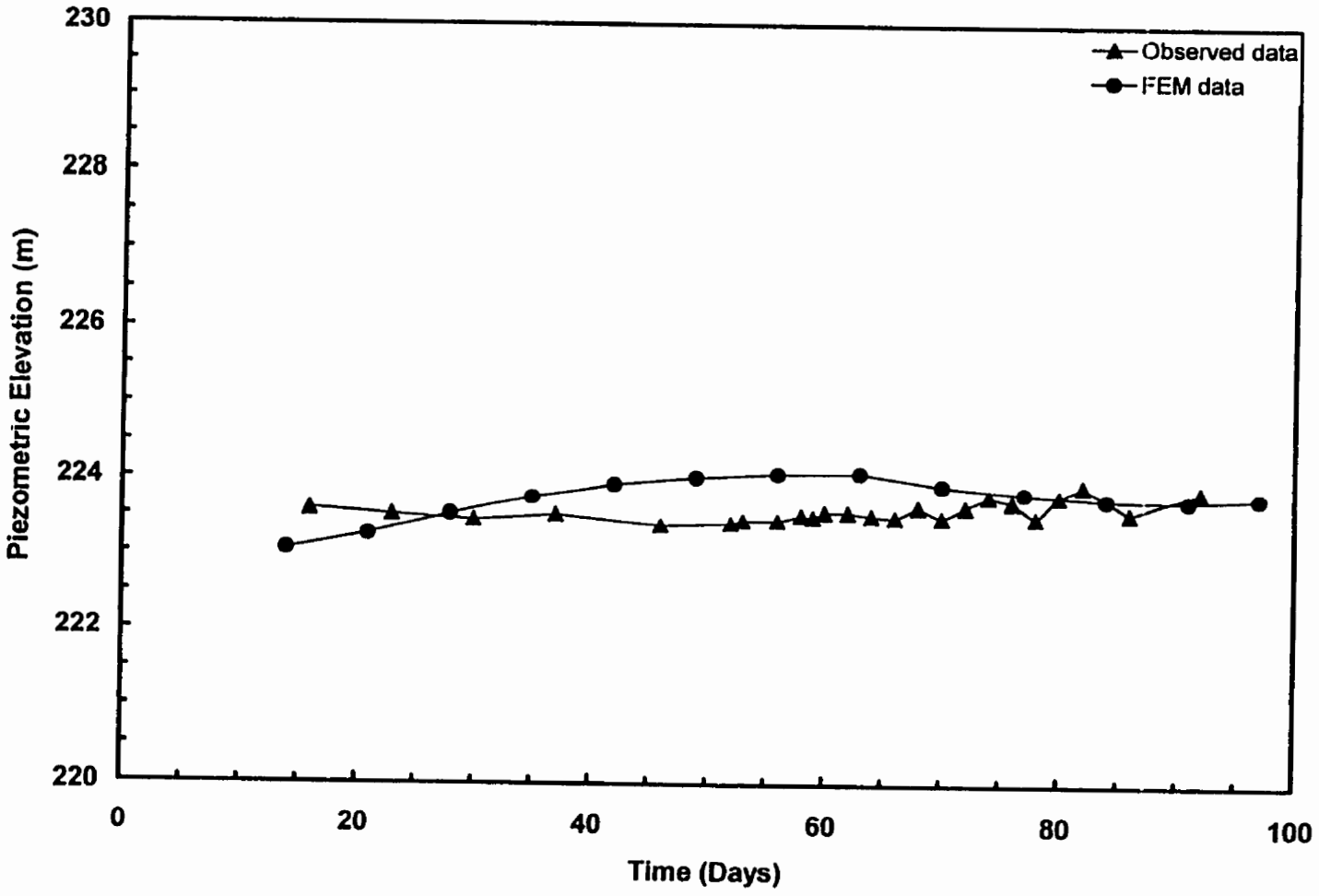

Figure 5.13 Comparison of observed piezometric elevation versus FE model data for P13 location

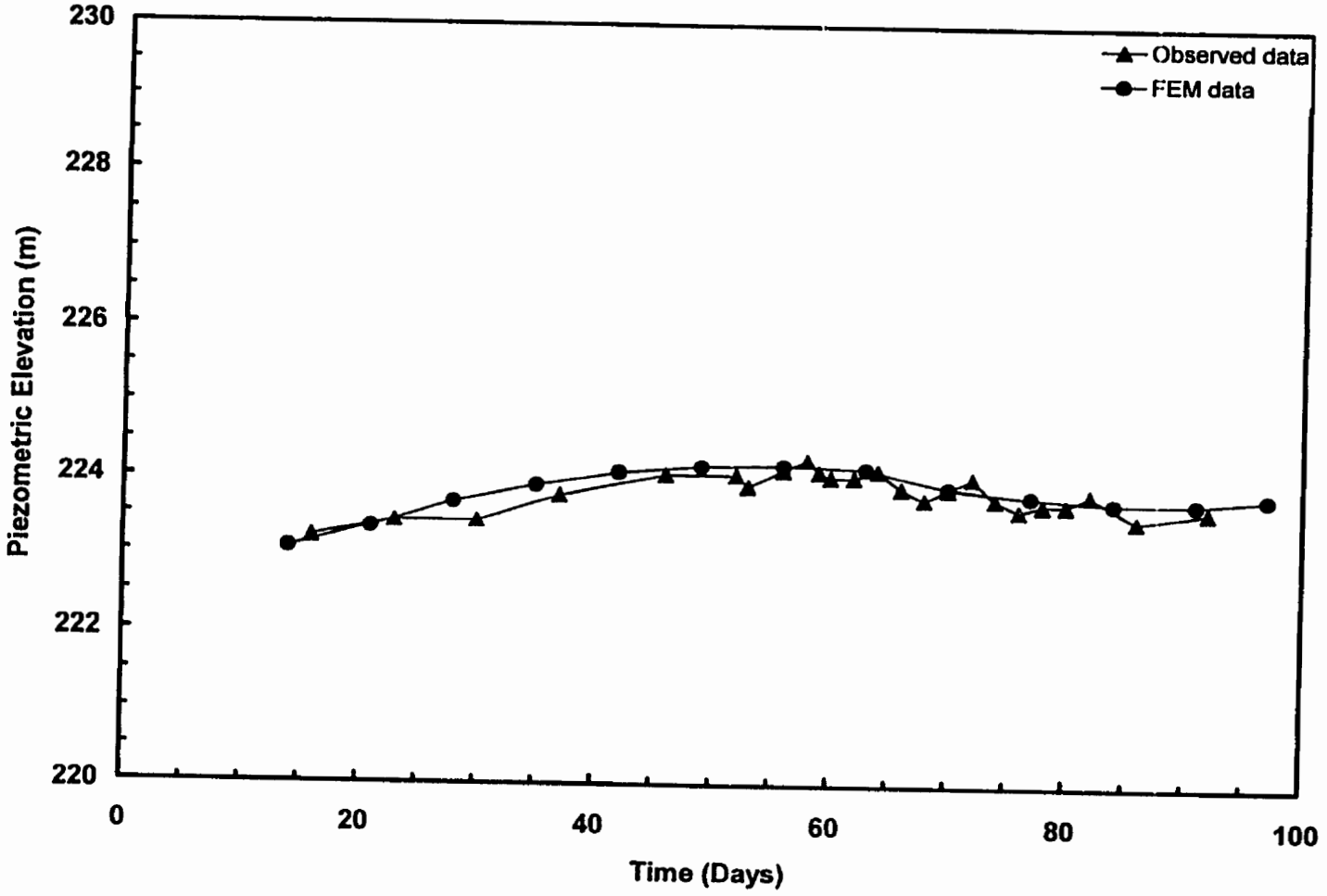

Figure 5.14 Comparison of observed piezometric elevation versus FE model data for P14 location

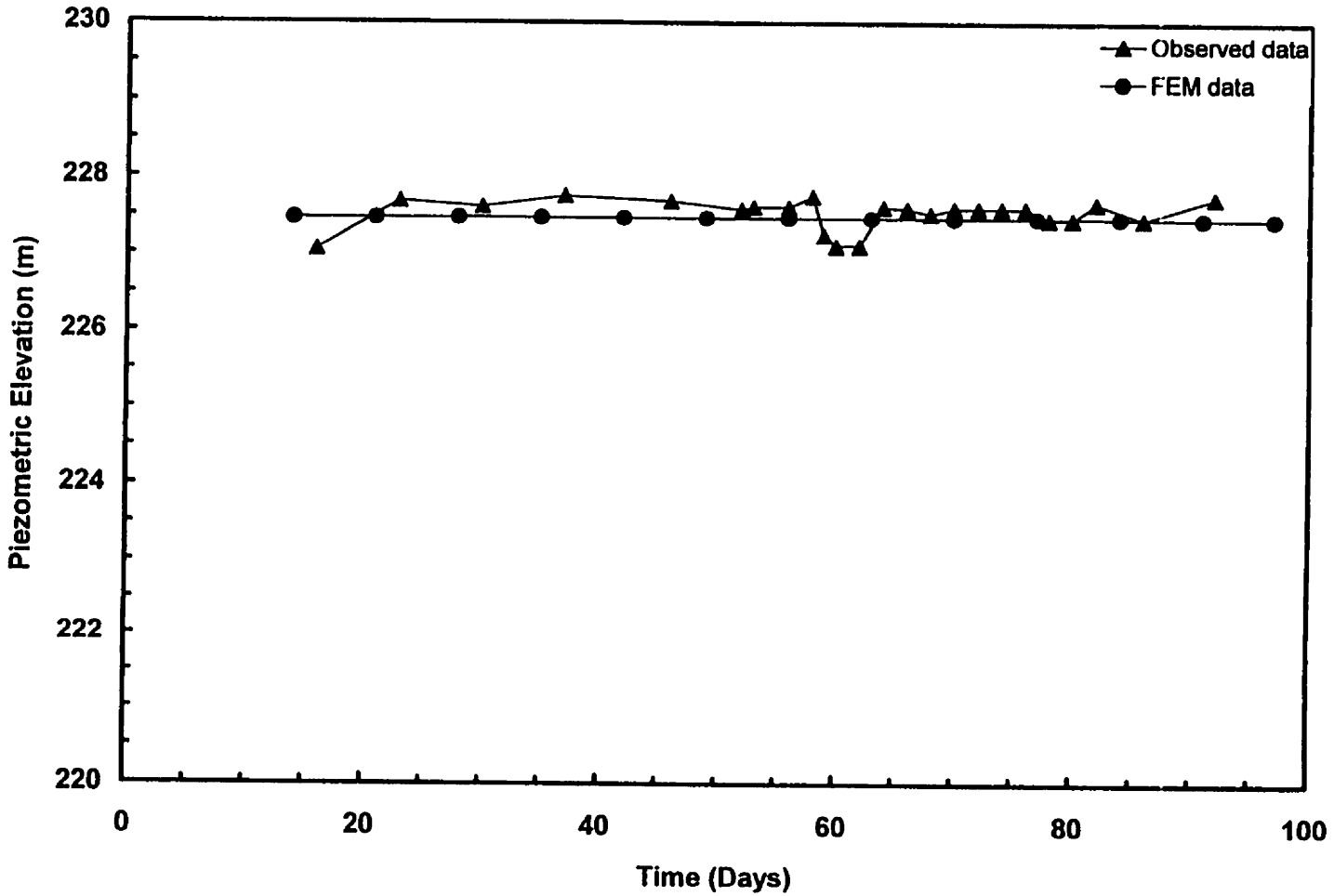

Figure 5.15 Comparison of observed piezometric elevation versus FE model data for P15 location

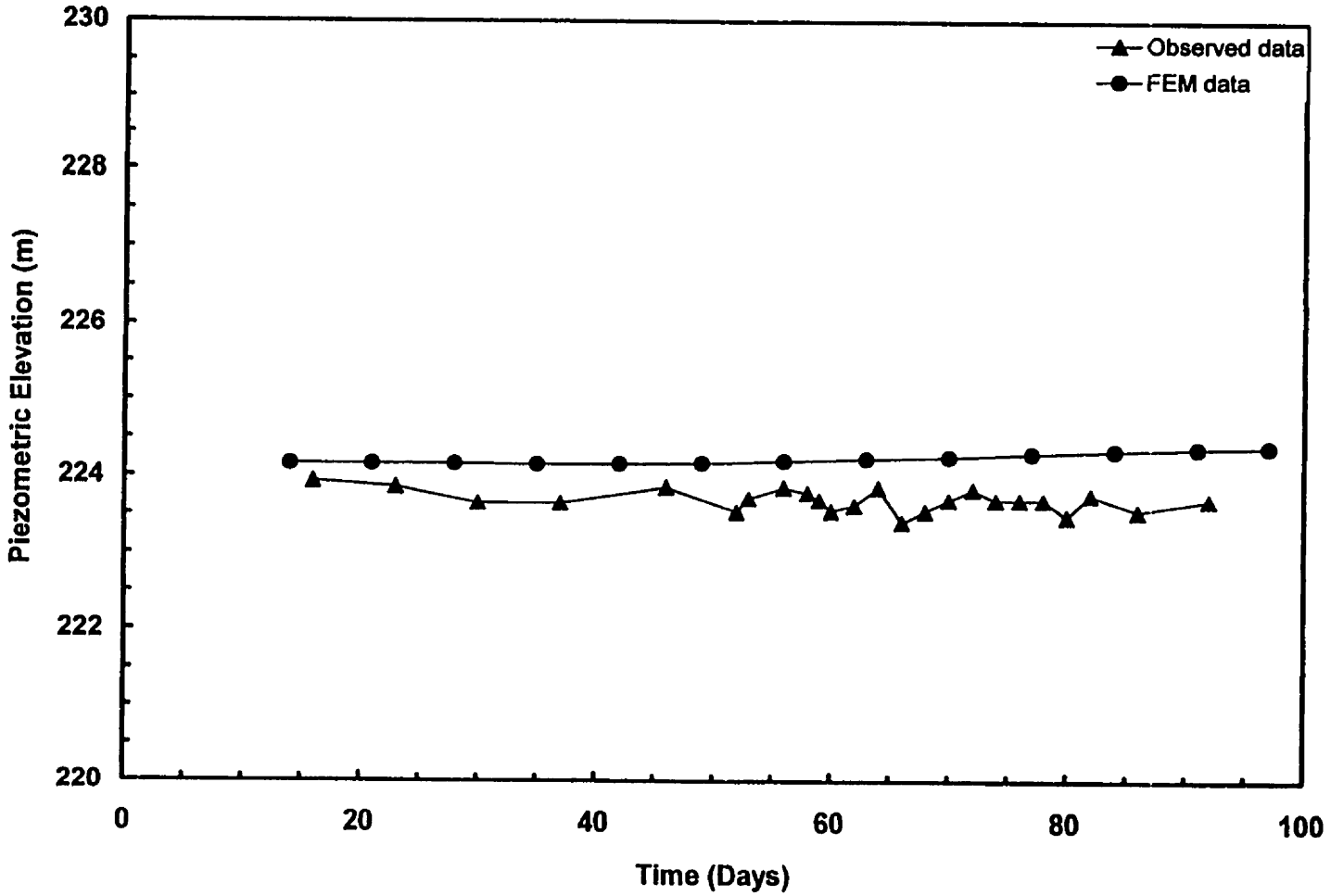

Figure 5.16 Comparison of observed piezometric elevation versus FE model data for P16 location

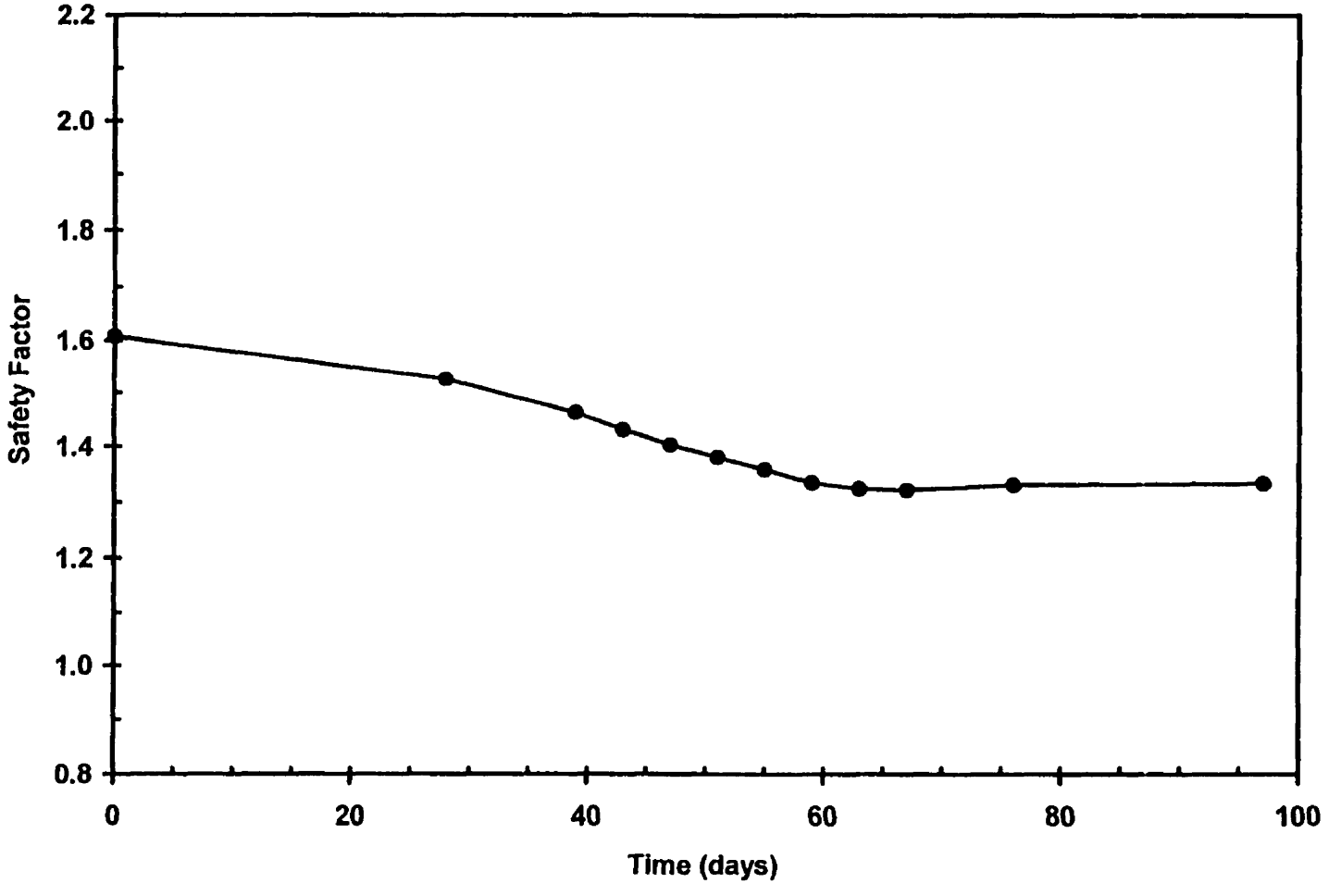

Figure 5.17 Safety factor versus time for FEM generated porewater pressures and weak clay layer at $c' = 3$ kPa, $\phi' = 12°$

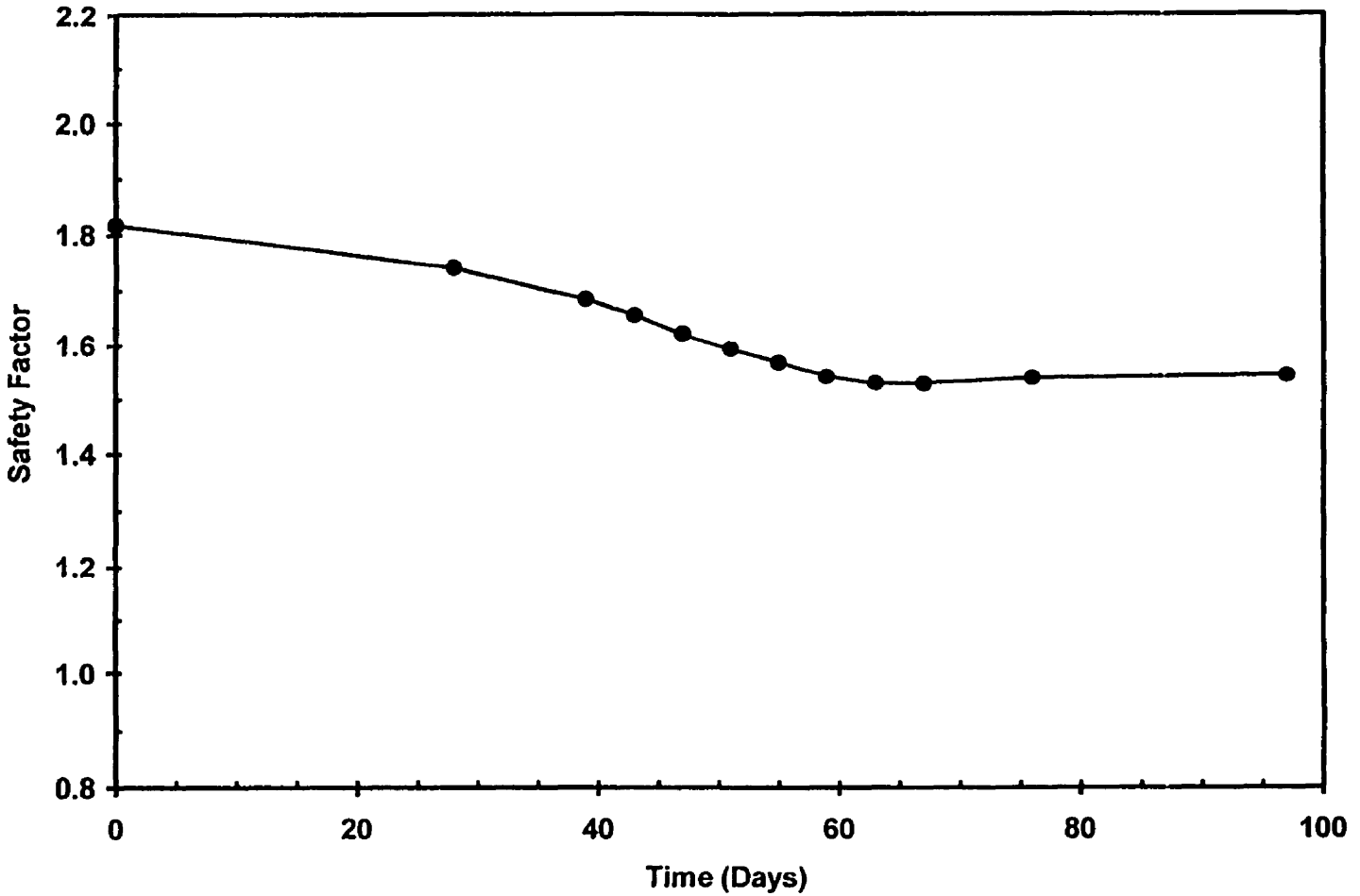

Figure 5.18 Safety factor versus time for FEM generated porewater pressures and weak clay layer at $c' = 4$ kPa, $\phi' = 15°$

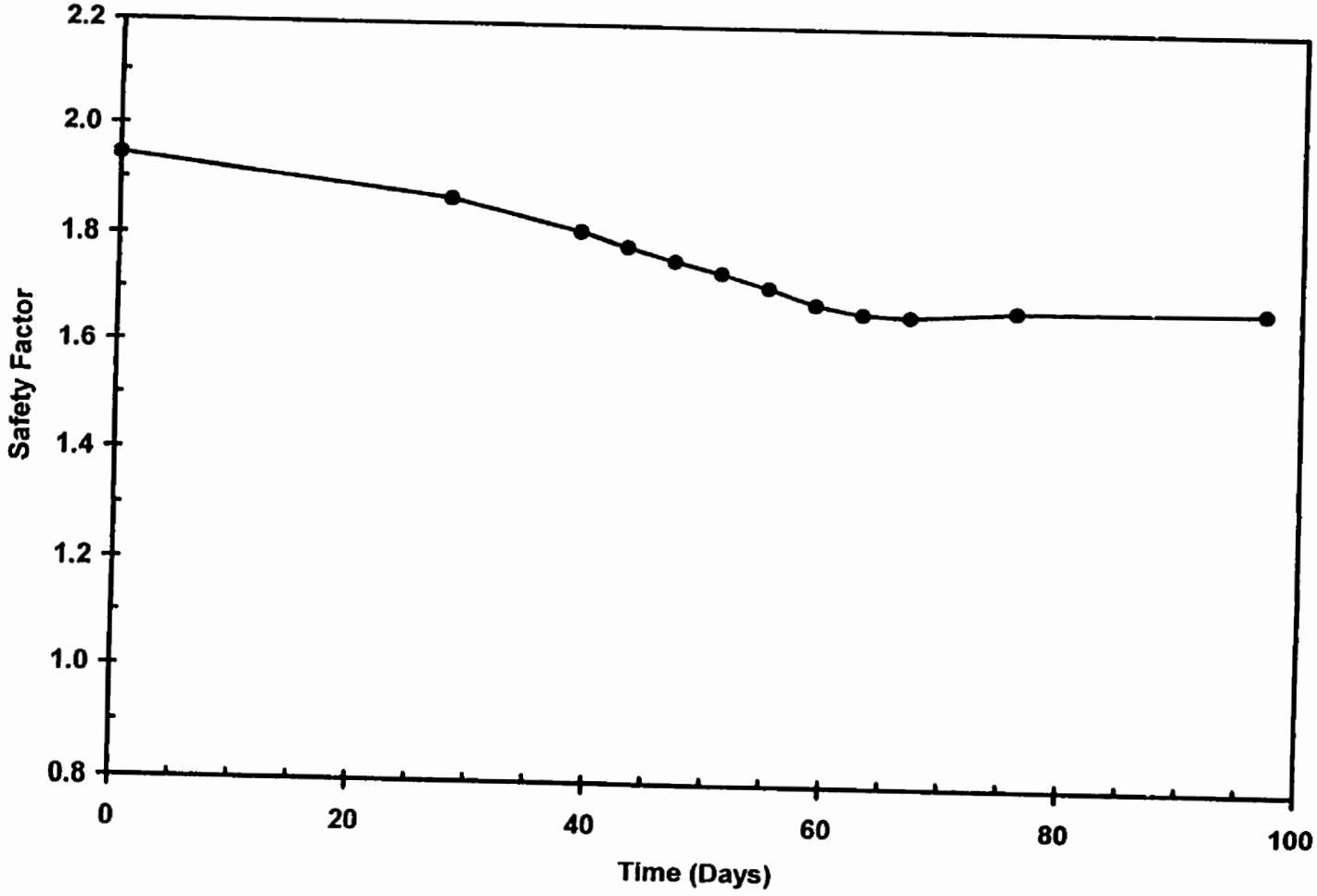

Figure 5.19 Safety factor versus time for FEM generated porewater pressures and no weak clay layer

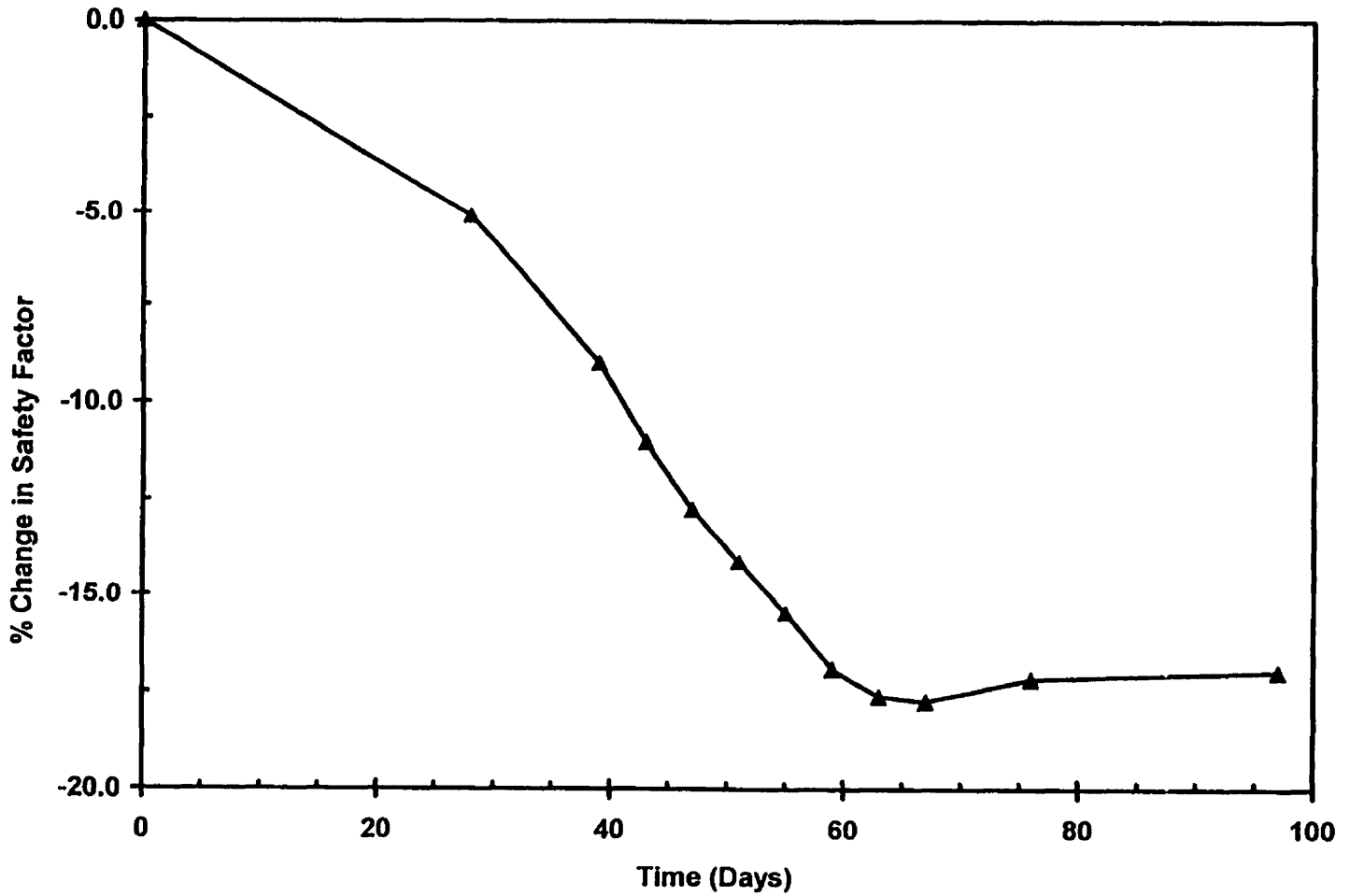

Figure 5.20 Percent decrease in safety factor for FEM generated porewater pressures and weak clay layer at $c' = 3$ kPa, $\phi' = 12°$

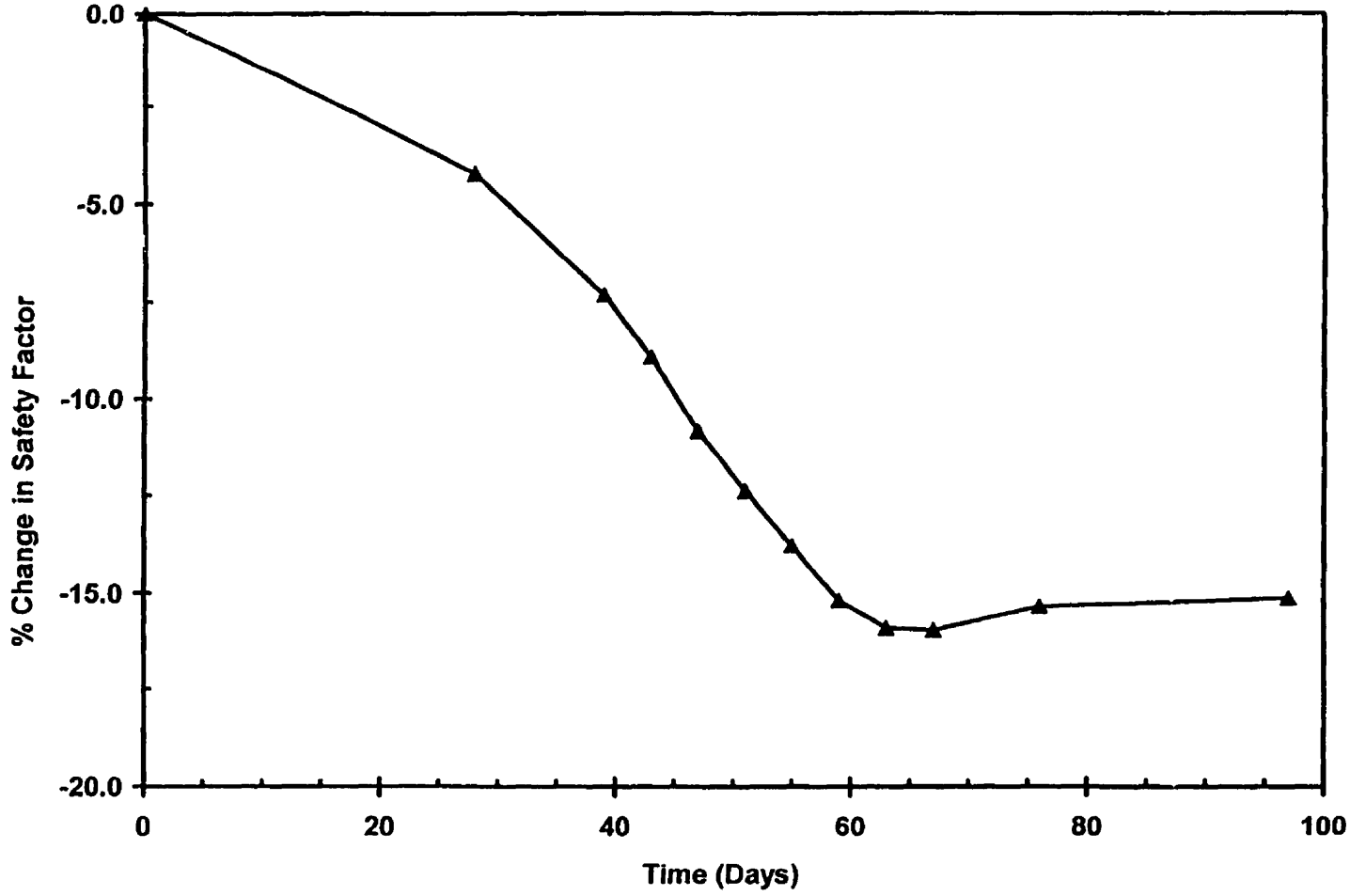

Figure 5.21 Percent decrease in safety factor for FEM generated porewater pressures and weak clay layer at $c' = 4$ kPa, $\phi' = 15°$

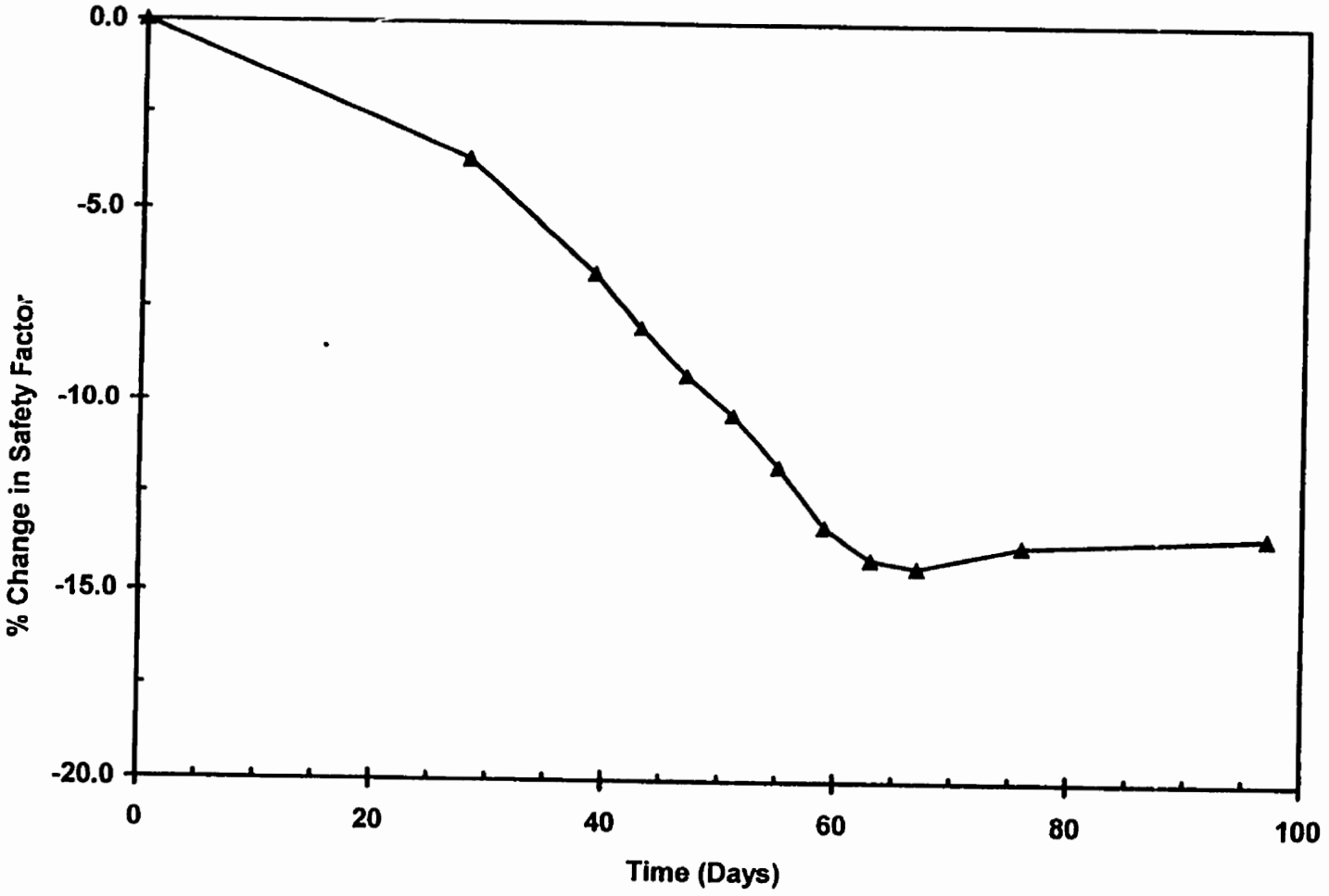

Figure 5.22 Percent decrease in safety factor for FEM generated porewater pressures and no weak clay layer

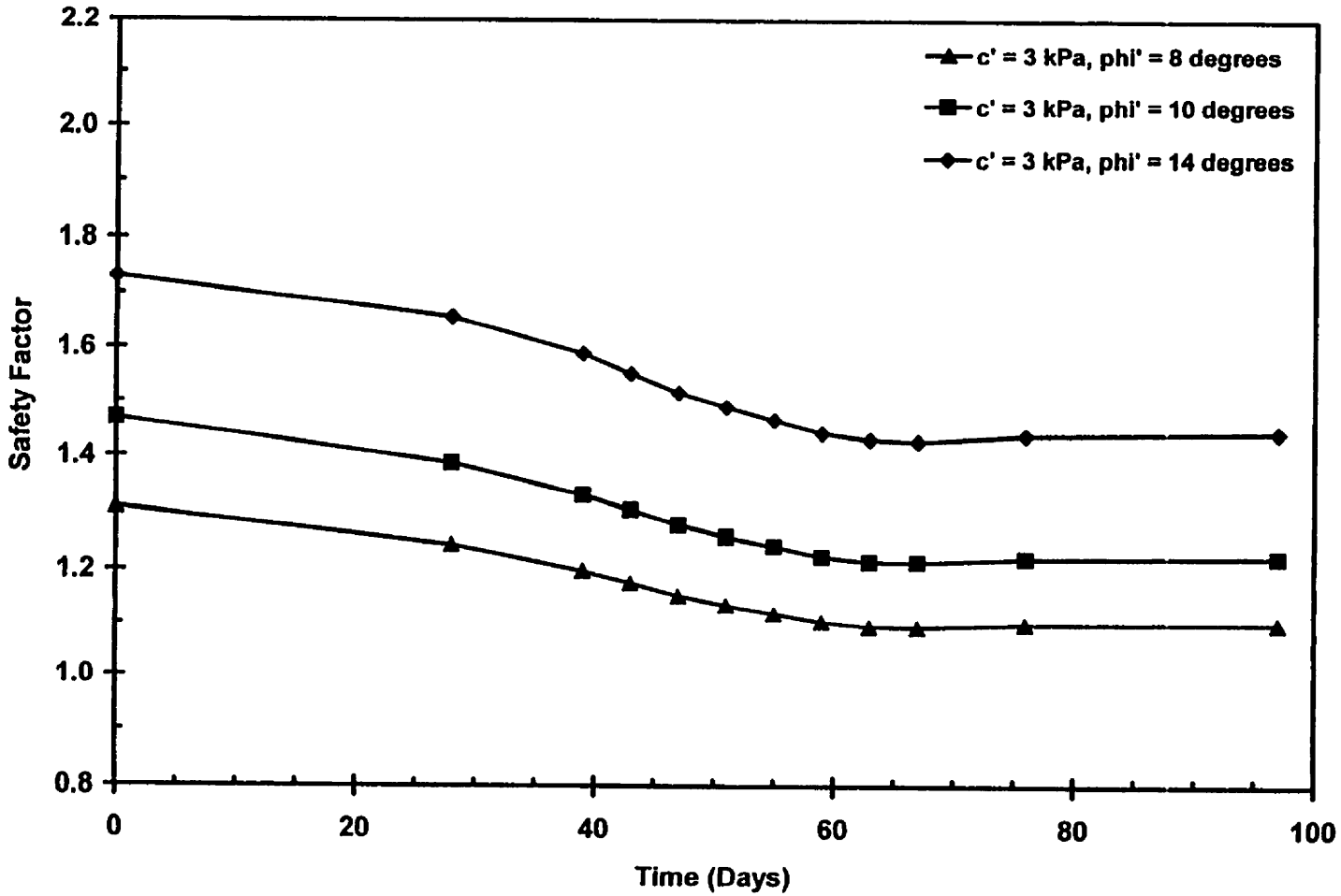

Figure 5.23 Safety factor versus time for FEM generated porewater pressures and three weak clay layer effective shear strength values

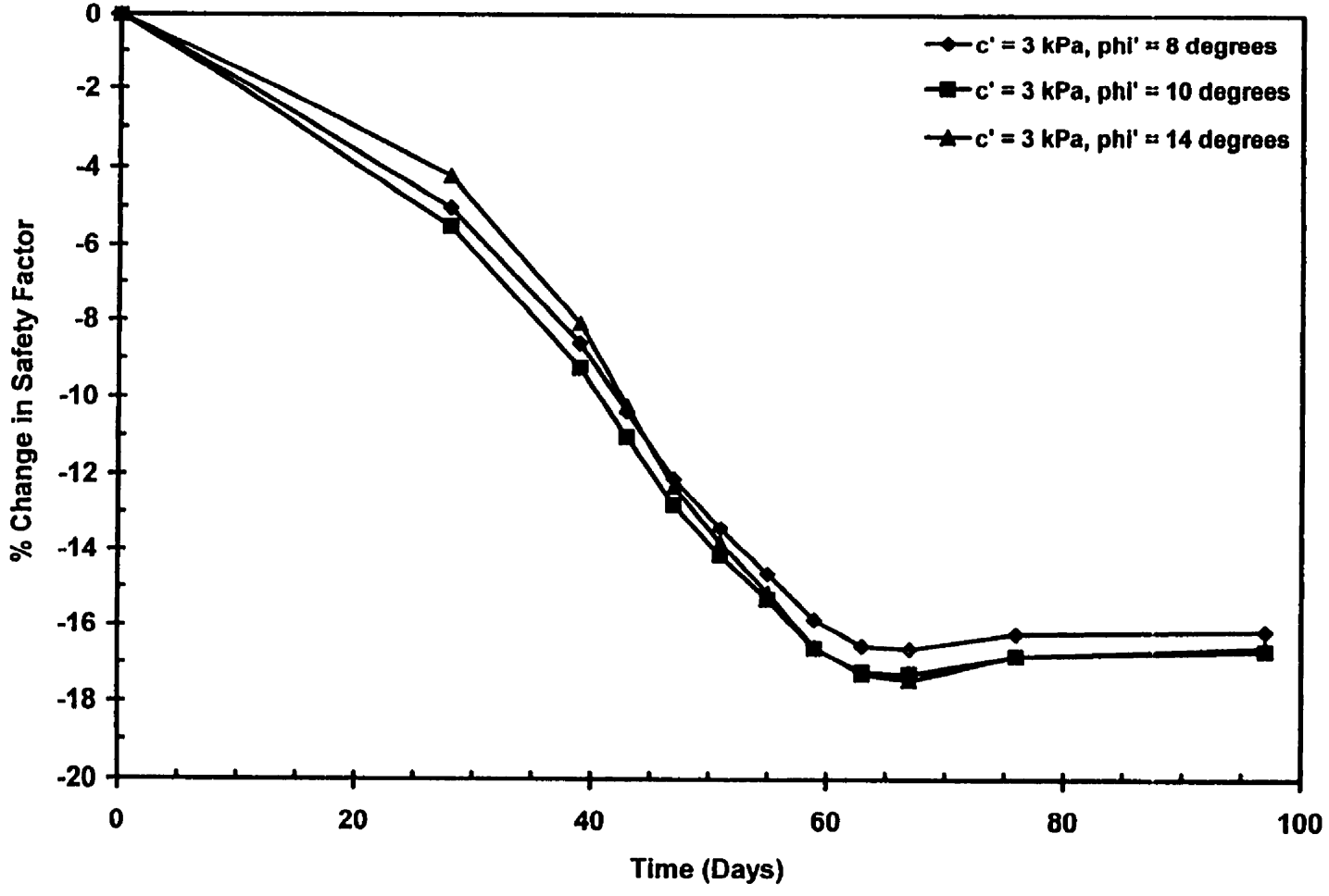

Figure 5.24 Percent decrease in safety factor for FEM generated porewater pressures and three weak clay layer effective shear strength values

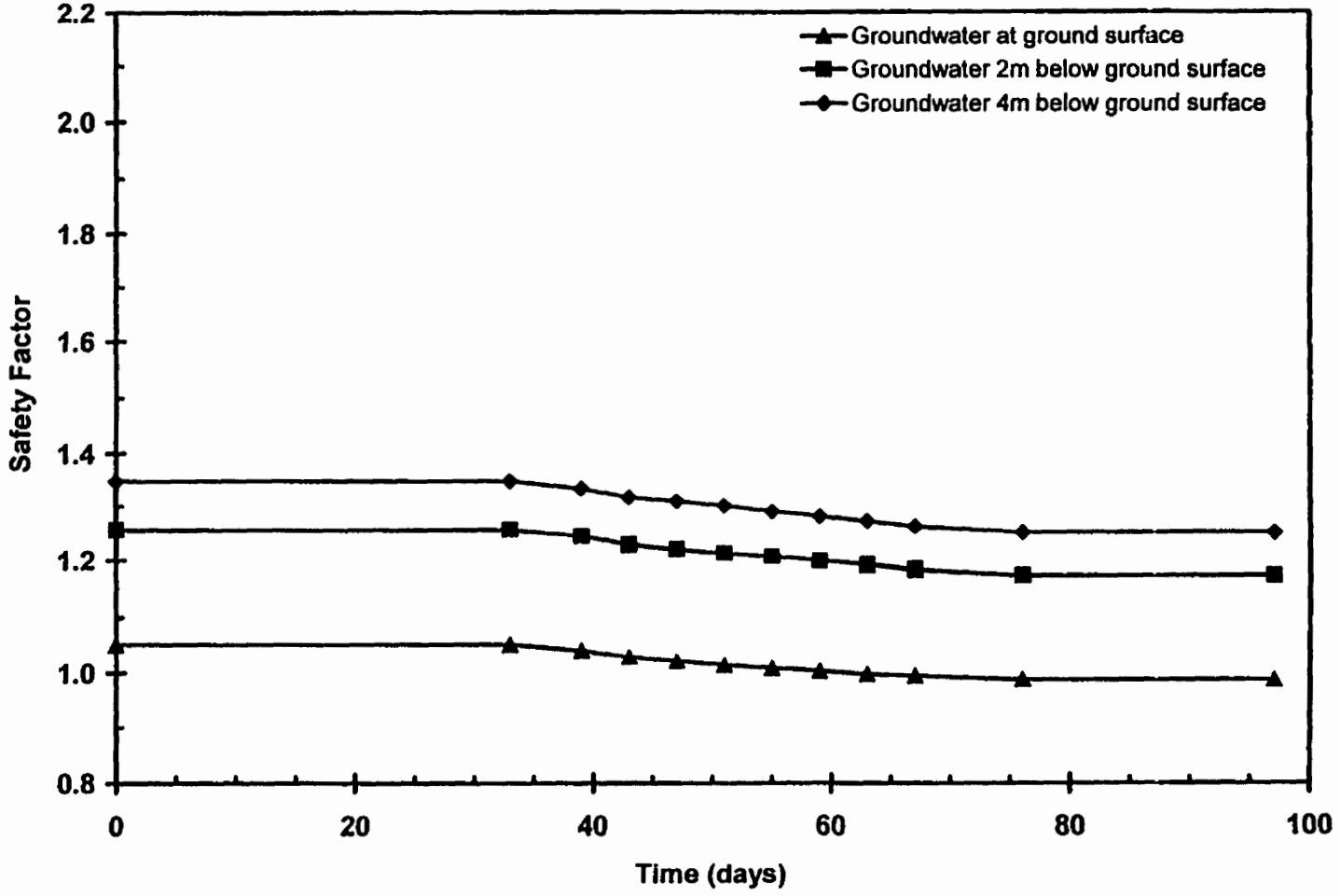

Figure 5.25 Safety factor versus time for three assumed groundwater levels and weak clay layer at $c' = 3$ kPa, $\phi' = 12°$

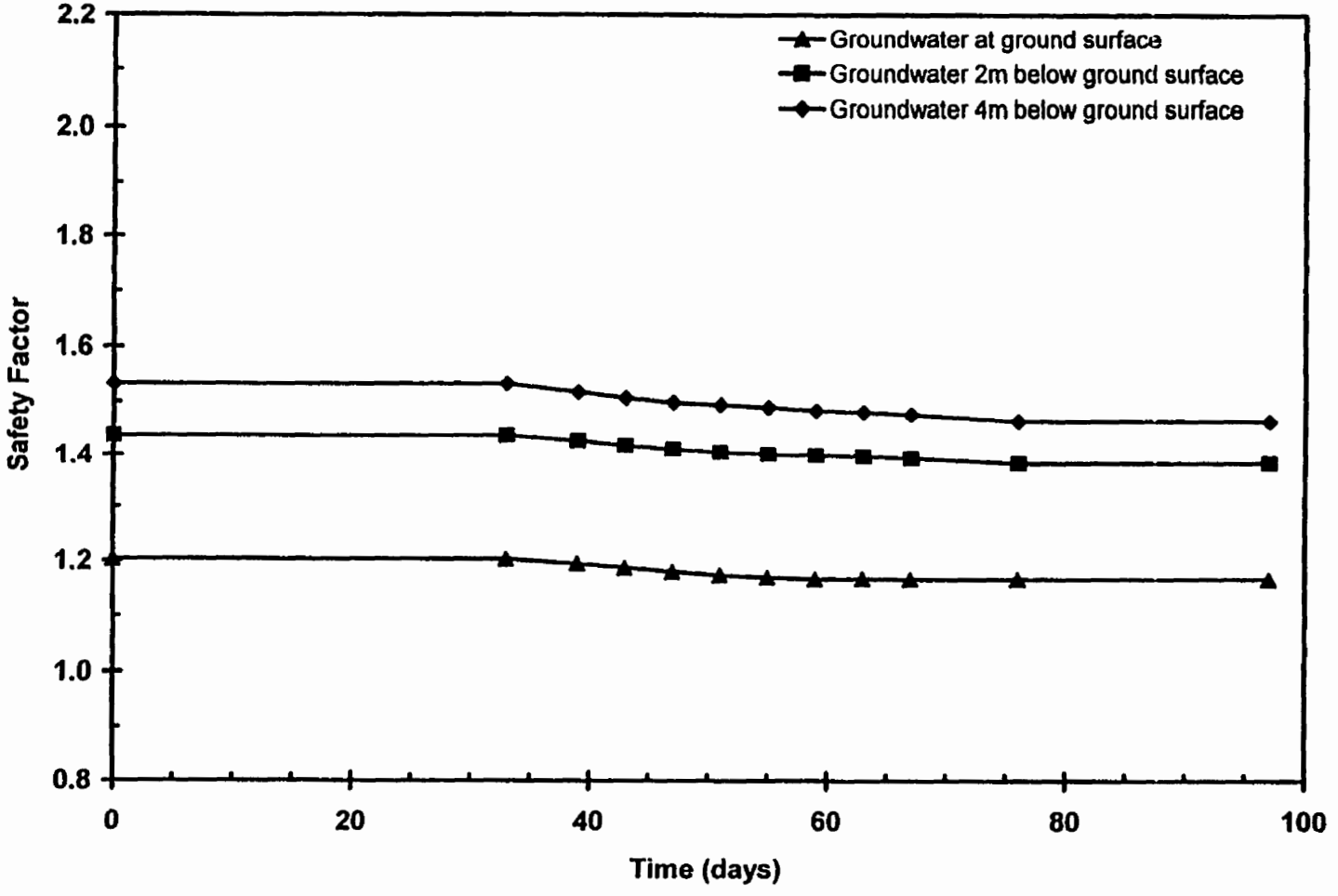

Figure 5.26 Safety factor versus time for three assumed groundwater levels and weak clay layer at $c' = 4$ kPa, $\phi' = 15°$

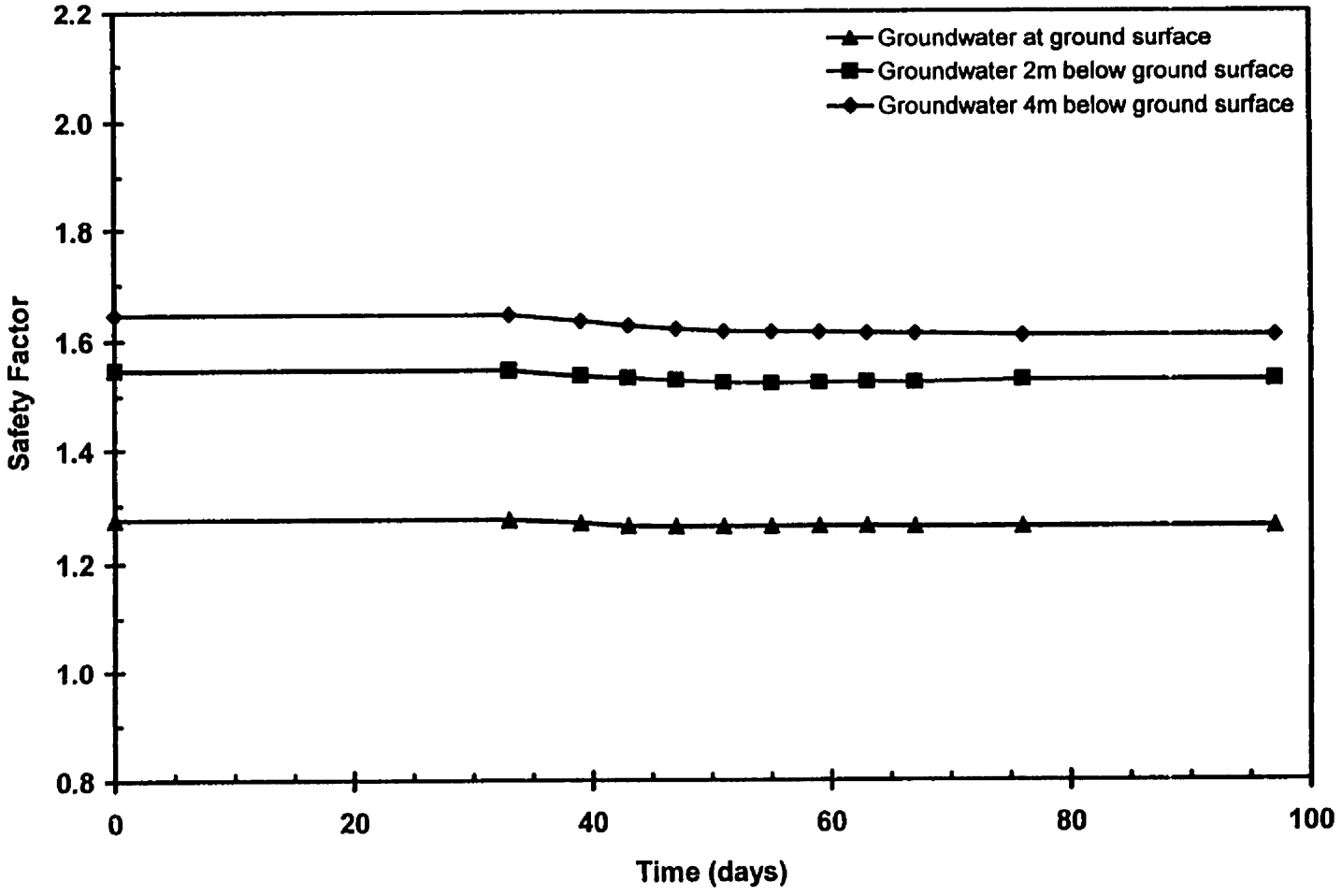

Figure 5.27 Safety factor versus time for three assumed groundwater levels and no weak clay layer

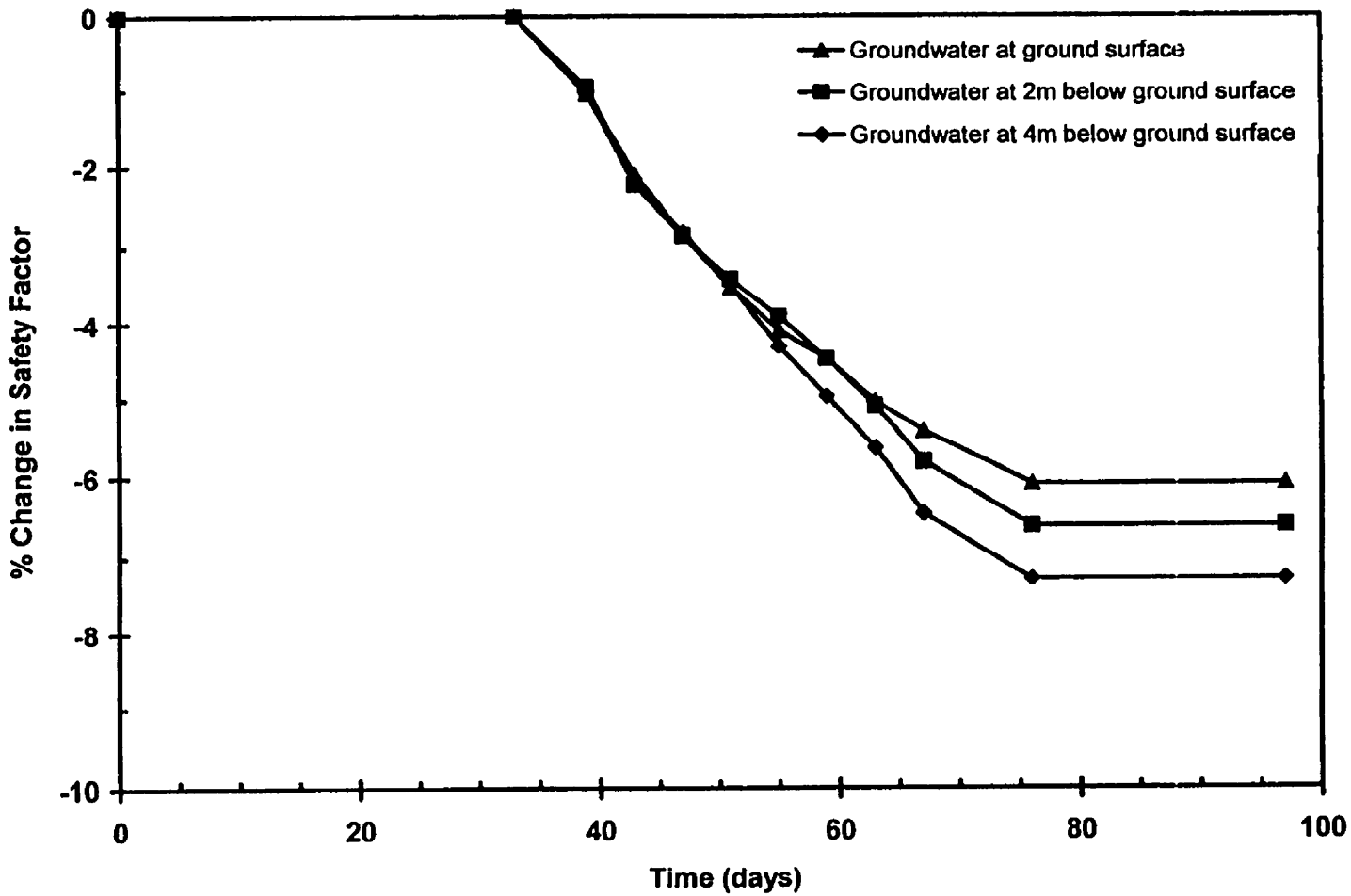

Figure 5.28 Percent decrease in safety factor for three assumed groundwater levels and weak clay layer at $c' = 3$ kPa, $\phi' = 12°$

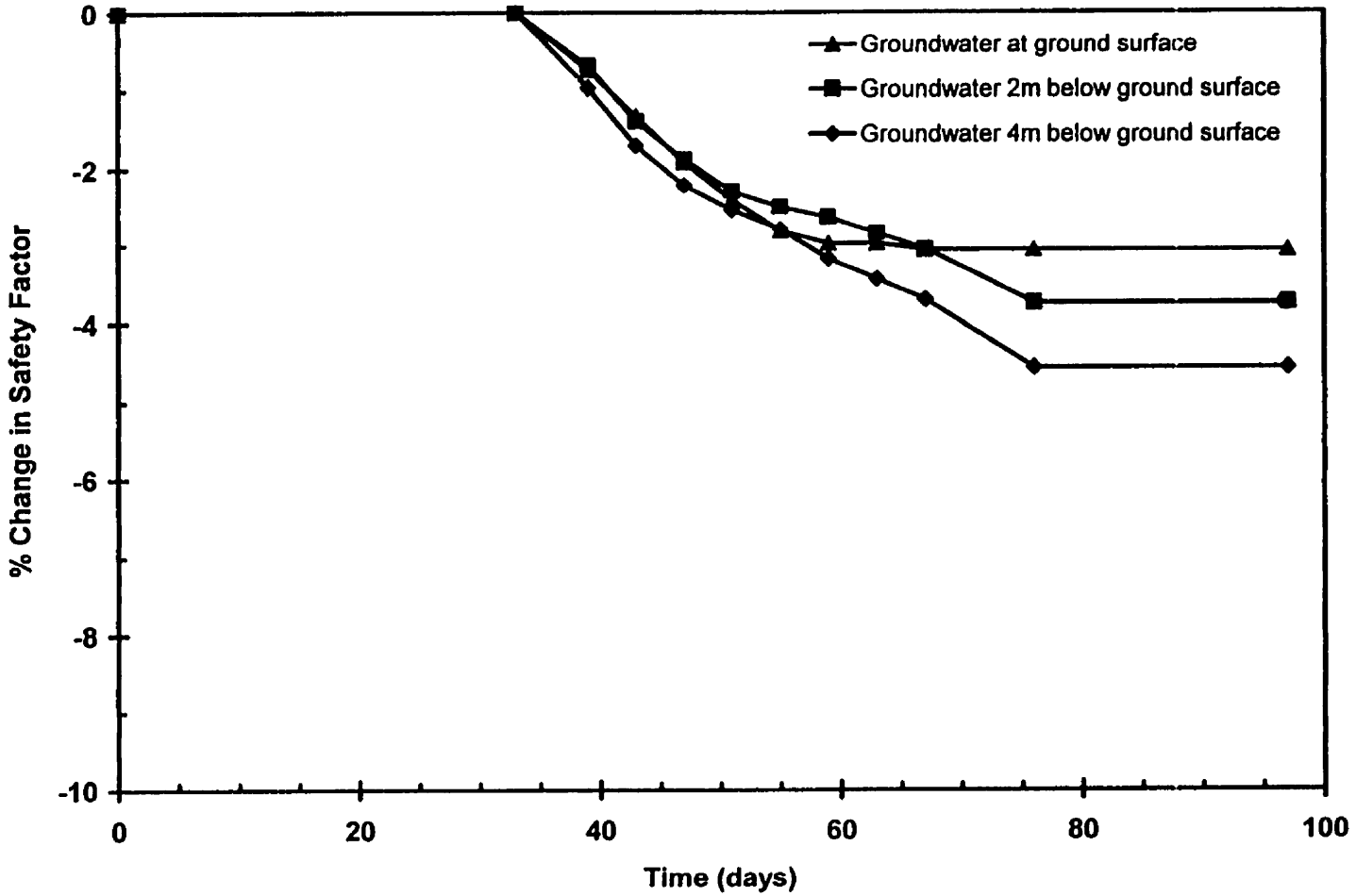

Figure 5.29 Percent decrease in safety factor for three assumed groundwater levels and weak clay layer at $c' = 4$ kPa, $\phi' = 15°$

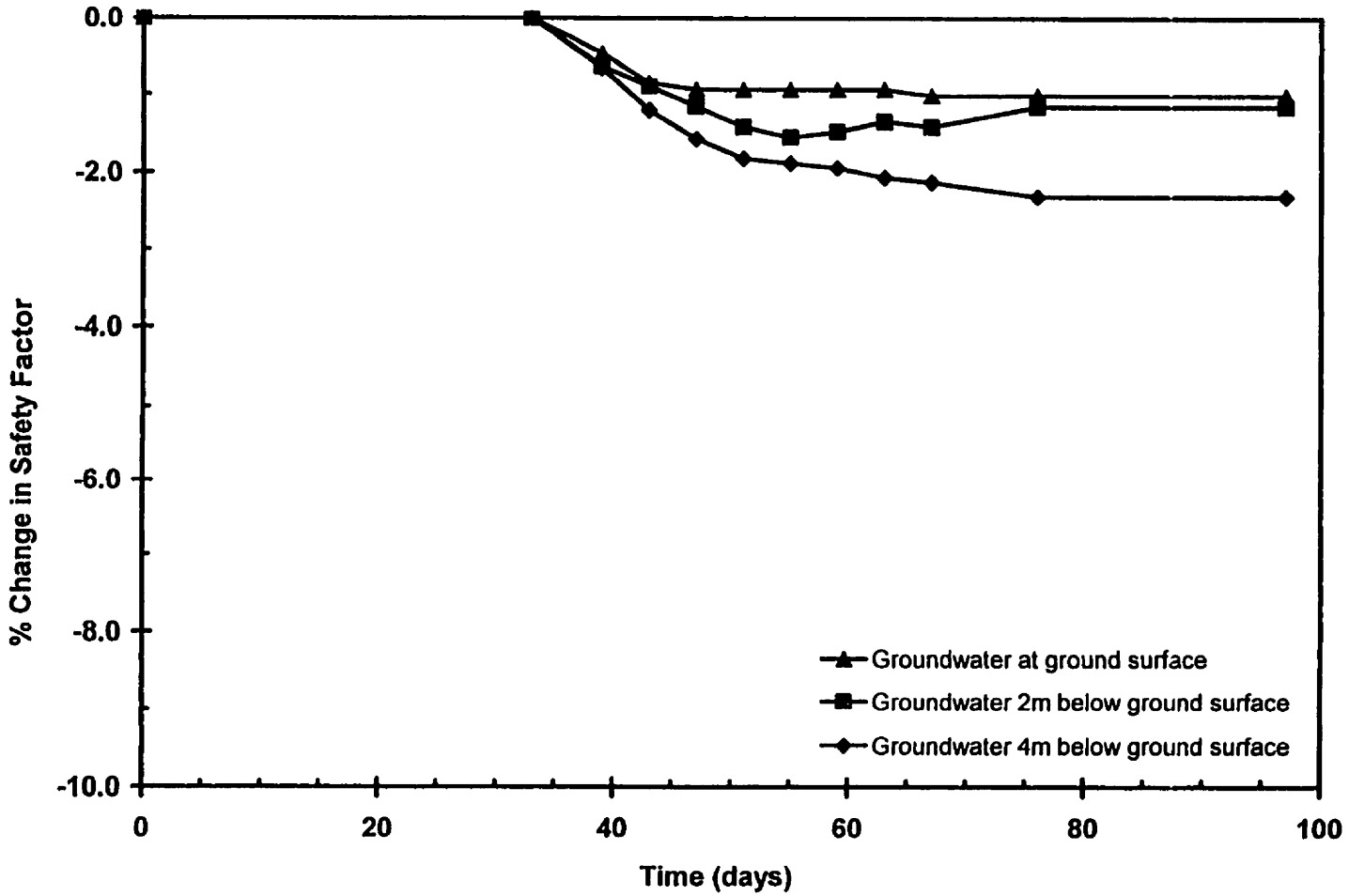

Figure 5.30 Percent decrease in safety factor for three assumed groundwater levels and no weak layer

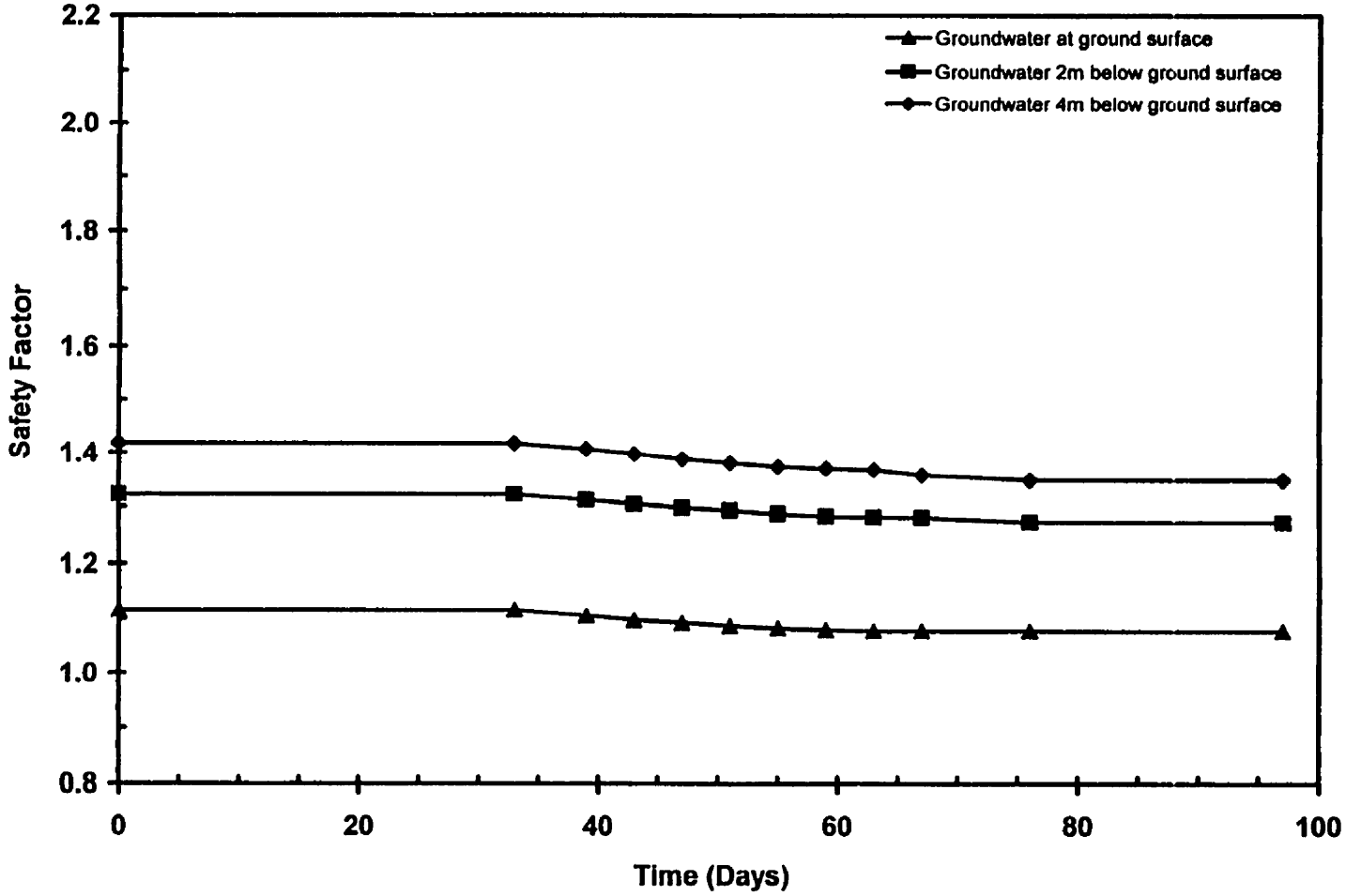

Figure 5.31 Safety factor versus time for three assumed groundwater levels and weak clay layer at c′ = 5 kPa, ϕ' = 12°

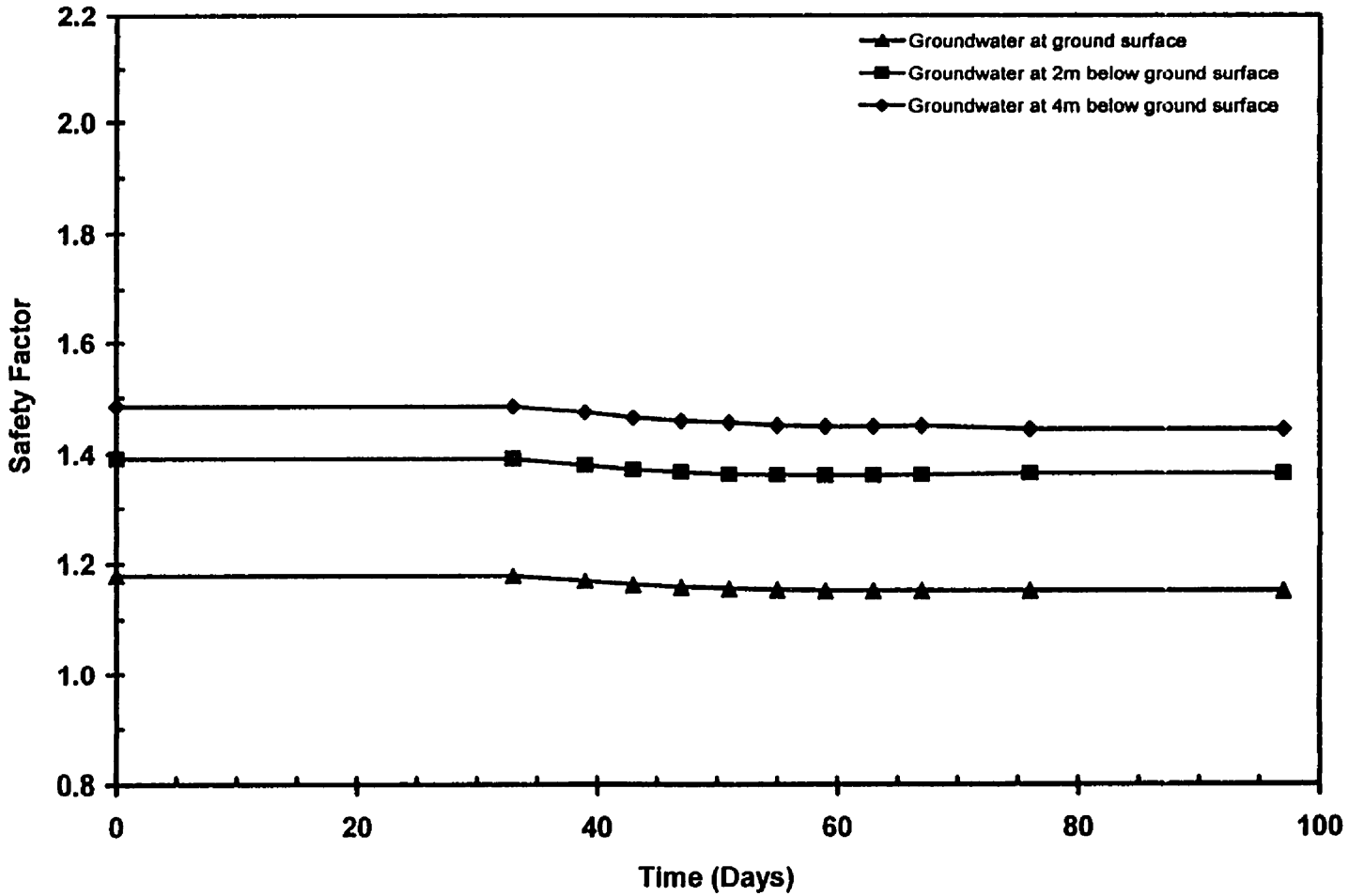

Figure 5.32 Safety factor versus time for three assumed groundwater levels and weak clay layer at $c' = 7$ kPa, $\phi' = 12°$

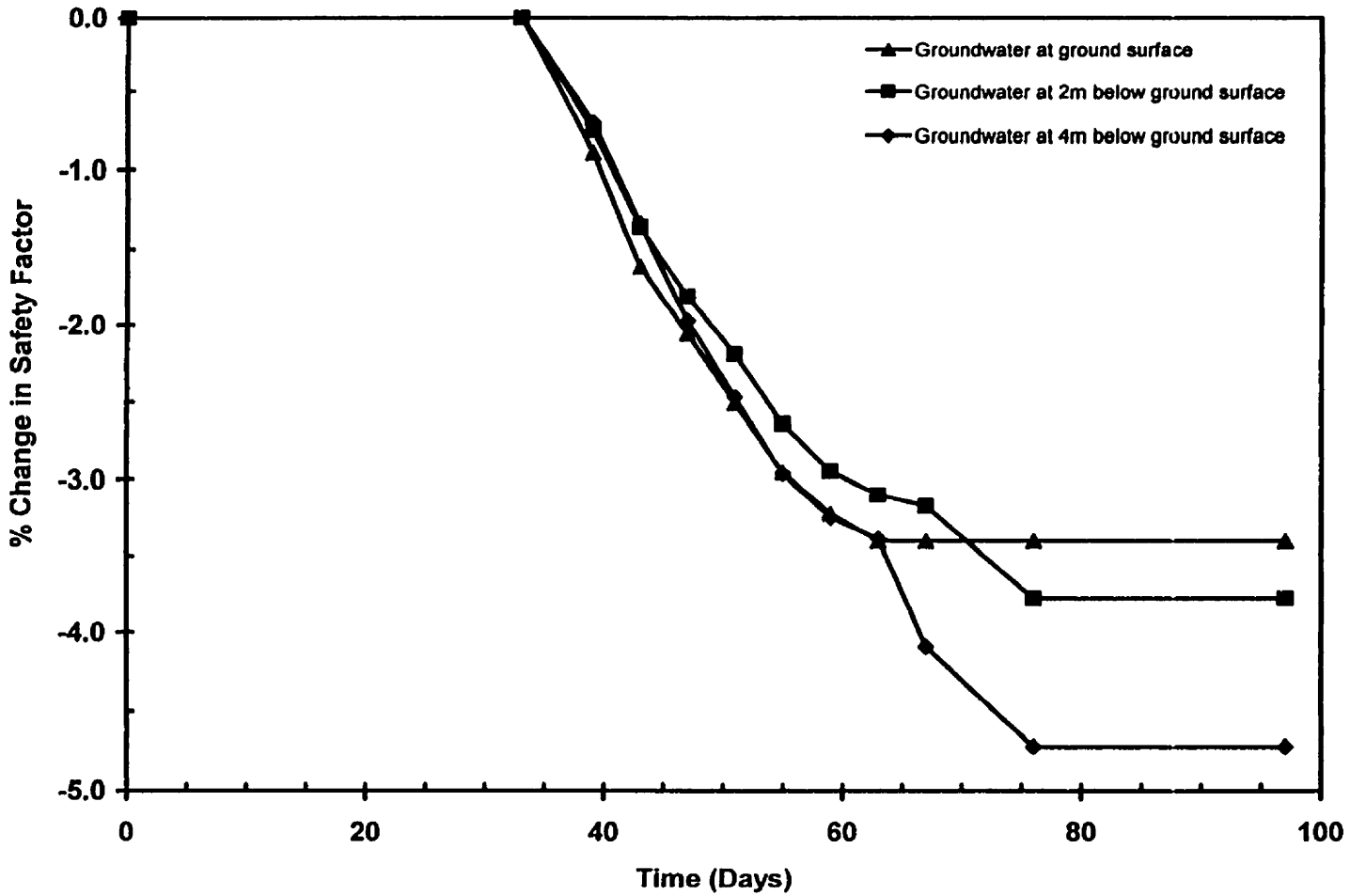

Figure 5.33 Percent decrease in safety factor for three assumed groundwater levels and weak clay layer at $c' = 5$ kPa, $\phi' = 12°$

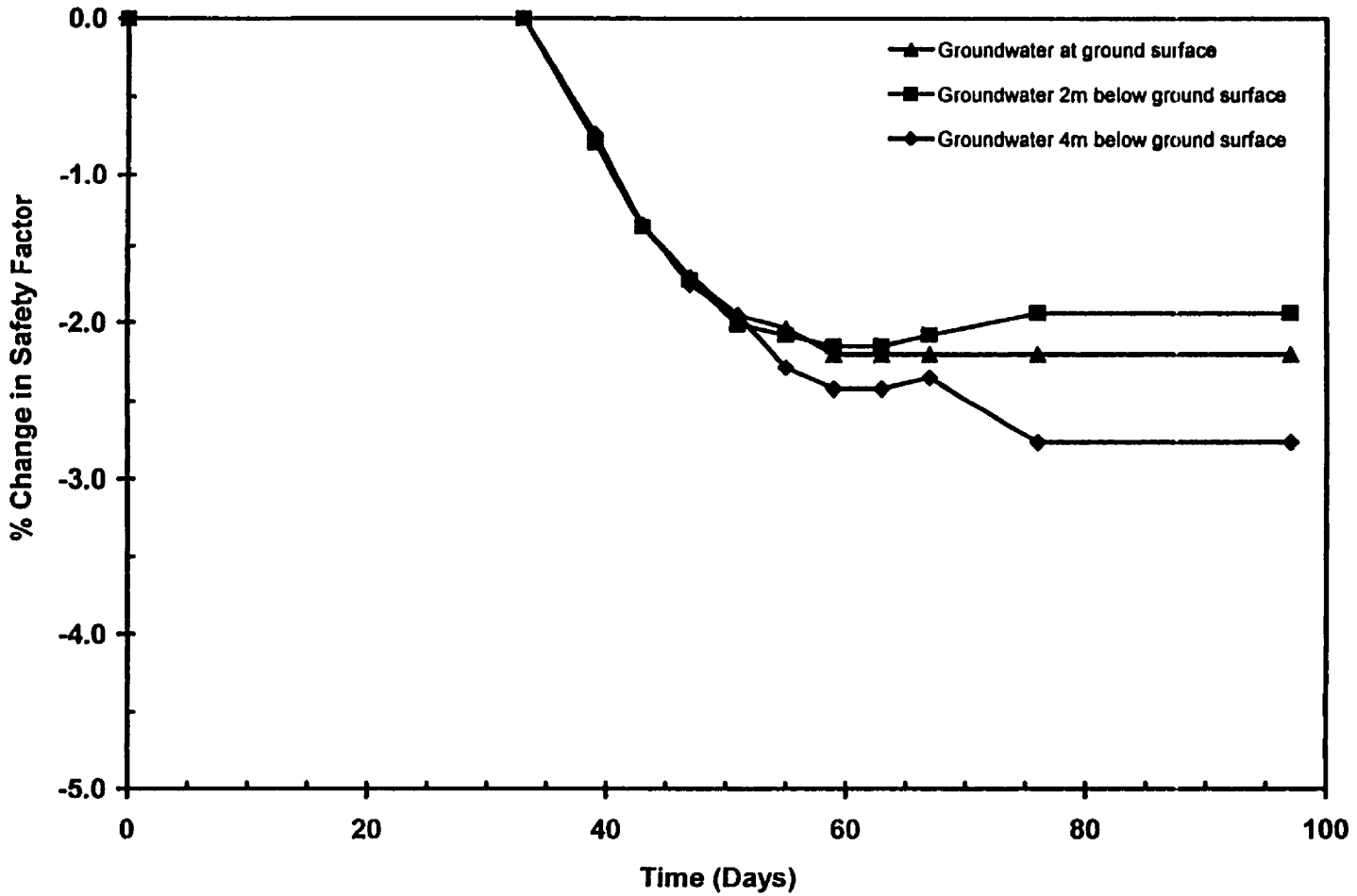

Figure 5.34 Percent decrease in safety factor for three assumed groundwater levels and weak clay layer at $c' = 7$ kPa, $\phi' = 12°$

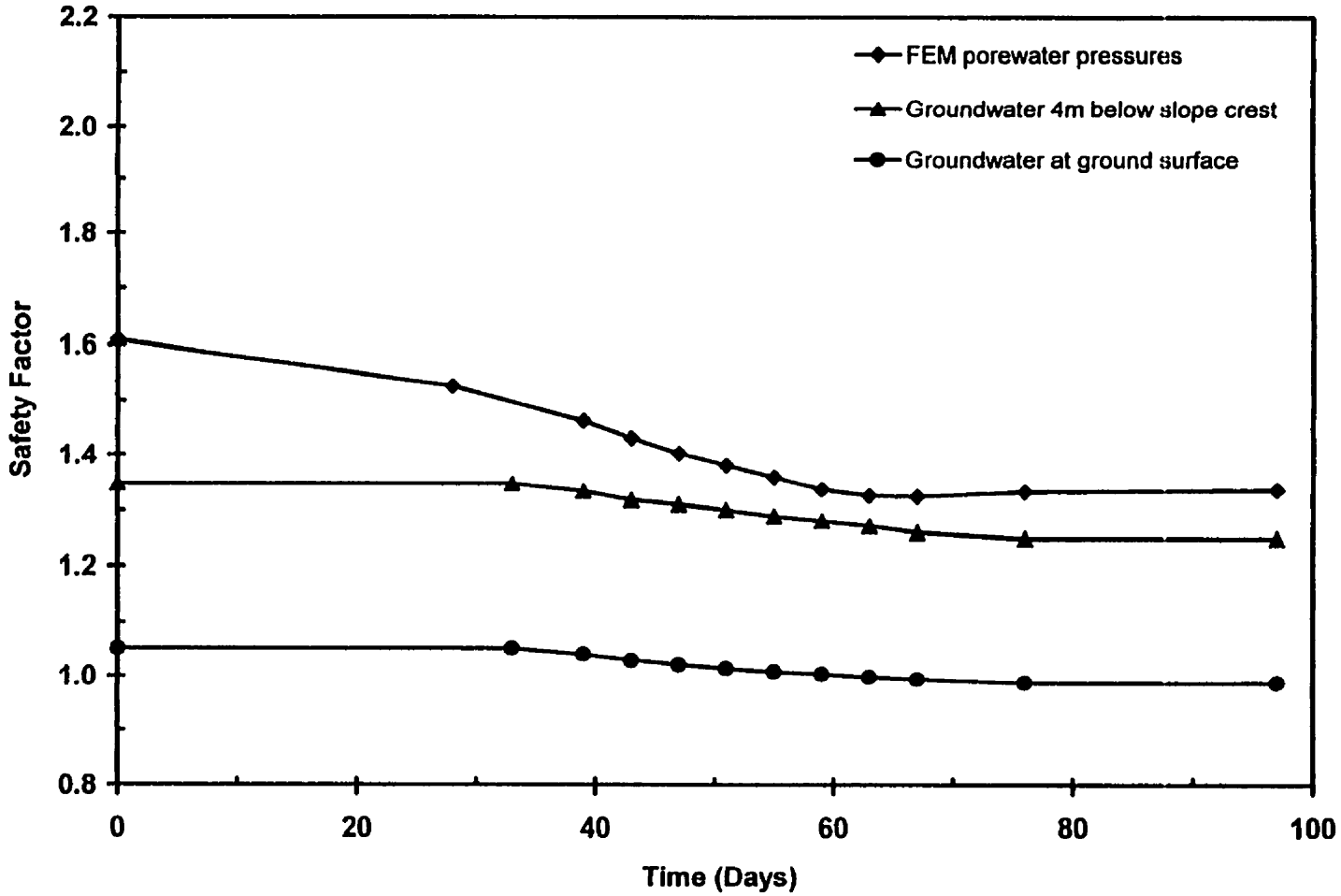

Figure 5.35 Safety factor versus time for three porewater pressure distributions with weak clay layer at $c' = 3$ kPa, $\phi' = 12°$

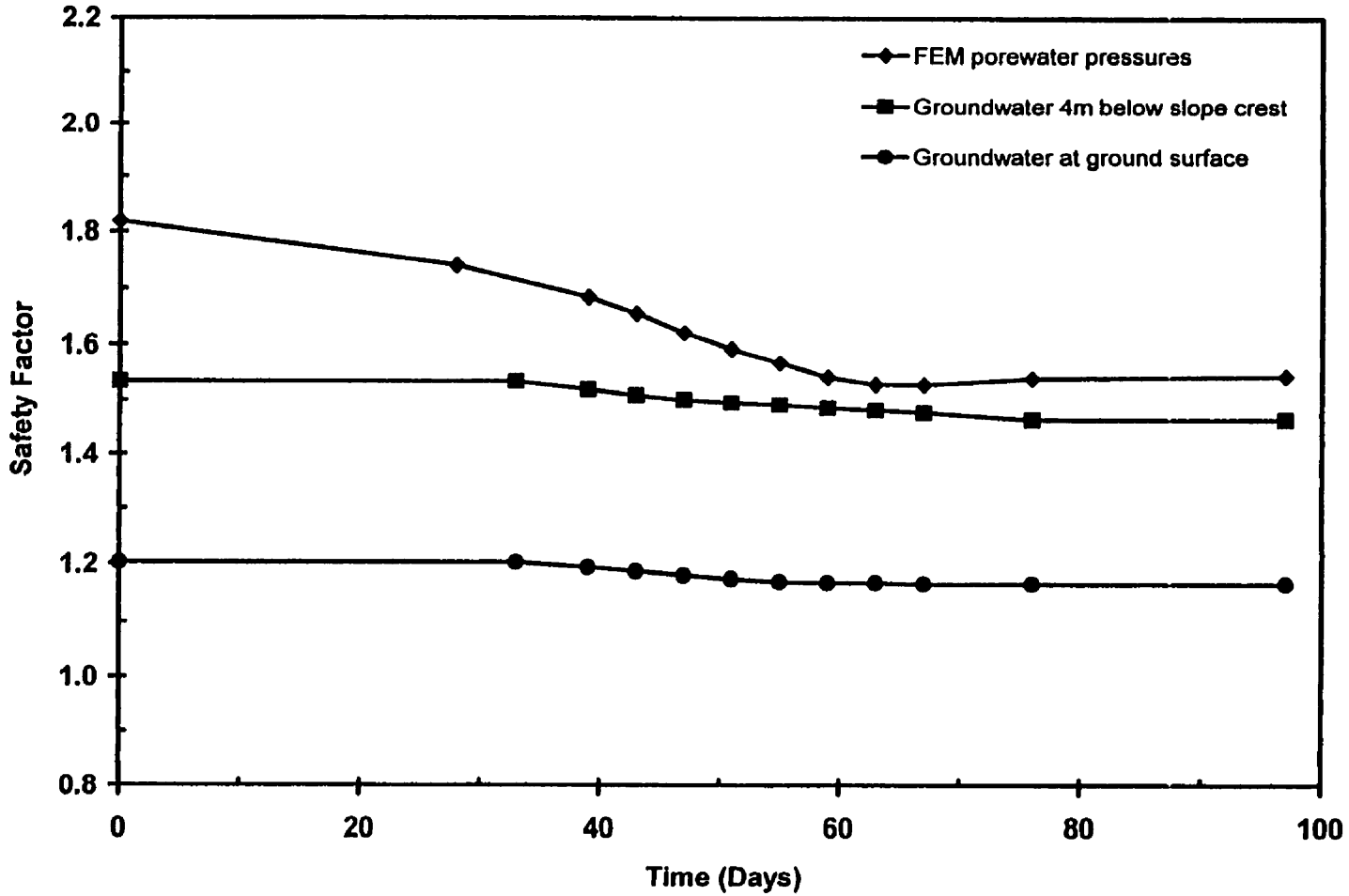

Figure 5.36 Safety factor versus time for three porewater pressure distributions with weak clay layer at $c' = 4$ kPa, $\phi' = 15°$

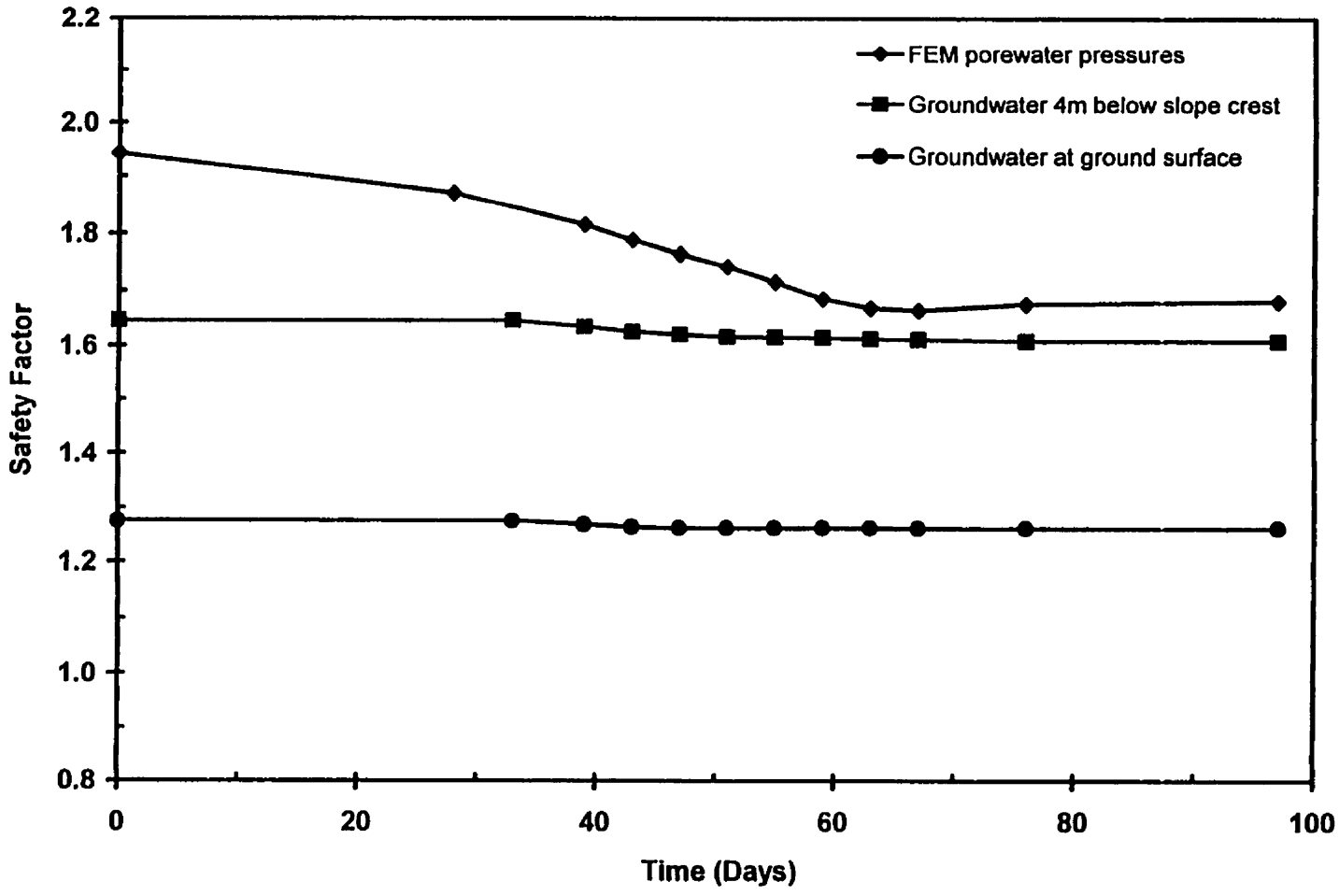

Figure 5.37 Safety factor versus time for three porewater pressure distributions with no weak clay layer

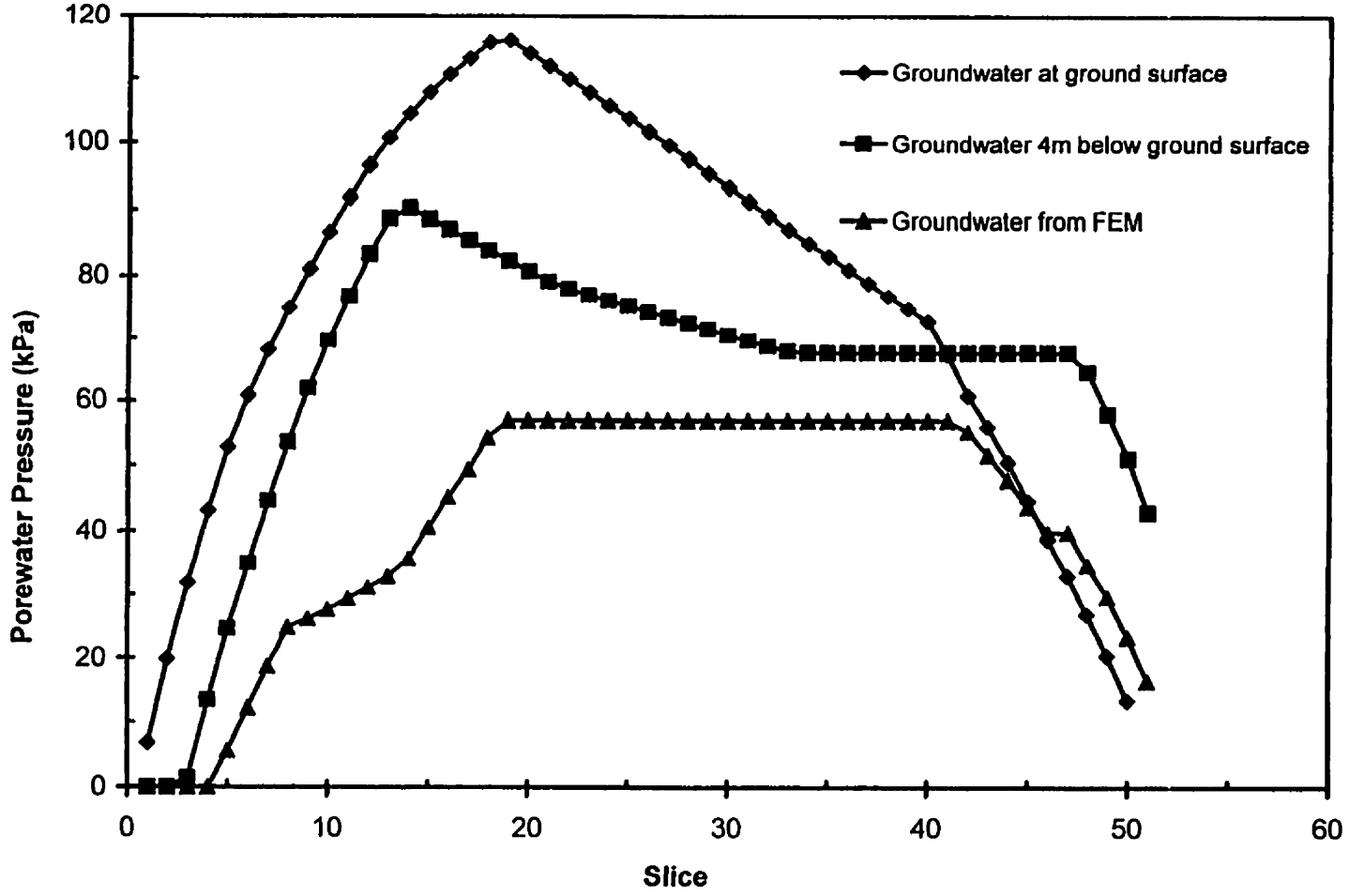

Figure 5.38 Porewater pressure distribution at the beginning of the modeling duration along the base of slip surface for three groundwater assumptions and weak clay layer at c′ = 3 kPa, ϕ′ = 12°

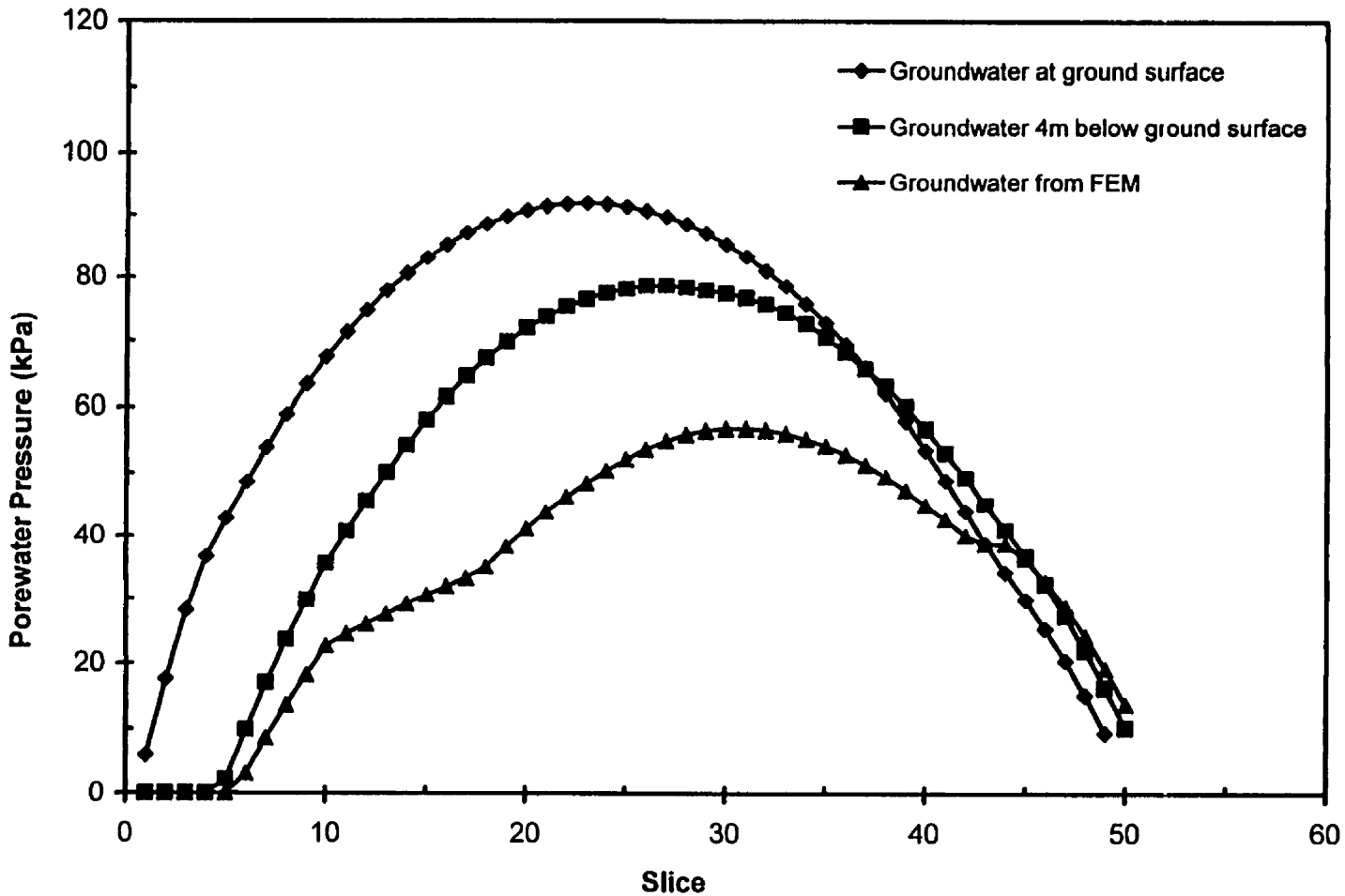

Figure 5.39 Porewater pressure distribution at the beginning of the modeling duration along the base of slip surface for three groundwater assumptions and no weak clay layer

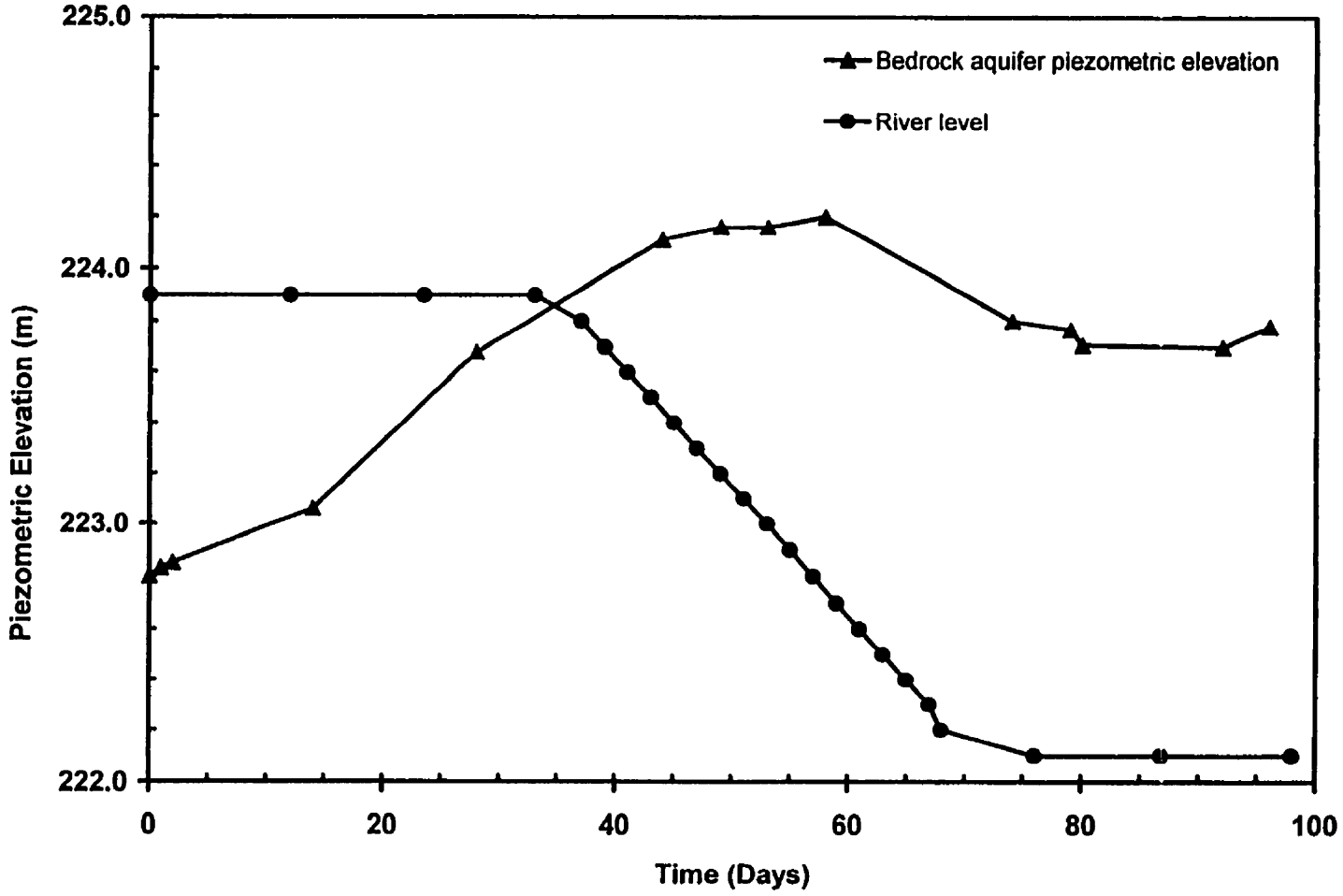

Figure 5.40 Bedrock aquifer piezometric elevations and river level versus time demonstrate the additive destabilizing influence for FEM computed porewater pressures

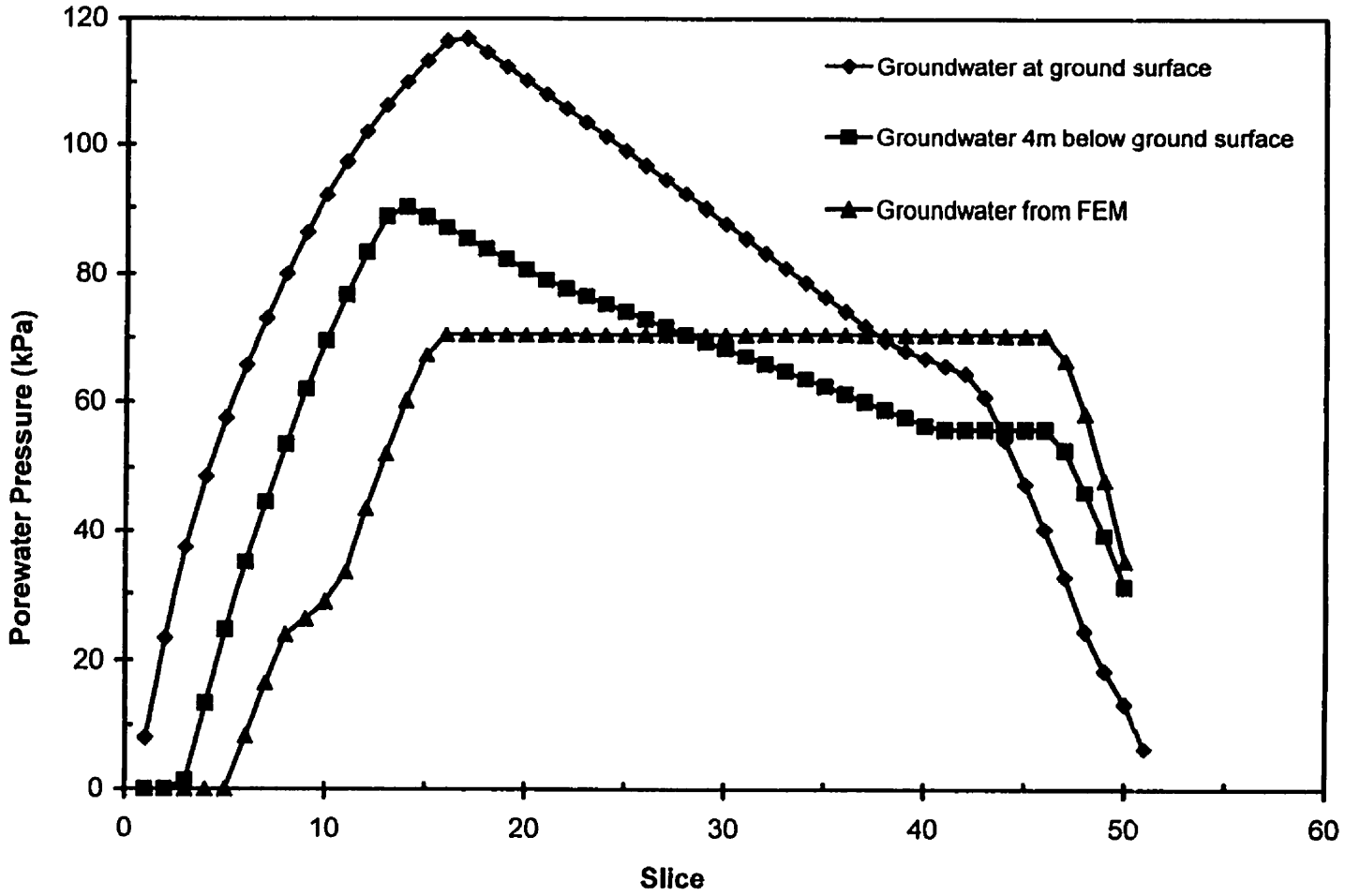

Figure 5.41 Porewater pressure distribution at the middle of the modeling duration along the base of slip surface for three groundwater assumptions and weak clay layer at $c' = 3$ kPa, $\phi' = 12°$

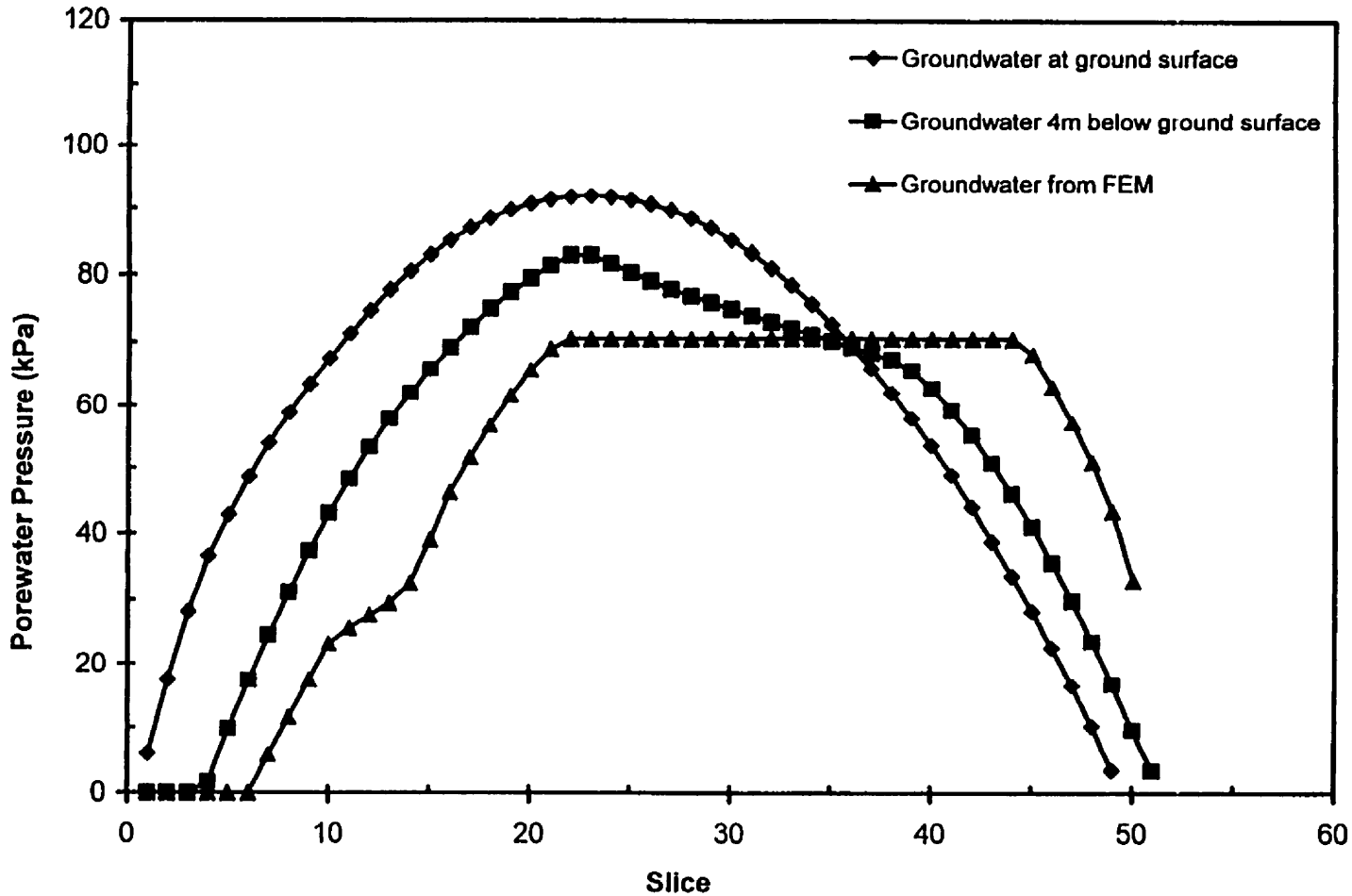

Figure 5.42 Porewater pressure distribution at the middle of the modeling duration along the base of slip surface for three groundwater assumptions and no weak clay layer

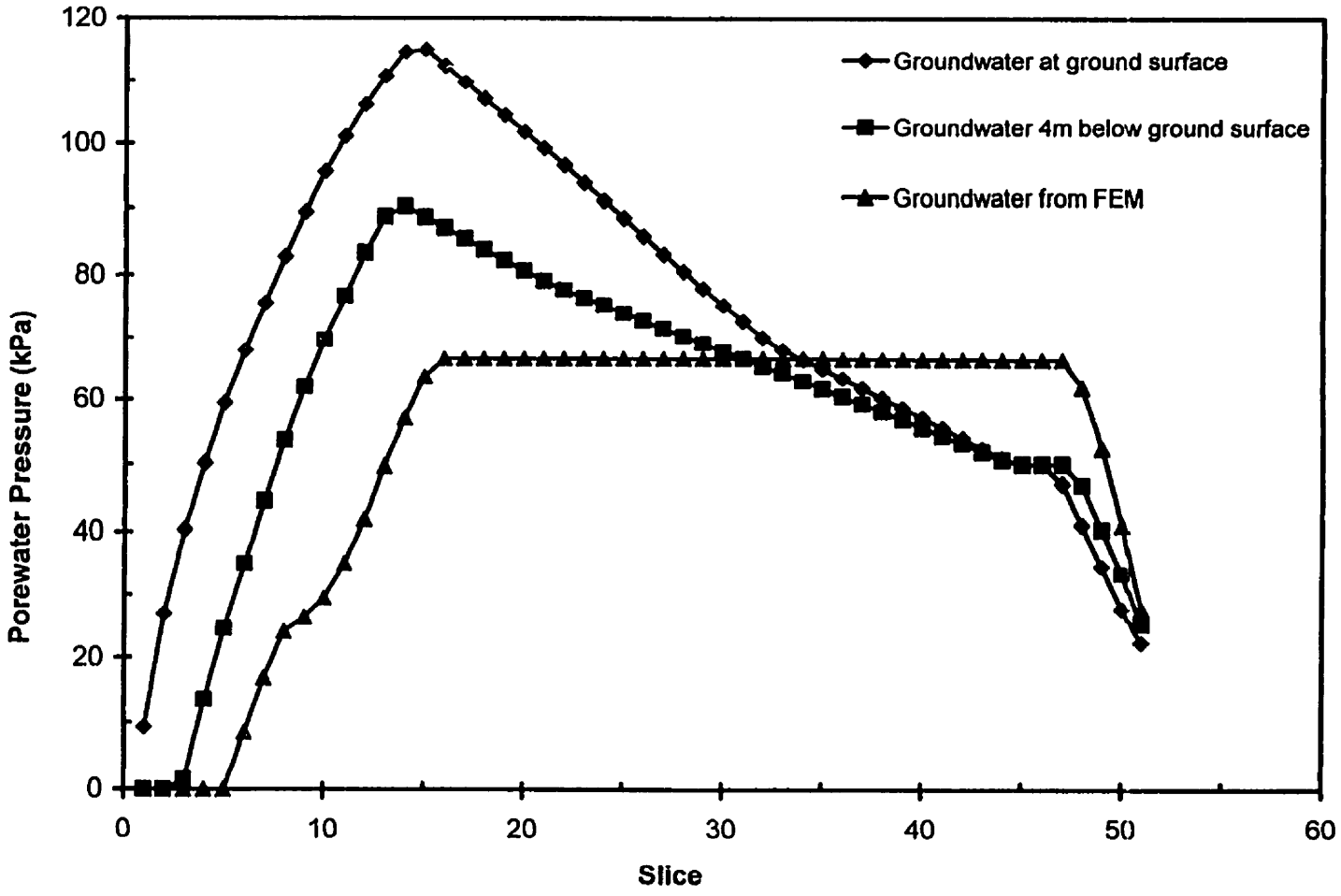

Figure 5.43 Porewater pressure distribution at the end of the modeling duration along the base of slip surface for three groundwater assumptions and weak clay layer at $c' = 3$ kPa, $\phi' = 12°$

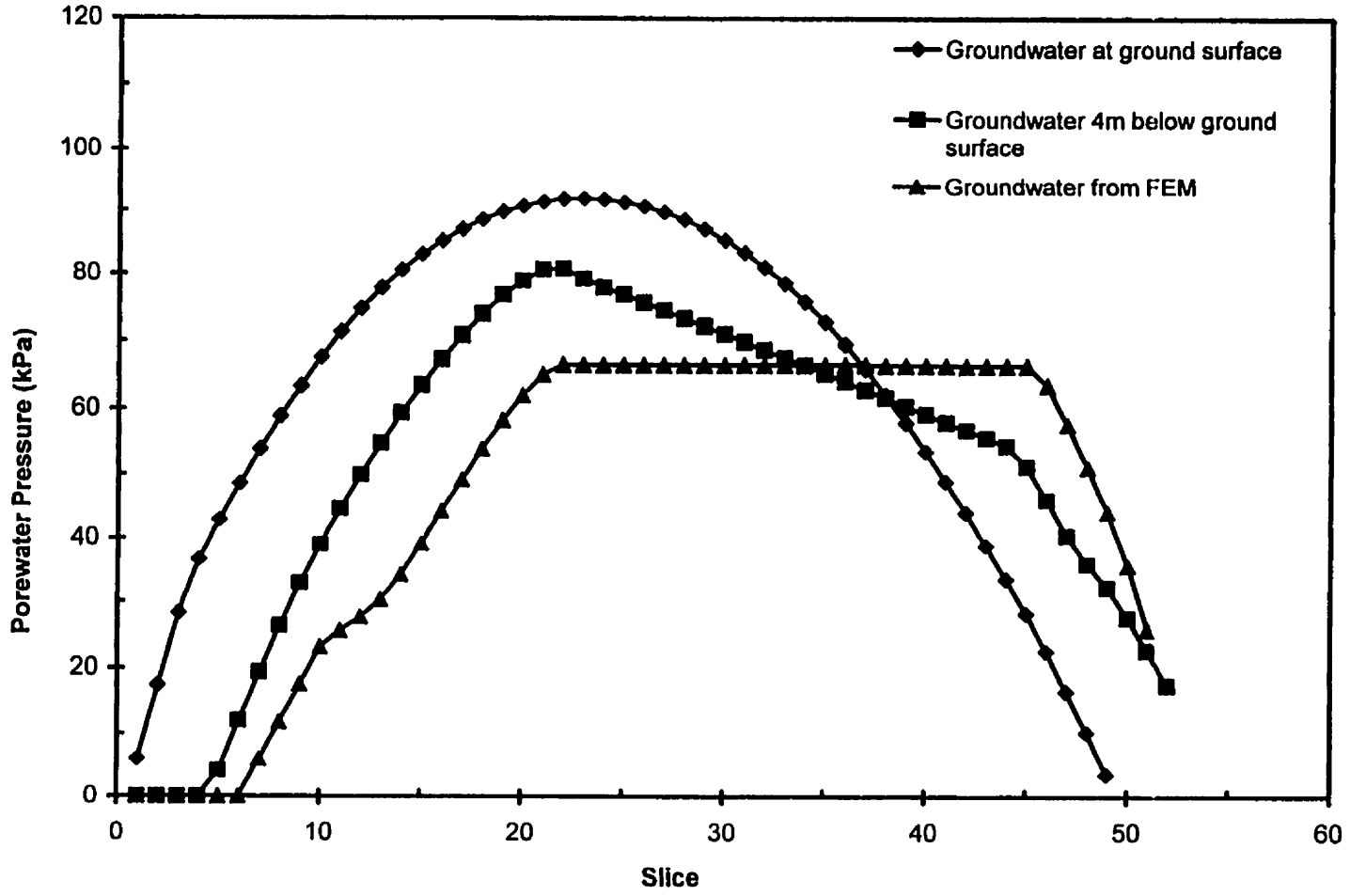

Figure 5.44 Porewater pressure distribution at the end of the modeling duration along the base of slip surface for three groundwater assumptions and no weak clay layer

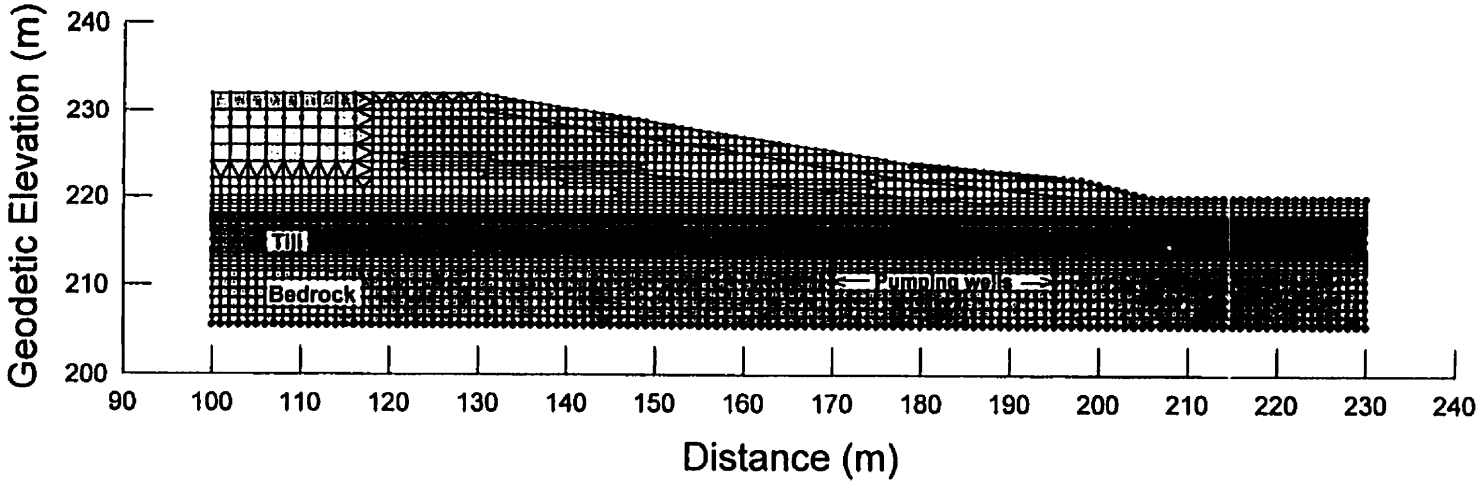

Figure 5.45 FE mesh with additional bedrock layer and pumping well locations

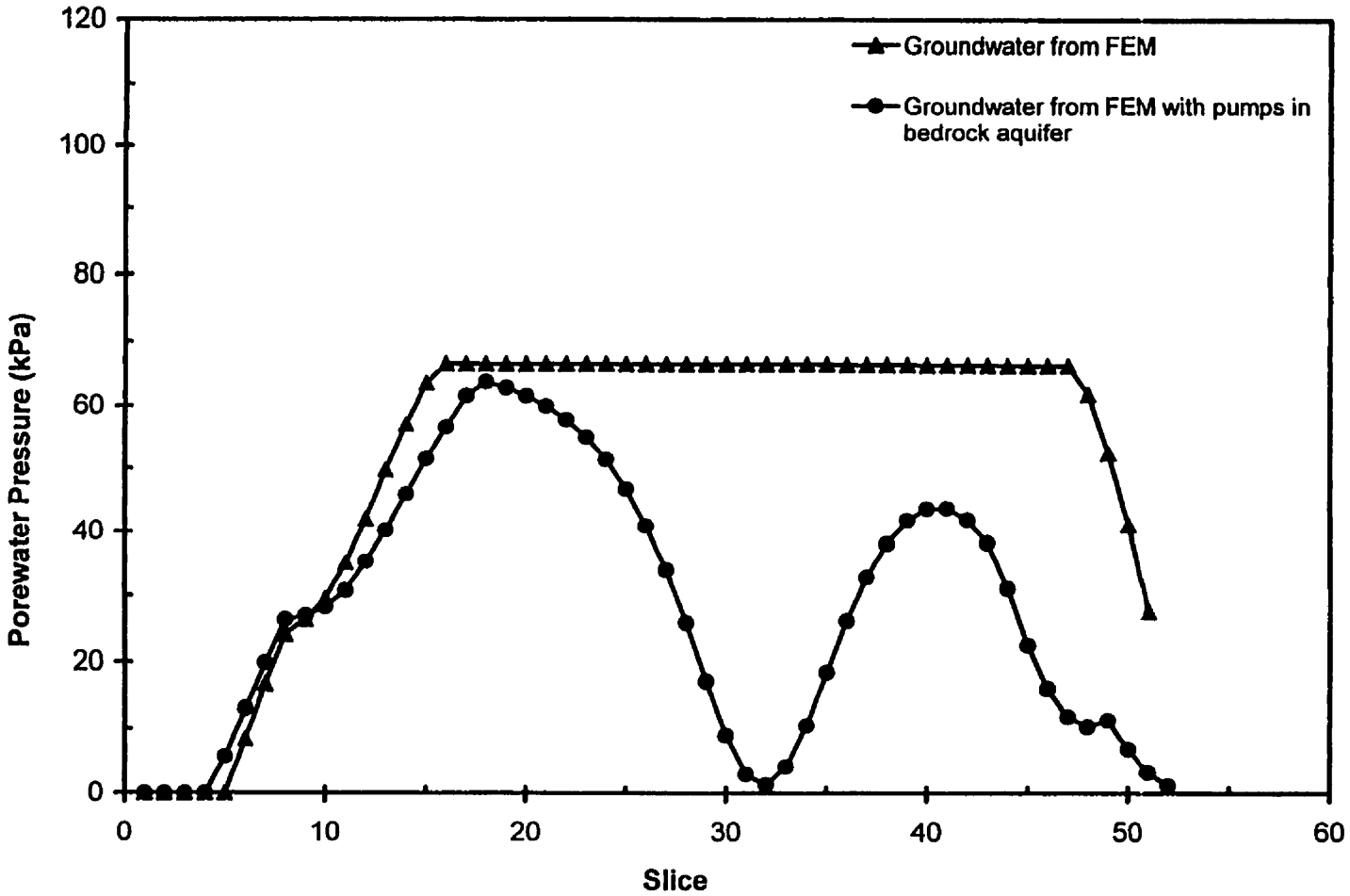

Figure 5.46 Porewater pressure distribution at the end of the modeling duration along the base of slip surface for pumping and non-pumping FE analysis and weak clay layer at $c' = 3$ kPa, $\phi' = 12°$

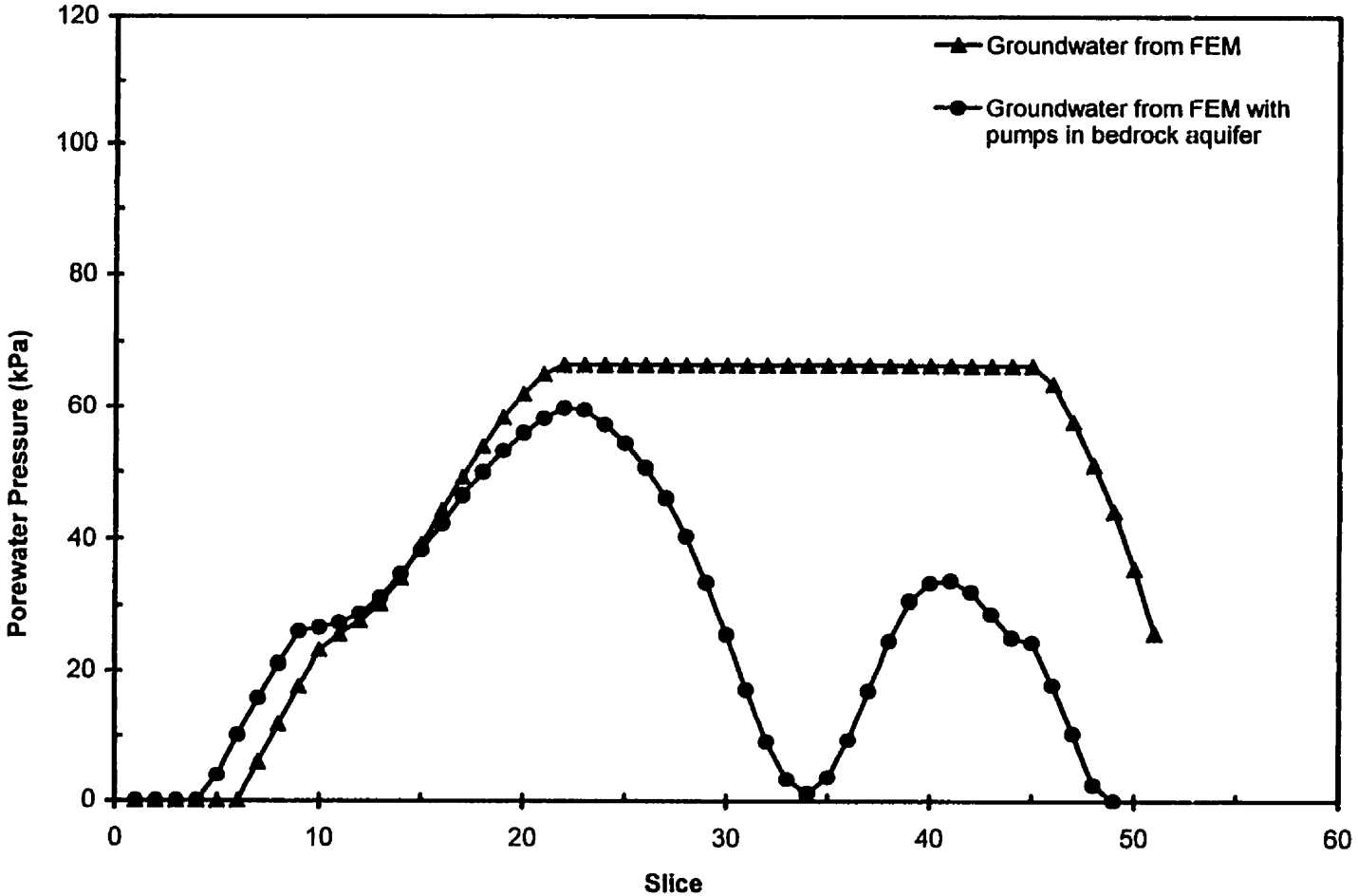

Figure 5.47 Porewater pressure distribution at the end of the modeling duration along the base of slip surface for pumping and non-pumping FE analysis and no weak clay layer

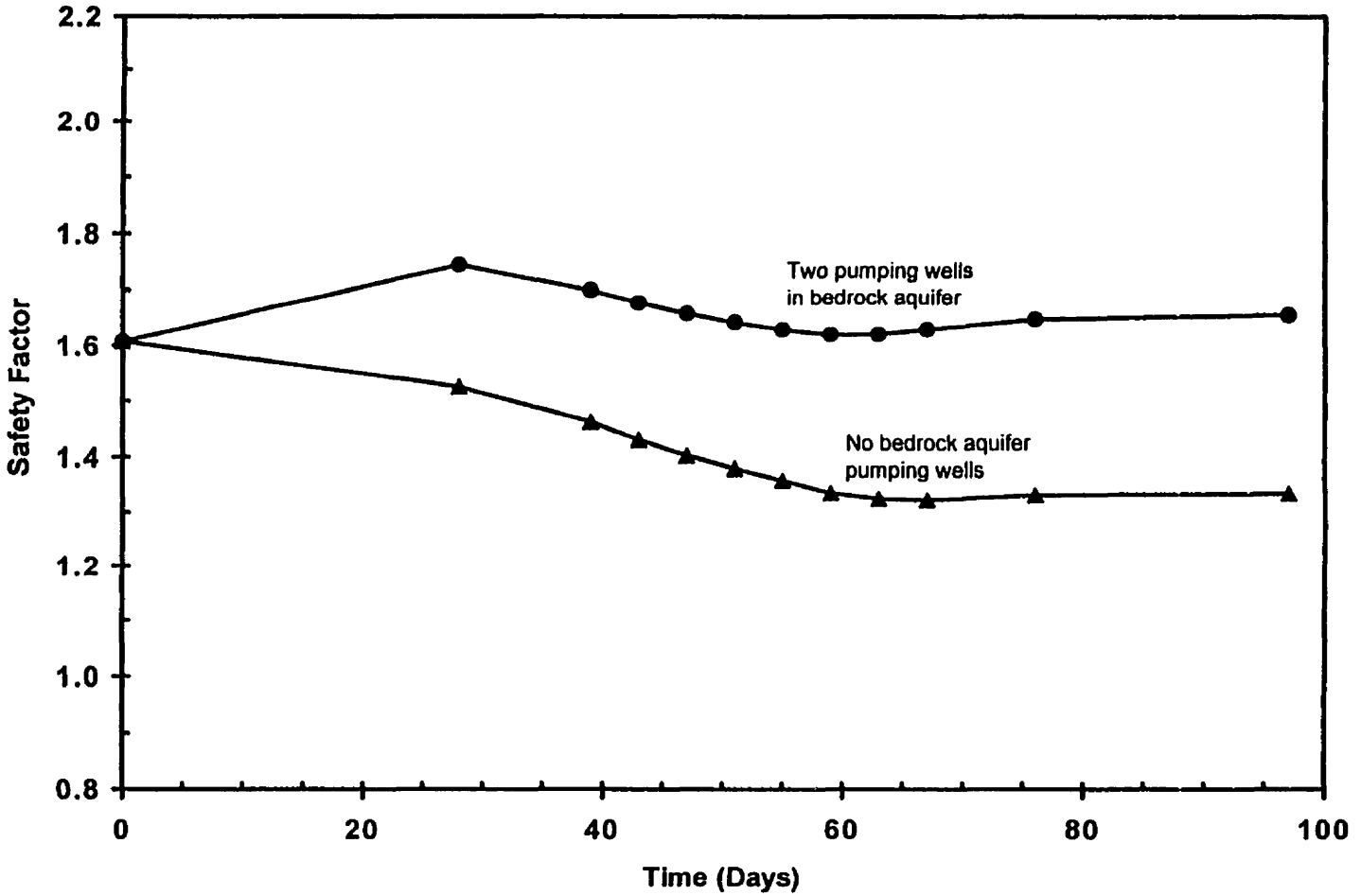

Figure 5.48 Safety factor versus time for pumping and non pumping stability analysis using FEM generated porewater pressures and weak clay layer at $c' = 3$ kPa, $\phi' = 12°$

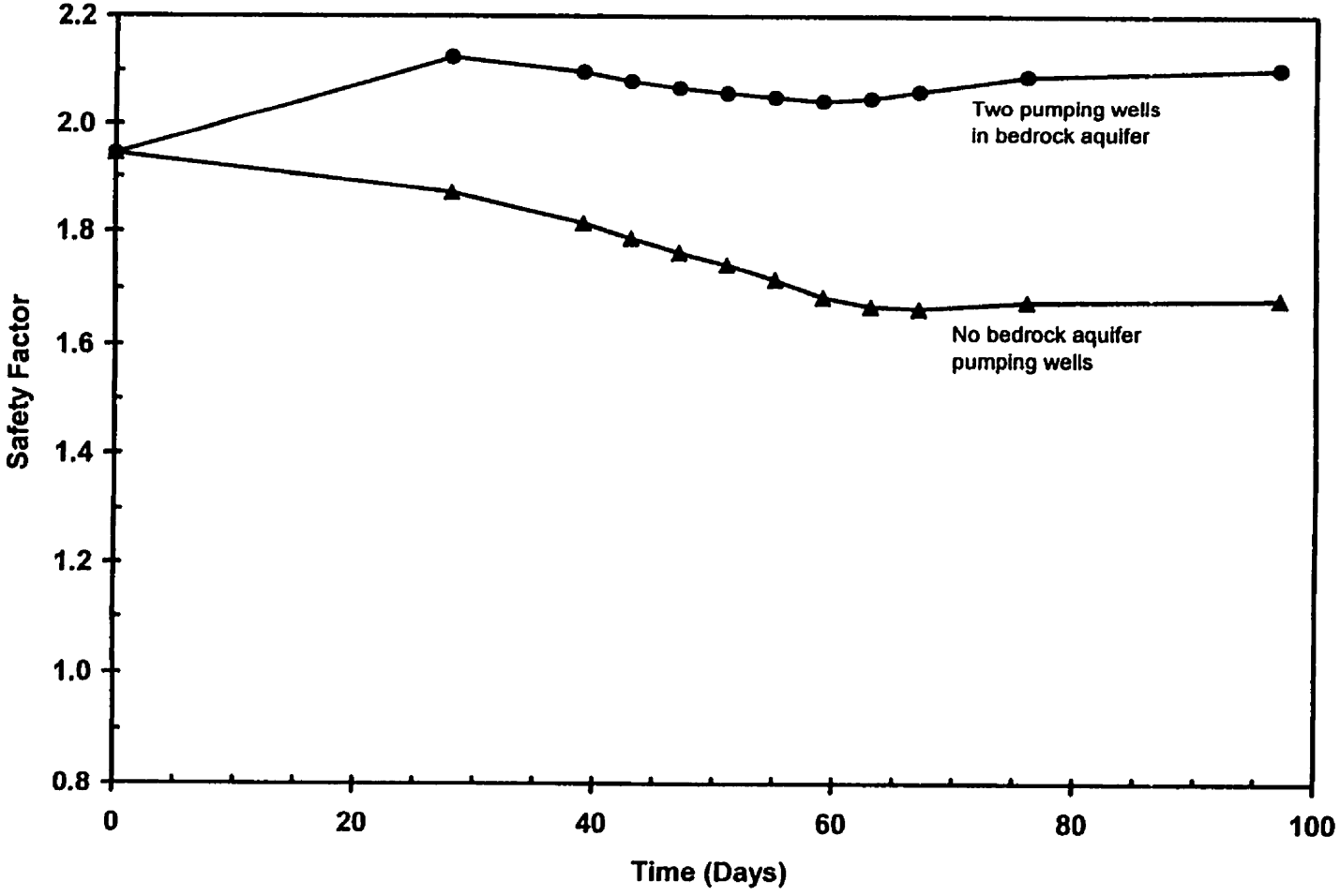

Figure 5.49 Safety factor versus time for pumping and non-pumping stability analysis using FEM generated porewater pressures and no weak clay layer

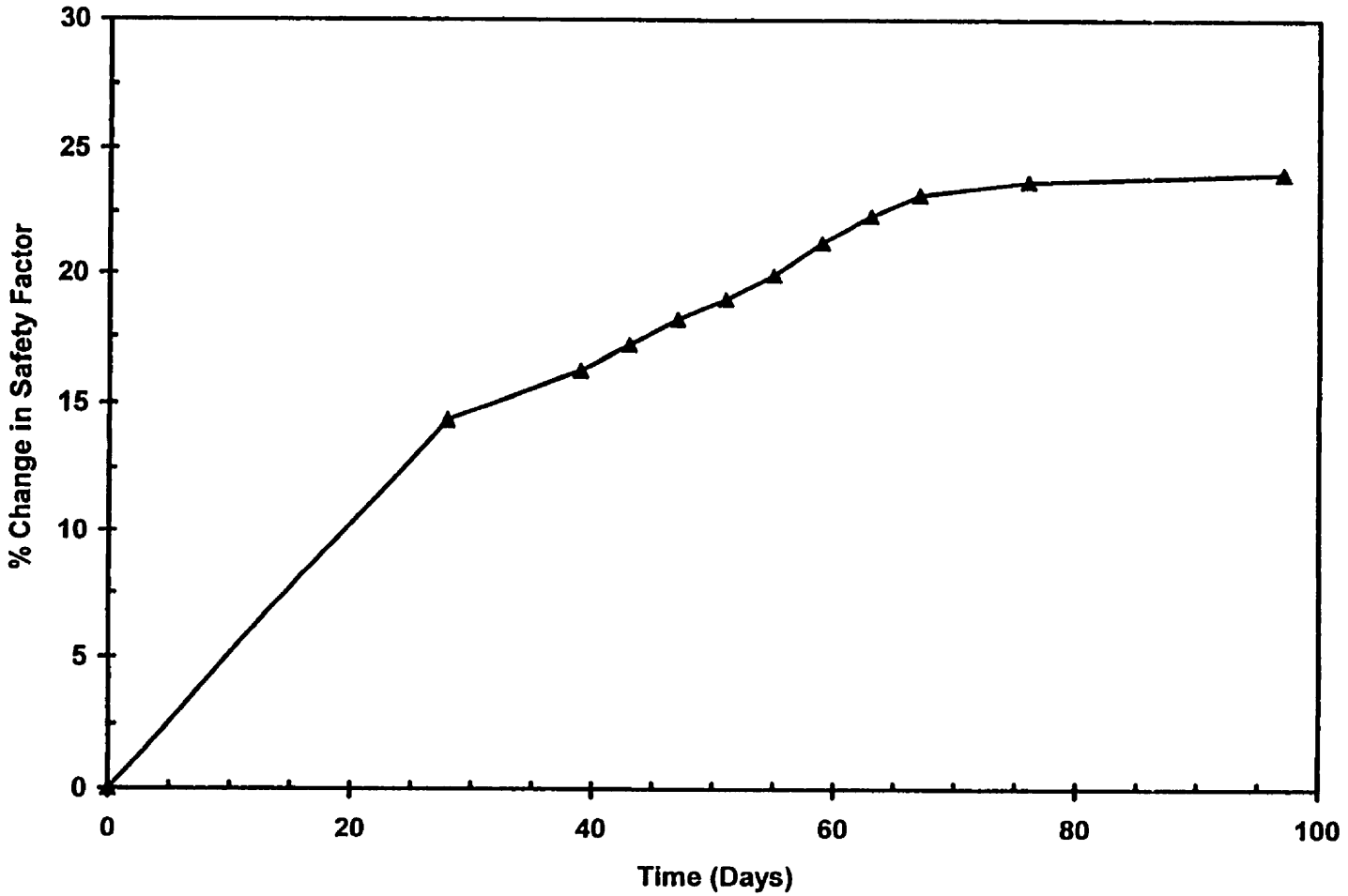

Figure 5.50 Percent increase in safety factor versus time for two pumps in bedrock aquifer and weak clay layer at $c' = 3$ kPa, $\phi' = 12°$

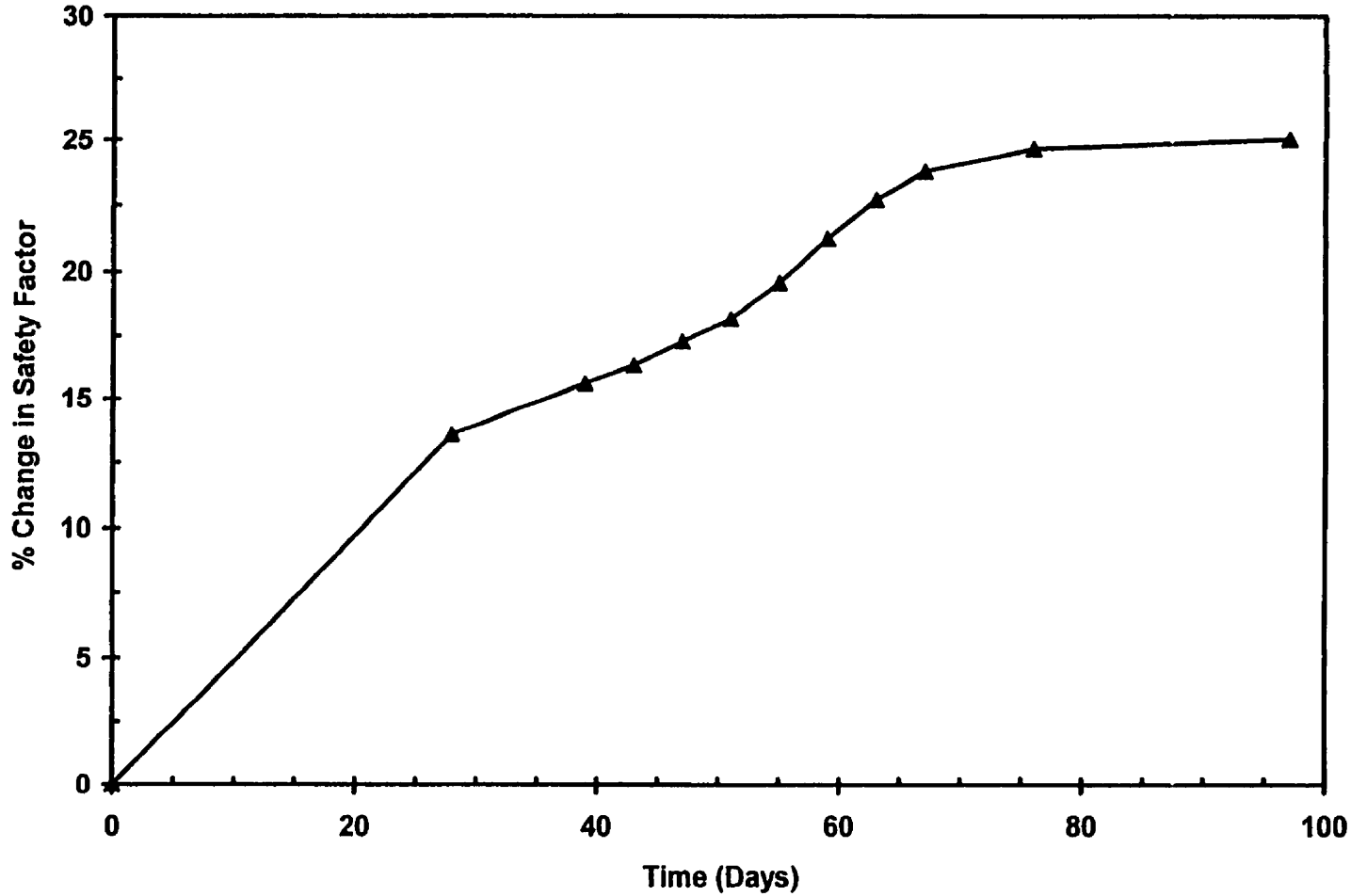

Figure 5.51 Percent increase in safety factor versus time for two pumps in bedrock aquifer and no weak clay layer

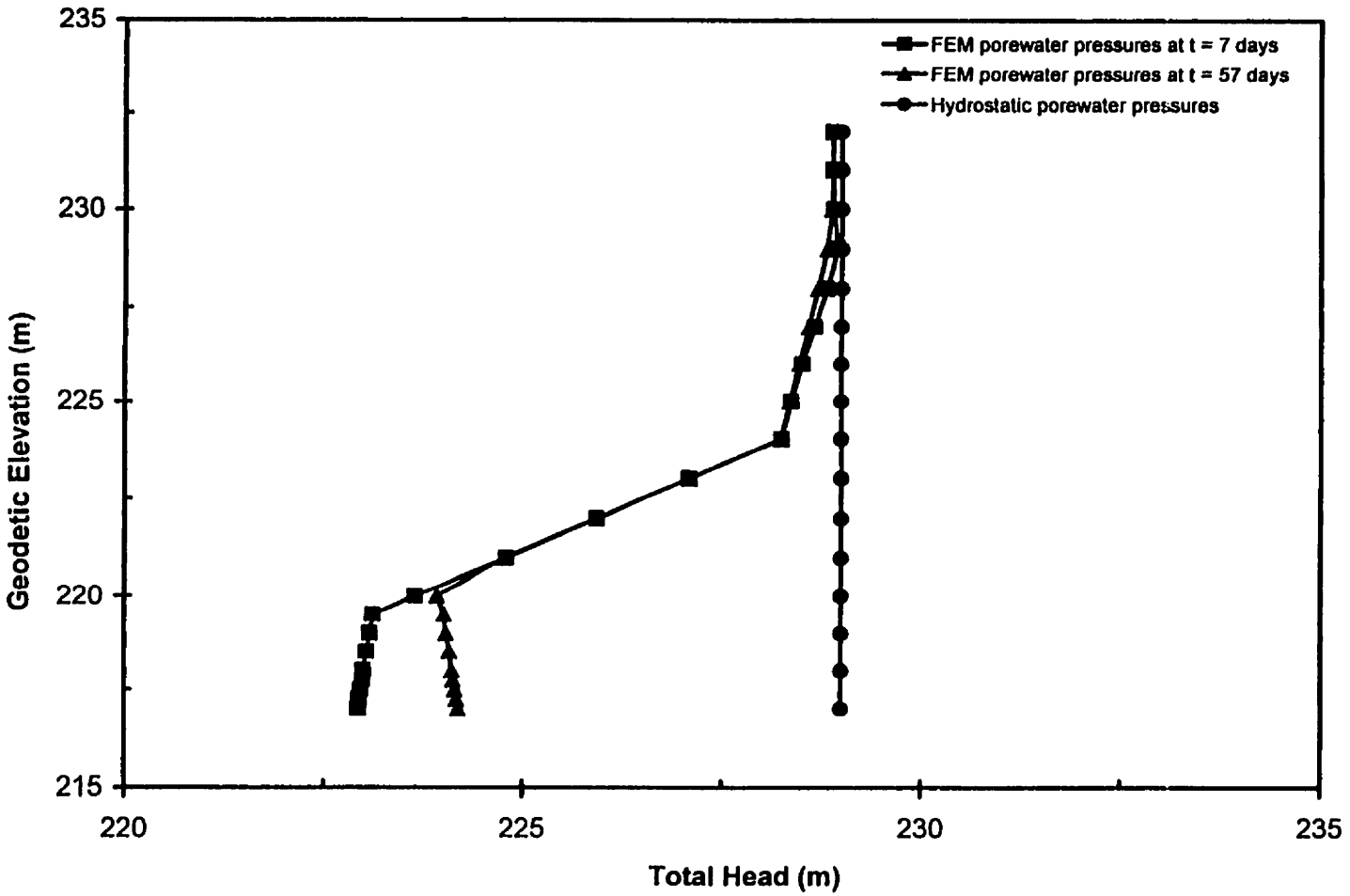

Figure 6.1 Porewater pressure distribution for FEM porewater pressures and assumed hydrostatic distribution.

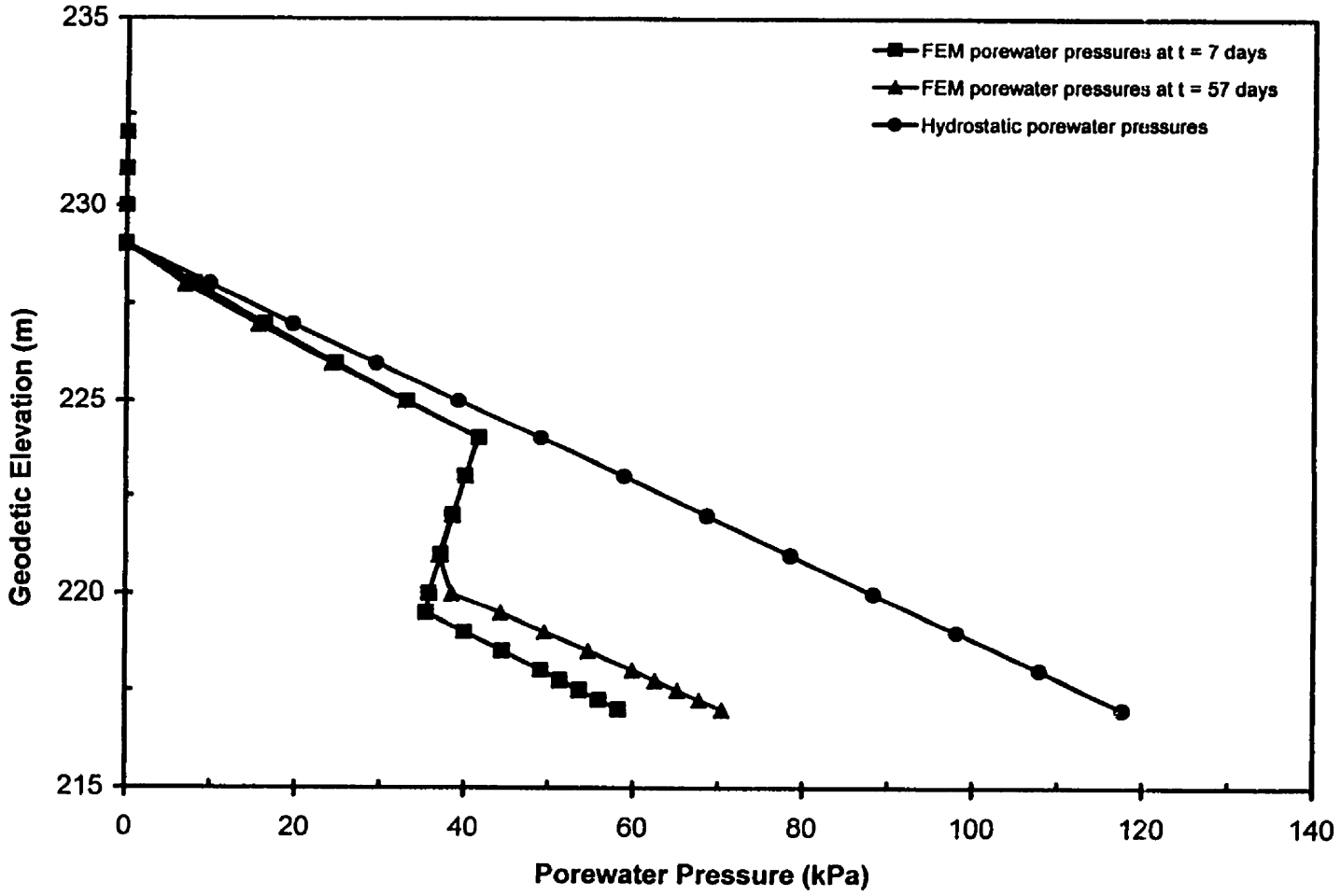

Figure 6.2 Porewater pressure versus depth for FEM porewater pressures and assumed hydrostatic distribution.

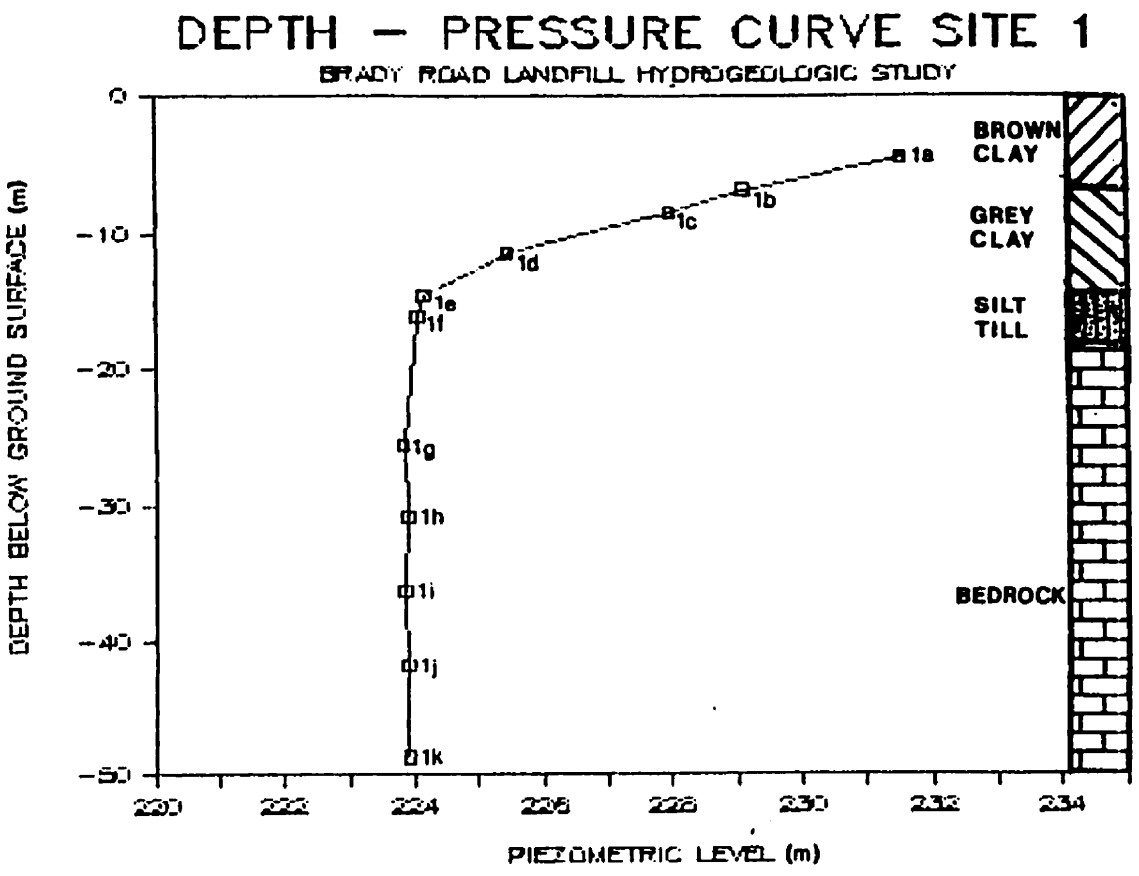

Figure 6.3 Piezometric elevation versus depth at the Brady Road Landfill site (UMA 1986)

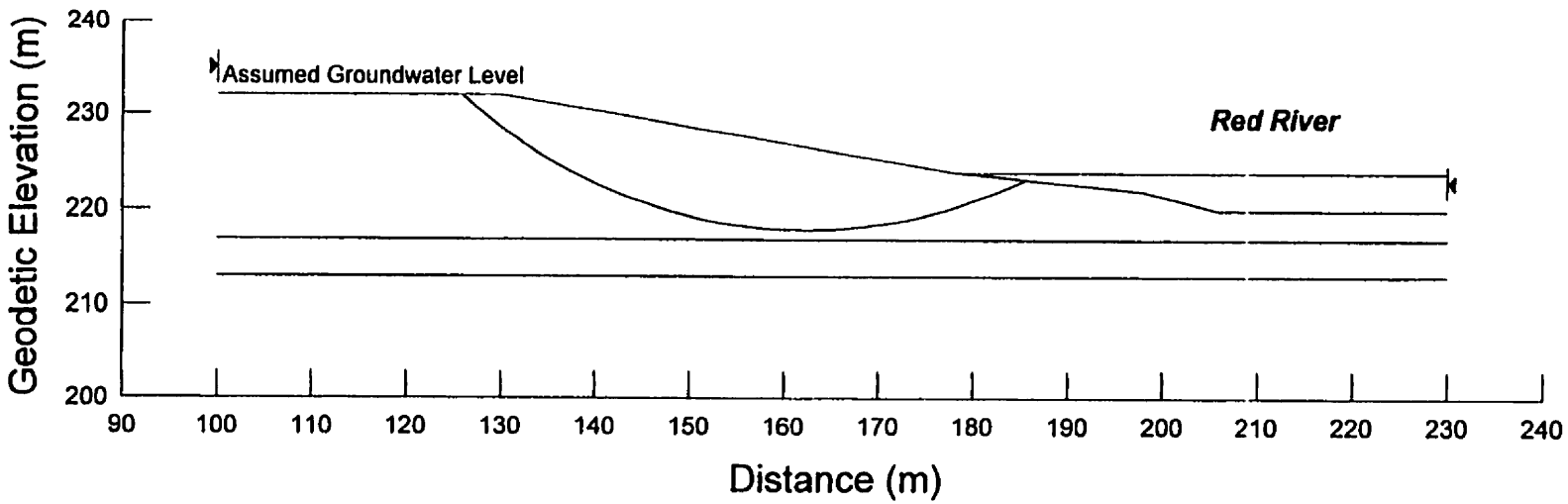

Figure 6.4 Slip surface at beginning of modeling duration for groundwater assumed at ground surface and no weak clay layer

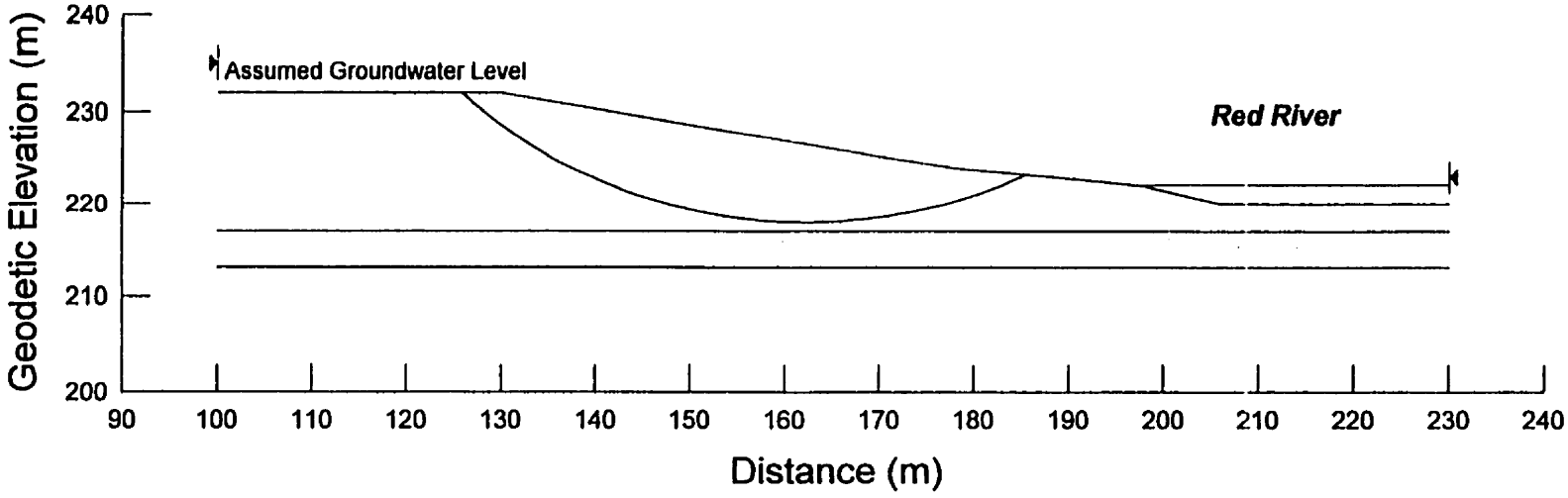

Figure 6.5 Slip surface at end of modeling duration for groundwater assumed at ground surface and no weak clay layer

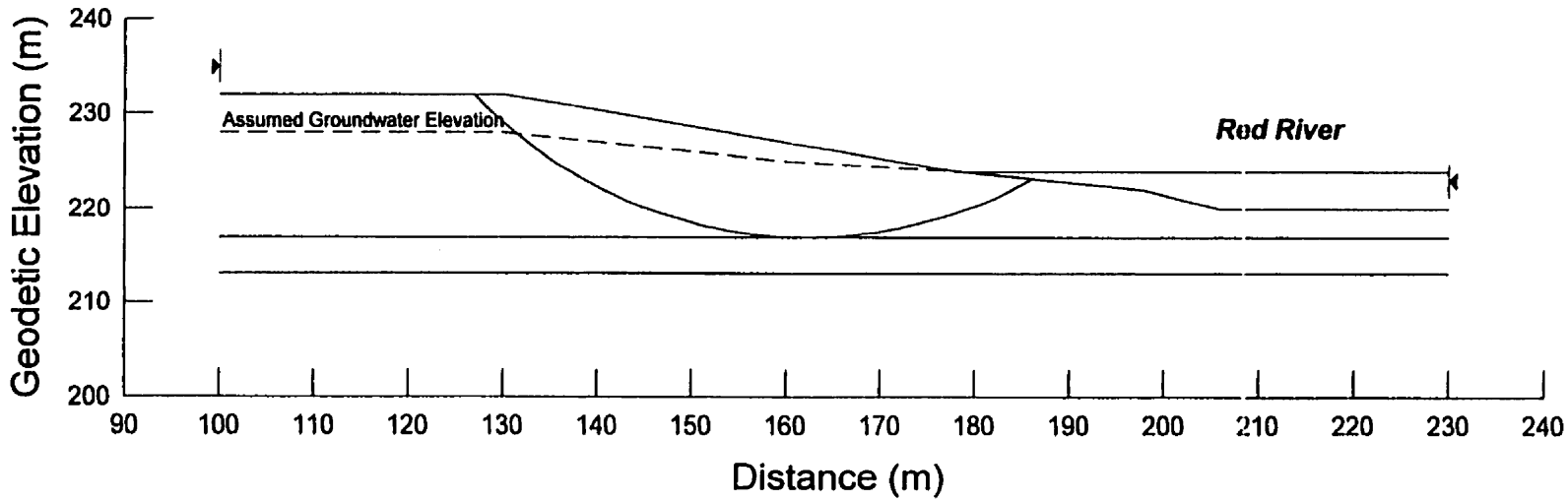

Figure 6.6 Slip surface at beginning of modeling duration for groundwater assumed at 4m below ground surface and no weak clay layer

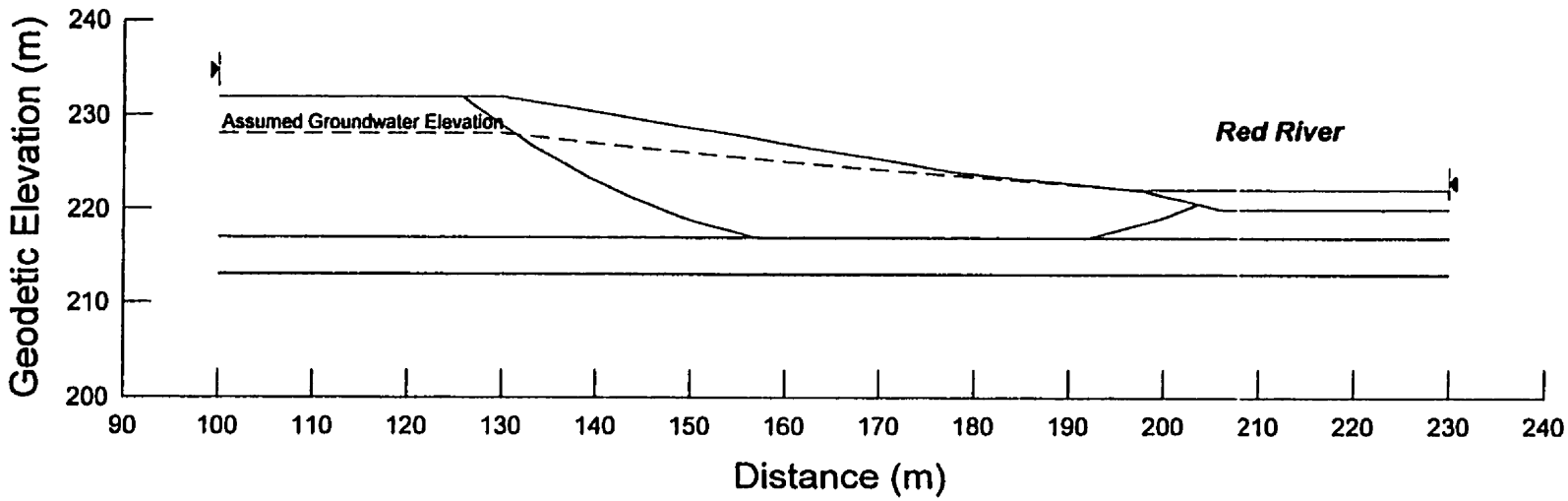

Figure 6.7 Slip surface at end of modeling duration for groundwater assumed at 4m below ground surface and no weak clay layer

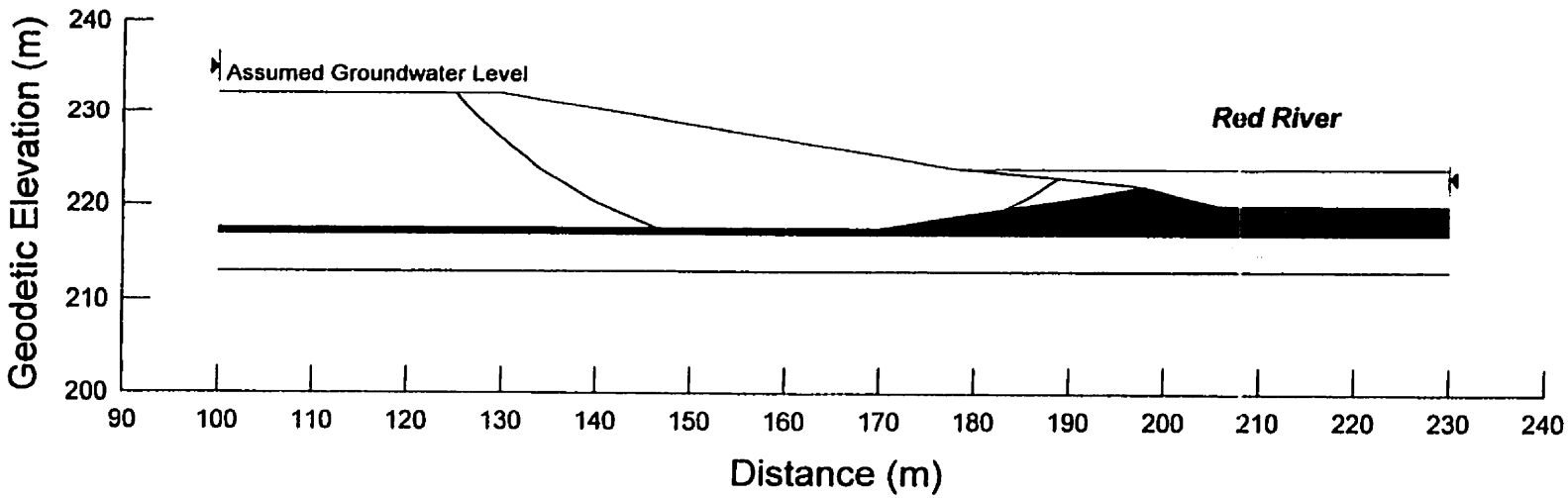

Figure 6.8 Slip surface at beginning of modeling period for assumed groundwater at ground surface and weak clay layer at $c' = 3$ kPa, $\phi' = 12°$

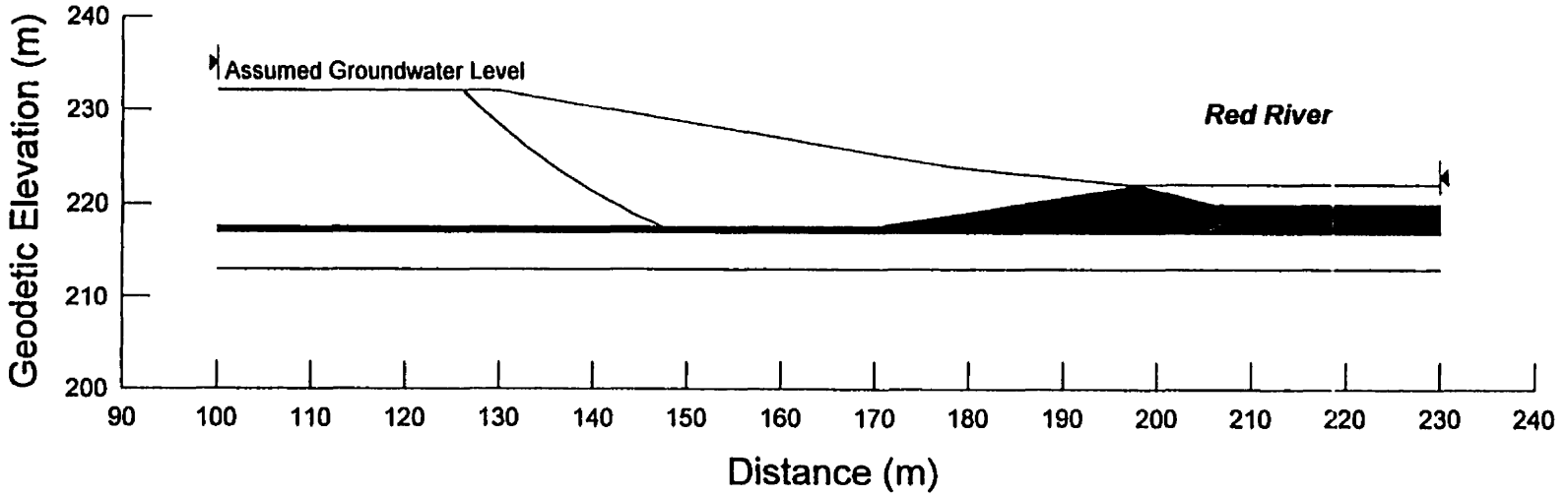

Figure 6.9 Slip surface at end of modeling period for assumed groundwater at ground surface and weak clay layer at $c' = 3$ kPa, $\phi' = 12°$

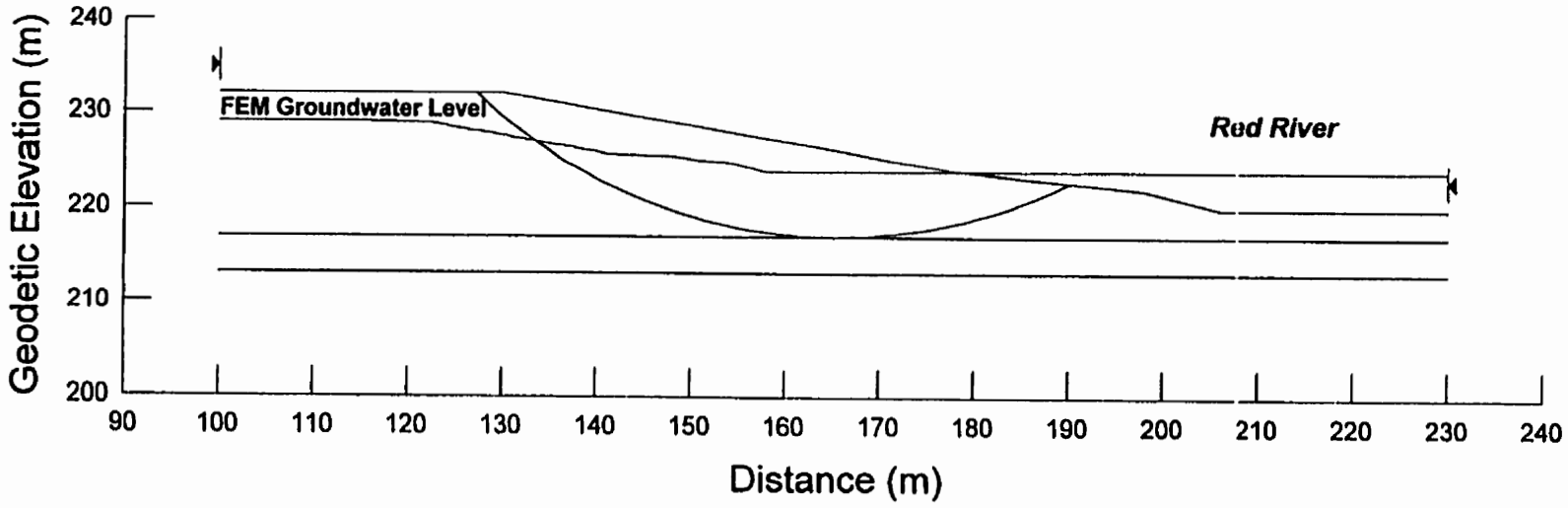

Figure 6.10 Slip surface at beginning of modeling period using FEM porewater pressures and no weak clay layer

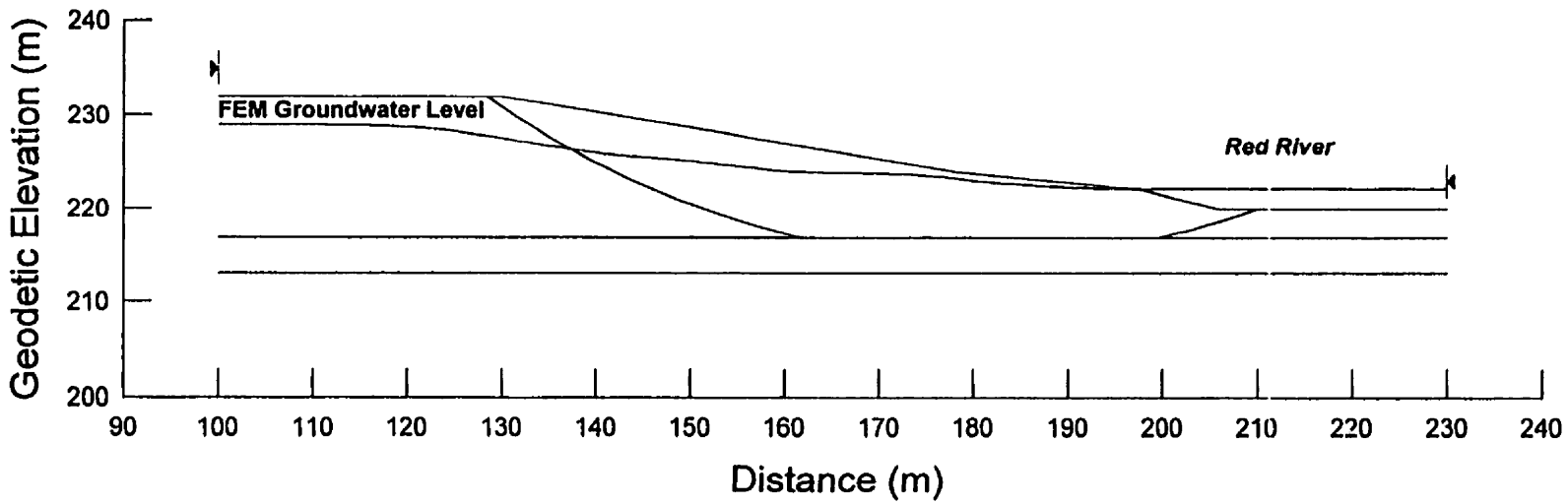

Figure 6.11 Slip surface at end of modeling duration with FEM porewater pressures and no weak layer

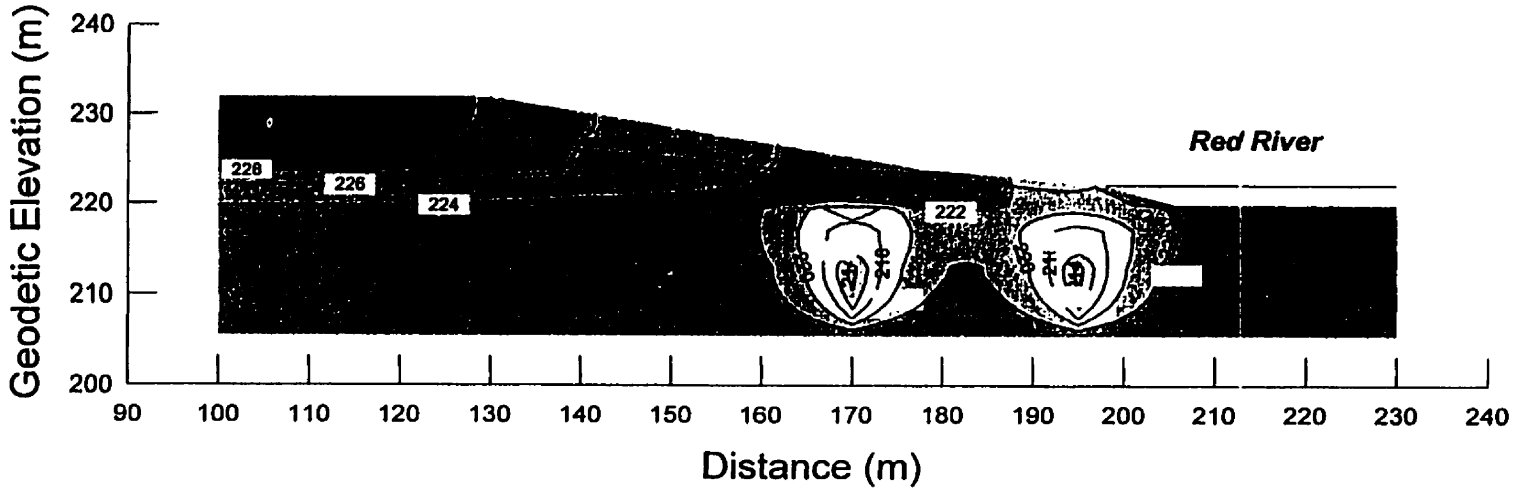

Figure 6.12 Porewater pressure distribution at end of modelling duration with two bedrock aquifer pumping wells

TABLES

Table 2.1 Summary of X-ray diffraction tests performed on Winnipeg soils (Baracos 1977)

Sample	Main minerals present (in order of decreasing showing)	
	Non-clay	Clay
Tan silt	Mostly dolomite Quartz Some calcite Some felspar Trace gypsum	Mostly illite Mixed layer (predominantly smectite) Some chlorite and/or kaolinite
Tan silt light colored layer	Mostly dolomite Quartz	Some illite
Brown clay	Some quartz Dolomite, Calcite } about equally Some felspar	Mostly mixed layer (predominantly smectite) Illite, Kaolinite } about equally
Inclusion in brown clay	Mostly calcite Dolomite, Quartz } about equally Some felspar	Some illite Some mixed layer
Grey clay	Mostly quartz Dolomite, Calcite } about equally Some felspar	Illite Mixed layer (predominantly smectite) Some chlorite and/or kaolinite
Inclusions in grey clay	Dolomite, Quartz, Calcite } about equally	Some mixed layer
Grey plastic clay	Quartz Dolomite Calcite	Illite Kaolinite Mixed layer (predominantly smectite)
Inclusions in grey plastic clay	Dolomite, Felspar, Calcite, Quartz } about equally	Some illite and mixed layer

Table 2.2 Three-section peak shear strength envelope for Winnipeg grey clay (after Baracos *et al.* 1980)

Section	Pressure σ'_{1c} (kPa)	c′ (kPa)	φ′ (degrees)
1	Low, < 60	6	31.7
2	intermediate, 60-200	33	13.0
3	high, > 200	3	22.5

Table 2.3 Ranges in residual shear strengths of Winnipeg clays (after Freeman and Sutherland 1974, Baracos 1978, Baracos *et al.* 1980, and Graham 1986)

Soil Type	Range of Residual Shear Strengths	
	c′ (kPa)	φ′ (degrees)
Brown Clay	0-6.7	8-13
Grey Clay	0-10.3	7-11.5

Table 2.4 Geotechnical properties of Winnipeg clays (Baracos *et al.* 1983(a))

Symbol	Soil Properties	Lower bound	Upper bound
E	deformation modulus [1]	3.5 MPa (500 psi)	21 MPa (3000 psi)
υ	Poisson's ratio	0.4	0.5
q_u	unconfined compressive strength [2]	50 kPa (1000 psf)	120 kPa (2500 psf)
S_u	undrained shear strength [3]	35 kPa (700 psf)	85 kPa (1775 psf)
ϕ'_r	residual angle of internal friction	8°	12°
C_c	compression index	0.5	1.0
P_s	swelling pressure	0 0	75 kPa (1550 psf)
K_0	coefficient of earth pressure at rest	0.6	0.8
OCR	overconsolidation ratio	1	5
γ	moist unit weight	16.2 kN/m^3 100 pcf)	18.2 kN/m^3 (115 pcf)
γ_d	dry unit weight	10.2 kN/m^3 (65 pcf)	13.3 kN/m^3 (85 pcf)
w_L	liquid limit	65	110
w_P	plastic limit	20	35
I_p	plasticity index	40	75
S_t	sensitivity	2	4

[1] based primarily on pressuremeter tests

[2] based on unconfined compression tests

[3] based on combination of unconfined compression tests, field vane and laboratory vane

Table 2.5 Geotechnical properties of Winnipeg glacial tills (Baracos *et al.* 1983(b))

Geotechnical Property		Typical Range Lower	Upper
Unit Weight (moist) (pcf)		-	150
Unit Weight (dry) (pcf)		-	140
Matrix material:	Liquid Limit (%)	13	20
	Plastic Limit (%)	11	13
Gradation:	Clay Size[1] (%)	10	20
	Silt Size (%)	30	40
	Sand Size (%)	25	35
Pressuremeter Modulus (ksi)		-	25-35

Notes: [1] Mostly rock flour, with limited clay minerals.
Information based on limited available data.
- Insufficient data.
1 ksi = 6.895 MPa, 1 pcf = 0.157 kN/m^3.

Table 2.6 Comparison of safety factors for common limit equilibrium methods of slope stability analysis (Fredlund and Krahn 1977)

Case no.	Example problem*	Ordinary method	Simplified Bishop method	Spencer's method			Janbu's simplified method	Janbu's rigorous method**	Morgenstern-Price method $f(x)$ = constant	
				F	θ	λ			F	λ
1	Simple 2:1 slope, 40 ft (12 m) high, $\phi' = 20°, c' = 600$ psf (29 kPa)	1.928	2.080	2.073	14.81	0.237	2.041	2.008	2.076	0.254
2	Same as 1 with a thin, weak layer with $\phi' = 10°, c' = 0$	1.288	1.377	1.373	10.49	0.185	1.448	1.432	1.378	0.159
3	Same as 1 except with $r_u = 0.25$	1.607	1.766	1.761	14.33	0.255	1.735	1.708	1.765	0.244
4	Same as 2 except with $r_u = 0.25$ for both materials	1.029	1.124	1.118	7.93	0.139	1.191	1.162	1.124	0.116
5	Same as 1 except with a piezometric line	1.693	1.834	1.830	13.87	0.247	1.827	1.776	1.833	0.234
6	Same as 2 except with a piezometric line for both materials	1.171	1.248	1.245	6.88	0.121	1.333	1.298	1.250	0.097

*Width of slice is 0.5 ft (0.3 m) and the tolerance on the nonlinear solutions is 0.001.
**The line of thrust is assumed at 0.333.

Table 4.1 Location of South Perimeter piezometer and FE observation nodes

South Perimeter Research Site			FE Seepage Model	
Piezometer Number	Ground elevation (m)	Piezometer Tip Elevation (m)	Ground Elevation (m)	Node Elevation (m)
P1	222.05	221.44	222.0	221.5
P2	222.05	216.87	222.0	217.0
P3	222.05	215.34	222.0	216.0
P4	222.7	221.18	222.7	221.0
P5	222.7	218.13	222.7	218.0
P6	223.4	220.96	223.4	221.0
P7	223.4	217.91	223.4	218.0
P8	223.4	215.78	223.4	216.0
P9	224.55	220.59	224.49	220.65
P10	224.55	218.15	224.49	218.0
P11	224.55	215.71	224.49	216.0
P12	229.2	221.58	229.16	221.5
P13	229.2	217.92	229.16	218.0
P14	229.2	215.5	229.16	216.0
P15	231.8	223.57	232.0	223.5
P16	231.8	220.52	232.0	220.5

Table 4.2 Summary of hydraulic conductivity values used in the FE seepage model

Material	Hydraulic Conductivity (m/s)
K1	$1x10^{-8}$
K2	$2x10^{-9}$
K3	$2x10^{-10}$
K4	$1x10^{-9}$
K5	$1x10^{-7}$
Bedrock	$6.5x10^{-4}$